INTERNATIONAL ACADEMIC RESEARCH AND REVIEWS IN

ENGINEERING

March 2023

EDITORS

PROF. DR. COŞKUN ÖZALP

DOÇ. DR. SELAHATTİN BARDAK

DOÇ. DR. ERTAÇ HÜRDOĞAN

SERÜVEN YAYINEVİ

Genel Yayın Yönetmeni / Editor in Chief • C. Cansın Selin Temana

Kapak & İç Tasarım / Cover & Interior Design • Serüven Yayınevi

Birinci Basım / First Edition • © Mart 2023

ISBN • 978-625-6399-76-1

Serüven Yayınevi / Serüven Publishing
Türkiye Adres / Turkey Address: Kızılay Mah. Fevzi Çakmak 1. Sokak Ümit Apt No: 22/A Çankaya/ANKARA
Telefon / Phone: 05437675765
web: www.seruvenyayinevi.com
e-mail: seruvenyayinevi@gmail.com

Baskı & Cilt / Printing & Volume
Sertifika / Certificate No: 47083

International Academic Research and Reviews in Engineering

March 2023

Editors

Prof. Dr. Coşkun ÖZALP
Doç. Dr. Selahattin BARDAK
Doç. Dr. Ertaç HÜRDOĞAN

CONTENTS

CHAPTER 1

DEVELOPMENT OF TANNIC ACID-CONTAINING FISH GELATIN-BASED GELS for ELECTRONIC SKIN APPLICATIONS

Hasan TÜRE[1]

1 Associate Prof. Dr.,Ordu University, Fatsa Faculty of Marine Science, Department of Marine Science and Technology Engineering, 52200 Ordu, Turkey. E-mail:hasanture@odu.edu.tr. (ORCID: 0000-0003-4883-0751)

1. INTRODUCTION

Numerous efforts are being made nowadays to develop high-performance materials for electronic skin, soft robotics, and human motion monitoring (Di et al., 2019). A substantial number of electronic materials with high responsiveness and conductivity have been developed by using conductive polymers (polypyrrole, polyaniline) or embedding nanofillers such as carbon nanotubes, graphene, and metallic nanoparticles into polymer networks. Although these materials fulfill the necessary conductivity requirements, their poor biocompatibility, stretchability, and bioadhesion restrict their practical applications (Di et al., 2019; Chen et al., 2021; Wang et al., 2021).

Hydrogels, cross-linked polymer networks containing abundant water, have been intensively investigated for use as electronic sensors because of their stretchability, surface compliance, and biocompatibility (Fan, Wang, & Jin, 2018; Qin, Owyeung, Sonkusale, & Panzer, 2019; Chen et al., 2021). On the other hand, the low mechanical properties and weak electrical conductivity of hydrogels severely limit their use as a matrix for soft sensor applications. Additionally, hydrogels rapidly dehydrate in their natural environment, requiring an additional sealing process for the long-term functionality of hydrogel-based devices. (Qin, Owyeung, Sonkusale, & Panzer, 2019; Chen et al., 2021). Although using ionic liquids (ILs) could be considered an ideal remedy to address these issues, their toxicity and high manufacturing costs prevent them from being widely used (Qin, Owyeung, Sonkusale, & Panzer, 2019). One possible solution to overcome these drawbacks is the use of deep eutectic solvents (DES) for the preparation of hydrogels.

DES are a new subclass of ILs that share physicochemical characteristics like being ionic, having low volatility, and having a moderate level of ionic conductivity. In addition, due to their low cost, high bio-based content, and environmentally friendly nature, DES-based gels have been produced for different types of applications such as wound dressing, water treatment, batteries, and capacitors (Joos et al., 2018; Joos et al., 2020; Gomes, Silva, & Reis, 2019; Wang et al., 2021). Several studies have also indicated that combining biopolymers with DES is a promising approach to obtain biocompatible, stretchable, and conductive gels for health monitoring and electronic skin applications (Wang et al., 2021; Qin, Owyeung, Sonkusale, & Panzer, 2019; Yamagata, Soeda, Ikebe, Yamazaki, & Ishikawa, 2013; Takada & Kadokawa, 2015). Though several biopolymers, such as chitosan, starch, and cellulose, have been used to prepare gels using DES, only a few attempts have been made to produce the gelatin-based DES gels for flexible devices (Qin, Owyeung, Sonkusale, & Panzer, 2019). To the best of my knowledge, no prior studies have detailed the prepara-

tion and evaluation of gelatin, tannic acid (TA), and DES-based biopolymer-supported gels.

The purpose of this study was to see if the use of TA could improve the mechanical, swelling, adhesive, and conductivity properties of gelatin-supported DES gels. In addition, the release properties of TA were studied in detail.

The novalty of this research is that gelatin, TA, and DES have been mixed for the first time to produce green and fully recyclable conductive gels and a simple method of synthesis. It appears that more precise and extensive research is required to evaluate the use of obtained gels as electronic devices. This work's main objective was to describe the *in vitro* characteristics of TA-containing gelatin-based DESs gels, but using the synthesized gels as electronic skin or devices on humans falls outside the scope of this article.

2. EXPERIMENTAL

2.1. Materials

Choline chloride (ChCl) was obtained from Sigma-Aldrich. Gelatin (cold-water fish skin) and glycerol (Gly) were obtained from Merck (Darmstadt). Tannic acid was purchased from Tekkim, Turkey.

2.2. Methods

2.2.1. DES/mixture formation and Gel preparation

DES was prepared by mixing a 1:2:0.5 molar ratio of ChCl, Gly, and water. This solution was heated at 60 °C with constant stirring at 150 rpm for half an hour to obtain a clear solution. The gelatin-based DES gel was prepared using the thermally modulated coil–helix transition process of gelatin caused by the subsequent heating and cooling of the gelatin/DES mixture. (Qin, Owyeung, Sonkusale, & Panzer, 2019). For this, gelatin powder was added to DES, and the solution was heated at 60 °C and 150 rpm for 1 hour to get a homogenous gelatin/DES mixture. The warm solution (20 mL) was then poured into plastic petri dishes (d= 90 mm) to define the gel shape. To create the supramolecular gel, the gelatin pre-gel was stored at 4 °C for 24 h, during which triple helix structures as a result of hydrogen bond associations were developed among gelatin chains as junction zones (Derkach et al., 2018; Qin et al., 2019). Thereafter, the obtained gel was dried at room temperature (23 ±2 °C) for 3 days. To prepare TA-containing gels, an appropriate amount of TA powder was added into the gelatin-DES mixture, and the same protocol used in the preparation

of pure gelatin gel was followed. The concentration of gelatin in the final gels was kept at 10 % (w/w), and the TA concentrations were varied to 1, 3, 5, and 7 % (w/w). Samples are denoted with respect to their TA content, whereby G-1 represents the gel containing (1% w/w TA). Fig. 1 shows the preparation process of gelatin-based gels.

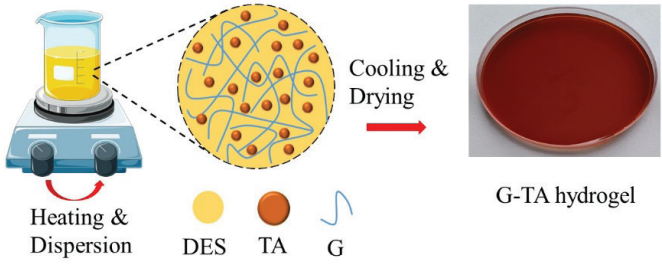

Figure 1. *Schematic illustration showing the preparation process of gelatin-based gels.*

2.2.2. Thickness measurement

The gels' thickness was measured using a digital micrometer. The average of ten random readings made on each gel was used to calculate the thickness of each gel (mm).

2.2.3. Swelling

To measure the swelling ratio of the gels, gels (3 mm in diameter, 14 mm thick) were first dried in a desiccator over silica gel for one week at room temperature (23 ±2 °C). Gels were then put into petri dishes with 40 ml of deionized water. The samples were left in water at room temperature for 0, 1, 3, 24, 28, 48, 168, 192, and 216 h. Then, the swollen samples were taken from the water, wiped with tissue paper, weighed, and placed again in water. The swelling (S) was calculated using the equation shown below:

$$S\,(\%) = \frac{(Ws - Wo)}{Wo} x\ 100 \qquad (1)$$

where, *Wo* is the dry weight of the gel and *Ws* is the weight of the gel after being treated with deionized water (Türe, 2019)

2.2.4. Adhesive properties of obtained gels

The simple and visual adhesion experiments were used to examine the adhesive behaviors of the gels on various substrates, including glass, plastics, metals, and paper.

2.2.5. Electrical conductivity

The electrical resistance of the gels (10 mm width and 50 mm length) was measured using an ohm-meter (Mastfuyi, FY107C, China) at room temperature (23 ±2 °C). The electrical conductivity was calculated using the following equation (Di et al., 2019).

$$\sigma\left(\frac{S}{cm}\right) = \frac{1}{tRs} \tag{2}$$

Where t represents the thickness of the hydrogel, Rs represents the resistance of the gels. Three samples were analyzed and the findings were averaged.

2.2.6. Tensile test

The mechanical properties of the samples were tested on a tensile tester (TA-TX Plus UK) with a 5 kg load cell and a crosshead speed of 1 mm/min at room temperature (23 ±2 °C). Before tensile testing, gel specimens with dimensions of 10 mm in width and 50 mm in length were punched out of the samples and allowed to condition for a week at room temperature in desiccators. The stress-strain curve was used to calculate the tensile strength (TS), the percentage of elongation at break (% E), and Young's modules. Each sample was tested using at least six replicates.

2.2.7. Release study

TA-containing gels were put in vessels containing 40 mL of water. Every predetermined amount of time, the amount of TA released from the gels was measured using a UV spectrometer (Shimadzu UV-1280, Japan) set at 275 nm. The sample that was collected for analysis was replaced with the same amount of water in order to maintain a constant release medium volume. The calibration curve was used to determine the amounts of TA released, and the cumulative release percentage (CD%) was calculated. (Leite et al., 2021).

2.2.8. Statistical analysis

The differences between the group averages were investigated using the Tukey test at a significance level of 0.05 after the data were subjected to an ANOVA analysis. KaleidaGraph 4.1.3 and Excel 15.25 (Microsoft, USA) were used to analyze the experimental results (Synergy Software, USA).

3. RESULTS AND DISCUSSION

3.1. Preparation of DES-supported gels

Initially, DES were prepared by mixing choline chloride as a hydrogen bond acceptor and glycerol as hydrogen bond donor (HBD) at a 1:2 molar ratio. To prepare gels with different polymer concentrations (10, 15, and 20 w/w %), gelatin powder was tried to be dissolved in prepared DES. However, even at the lowest gelatin concentration, a homogeneous solution could not be obtained. Insoluble gelatin lumps and lots of bubbles were observed. The reason for this can be explained by high viscosity of DES due to the presence of a strong hydrogen bond network between the components as well as electrostatic and Van der Waals interactions, which limit the mass-transfer of free species inside the DES (Gabriele, Chiarini, Germani, Tiecco, & Spreti, 2019). It was revealed that water could act as a co-HBD in a hydrated DES mixture at a low concentration, leading to a decrease in the mixture's viscosity and increasing both ionic conductivity and liquid processability (Owyeung, Sonkusale, & Panzer, 2020). Therefore, small amounts of water (0.5 mol fraction) were added to the DES mixture to obtain a clear and bubble-free gel solution. Gels with a gelatin concentration of 10% (w/w) were easily prepared without any additional steps after the addition of water. In addition, when water was added to the mixture, homogeneous, smooth, and pliable gels were obtained. The incorporation of up to 7 wt.% TA did not significantly change the preparation of TA-containing gels. However, at higher TA concentrations, the viscosity of the mixture increased, resulting in gels with undissolved TA powders. As can be seen in Fig. 2, gelatin gels turned from pale yellow to brownish as the TA concentration increased, and the transparency of gels decreased as the TA level increased.

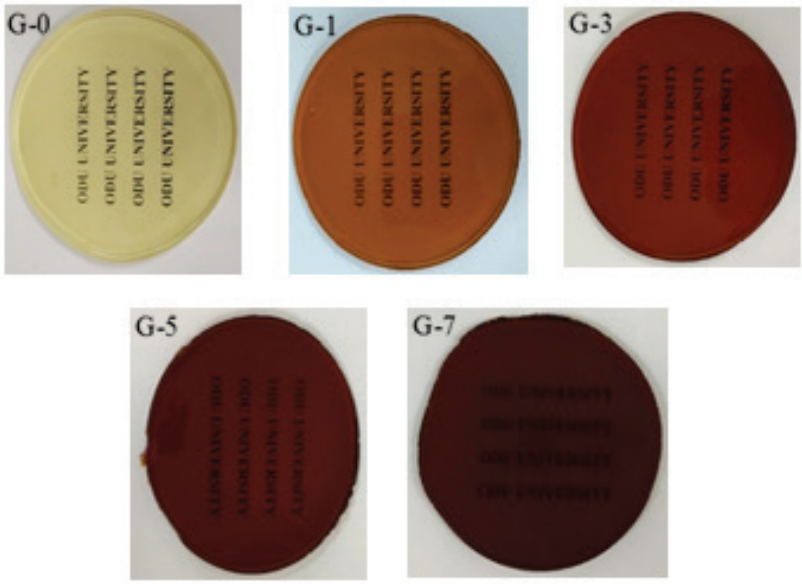

Figure 2. *Photographs of the gels with different TA concentration*

3.2. Adhesive properties

It was observed that TA-containing gels can adhere to various substrates, such as paper, glass, plastic, and metal (Fig. 3). Notably, the TA-7 gel adheres quite well to the metal surface. Because of its pyrogallol and catechol groups, TA is adhesive to a variety of substrates and can form hydrogen and covalent bonds, hydrophobic interactions, and metal coordination bonds (Zhao et al., 2021).

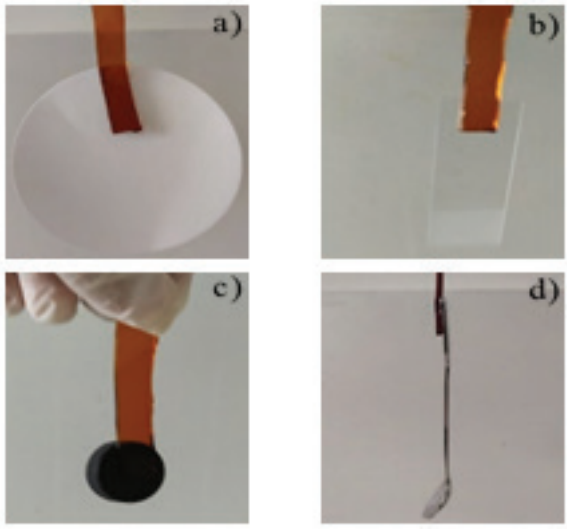

Figure 3. *Adhesive properties of G-3 gels. (a) paper, b) glass, c) plastic, d) metal*

3.3. Swelling

The swelling degrees of the gels containing different amounts of TA are shown in Fig. 4. As can be seen from Fig. 4, at the end of the first hour, G-0 had the highest swelling value, and as the amount of tannic acid in the gels increased, the swelling ratio of the samples decreased. This drop can be explained by the increase in crosslinking density due to the interaction between TA and G. At the end of the second hour, while the water holding capacity of the G-1 and G-3 gels continued to increase, no significant change was observed in the swelling value of the G-5 gel. The swelling value of the G-7 gel, however, continued to decrease. Notably, the swelling values of the G-0 and G-1 gels could not be measured after 2 and 3 hours, respectively. This is because G-0 gel dissolved in water while G-1 gel disintegrated into small pieces, probably due to insufficient crosslinking. At the end of the 24th hour, the swelling value of the G-3 gel reached its highest value, whereas the swelling value of the G-5 gel started to decrease. Then, the swelling values of both gels reached equilibrium within one week. Noteworthy is that the G-7 gel started to show a negative swelling value by the 24th hour, and then it began to gradually decline before reaching equilibrium. The swelling values of the G-7 gels at the end of 24, 28, 48, and 168 hours were found to be approximately -14, -15, -20, and -27 %, respectively.

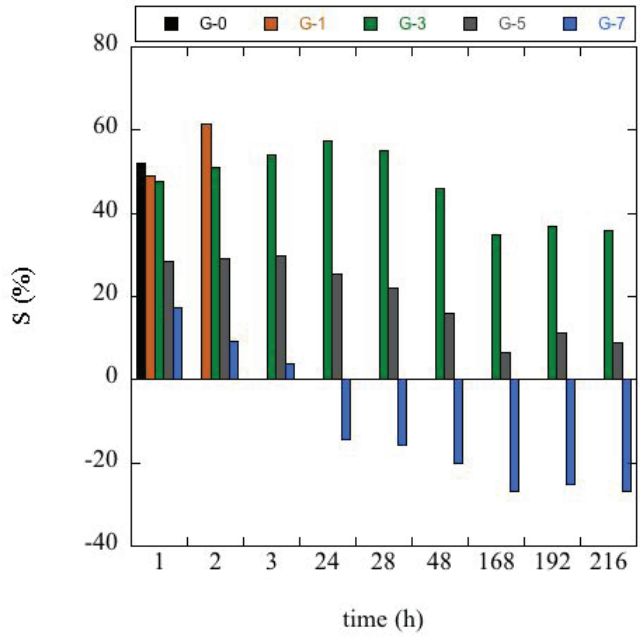

Figure 4. *Swelling degree of gels containing different concentration of TA*

A phenomenon known as "negative swelling" refers to the reduction in solid volume that occurs after solvent absorption. (Curatolo, 2018). It is a relatively uncommon event, and this is, to the best of my knowledge, the first success in achieving negative volume changes in composite materials made of gelatin. The reason for the negative swelling value seen in the G-7 gel can be explained by the high cross-linking reaction between the gel and TA. When G-7 gel is immersed in water, it shrinks, with most triple helix joints collapsed and more hydrogen bonds formed between gelatin and TA during the immersion time. Although this is the first report to show that gelatin-supported DES gel can have a negative degree of swelling, more research into how TA accomplishes this during the swelling process is needed.

It can be concluded that by varying the TA concentration, the swelling of Gel-based DES gels could be systematically controlled in the range of 0% to -27%. The suggested approach can be easily adapted to different biopolymers and DES to control the swelling of gels and improve their mechanical properties.

3.4. FTIR

The secondary structural changes in gelatin gels were investigated using FTIR analysis. The amide I region (1600–1700 cm^{-1}) was chosen because it gives information regarding the secondary structure of polypeptide chains (Owyeung, Sonkusale, & Panzer, 2020) (Fig. 5). The exact placement of the amide I is determined by hydrogen bonding and protein structural conformation (Peña-Rodriguez et al., 2015). Fig. 5 shows the FTIR spectra of neat and TA-gels in the amide I region. Previously, the broad signals in this band were attributed to both gelatin triple helices and nonhelical gelatin strands (Owyeung, Sonkusale, & Panzer, 2020). As can be seen in Fig. 5, all gels have broad spectra, showing the presence of both triple helix and random coil formations of gelatin within them. In addition, no significant variations in the position of amide I were identified, suggesting that the incorporation of TA into the gels has a minor effect on protein conformation.

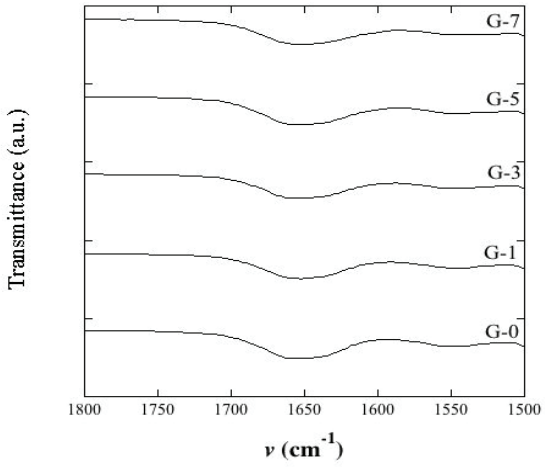

Figure 5. *FTIR spectra of the gels in the amide-I region*

3.5. Electrical study

As shown in Fig. 6, the conductivity of gels was significantly increased with the increase in concentration of TA from 0 wt.% to 3 wt.%. However, when the concentration of TA was further increased, the conductivity of gels decreased from 5.97 to 4.55 S cm^{-1}. This might be owing to the formation of less conductive pathways inside the gels with the increase in TA concentration. Wang et.,al (2021) reported that the conductivity of the WPU-DES gels decreased with increasing TA concentration. Thus, considering the ionic conductivity, the G-3 gel was chosen for the following studies. The next step involved investigating how sensitively G-3 gel can translate mechanical deformation into a change in resistance. The circuit of LED beads was used to demonstrate visually how the resistance of G-3 gel changed as the tensile strain increased. As illustrated in Fig. 7, the LED bead darkened steadily as the tensile strain of G-3 gel increased, revealing that the conductivity of G-3 gel was significantly reduced with the increase in tensile strain.

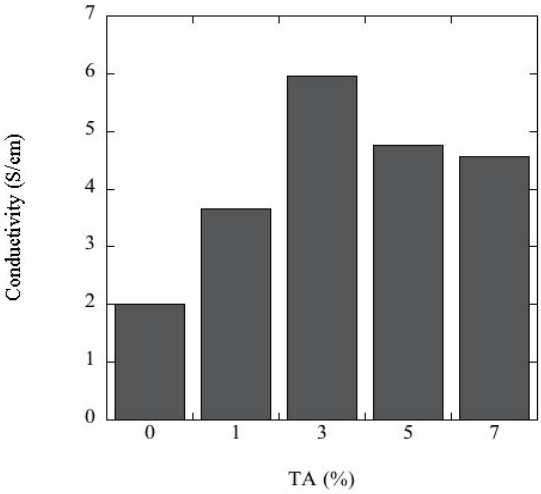

Figure 6. *Electrical conductivity of the gels with different TA concentration*

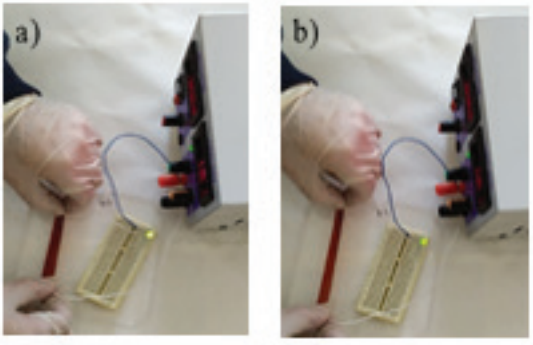

Figure 7. *Photographs of the changes of bulb brightness at different elongation a) unstreched b) stretched*

3.6. Tensile properties

Gels can be stretched or twisted easily, as shown in Fig. 8. The mechanical characteristics of gels with various TA loadings are shown in Fig. 9. When compared to a neat gel, adding TA to the gels greatly improved their mechanical properties. With increased TA loading, the gelatin-supported gels' Young's modulus and max stress (MS) improve, while the elongation at break decreases. The increase in MS might be related to the development of a more stable network because of interactions between gelatin and TA

(Peña, De La Caba, Eceiza, Ruseckaite, & Mondragon, 2010). As reported by other authors, for gelatin gels cross-linked with various aldehydes, ferrulic acid, glutaraldehyde, and TA, tensile strength increases, elongation at break decreases with an increase in the level of the cross-linking agent (Peña, De La Caba, Eceiza, Ruseckaite, & Mondragon, 2010).

The Young's modulus of the G-7 gel is 4.86 kPa, which is comparable to that of human skin, which ranges from 3 kPa to 7.7 MPa. However, it was found that its elongation at break value was 678 %, which is much higher than human skin (Wang et al., 2021). Because the gels are highly conformable when applied to or worn on the human body, their low Young's modulus and high strain make them perfect for ionic skin devices. (Qin, Owyeung, Sonkusale, & Panzer, 2019).

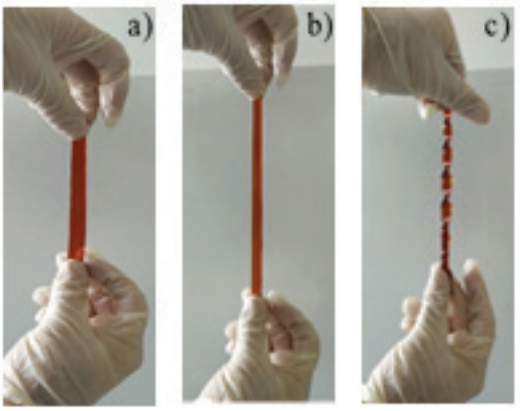

Figure 8. *Photographs of the mechanical performances of the G-3 gels. a) original gel, b) stretching, c) twisting*

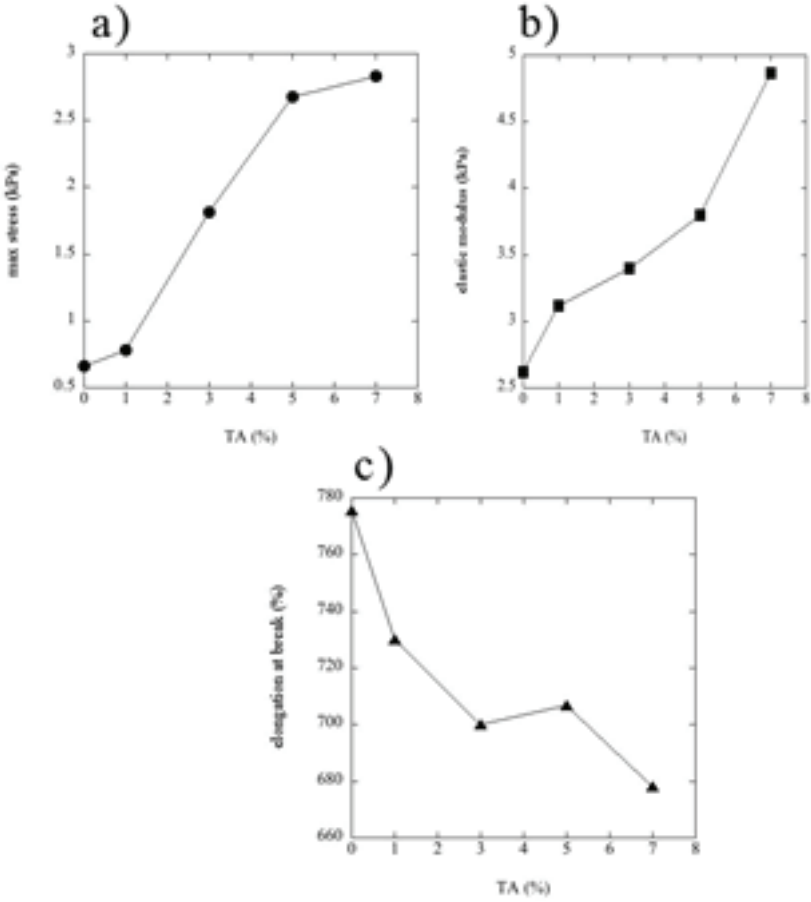

Figure 9. *Mechanical properties of the TA containing gels. a) Max stress, b) elastic modulus, c) elongation at break*

3.7. Release of TA

Fig. 10 shows the cumulative release of TA from the gels. The release of TA from the gels within the first 3 hours was rapid, and then it began to gradually decline before settling into equilibrium. After 168 hours, the amount of TA released from the G-1, G-3, G-5, and G-7 gels was found to be 58.03, 45.53, 43.64, and 36.50%, respectively. Results showed that as the amount of TA in the gel increased, the amount of TA released decreased. This can be explained by the fact that the more tannic acid there is, the more interaction/crosslinking there is between tannic acid and gelatin, thus resulting in less TA release. The amount of free TA extracted from the samples and the initial amount of TA added to the gels could be used to estimate the degree of crosslinking. (Leite et al., 2021). It was found that the highest degree of cross-linking (63.50%) was found in the G-7 gel.

Swelling behavior and TA release followed a similar trend in this study. A more compact gel structure is obtained as the amount of TA in the gel formulation rises, resulting in less TA release.

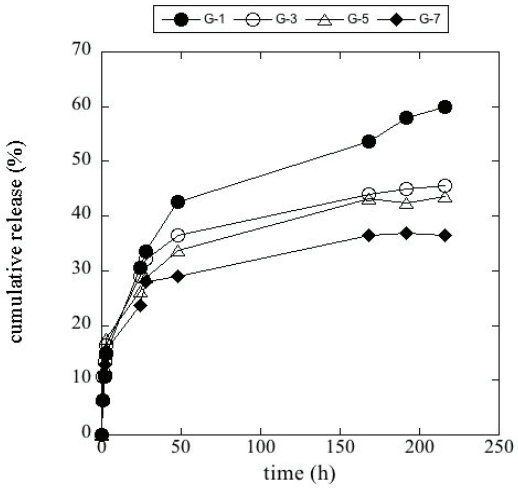

Figure 10. *Release of TA from gels*

The mechanism of TA release from gels was investigated by fitting the cumulative TA release data to kinetic models including zero-order, first-order, Higuchi, and Hixon-Crowell (Iftime et al., 2020). The obtained results are shown in Table 1. When the correlation coefficients (R^2) for the several release kinetic models were compared, it was clear that Higuchi's model best described the release kinetics. This indicates that the TA is dispersed uniformly throughout the matrix and that diffusion occurs solely in one direction from the insoluble matrix (Ninan, Forget, Shastri, Voelcker, & Blencowe, 2016). In addition, a close relationship was also found with the first order and the Hixson-Crovell model. According to the first-order model, release is dependent on the concentration of TA, and the Hixson-Crovell model suggests a change in the surface area and diameter of the gels (Merchant, Shoaib, Tazeen, & Yousuf, 2006).

Table 1. *Mathematical modelling of TA release from gels*

Kinetic model	R^2			
	G-1	**G-3**	**G-5**	**G-7**
Zero-order	0.9170	0.8336	0.8123	0.7702
First-order	0.9507	0.8754	0.8529	0.8025
Hixson-Crowell	0.9403	0.8619	0.8396	0.7918
Higuchi	0.9916	0.9583	0.9362	0.9144

4. Conclusions

Due to their numerous applications in soft robotics and healthcare, there is an increasing demand for devices that have sensory capabilities similar to those of human skin. Long-term use of hydrogel-based devices can be hampered by dehydration problems caused by the volatility of water, despite studies on ionically conductive hydrogels for wearable, flexible sensor applications. For "ionic skin" sensor applications, deep eutectic solvent gels have recently come to light as promising substitutes for ionic liquid- or water-based gels. The transparent, nonvolatile, and ionically conductive DES gels in this study were easily made by combining DES with gelatin and then going through a few quick heating and cooling steps. Interestingly, the DES gel containing 10% gelatin and 3% tannic acid displayed high stretchability and a room temperature ionic conductivity of 5.97 S cm^{-1}. This is likely due to intermolecular interactions between both DES components and the gelatin gels, which alter the biopolymer scaffold assembly in comparison to its hydrogel analogue.

The gels were also adhesive to various substrates, which made it possible to assemble them into a flexible epidermal sensor for prolonged human-machine interfacial contact without worrying about the use of external adhesive tapes. Additionally, since the prepared gels exhibit negative swelling behavior, the design of such systems may find use in other fields where targeted and extreme volume changes may be necessary, such as optical engineering and aerospace. This research is expected to offer a promising method for producing conductive hydrogels quickly for use in soft robotics, biomedical devices, and flexible electronic skin.

ACKNOWLEDGEMENTS

The author wishes to thank Associate Prof Dr. Ali Ekber Özdemir for helping with electrical measurements. Dr. Caner Şirin is thanked for his assistance with the photography.

REFERENCES

Chen, K., Hu, Y., Liu, M., Wang, F., Liu, P., Yu, Y., Xiao, X. (2021). Highly stretchable, tough, and conductive Ag@ Cu nanocomposite hydrogels for flexible wearable sensors and bionic electronic skins. *Macromolecular Materials and Engineering, 306*(10), 2100341.

Curatolo, M. (2018). Effective negative swelling of hydrogel-solid composites. *Extreme Mechanics Letters, 25*, 46-52.

Derkach, S., Voron'Ko, N., Kuchina, Y. A., Kolotova, D., Gordeeva, A., Faizullin, D., Makshakova, O. (2018). Molecular structure and properties of κ-carrageenan-gelatin gels. Carbohydrate Polymers, 197, 66-74.

Di, X., Kang, Y., Li, F., Yao, R., Chen, Q., Hang, C., Wu, G. (2019). Poly (N-isopropylacrylamide)/polydopamine/clay nanocomposite hydrogels with stretchability, conductivity, and dual light-and thermo-responsive bending and adhesive properties. *Colloids and Surfaces B: Biointerfaces, 177*, 149-159.

Fan, H., Wang, J., & Jin, Z. (2018). Tough, swelling-resistant, self-healing, and adhesive dual-cross-linked hydrogels based on polymer–tannic acid multiple hydrogen bonds. *Macromolecules, 51*(5), 1696-1705.

Gabriele, F., Chiarini, M., Germani, R., Tiecco, M., & Spreti, N. (2019). Effect of water addition on choline chloride/glycol deep eutectic solvents: Characterization of their structural and physicochemical properties. *Journal of Molecular Liquids, 291*, 111301.

Gomes, J. M., Silva, S. S., & Reis, R. L. (2019). Biocompatible ionic liquids: fundamental behaviours and applications. *Chemical Society Reviews, 48*(15), 4317-4335.

Iftime, M. M., Dobreci, D. L., Irimiciuc, S. A., Agop, M., Petrescu, T., & Doroftei, B. (2020). A theoretical mathematical model for assessing diclofenac release from chitosan-based formulations. *Drug Delivery, 27*(1), 1125-1133.

Joos, B., Vranken, T., Marchal, W., Safari, M., Van Bael, M. K., & Hardy, A. T. (2018). Eutectogels: a new class of solid composite electrolytes for Li/Li-ion batteries. *Chemistry of Materials, 30*(3), 655-662.

Joos, B., Volders, J., da Cruz, R. R., Baeten, E., Safari, M., Van Bael, M. K., & Hardy, A. T. (2020). Polymeric backbone eutectogels as a new generation of hybrid solid-state electrolytes. Chemistry of Materials, 32(9), 3783-3793.

Leite, L. S. F., Pham, C., Bilatto, S., Azeredo, H. M., Cranston, E. D., Moreira, F. K.,Bras, J. (2021). Effect of tannic acid and cellulose nanocrystals on antioxidant and antimicrobial properties of gelatin films. *ACS Sustainable Chemistry & Engineering, 9*(25), 8539-8549.

Merchant, H. A., Shoaib, H. M., Tazeen, J., & Yousuf, R. I. (2006). Once-daily tablet formulation and in vitro release evaluation of cefpodoxime using hydroxypropyl methylcellulose: a technical note. *AAPS PharmSciTech, 7*(3), E178-E183.

Ninan, N., Forget, A., Shastri, V. P., Voelcker, N. H., & Blencowe, A. (2016). Antibacterial and anti-inflammatory pH-responsive tannic acid-carboxylated agarose composite hydrogels for wound healing. *ACS Applied Materials & Interfaces, 8*(42), 28511-28521.

Owyeung, R. E., Sonkusale, S. R., & Panzer, M. J. (2020). Influence of hydrogen bond donor identity and intentional water addition on the properties of gelatin-supported deep eutectic solvent gels. *The Journal of Physical Chemistry B, 124*(28), 5986-5992.

Peña, C., De La Caba, K., Eceiza, A., Ruseckaite, R., & Mondragon, I. (2010). Enhancing water repellence and mechanical properties of gelatin films by tannin addition. *Bioresource Technology, 101*(17), 6836-6842.

Peña-Rodriguez, C., Martucci, J. F., Neira, L. M., Arbelaiz, A., Eceiza, A., & Ruseckaite, R. A. (2015). Functional properties and in vitro antioxidant and antibacterial effectiveness of pigskin gelatin films incorporated with hydrolysable chestnut tannin. *Food Science and Technology International, 21*(3), 221-231.

Qin, H., Owyeung, R. E., Sonkusale, S. R., & Panzer, M. J. (2019). Highly stretchable and nonvolatile gelatin-supported deep eutectic solvent gel electrolyte-based ionic skins for strain and pressure sensing. *Journal of Materials Chemistry C, 7*(3), 601-608.

Qin, Z., Dong, D., Yao, M., Yu, Q., Sun, X., Guo, Q., Li, J. (2019). Freezing-tolerant supramolecular organohydrogel with high toughness, thermoplasticity, and healable and adhesive properties. *ACS Applied Materials & Interfaces, 11*(23), 21184-21193.

Takada, A., & Kadokawa, J.-i. (2015). Fabrication and characterization of polysaccharide ion gels with ionic liquids and their further conversion into value-added sustainable materials. *Biomolecules, 5*(1), 244-262.

Türe, H. (2019). Characterization of hydroxyapatite-containing alginate–gelatin composite films as a potential wound dressing. *International Journal of Biological Macromolecules, 123*, 878-888.

Wang, S., Cheng, H., Yao, B., He, H., Zhang, L., Yue, S., Ouyang, J. (2021). Self-adhesive, stretchable, biocompatible, and conductive nonvolatile eutectogels as wearable conformal strain and pressure sensors and biopotential electrodes for precise health monitoring. *ACS Applied Materials & Interfaces, 13*(17), 20735-20745.

Yamagata, M., Soeda, K., Ikebe, S., Yamazaki, S., & Ishikawa, M. (2013). Chitosan-based gel electrolyte containing an ionic liquid for high-performance nonaqueous supercapacitors. *Electrochimica Acta, 100*, 275-280.

Zhao, L., Ren, Z., Liu, X., Ling, Q., Li, Z., & Gu, H. (2021). A multifunctional, self-healing, self-adhesive, and conductive sodium alginate/poly (vinyl alcohol) composite hydrogel as a flexible strain sensor. *ACS Applied Materials & Interfaces, 13*(9), 11344-11355.

CHAPTER 2

RENEWABLE ENERGY RESOURCES AND MITIGATING THE ENERGY CRISIS

Yasin Furkan GORGULU[1]

1 Assistant Prof. Dr., Isparta University of Applied Sciences, Department of Machinery and Metal Technologies, ORCID: 0000-0002-1828-2849, yasingorgulu@isparta.edu.tr

INTRODUCTION

Every facet of development, prosperity, health, nutrition, infrastructure, and education depends on energy. Our civilization depends on energy as one of its fundamental needs, thus its supply should be sufficient and safe (Poudyal, Loskot, Parajuli, & Khadka, 2019). Many development indicators are strongly correlated with the amount of energy consumed per capita. Enhanced global action is also needed to address emissions issues. The most conventional energy source is a fossil fuel, but using it can be dangerous since when economies expand, greenhouse gas emissions rise along with it. The use of fossil fuels also produces a vast amount of harmful waste that affects all other forms of life. There are transitions between energy, water, food, soil, and climate, and they are all interconnected. It can be handled transitions and identify synergies between them thanks to these relationships. Any component that is under pressure will also have an impact on other components. Our natural environment's basic resources energy, water, food, soil, and climate support our quality of life. Globally, there is more competition for these resources, which is made worse by climate change. Enhancing resource usage efficiency will be necessary to ensure resource availability. At the national and international levels, several policies and initiatives are addressed (Ambika et al., 2022; Gorgulu, 2022).

The world's energy need is increasing day by day in parallel with the increase in population and the development of technology. The limited use of fossil fuels and the harms of their use in obtaining energy are driving the world to use alternative energy sources. Although the trend is towards renewable energy sources and less harmful sources, it seems that this has not yet replaced fossil fuels. To achieve this, studies are continuing on new-generation energy production technologies and how to increase the performance of existing energy production resources. Significant decarbonization of the energy system is needed to combat climate change (Ambika et al., 2022; Fawzy, Osman, Doran, & Rooney, 2020; Gorgulu, 2022). However, aspects of the energy system, such as long-term changes in climatic parameters, instability, and extreme weather conditions (Ambika et al., 2022; Field et al., 2014), frequently have an impact on climate change itself. Real global challenges like energy security and climate change are influencing public policy discussions all across the world. Reviewing the literature measuring effects and assessing how this data is utilized to construct models of energy systems is essential in this dynamic field of study that is always evolving. Utilizing many energy sources has always been crucial to the survival of humans and the development of civilization. Prehistoric people relied on food and fire produced from the burning of dry material as their main sources of energy for nearly 500,000 years. Fire was utilized for more than just heating and lighting; it also served as a source of

fuel for cooking and the primary defense against the elements. Later, when people began to invest their resources in the creation of new land, energy utilization also advanced. As a result, the energy era, which began with fire and firewood and progressed to innovations in food energy production, has been a significant step toward the development of civilization and urbanization. During this period, biomass sources such as fire and wood were both recognized as renewable. Additionally, James Watt's steam engine enabled the industrial revolution to take off in the seventeenth and early eighteenth centuries by utilizing non-renewable energy sources like "fossil fuels," mainly natural gas, oil, and coal. From an energy viewpoint, fossil fuels have been one of the main forces behind economic growth in the twenty-first century. However, since the start of the industrial revolution, the intensive use of fossil fuels has led to several significant environmental issues, such as air pollution, photochemical smog, and global warming, all of which have been well documented in the scientific literature. It is a known truth that events leading to unfavorable changes in the environment would precipitate a cascade with a considerable impact on human civilization and the economy if the rise in greenhouse gas emissions is not reversed. The ongoing rise in energy demand and environmental degradation has prompted efforts to find sustainable and alternative energy sources. Many nations throughout the world are already working to develop the materials and methods necessary for the effective use of alternative fuel sources. These advanced or unconventional fuels, usually referred to as alternative fuels, are substances that can be utilized as fuels in place of traditional fuels. Oil, coal, propane, and natural gas all fall within the standard definition of fuel, which also includes nuclear elements like uranium. Alternatives include non-fossil fuels like biodiesel, bioethanol (ethanol, methanol), hydrogen, chemically stored energy (batteries, fuel cells), non-fossil natural gas, non-fossil methane, and vegetable oils. According to a current study, 23% of the world's anthropogenic greenhouse gas emissions are caused by forestry, livestock, and other land-based activities. These emissions are caused by changes in land use, such as deforestation, which makes room for industries, farms, and other buildings. The destruction of peatlands, other land resources, and human-led agriculture account for another 44% of the powerful greenhouse gas methane (IPCC, 2019).

As energy contributes to over 60% of global emissions, managing energy emissions is essential to achieving climate reduction targets (Baumert, Herzog, & Pershing, 2005). Additionally, energy management serves as a strategic foreign policy not just from a local standpoint (Giddens, 2009). Climate change will undoubtedly influence the energy industry, but actions enacted to combat it are anticipated to have immediate and possibly larger repercussions. Modern energy policy, renewable resource use, and energy

conservation are all aspects of climate change that eventually support economic expansion.

RENEWABLE ENERGY SOURCES

Because it will be accessible as long as the sun shines, solar energy is referred to be renewable or sustainable energy. It is predicted that the sun's main stage will continue to exist for another 4 to 5 billion years. Insolation is the name for the electromagnetic radiation that comes from the sun. Wind, bioenergy, geothermal, hydro, tides, and waves are some of the other primary renewable energy sources. The uneven heating of the Earth's surface caused by greater heat entering near the equator, together with the concomitant movement of water and thermal energy through evaporation and precipitation, is the source of wind energy. In this sense, solar energy is stored in rivers and dams that produce hydroelectricity. The third significant use of solar energy is the photosynthesis process, which turns solar energy into biomass. Solar energy is used to produce animal products like biogas from manure and oil from animal fat. Geothermal energy is another type of renewable energy that is produced by the Earth's internal heat produced by radioactive particle decay and by gravitational leftover heat from the Earth's creation. Volcanoes are blazing instances of how hotter-than-surface geothermal energy may travel from the deep to the surface. The gravitational contact between the Earth and the moon is what produces most of the tidal energy. In total, 14% of the world's energy is produced by bioenergy, largely using wood and charcoal for cooking and some heating but also using agricultural waste and even animal manure. In poorer nations, this adds to deforestation and soil erosion. Nowadays, notably in Brazil and the United States, the production of ethanol from biomass contributes to the supply of liquid fuels for transportation. Fossil fuels, on the other hand, are the accumulated sun energy of earlier geological eras. Even if there is a lot of oil, gas, and coal, it is limited, and it cannot be sustained for a long period (Nelson, 2011).

Hydro Power

Hydroelectric energy is a form of energy that utilizes the movement of water to generate electricity. This energy is produced in facilities that are based on dams and tunnels. Worldwide, hydroelectric energy accounts for approximately 16% of installed power capacity and roughly 70% of electricity production (International Energy Agency (IEA), 2021b) The largest hydroelectric energy producers include China, Canada, Brazil, Russia, and Norway. These countries carry out a significant portion of hydroelectric energy production worldwide (Office of Energy Efficiency & Renewable Energy, 2021c). Hydroelectric energy is considered an environmentally

friendly energy source. This is because it utilizes a natural process, the movement of water, and therefore does not emit carbon (Union of Concerned Scientists, 2021a). Additionally, hydroelectric energy is a long-lasting energy source and can produce electricity for many years. However, hydroelectric energy production can also have some environmental impacts. For example, the construction of dams can affect natural water flows and disrupt water movements (Union of Concerned Scientists, 2021a). Also, the construction of dams can lead to the destruction of natural habitats. Therefore, hydroelectric energy production should be carefully planned concerning environmental impacts. Hydroelectric energy is a significant energy source worldwide. It is considered an environmentally friendly energy source, but its production process should also consider environmental impacts. Therefore, the planning and implementation of hydroelectric energy production should become a part of environmental and energy policies.

Solar Energy

Solar energy is the energy that is harnessed from the sun's rays. This energy is generally captured using solar panels, which convert sunlight into electricity. Worldwide, solar energy accounts for approximately 1% of installed power capacity and is expected to grow rapidly in the coming years (International Energy Agency (IEA), 2021d). The largest solar energy producers include China, the United States, India, Japan, and Germany. These countries carry out a significant portion of solar energy production worldwide (Office of Energy Efficiency & Renewable Energy, 2021d). Solar energy is considered an environmentally friendly energy source. This is because it utilizes a renewable energy source, the sun, and therefore does not emit carbon (Union of Concerned Scientists, 2021b). Additionally, solar energy is a clean energy source that does not produce any air or water pollution. However, the production and disposal of solar panels can have some environmental impacts. For example, the manufacturing of solar panels requires the use of toxic chemicals and generates hazardous waste (Union of Concerned Scientists, 2021b). Also, the disposal of solar panels can be a challenge as they contain toxic materials and need to be recycled properly. Therefore, solar energy production should be carefully planned about environmental impacts. Solar energy is a rapidly growing energy source worldwide.

Wind Energy

Wind energy is the energy that is harnessed from the wind. This energy is captured using wind turbines, which convert the kinetic energy of the wind into electricity. Worldwide, wind energy accounts for approximate-

ly 7% of installed power capacity and is expected to grow rapidly in the coming years (IRENA, 2021c). The largest wind energy producers include China, the United States, Germany, India, and Spain. These countries carry out a significant portion of wind energy production worldwide (Office of Energy Efficiency & Renewable Energy, 2021e). Wind energy is known as an environmentally friendly energy source. This is because it utilizes a renewable energy source, wind, and therefore does not emit carbon (World Wildlife Fund (WWF), 2021b). Additionally, wind energy is a clean energy source that does not produce any air or water pollution. However, the construction and maintenance of wind turbines can have some environmental impacts. For example, the construction of wind turbines can affect wildlife and their habitats, particularly birds and bats (World Wildlife Fund (WWF), 2021b). Also, the maintenance of wind turbines can cause noise pollution and visual impact in some cases.

Geothermal Energy

Geothermal energy is the energy that is harnessed from the Earth's heat. This energy is captured using geothermal power plants, which convert the heat energy from the Earth's interior into electricity. Worldwide, geothermal energy accounts for approximately 3% of installed power capacity and has the potential to grow in the coming years (Geo Energy, 2023). The largest geothermal energy producers include the United States, the Philippines, Indonesia, Mexico, and Iceland. These countries carry out a significant portion of geothermal energy production worldwide (Office of Energy Efficiency & Renewable Energy, 2021b). Geothermal energy is considered an environmentally friendly energy source. This is because it utilizes a renewable energy source, the Earth's heat, and therefore does not emit carbon (EIA, 2021). Additionally, geothermal power plants emit low levels of greenhouse gases and air pollutants. However, the construction and maintenance of geothermal power plants can have some environmental impacts. For example, the construction of geothermal power plants can affect the local ecosystems and the use of water resources (EIA, 2021). Also, the maintenance of geothermal power plants can cause noise pollution and visual impact in some cases.

Biomass

Biomass energy is the energy that is harnessed from organic materials such as plants, wood, and waste. This energy is captured using various technologies, such as combustion and gasification, which convert biomass into heat, electricity, or liquid fuels. Worldwide, biomass energy accounts for approximately 10% of installed power capacity and is expected to grow in the coming years (International Energy Agency (IEA), 2021a).

The largest biomass energy producers include the United States, Brazil, China, Germany, and Canada. These countries carry out a significant portion of biomass energy production worldwide (Office of Energy Efficiency & Renewable Energy, 2021a). Biomass energy is considered an environmentally friendly energy source. This is because it utilizes a renewable energy source, organic materials, and can reduce the amount of waste in landfills (Food and Agriculture Organization (FAO), 2021). Additionally, when sustainably managed, biomass energy can have a lower carbon footprint than fossil fuels. However, the production and use of biomass energy can also have some environmental impacts. For example, the production of biomass energy can lead to deforestation and habitat destruction if not sustainably managed (Food and Agriculture Organization (FAO), 2021). Also, the transportation and processing of biomass can contribute to air and water pollution. Therefore, biomass energy production should be carefully planned with regard to environmental impacts.

Tidal Energy

Tidal energy is the energy that is harnessed from the tidal movements caused by the gravitational pull of the moon and the sun on the Earth's oceans. This energy is usually captured using tidal turbines, which convert the kinetic energy of the tides into electricity. Worldwide, tidal energy accounts for a small portion of installed power capacity but has the potential to grow in the coming years (IRENA, 2021b). The largest tidal energy producers include France, Canada, China, the United Kingdom, and South Korea. These countries carry out a significant portion of tidal energy production worldwide (Office of Energy Efficiency & Renewable Energy, 2021e). Tidal energy is considered an environmentally friendly energy source. This is because it utilizes a renewable energy source, the tides, and therefore does not emit carbon (World Wildlife Fund (WWF), 2021a). Additionally, tidal power plants emit low levels of greenhouse gases and air pollutants. However, the construction of tidal power plants can affect the local ecosystems and the use of water resources (World Wildlife Fund (WWF), 2021a). Also, the maintenance of tidal power plants can cause noise pollution and visual impact in some cases.

MITIGATING THE ENERGY CRISIS

The energy crisis refers to the growing demand for energy and the limited availability of non-renewable energy sources such as fossil fuels. This crisis has led to increasing concerns about energy security, environmental degradation, and economic instability. The causes of the energy crisis are multifaceted and include increasing population, economic growth, urbanization, and industrialization. One major cause of the energy crisis

is the increasing population. As the global population continues to grow, so does the energy demand. According to the United Nations (UN, 2022), the world's population is expected to reach 9.7 billion by 2050, which will lead to an increased demand for energy for basic needs such as heating, lighting, and transportation.

Another major cause of the energy crisis is economic growth. Economic growth is often associated with increased energy consumption. As countries continue to develop and industrialize, the demand for energy increases. According to the International Energy Agency (International Energy Agency (IEA), 2022), the global energy demand is expected to increase by 30% by 2040, due to economic growth and population growth.

Urbanization is also a significant cause of the energy crisis. Urbanization leads to an increase in energy consumption, as more people move into cities and require energy for transportation, heating, and cooling. According to the United Nations (UN, 2022), urbanization is expected to continue and by 2050, 68% of the world's population will live in urban areas. Some reasons affecting the energy crisis are given in Figure 1 (Poudyal et al., 2019).

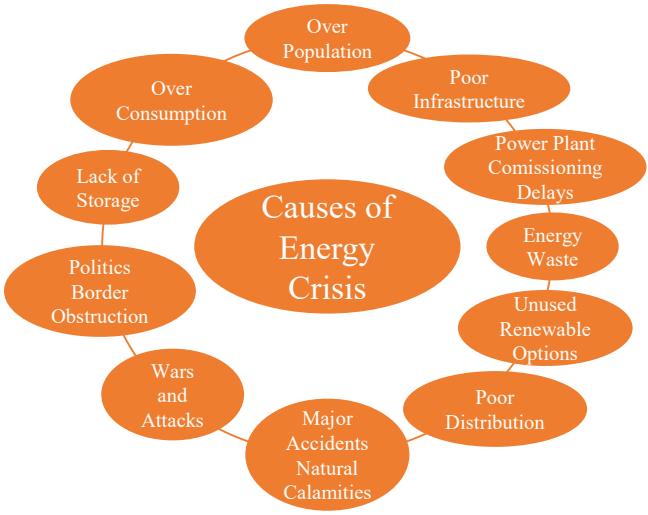

Figure 1. *Causes of energy crisis.*

By expanding the supply of clean, sustainable, and dependable energy, renewable energy sources including solar, wind, hydro, geothermal, biomass, and tidal energy provide a workable answer to the energy dilemma. One of the most promising renewable energy sources is solar energy. It might help the world satisfy a sizable amount of its energy needs while reducing reliance on fossil fuels. The International Energy Agency (International Energy Agency (IEA), 2021c) estimates that by 2050, solar energy might meet up to 16% of the world's electricity needs. Additionally, using

solar energy helps lessen greenhouse gas emissions and the effects of climate change.

Another promising renewable energy source is wind energy. It is regarded as one of the energy sources with the highest cost competitiveness and the fastest rate of growth. The International Renewable Energy Agency (IRENA, 2021a) estimates that by 2050, wind energy might meet up to 18% of the world's electricity needs. Additionally, using wind energy helps lessen greenhouse gas emissions and the effects of climate change.

One of the dependable and sustainable renewable energy sources is hydroelectricity. The International Energy Agency (International Energy Agency (IEA), 2021c) estimates that hydroelectric energy already makes for around 16% of installed power capacity and nearly 70% of the world's electricity output. Utilizing hydroelectric power can lessen the effects of climate change and minimize greenhouse gas emissions.

Geothermal energy is a reliable and sustainable energy source that can provide baseload power. According to the Geothermal Energy Association (Geo Energy, 2023), geothermal energy already accounts for approximately 3% of installed power capacity worldwide and has the potential to grow in the coming years. Utilizing geothermal energy can also lessen greenhouse gas emissions and climate change's effects.

Biomass energy is also a significant and versatile energy source that can provide baseload power. According to the International Energy Agency (International Energy Agency (IEA), 2021c), biomass energy already accounts for approximately 10% of installed power capacity worldwide and is expected to grow in the coming years. The use of biomass energy can also help to reduce the amount of waste in landfills and mitigate the impacts of climate change if sustainably managed.

Finally, by increasing the supply of clean, sustainable, and dependable energy, renewable energy sources like solar, wind, hydro, geothermal, and biomass offer a workable answer to the energy dilemma. Utilizing these energy sources can lessen the effects of climate change and greenhouse gas emissions. Therefore, in order to alleviate the energy crisis and provide energy security, environmental sustainability, and economic stability, it is imperative to invest in the research and implementation of renewable energy technologies.

CONCLUSION

By increasing the supply of clean, sustainable, and dependable energy, renewable energy sources like solar, wind, hydro, geothermal, biomass, and tidal offer a workable answer to the energy dilemma. Utilizing these energy sources can lessen the effects of climate change and greenhouse gas emissions. The potential of these renewable energy sources is significant and can contribute a large portion of the global electricity demand by 2050. However, it is crucial to invest in the development and deployment of renewable energy technologies and ensure the sustainable management of these resources to mitigate the energy crisis and ensure energy security, environmental sustainability, and economic stability. It is also essential to have policies and regulations in place that support the development and implementation of renewable energy projects. The shift towards renewable energy sources is an important step toward a sustainable future and it is necessary to take action now to ensure a secure energy supply for future generations.

REFERENCES

Ambika, Jadhav, S. K., Agrawal, S., Koreti, D., Ahmad, F., Kosre, A., … Yadav, K. (2022). Energy Crises, Challenges and Solutions. In P. Singh, S. Singh, G. Kumar, & P. Baweja (Eds.), *Wiley Blackwell*.

Baumert, K. A., Herzog, T., & Pershing, J. (2005). Navigating the numbers. In *Greenhouse Gas Data and International Climate Policy*.

EIA. (2021). Geothermal Power. Retrieved from www.eia.gov/energyexplained/renewables/geothermal-power.php

Fawzy, S., Osman, A. I., Doran, J., & Rooney, D. W. (2020). Strategies for mitigation of climate change: a review. *Environmental Chemistry Letters*, *18*(6), 2069–2094. https://doi.org/10.1007/s10311-020-01059-w

Field, C. B., Barros, V. R., Mach, K. ., Mastrandrea, M. D., Aalst, M. van, Adger, W. N., … Yohe, G. W. (2014). Technical Summary. In *Climate Change 2014: Impacts, Adaptation, and Vulnerability. Part A: Global and Sectoral Aspects. Contribution of Working Group II to the Fifth Assessment Report of the Intergovernmental Panel on Climate Change*.

Food and Agriculture Organization (FAO). (2021). Biomass Energy. Retrieved from www.fao.org/biomass/biomass-energy/en/

Geo Energy. (2023). Geothermal Energy. Retrieved January 22, 2023, from https://www.geo-energy.org/geothermal-energy/

Giddens, A. (2009). The Politics of Climate Change. In *Environmental Politics* (1st ed.). Polity Press. https://doi.org/10.1080/09644019308414108

Gorgulu, Y. F. (2022). Enerji Krizi ve Yenilenemez Enerji Kaynakları. In C. Karaman (Ed.), *Teknobilim-2022 Enerji Krizi ve Yenilenebilir Enerji* (1st ed., pp. 7–18). İstanbul: Efe Akademi Yayınları.

International Energy Agency (IEA). (2021a). Biomass for Power and Heat. Retrieved from www.iea.org/reports/biomass-for-power-and-heat

International Energy Agency (IEA). (2021b). Hydropower Status Report 2021. Retrieved from https://www.iea.org/reports/global-hydropower-status-report-2021

International Energy Agency (IEA). (2021c). Renewable Energy Progress 2020. Retrieved from www.iea.org/reports/renewable-energy-progress-2020

International Energy Agency (IEA). (2021d). Solar Power. Retrieved from www.iea.org/topics/renewables/subtopics/solar-power

International Energy Agency (IEA). (2022). *World Energy Outlook 2022*.

IPCC. (2019). *Special Report: The Ocean and Cryosphere in a Changing Climate*. https://doi.org/https://www.ipcc.ch/report/srocc/

IRENA. (2021a). Global Renewable Energy Outlook 2021. Retrieved from www.irena.org/global-outlook

IRENA. (2021b). Tidal Power. Retrieved from www.irena.org/tidal-power

IRENA. (2021c). Wind Energy. Retrieved January 22, 2023, from https://www.irena.org/Energy-Transition/Technology/Wind-energy

Nelson, V. (2011). *Introduction to Renewable Energy* (A. Ghassemi, Ed.). CRC Press.

Office of Energy Efficiency & Renewable Energy. (2021a). Bioenergy Technologies Office. Retrieved January 22, 2023, from https://www.energy.gov/eere/bioenergy/bioenergy-technologies-office

Office of Energy Efficiency & Renewable Energy. (2021b). Geothermal Technologies Office. Retrieved from www.energy.gov/eere/geothermal/geothermal-technologies-office

Office of Energy Efficiency & Renewable Energy. (2021c). Hydropower Program. Retrieved January 22, 2023, from https://www.energy.gov/eere/water/hydropower-program

Office of Energy Efficiency & Renewable Energy. (2021d). Solar Energy Technologies Office. Retrieved January 22, 2023, from https://www.energy.gov/eere/solar/solar-energy-technologies-office

Office of Energy Efficiency & Renewable Energy. (2021e). Wind and Water Power Technologies Office. Retrieved from www.energy.gov/eere/wind/wind-and-water-power-technologies-office

Poudyal, R., Loskot, P., Parajuli, R., & Khadka, S. K. (2019). Mitigating the current energy crisis in Nepal with renewable energy sources. *Renewable and Sustainable Energy Reviews*, *116*(April), 109388. https://doi.org/10.1016/j.rser.2019.109388

UN. (2022). World Population Prospects - Population Division. Retrieved January 22, 2023, from https://population.un.org/wpp/

Union of Concerned Scientists. (2021a). The Environmental Impact of Hydroelectric Power. Retrieved from www.ucsusa.org/clean-energy/renewable-energy/environmental-impacts-of-hydroelectric-power

Union of Concerned Scientists. (2021b). The Environmental Impact of Solar Power. Retrieved from www.ucsusa.org/clean-energy/solar-power/environmental-impacts-of-solar-power

World Wildlife Fund (WWF). (2021a). Tidal Energy. Retrieved from www.worldwildlife.org/industries/tidal-energy

World Wildlife Fund (WWF). (2021b). Wind Energy. Retrieved from www.worldwildlife.org/industries/wind-energy

CHAPTER 3

HEATING MODES OF SOLAR ASSISTED HEAT PUMPS

Kutbay SEZEN[1]

1 Öğr. Gör. Dr.; Alanya Alaaddin Keykubat Üniversitesi Alanya Ticaret ve Sanayi Odası Meslek Yüksekokulu Elektrik ve Enerji Bölümü İklimlendirme ve Soğutma Teknolojisi Programı. kutbaysezen@gmail.com ORCID No: 0000-0003-1018-5793

INTRODUCTION

The energy demand of mankind has increased rapidly with industrialization and the increasing population and urbanization, and unfortunately at the present time, this need is met by 80% non-environmentally friendly fossil resources (Buker, and Riffat, 2016:399). The use of fossil resources poses a threat to sustainable world by causing the rapid depletion of these limited resources, as well as global warming due to high greenhouse gas emissions. According to the International Energy Agency, CO2 emissions from fossil fuel combustion increased 37% from 1990 to 2021, and this increase is projected to reach 42% by 2040 (EIA, 2022). The energy need of buildings accounts for 40% of the world's total energy demand, and heating accounts for at least half of this demand in industrialized countries, depending on climatic conditions. For example, the share of heating in building energy demand is 55% in the USA, 70% in China and 80% in Europe (Cao vd., 2016:198). Heat pumps, which are energy efficient and environmentally friendly heating systems, stand out as suitable systems that can meet the high heating demands of buildings, moreover these systems can be assisted by solar energy with different configurations (Sezen vd., 2021:146362).

In the literature, solar assisted heat pumps (SAHP) are divided into basic classes and subclasses considering their structures. In this study, besides these classifications, the operating modes of SAHP systems are explained and the limitations on the operating conditions of the systems are revealed.

Solar assisted heat pump (SAHP) systems classification

SAHP systems are divided into two basic classes according to whether the heat gained by solar collectors is transferred directly or indirectly to the heat pump refrigerant cycle (Sezen ve Gungor, 2023:424). In indirect expansion solar assisted heat pump (IDX-SAHP) systems, the heat transmitter fluid, which is mostly a water antifreeze solution, provides heat transfer between the collector and the heat pump evaporator. In direct expansion solar assisted heat pump (DX-SAHP) systems, no intermediary is used for the transfer of the heat gained, and the refrigerant circulates in the collector and evaporates directly with the heat taken from the air and the sun. IDX-SAHP systems are subdivided into series, parallel and dual source, depending on their construction and equipment, which allows switching between different heating modes. In DX-SAHP systems, on the other hand, since there is no optional heating mode option, sub classifications are not generally made in the literature. Illustration of operating diagrams of SAHPs are given in Figure 1.

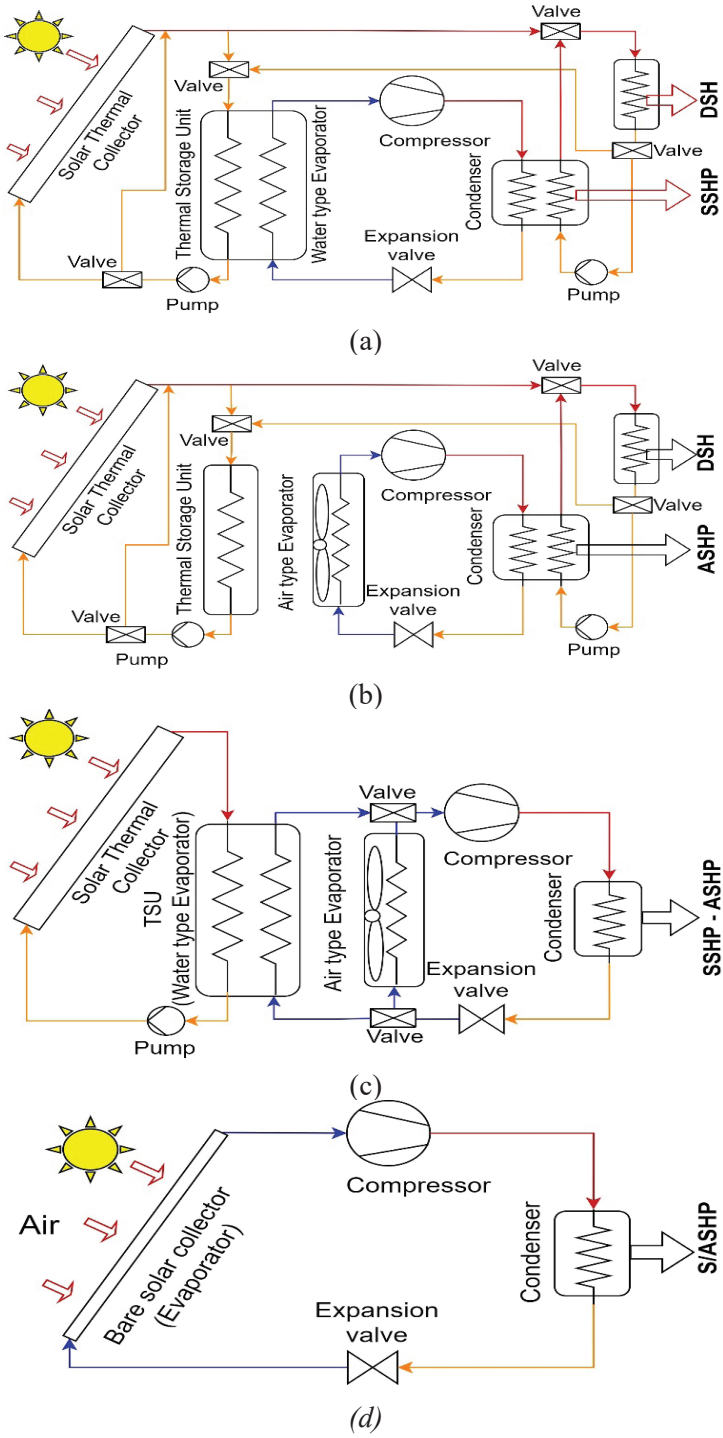

Figure 1: *Illustration of Operating Diagrams of SAHPs; (a) Series IDX-SAHP, (b) Parallel IDX-SAHP, (c) Dual Source IDX-SAHP, (d) DX-SAHP*

Heating modes of SAHPs

In SAHP systems, heating can be provided by means of a heat pump or directly by solar energy. In the case of using a heat pump, the heat source used may vary according to ambient conditions or user preference.

In direct solar heating (DSH) mode, the heat collected by the collectors is transferred to the indoor heat exchanger with a heat transmitter fluid, and heating is performed. With the use of a heat storage tank, the heat stored throughout the day can be used for a short time at a high rate. The high collector temperature values required to use this mode can be achieved with only high solar irradiation and low heat loss to ambient.

In solar source heat pump (SSHP) mode, the heat pump supplies the heating need by using the solar as the heat source in the evaporator. In IDX-SAHP systems, the heat absorbed from the solar by the collector is transferred with the heat transmitter fluid to a heat storage tank in which a liquid type evaporator is placed. In this insulated heat storage tank, if the heat requirement of the evaporator can be adequately met by the solar, the evaporation temperature can be kept above the value that the air heat source can provide. Therefore, it should be kept in mind that in the absence of solar irradiation, the temperature of the insulated tank may drop excessively with the evaporation of the refrigerant, and cause a dramatic performance loose.

Solar/air source heat pump (S/ASHP) mode is possible for DX-SAHP systems with a bare evaporator-collector structure. If the temperature of the bare solar collector, which acts as an evaporator, remains below the air temperature, there will be heat gain from the air as well as solar and the heat pump operates as double source. If the collector rises above the ambient temperature with the increase in solar irradiation, the system will start to operate in SSHP mode and heat loss will occur from the bare surface to the air. For this reason, in night conditions, the system works in ASHP mode with a flat air-type evaporator.

In IDX-SAHP systems, heating can be provided by air source heat pump (ASHP) mode at night or in cloudy weather conditions with low or no solar radiation. With the conventional air source evaporator added to the system and the valve-pipe systems where the refrigerant circulation direction can be changed optionally, the system can switches from the solar type evaporator to the air type evaporator. The ASHP mode may also allow time for the solar collector system to store enough heat for the use of solar heating modes. Heating modes allowed by SAHP types are given in Table 1.

Table 1: *Heating Modes of SAHP Types*

	Heating Modes			
SAHP type	DSH	SSHP	S/ASHP	ASHP
Series IDX-SAHP	X	X		
Parallel IDX-SAHP	X			X
Dual source IDX-SAHP		X		X
DX-SAHP		X	X	X

CONCLUSION

In this study, besides the structural classification of SAHP systems, the heating modes that the systems allow are defined and explained. The required high temperatures for DSH can be achieved only at high solar irradiations with low heat loss from collector. The SSHP mode is advantageous over the ASHP mode only if the evaporator placed in the insulated heat tank provides a higher evaporation temperature than the air can supply. DX-SAHP systems automatically switch between S/ASHP, SSHP and ASHP modes depending on whether the collector temperature due to radiation is higher or lower than the ambient air temperature.

REFERENCES

Buker, M. S., and Riffat, S. B. (2016). Solar assisted heat pump systems for low temperature water heating applications: A systematic review. *Renewable and Sustainable Energy Reviews*, (55), 399-413.

Cao, X., Xilei, D., and Liu, J. (2016). Building energy-consumption status worldwide and the state-of-the-art technologies for zero-energy buildings during the past decade. Energy and Buildings, (128), 198-213.

IEA (2022). *World Energy Outlook 2022*. International Energy Agency. Retrieved February 3, 2023, from https://www.iea.org/reports/world-energy-outlook-2022.

Sezen, K., and Gungor, A. (2023). Comparison of solar assisted heat pump systems for heating residences: a review. Solar Energy, (249), 424-445.

Sezen, K., Tuncer, A. D., Akyuz, A. O., and Gungor, A. (2021). Effects of ambient conditions on solar assisted heat pump systems: a review. Science of The Total Environment, (778), 146362.

CHAPTER 4

USING 3D PRINTING TECHNOLOGY TO BUILD A LOW-COST PROSTHETIC HAND PROTOTYPE

Alban RAKIPI[1], Olimpjon SHURDI[2]

1 Department of Electronics and Telecommunications, Polytechnic University of Tirana, Albania, arakipi@fti.edu.al
2 Department of Electronics and Telecommunications, Polytechnic University of Tirana, Albania

I. Introduction and Related Works

Adaptive hands that use underactuation and compliance are becoming more popular, according to recent trends [1].

Modern prosthetic limbs are primarily made of sophisticated plastic and carbon fiber, which is one of the most expensive and lightest materials available in terms of both weight and craftsmanship [2]. Technology advancements have made automatic control and operation of electronic components much simpler.

There are three main categories for prosthetic hands [3]), which are: passive prosthetic hand, conventional prosthetic hand (body-powered hand prostheses) and electric prosthetic hand (myoelectric hand prostheses). They are put into practice based on these categories as well as the preferences of the patients, which are determined by their financial and physical capabilities [2].

Three-dimensional (3D) printing is a new technique that can be used to quickly produce affordable prosthetics [4].

A wide range of requested equipment could be delivered on demand with the help of 3D printing in low-income nations, especially when open source designs are used [5].

For models that can accomplish basic functionality, a 3D printer can considerably lower the production cost [6].

In [4] are evaluated all the published designs of openly accessible 3D printed prosthetic hands for their suitability to those with congenital loss of hands or war-related amputation.

The paper [5] presents a methodology to design and manufacture an artificial hand for prosthetic application. The proposed design is a five finger hand with the forearm actuated by under-actuated system composed of tendons and servomotors.

A. Passive prosthetic hand

The passive prosthetic hand has no mobility of any kind and is seen more as a replacement for the lost hand than a functional one. However, it can be used to hold or move non-heavy items. Usually, such implementations are used in case of loss of fingers and the color they get is dependent on the pigment of the hand, in order to make a more realistic appearance.

B. Conventional prosthetic hand

This hand uses a system that is placed on the upper body (harness system). Through this system the control of the hand can be done by moving

a specific part of the body. The electronic parts that also provide finger movement are directly connected to the system.

The conventional prosthetic hand is divided into two main categories; voluntary opening: the hand is opened the moment pressure is exerted on it and voluntary closure: the hand closes the moment pressure is exerted on it.

C. Electric prosthetic hand

The electric prosthetic hand is the only one that is similar to the human hand, both in its function and in its appearance and construction. The latter are controlled by nerves and electrical impulses of the patient's remaining limb, which are captured and processed by sensors contained in the forearm. The electric motor, which enables the operation of this hand is equipped with rechargeable or replaceable batteries. The only disadvantage of this model is the extremely high cost, which comes due to the technology used and guaranteed quality.

One model of the electric prosthetic hand that is worth mentioning is the Michelangelo prosthetic hand, which is a robotic prosthetic hand manufactured by the German company Ottobock [7]. It is the first prosthetic hand, which contains an electronic finger that mimics all the human movements. Its first implementation took place in 2010. The hand is made of metal and plastic elements and operates by means of a rechargeable battery. It falls into the category of electric prosthetic hand, as its movement is done through electrodes, which capture the movements of the rest of the arm. A Michelangelo [8] prosthetic hand costs about $ 60,000.

II. Materials and Method

To build a functional prosthetic hand several key points need to be considered [9]. Since its construction involves several areas, the physical model of the hand should be considered first. Accurate construction of the physical model will also determine the accuracy of its operation. Each part of the modeled hand must be conceived in such a way that it imitates the movement of the human hand.

The next point to be considered is how the hand will be controlled, since it is attempted to create a prosthetic electric hand. For this reason, the appropriate electronic elements must be selected, to enable the movement of the physical model.

Finally, the total cost of the project must be evaluated. Comparing it with prosthetic hands, which are offered nowadays, an alternative should be presented, which best competes with those highly priced. The process

for designing specifically for the end user with significant reduction in costs may radically change the accessibility of functional prosthesis for patients [10].

III. Design of the prosthetic hand prototype

After reviewing the hand models presented in [11] and [2] , it was decided to create three main parts for this prototype. The first part of the model consists of creating the five fingers and creating an idea of how these parts will move and be joined together. The second part is the design process of the palm. For the created model to resemble a human palm, measurements were made in terms of size. The palm was divided into five parts, and the angles at which the fingers would be placed were estimated. The last part of the model will be the forearm, which will serve to hold the electronic part, that is going to be used for finger movement. Figure 1 shows the first two parts of the model.

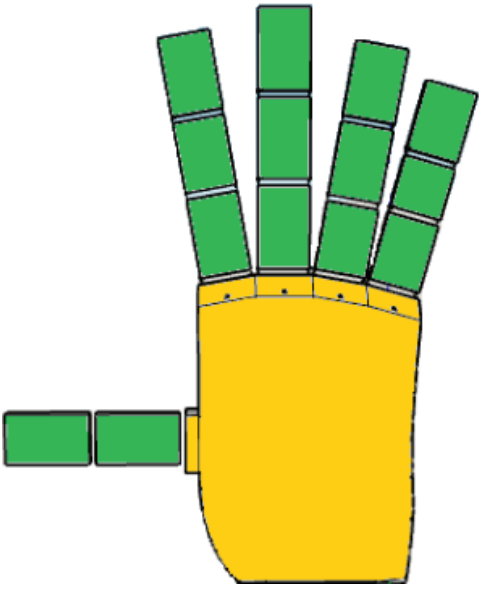

Fig. 1 The first two parts of the model

It is thought that the forearm part is adjacent to the palm part and therefore we will not have movement of the palm part, as the created model does not contain a part which represents the functions of the wrist. The mobility of the whole hand in this case will be performed by the fingers.

Regarding how the parts of the fingers will be joined with each other, two options were considered that would allow the movement of the fingers.

The first option that was considered was joining them by means of small springs, which can be found on pens, and the second option was joining them by means of thin elastic threads. Since the first option would have a visible separation between the parts of the fingers and also their durability would not be high due to the deformation of the spring during different tests, then it was considered the best option would be elastic fibers.

A. Full hand model

The complete hand model consists of 17 individual 3D printed parts. The printing process for all parts took about a day. This complete model is shown in figure 2.

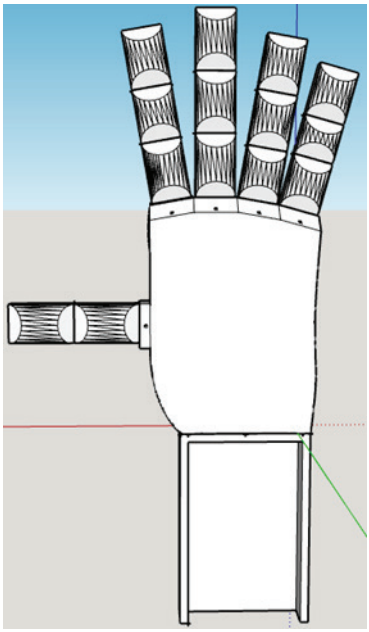

Fig. 2 Full hand model

B. 3D printing process

The program chosen to model the hand design is Sketchup Pro 2019. This program enables 3D modelling and is widely used in various engineering fields. There is a section dedicated to 3D printing only and it makes it possible to create STL files. STL (Stereolithography) is a file format used by 3D systems' Stereolithography CAD applications. This file format is commonly used for Rapid Prototyping and is supported by many other software packages [12].

3D printing is the process of creating a three-dimensional object based

on a digital file. The way these objects are created is by placing the selected material layer by layer. The materials that can be used in 3D printing are plastic, paper, and filament.

Before printing the object in 3D from the STL file, it is suggested to check for possible errors which may appear in the model. Errors, which appear most often are holes in the created pattern. For the model to be printed correctly these errors will need to be repaired with specific software.

Once the possible errors have been corrected, the model is divided into different layers and a G-code file is generated, which contains detailed instructions for the printer. For different printers we will have layers in different sizes, depending on the capacity of the printer. The model was 3D-printed using polylactic acid (PLA).

Fig. 3 The result of the first test

IV. Results

To observe the functionality of the created prosthetic hand, several tests have been performed. Each of them will be explained below and will be accompanied by the results obtained.

The first test performed consists of joining the index finger with the thumb. It is a test that is performed to verify the flexibility of the created model. A script has been created on Arduino, which will command the two motors that are connected to the respective fingers. The result obtained is given in figure 3.

For this test all the fingers of the hand will be pulled to prove the strength of the model. The angle of motion in this case will be from 0 to 180˚. The obtained results are given in figure 5.

As can be seen from figure 4, this test is successful as the complete pulling of all the fingers is done. The part that needs to be considered, is finding the correct angle for the thumb, since the base on which it is placed does not have an arc as in all other cases.

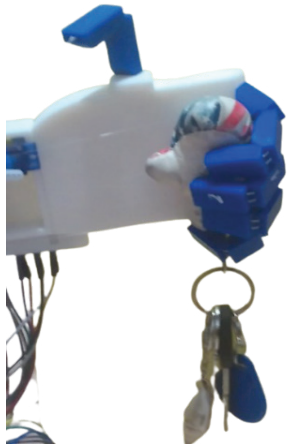

Fig. 4 The result of the second test

In the final test the hand's pointing ability will be tested. All fingers of the hand will be pulled except for the index finger, which will be positioned at an angle of 0˚. The obtained result is given in figure 5 and it can be noticed that this test is also successful.

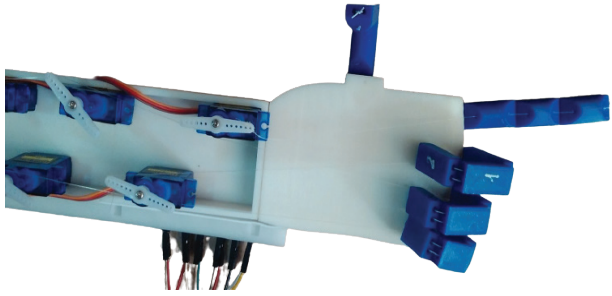

Fig. 5 The result of the third test

The total cost of the project is detailed in table 1.

If we make a comparison with other prosthetic limbs [2], we could say that the cost of the project is negligible. Such a cost comes because all selected electronic products have a performance many times lower than the elements used by large companies. Also, the model chosen to print is not very detailed as its purpose is only for testing.

Table 1. Cost structure of the project

Item description	Unit	Price ($)
3D printing	1	180
Wavgat board	1	2.7
Servo motors	5	7.3
9V battery	1	1
Breadboard	1	2.2
Total	-	**193.2**

V. CONCLUSION

The process of designing and printing in 3D of such a device is extremely difficult. Before designing the model, accurate data must be obtained regarding the dimensions, but also the angles of placement of the fingers. The correct way of modelling is a key element in relation to the most accurate functioning of the limb.

The total weight of this model, it is estimated to be around 300 gr. This weight makes this system more ideal if its real implementation would take place. The material, which is used is extremely light, but also the selected electronic devices are minimalist and do not affect the total weight. What should be considered in these cases is the fact that the created model is chosen to be non-detailed and not have all the parts of a real prosthetic hand, which allows the greatest reduction in weight.

In this case, the advantage of 3D printing can be mentioned, which allows working with different materials. In this way the work with a very light material can be chosen.

A key point to be considered for a better model would be a greater detail of the model to resemble an improved functional prosthetic hand. A greater focus should also be placed on the positioning of each modelled part, to have a successful passage in each test. Robotic components can be added to the prosthetic hand to further improve it.

References

[1] F. Negrello, H. S. Stuart, and M. G. Catalano, "Hands in the Real World," *Frontiers in Robotics and AI*, vol. 6. 2020, doi: 10.3389/frobt.2019.00147.

[2] J. ten Kate, G. Smit, and P. Breedveld, "3D-printed upper limb prostheses: a review," *Disability and Rehabilitation: Assistive Technology*, vol. 12, no. 3. 2017, doi: 10.1080/17483107.2016.1253117.

[3] T. Kulkarni and R. Uddanwadiker, "Overview: Mechanism and control of a prosthetic arm," *MCB Molecular and Cellular Biomechanics*, vol. 12, no. 3. 2015.

[4] J. J. Cabibihan *et al.*, "Suitability of the Openly Accessible 3D Printed Prosthetic Hands for War-Wounded Children," *Front. Robot. AI*, 2021, doi: 10.3389/frobt.2020.594196.

[5] A. Al-Sahib, N. Kadhim, A. Muhammed, and A. Abdulghani, "Low Cost Design of 3D printed Wearable Prosthetic Hand," *Am. J. Eng. Res. (AJER*, no. 7, 2018.

[6] S. Omar, A. Kasem, A. Ahmad, S. R. Ya'akub, S. Ahman, and E. Yunus, "Implementation of low-cost 3D-printed prosthetic hand and tasks-based control analysis," in *Advances in Intelligent Systems and Computing*, 2019, vol. 888, doi: 10.1007/978-3-030-03302-6_19.

[7] Ottobock, "Be-Bionic Prosthetic," 2019. https://www.ottobock.it/ (accessed Jan. 11, 2023).

[8] Ottobock, "Ottobock Michelangelo Prosthetic," 2019. https://www.ottobock.it/ (accessed Jan. 10, 2023).

[9] B. Maat, G. Smit, D. Plettenburg, and P. Breedveld, "Passive prosthetic hands and tools: A literature review," *Prosthet. Orthot. Int.*, vol. 42, no. 1, 2018, doi: 10.1177/0309364617691622.

[10] A. Manero *et al.*, "Implementation of 3D printing technology in the field of prosthetics: Past, present, and future," *Int. J. Environ. Res. Public Health*, vol. 16, no. 9, 2019, doi: 10.3390/ijerph16091641.

[11] L. Dunai, M. Novak, and C. G. Espert, "Human hand anatomy-based prosthetic hand," *Sensors (Switzerland)*, vol. 21, no. 1, 2021, doi: 10.3390/s21010137.

[12] B. Satyanarayana and K. J. Prakash, "Component Replication Using 3D Printing Technology," *Procedia Mater. Sci.*, vol. 10, 2015, doi: 10.1016/j.mspro.2015.06.049.

CHAPTER 5

CURRENT SITUATION OF RENEWABLE ENERGY UTILIZATION IN TURKEY AND RECOMMENDATIONS FOR FUTURE POLICIES: A CASE STUDY OF YEARS 2030 FOR MALATYA PROVINCE

Ozan AKDAĞ[1]

1 Turkish Electricity Transmission, Malatya, Turkey, ORCID ID: https://orcid.org/

1. A brief overview of renewable energy policies in the world

Energy is one of the most important agenda in the world. Major part of energy production from past to present is provided by nonrenewable energy sources (such as fossil fuels: coal, petroleum, and natural gas). This case leads to environmental disasters and the energy crisis. To prevent these problems, sustainable energy policies should be developed. Sustainable energy means that to meet today's energy demand without destroying the energy demand of future generations. Therefore, the sustainability of the energy supply should be base on increasing the use of renewable energy (Guney, 2019). Today, due to such issues, the tendency towards renewable energy resources is increasing in the world. Renewable energy policies are an agenda topic worldwide. The European Union aims to move to a low carbon economy that will reduce greenhouse gas emissions and minimize dependence on imported petroleum-coal-natural gas to deal with environmental problems (Ayhan, 2006). The European Union targets increasing renewable energy share to 45% in 2030 energy strategy goals (with Fit for 55 package). According to the report held by the International Renewable Energy Agency (IRENA) in 2022, all sectors are expected to increase the total amount of energy generated from renewable energy to 40% (IRENA, 2022). The German government has promised to reduce GHG emissions by 85% by 2050 after nuclear accidents around the world (UBA, 2019). The Government of India has also shared its dream for a long-term renewable energy target of 450 GW by 2030, (Singh et al. 2022) . The Chinese government has announced its greenhouse gas emission targets after 2060. Accordingly, by 2060, China aims to increase its share of renewable energy sources to 100% (or zero greenhouse emissions) (Qui et al., 2021). The Russian government aims to reduce carbon emissions by 70% by 2030 compared to 1990 (Malysheva and Shlyamina, 2021). The Swedish government aims for 100% renewable electricity capacity by 2040 (SRE, 2019). The Nigerian government has stated that it will start to use solar energy efficiency within the framework of sustainable energy policies. Within the framework of the studies, it aims to install a solar power plant of 500 MW in 2025 (Aliyu et al., 2018). The South Africian government aims for 8400 MW solar electricity capacity by 2030 (Aliyu et al., 2018). The Brazilian government has approved a renewable energy project of 1.5 GW, which will be completed by 2024 (PDE24, 2018). Japan aims to meet its energy from 100% renewable energy plants by 2050 (RIST, 2017). The Iranian government has stated that it will work to achieve zero emissions targets by 2050 (Ghorbani et al., 2020). With these policies for the use of renewable energy in the world, the capacity of renewable energy power plants is increasing every year. The change in the total installed

capacity of renewable energy plants in the world by years is given in Fig. 1. It is seen that the installed power of these power plants in the world is constantly increasing over the years.

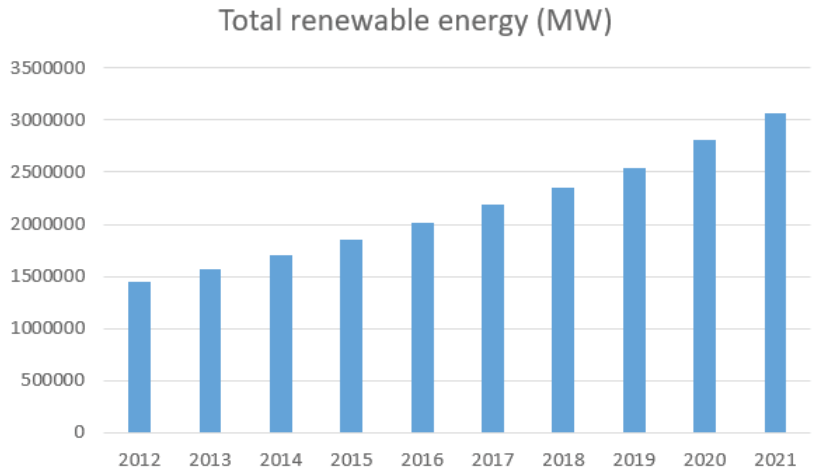

Fig. 1. Total renewable power plant installed capacity by years for world (IRENA, 2022)

In summary, many renewable energy policies have been put into practice within the scope of sustainable energy policies in the world.

In this study, while discussing Turkish renewable energy policies, Turkey's renewable energy potential is investigated. In line with this information, a sustainable energy model proposes for Turkey. This model has explicated by applying it to the Malatya province in Turkey. As a result, precautions that should be taken to wipe out energy bottleneck and to make more efficient use of renewable energy potential has discussed to contribute to sustainable energy policies.

2. Turkey's renewable energy policy

Turkey's energy needs are increasing due to its population, emerging technology, and urbanization. Turkey imports mostly coal, oil, natural gas to use in energy production. For this reason, Turkey has prepared new long-term energy policies to reduce the share of fossil fuels in power production. Fossil-based energy production, which currently tends to increase in the world, leads to an increase in emissions of greenhouse gases, most of which are CO2-CH4-N2-CO. With this increase, the world is experiencing an ecological imbalance. The World Climate Research Program (WCRP)

reported that emissions have reached the highest level of all time in 2018 (WCRP, 2018). With its increasing population and developing industry, Turkey's CO2 emissions are constantly increasing over the years. This case is given in Figure 2 (Stastica, 2022).

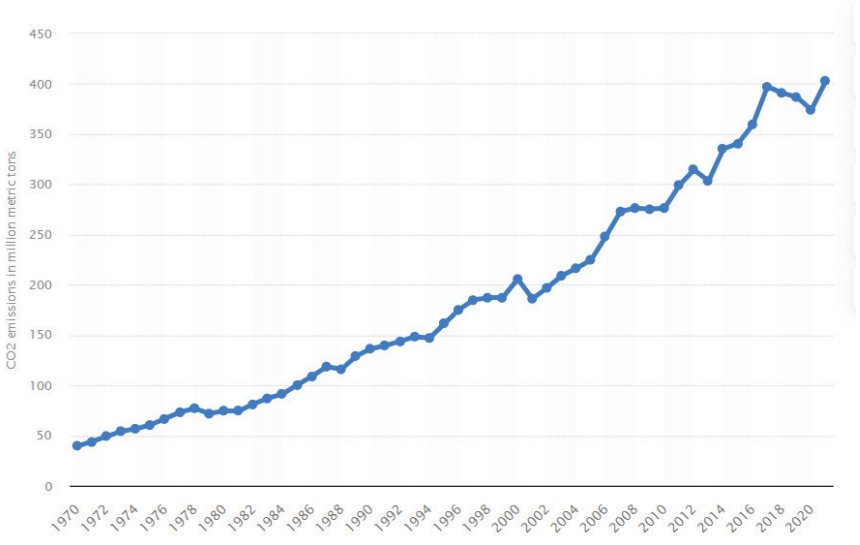

Fig.2. *Turkey's 1971-2022 annual CO_2 emission quantities (Stastica, 2022)*

In Turkey, especially until the beginning of the 2000s, there were no serious investments and incentive policies in both reducing carbon emissions and establishing renewable energy power plants. After 2001, serious policies have been developed in this regard (RTMENR, 2005; RTMENR, 2007). In 2009, Turkey became a party to the Kyoto Protocol. The Kyoto Protocol is an agreement to reduce the use of greenhouse gases. The articles of the agreement were created in 1992, and the protocol was signed on 11 December 1997. Turkey has agreed to reduce greenhouse gas emissions by becoming a party to the Kyoto protocol (Bayrak, 2012). In the following years, in accordance with this protocol, various laws have been published that promote renewable energy in Turkey and raise awareness of this issue (NREA, 2010; NREA, 2011; NREA, 2013). In Turkey's 2023 energy targets, it is aimed to increase the total production of renewable energy share by 30% in 2023. In the plan, a total of 61 GW renewable energy power plant capacity was targeted which includes 34000 MW hydroelectric, 20000 MW wind energy, 5000 MW solar energy, 1000 MW geothermal energy and 1000 MW biomass (TNREP, 2012). In the following years, the scope of Law No. 5346 on Electricity Production from Renewable Energy Resources was expanded and various incentives were introduced for

the establishment of renewable energy power plants (Law 5346, 2005). Turkey's annual electricity consumption increase rate has been over 5% in recent years. İn addition to, the increases in electrical energy demand have been over 6%. A significant share has been obtained from renewable energy sources of Turkey's installed power. In this share, undoubtedly, energy policies in recent years have been effective. Table 1 shows the installed power (all) in Turkey from the past to the present day (TEIAS, 2022).

Table 1. *Turkey's renewable resources capacity in between 2003 and 2021*

Years	Hydroelectric (MW)	Geothermal (MW)	Wind (MW)	Solar (MW)	Biomass (MW)	Renewable total installed power	Total installed power	Rewable %
2003	12575	15.1	18.7	-	27.2	12636	35575	35.51
2004	12641	15.2	18.7	-	27.2	12702.1	36818	34.49
2005	12900	15.2	19.9	-	34.9	12970	38841	33.39
2006	13059	22.85	58.8	-	41	13181.65	40545	32.51
2007	13385	22.99	146.8	-	42.5	13597.29	40824	33.333
2008	13822	29.75	362.9	-	58.9	14273.5	41804	34.143
2009	14552.9	76.9	790.9	-	85.9	15506.6	44759	34.6
2010	15830.9	93.9	1319.1	-	106.8	17350.7	49511	35.04
2011	17136.9	113.8	1727.5	-	124.9	19103.1	52888	36.11
2012	19610	161.9	2259	-	167.9	22198.8	57044	38.91
2013	22279	309.9	2758.5	-	234.8	25582.2	63999	39.97
2014	23639	402.8	3618.5	40.1	298.9	27999.3	69518.2	40.27
2015	25859.4	622.85	4502.9	247.9	369.9	31602.95	73139.8	43.208
2016	26679	819.5	5749	829	494.9	34571.4	78495.8	44.04
2017	27259	1059.9	6959.8	3416.5	577	38542.2	84999	45.34
2018	28349.9	1302	7504.9	4791.8	810.9	42759.1	88299	48.42
2019	28503	1514	7591	5995	810.9	44413.9	91267	48.66
2020	30983	1613.2	8832.4	6667	1115.6	49211.2	95890	51.32
2021	31492.6	1676.2	10607	7815.6	1644	53235.4	99819	53.33

Table 1 is examined, it is seen that the installed power of renewable energy power plants has increased over the years. Especially when it comes to 2021, it is seen that the installed power of renewable energy plants is 53.3% of total installed power.

3. Turkey's renewable energy potential

3.1.Wind Power

The wind potential of Turkey is quite high due to facts that the 3 sides of Turkey surrounded by seas, the sharp climate change, and the excessive sunbathing time. In a technical study carried out in Turkey, Turkey's has determined to be 88 GW of wind potential (Ilkilic, 2012). The installed power of wind power plants in Turkey has approached the level of 12 GW as of 2022. With this new capacity, Turkey has been in the top 10 in the world (GWEC, 2022). The potential of wind is quite high in the Marmara, Aegean and southeastern Anatolia (Celik, 2004). The wind speed map of Turkey is shown in Fig. 3. In Turkey, wind energy potential lies along the coastline (WindMap, 2022). Apart from these regions, in the southeastern region, Adiyaman-Sincik, Mardin, Malatya-Arapgir, Şanlıurfa-Siverek; in the Mediterranean region the eastern parts of the province of Antakya and Northern Osmaniye has high wind potential.

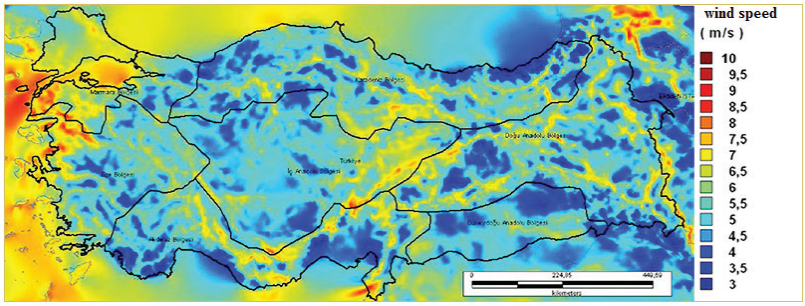

Fig. 3. *Wind speed map in Turkey 50 m (WindMap, 2022)*

With the renewable energy policies in Turkey, there has been a significant increase in the number of renewable energy power plants in recent years. With the energy vision of 2023, the installed power of wind energy will increase to 20 GW, and the share of imported coal and natural gas in electricity generation will be reduced (Law5346, 2005). With this energy vision, in recent years, a significant number of wind farms have been established. Turkey's total wind energy generation by years is shown in Fig. 4.

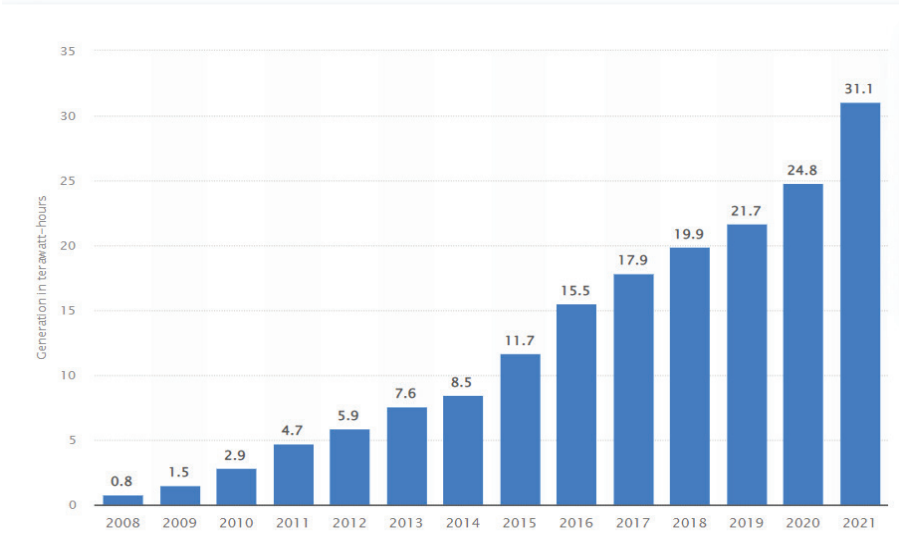

Fig. 4. *Wind energy generation ftom 2008 to 2021 in Turkey (terawatt hours) (Stastica, Dierks 2022)*

3.2. Solar Energy

The world benefits from solar energy in the forms of thermal and electrical (Kahraman, 2018). The energy of the sun reaching the earth is 0-100 W / m2 (Ceylan, 2014). Turkey is a country with a very high potential for solar energy due to its geographical location. Turkey has an average sun time of approximately 2737 hours per year, 7.5 hours a day. The average amount of radiation is as 1.311 kWh/m2 per year, 3.6 kWh/m2 per day (IRENA, 2022). Turkey's Solar Map is seen in Fig. 5. This map shows that there is a important solar energy potential in the south. Turkey's renewable energy policies are increasing the installed power capacity of solar energy day by day. As of 2022, Turkey's installed solar power capacity has reached 8 GW (licensed).

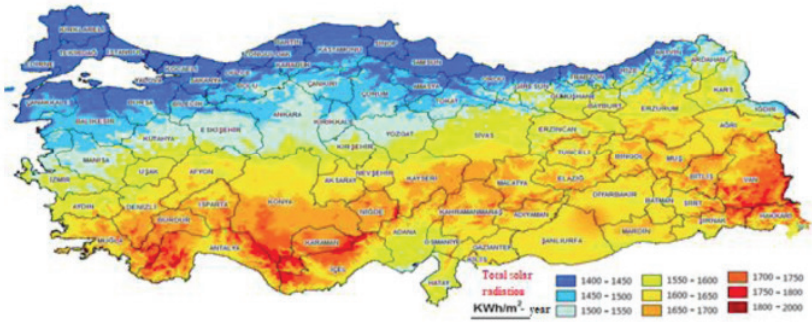

Fig. 5. *Sun Map of Turkey (Serteller, 2017)*

3.3. Biomass Energy

Biomass is a type of fuel derived from wood, animal/plant wastes, and biological sources (Kaygusuz and Turker, 2002; EnergyReport, 2022). Energy production from biomass has become popular in recent years. In recent years, Turkey has made many attempts to use agricultural and animal waste for energy production (Toklu, 2017). Turkey has a large agricultural/livestock potential and therefore biomass reserves. While 70% of these areas is used for grain cultivation, the rest uses as vegetable production, garden or fallow land (Avcioglu et. Al., 2019). In addition, 20-25% of Turkey is approximately forested area. This provides a significant advantage in terms of biomass reserve. It is estimated that Turkey's annual biomass potential is approximately 32 MTEP, and the total usable bioenergy potential is approximately 16.92 MTEP (Kapluhan, 2014). Turkey biomass energy potential map is shown in Fig 6.

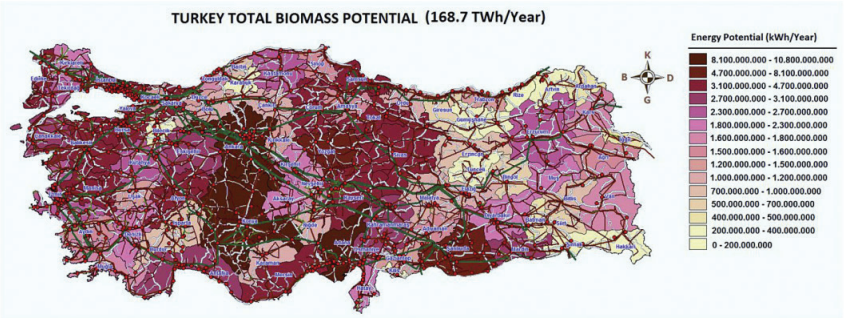

Fig. 6. *Turkey's biomass energy potential map (MEF, 2009)*

Turkey has implemented various policies to increase energy generation of the biomass potential seen in Figure 6. According to the strategic

plan of the Ministry of Energy 2010-2014, Turkey has set its goal to increase biomass installed power plant to 2000 MW within the framework of the energy policy of 2023 (TNREP, 2012). With these and similar policies, biomass installed power, which was 27.2 MW in 2003, has been increased to 1644 MW by the end of 2021.

3.4. Geothermal Energy

Turkey reached 1686 MW installed power in geothermal energy at the end of 2021. It was the fourth in the world and the first in Europe. Geothermal energy has significant potential in America, Southeast Asia Turkey and Italy. Turkey has geothermal potentials with an estimated value of 35000 MW (Agacayak, 2017). Turkey, the young tectonic structure, located on the Alpine-Himalayan mountain belt, is an important geothermal center due to the presence of warm and minarel sources (Aksoy, 2014). There are approximately 1000-1100 natural sources of geothermal output in Turkey located 78-80% in western Anatolia. While electricity can be produced from only 10% of these wells in Turkey, the rest can be used for health and tourism. Fig. 7 shows Turkey's geothermal energy potential at a depth of 50 meters.

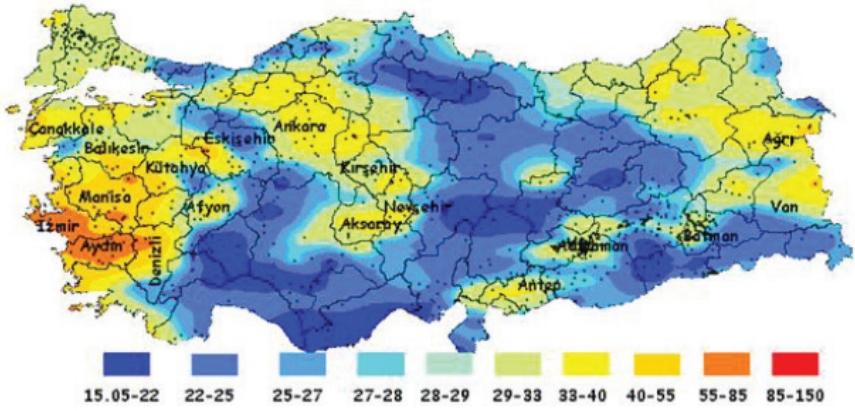

Fig. 7. Turkey's 500 m depth temperature distribution map (TMMBO, 2009)

In Turkey's 2023 energy policies, 1000 MW installed power envisaged in geothermal energy (TNREP, 2012). Since this target was reached early, this target was later updated to 4000 MW.

3.5. Hydroelectric Energy

Turkey is ranked first in hydroelectric potential in Europe with 25 Basin units (Bilgili et al., 2018; Bilgili and Sahin, 2009). Turkey has 30-35% of its hydroelectric potential in the eastern and southeastern Anatolia region where the Euphrates River located. There are large-scale power plants in this region. The most important of them are Atatürk Dam (2405 MW), Karakaya (1800 MW), Keban (1330 MW), Birecik (7003 MW). The region with second high hydroelectric potential is the eastern Black Sea region. The mountainous and high-altitude flow rates of this region are the main reason of this hydropower potential. Some of the most important dams in the region are: Deriner Dam (670 MW), Artvin Dam (332 MW). There are 708 hydroelectric power plants with large and small scales in Turkey. As of the end of 2021, the hydroelectric plant has reached 30000 MW installed power. Turkey has implemented many policies to increase hydroelectric power plant capacity. The most important of these policies is the target of increasing the hydroelectric installed capacity to 42.000 MW, which is announced by Turkey's 2023 energy vision (TNREP, 2012; Law No. 5539, 2006; Law No. 6446, 2013).

4. Possible suggestions for Turkey

Turkey has taken important steps in renewable energy especially with its energy policies developed after 2002 and achieved some of its goals in the energy vision of 2023. However, despite its renewable energy potential, Turkey is still unable to benefit from this potential enough. In particular, Turkey must continue to work both in the technological/academic area and the practical field by adopting policies that will cover longer years of renewable energy. In this study, a proposal, based on distributed production systems, is presented to increase the capacity of renewable energy power plants according to the structure of Turkey.

4.1. Disturbed Generation

Distributed Generation (DG) is the power generation plants directly integrated into the power systems from the distribution level. In power systems, wind power plants, photovoltaic systems, hydropower/biomass power plants may integrate from distribution level to power systems. DGs are installed close to the region where they are used to contribute to reducing the losses of transmission lines in power systems and contribute significantly to the supply/demand balance. A DG plant with sufficient capacity may allow the respective consumption zone to be operated separately from the mains. This is important for energy continuity. Due to their low capacity DGs can quickly enter/exit the grid. DGs reduce the installation cost of large-scale high-cost power plants. There are also some difficulties in

integrating DGs into power systems (impact on power quality, bidirectional energy flow, protection coordination, etc.). These challenges are widely overcome by technological advances in recent years (Cetinkaya and Dumlu, 2013).

4.2. Suggestions

In this study, some suggestions have been offered to increase Turkey's renewable energy power capacity considerably as follows:

- Turkey's energy supply and the installed capacity of each province (with type) should be determined.

- The renewable energy potential of each province should be evaluated in detail. A feasibility study should be carried out for renewable power plants that can be established later.

- Afterward, in order to determine the location and capacity of the power plant, various power engineering analysis should be carried out by modeling the DGs with the existing networks in a virtual environment.

- According to the target year determined by the detailed analysis results, related DGs projects should be submitted.

Thus, instead of costly power plant projects in Turkey, smaller-scale, fast-to-install, cost-effective and local energy generation systems can be established to increase renewable energy capacity. The suggestion presented in this study has applied with a case study based on Malatya province.

4.3. A Case study for Malatya province

Malatya is located in the Upper Euphrates Basin in the Eastern Anatolia Region and has connecting highways to the Central Anatolia, Mediterranean, Eastern Anatolia, and South-Eastern Anatolia Regions. Malatya is located in the southwest of the Eastern Anatolia Region and is surrounded by Elazığ to the east, by Erzincan to the northeast, by Sivas to the northwest, by Kahramanmaraş to the west, by Adıyaman to the south and by Diyarbakır to the southeast. The landscape in Malatya is formed mostly of high plateaus and mountains. The mountain chain which forms the high western part of the South Eastern Taurus Mountains covers a large area in the southern province. According to the geographical coordinate system, it is located in between 8°21′0.65″K 38°19′0.01″D / 38.3501806°K 38.3166694°D.

As of 2022, there are 26 active power plants (licenced) with an electric installed capacity of 116.4 MW (licenced)/115 MW (unlicensed) in Malatya (EnergyMalatya, 2022). The installed power and number of these power plants according to their source are in given Table 2 (appromiexly).

Thus, it is planned to reach 379.4 MW installed capacity in Malatya As of 2022, the hourly maximum power demand of Malatya is 250-270 MWh (appromiexly). Based on the rate of increase in previous years, It foresees that this figure will increase to 440 MWh (maximum) by 2030. To meet the total demanded power for the year 2030 from the installed capacity, totaling 50-60 MW power plant construction is needed. New sources should be sought for this energy need. Malatya has high hydro, solar, and wind potential and considerable biomass resources. Since Malatya is considered to be a sufficient hydroelectric power plant, research has been carried out in the other three sources (wind, solar and biomass). Following DGs may be planned to establish in Malatya;

- Solar Power Plants: Figure 8 shows the solar radiation map for Malatya obtained from the Renewable Energy Directorate. In Akdağ and Yeroglu (Akdag and Yeroglu, 2019a), four regions were determined, where solar radiation is high in Malatya and marked as shown in Fig. 9. PVsyst 6.7.3 and DigSilent simulation software has been used in the detection of these regions and solar power plant installation, respectively. The total installed capacity for these four regions is 22.61 MW. Thus, solar power plants may be proposed for these locations.

- Wind Power Plant; Akdağ and Yeroğlu (Akdag and Yeroglu, 2019b) selected a location in Darende, one of the regions with high wind potential in Malatya province in Fig. 10, and they made a wind power plant simulation (DigSilent simulation program) and proposed a 25 MW DG. Thus, wind power plants may be offered for this region in Malatya.

- Biomass Power Plant; Malatya is one of the provinces where agriculture is actively carried out. In the study, conducted by Kurt and Koçer (Gizem and Kocer, 2010), the average dry biomass amount obtained in one year in Malatya and the average thermal value of dry biomass were calculated in terms of Tons of Equivalent Oil (TEO) as; in average 142576.5 TEO for Darende, 70116.2 TEO for Hekimhan and 127083 TEO for Arapgir. The study proposes biomass power plants in Darende, Arapgir, and Hekimhan districts due to their proximity to the existing transformer centers in Malatya and active agriculture. Assuming that the total agricultural area allocates for 10 % biomass power plant capacity in these 3 centers, a biomass production plant with a total installed power of 18 MW in Darende, 9.3 MW in Arapgir, and 16.8 MW in Hekimhan can be installed. These generation plants can be integrated into the distribution feeders of the relevant substations and integrated from the DG level.

Thus, in the province of Malatya, a total of 91.71 MW of power can be installed in these 3 energy types by 2030. As a result, Malatya province can reach a level that can meet the power demanded. If these suggestions

can be extended to Turkey, rapid renewable energy transformations can be achieved in every province.

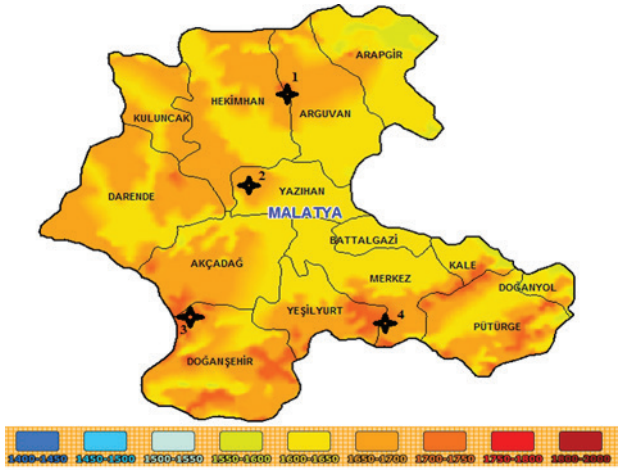

Fig. 8. *Solar radiation map of Malatya province (Akdag and Yeroglu, 2019a)*

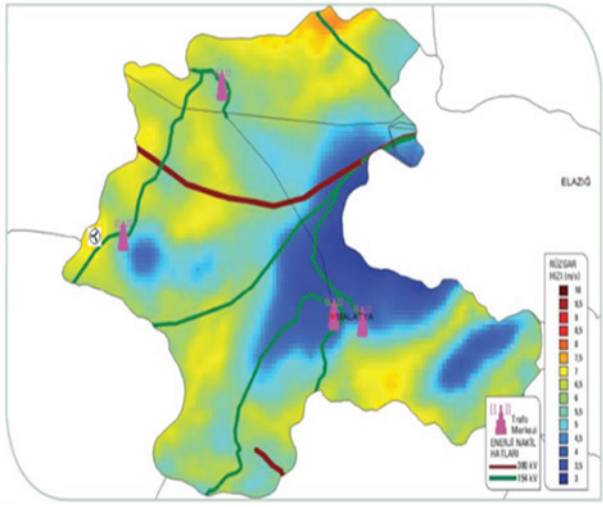

Fig. 9. *Malatya wind map (Akdag and Yeroglu, 2019a)*

Table 2. *Malatya province installed power plant capacities*

Case	Solar (MW)	Wind (MW)	Biomass (MW)	Hydroelectric (MW)	Other (MW)	Total (MW)
Current State	19.765	10	16	65.23	5.44	116.43
Under Construction	9.9	-	-	17	-	26.9
Licenced	-	30	-	7.26	-	37.26
Pre-Licenced	-	-	-	84.01	-	84.01
Planned by 2030	22.61	25	44.1	-	-	91.71

5. Conclusion

In the world, the gradual abandonment of fossil fuel use in energy production, technological developments in renewable energy, incentives brought by countries to renewable energy sources and tax reductions have increased the share of renewable energy in power production. Renewable energy is a collection of energy sources that are not monopolized such as fossil fuels, which reduce ongoing energy battles in the world, which are accessible by everyone, and reduces loyalty to central units. In this respect, it contributes to world peace and the development of countries. Since Turkey is a continuously developing country, national energy consumption is constantly increasing. Turkey, considering 2018 data for electricity generation, produces 38% of its energy from imported coal and natural gas. This rate increases Turkey's dependence on foreign trade. In addition, fossil fuel plants, which cause the emission of harmful gases to nature, take a significant part of this ratio. Turkey has made a breakthrough in renewable energy, especially since 2002, with no indifference to the development of renewable energies in the world for these reasons.

In this study, a general overview of renewable energy policies in the world, Turkey's reflection on these policies, and the original policies issued in Turkey are discussed. Further, Turkey's renewable energy potential has been discussed and recent studies in the field of renewable energy have been evaluated. In the last part of the study, some suggestions have been given based on the energy policies carried out in Turkey, renewable energy potential and developments in the world, and Turkey's renewable energy policy. The suggestions presented in this study have been applied to a case study based in Malatya province.

REFERENCES

Agacayak, A.C. (2017). Investıgatıon Of The Factors Affectıng The Electrıc Energy Productıon Of Thermoelectrıc Generators By Usıng Geothermal Energy: Master Thesis, Afyon Kocatepe University, 125s.

Akdağ, O., & Yeroğlu, C (2019a). Malatya Yöresi İçin Örnek Bir Güneş Santrali Modelinin Benzetimi Ve Şebekeye Etkilerinin İncelenmesi. *Mühendislik Bilimleri Ve Tasarım Dergisi*, *7*(3), 552-560.

Akdağ, O., & Yeroğlu, C. (2019b). Offshore/Onshore Rüzgâr Santralinin Modellenmesi ve Şebekeye Bağlantısı. *Avrupa Bilim ve Teknoloji Dergisi*, (16), 505-520.

Aksoy, N. (2014). Power generation from geothermal resources in Turkey. *Renewable Energy*, *68*, 595-601.

Aliyu, A. K., Modu, B., & Tan, C. W. (2018). A review of renewable energy development in Africa: A focus in South Africa, Egypt and Nigeria. *Renewable and Sustainable Energy Reviews*, *81*, 2502-2518.

Avcıoğlu, A. O., Dayıoğlu, M. A., & Türker, U. (2019). Assessment of the energy potential of agricultural biomass residues in Turkey. *Renewable Energy*, *138*, 610-619.

Bayrak, M. R. (2012). Sürdürülebilir Kalkınma İçin Türkiye'de Düşük Karbon Ekonomisi ve Kyoto Protokolü'nün Finansman Kaynakları/Low Carbon Economy and Financial Sources of The Kyoto Protocol for Sustainable Development In Turkey. *Journal of History Culture and Art Research*, *1*(4), 266-279.

Bilgili, M., and Şahin, B. (2009). Electric power plants and electricity generation in Turkey. *Energy Sources, Part B: Economics, Planning, and Policy*, *5*(1), 81-92.

Bilgili, M., Bilirgen, H., Ozbek, A., Ekinci, F., & Demirdelen, T. (2018). The role of hydropower installations for sustainable energy development in Turkey and the world. *Renewable Energy*, *126*, 755-764.

Celik, A. N. (2004). A statistical analysis of wind power density based on the Weibull and Rayleigh models at the southern region of Turkey. *Renewable energy*, *29*(4), 593-604.

Ceylan, (2014). The Analysıs Of Turkey's Solar Energy Potentıal And The Posıtıon Of Solar Power In The Energy Polıcy: Master Thesis, Bahcesehir University, 114s.

Çetinkaya, H. B., & Dumlu, F. (2013). Dağıtık üretim tesislerinin şebeke entegrasyonunda yaşanabilecek olası problemler ve entegrasyon analizleri. *Akıllı Şebekeler Ve Türkiye Elektrik Şebekesinin Geleceği Sempozyumu*, 26-27.

Demirbaş, A. (2006). Turkey's renewable energy policy. *Energy Sources, Part A*, *28*(7), 657-665.

EnergyMalatya, 2022. https://www.enerjiatlasi.com/sehir/malatya/ [Accessed 16 09 2022].

EnergyReport, (2022). Dünya Enerji Konseyi, World Energy Resources: 2013 Survey http://www.dektmk.org.tr/upresimler/Enerji-Raporu-2013.pdf, [Accessed 02 03 2022].

Ghorbani, N., Aghahosseini, A., & Breyer, C. (2020). Assessment of a cost-optimal power system fully based on renewable energy for Iran by 2050–Achieving zero greenhouse gas emissions and overcoming the water crisis. *Renewable Energy*, *146*, 125-148.

Gizem, K., and Koçer, N. N. (2010). Malatya ilinin biyokütle potansiyeli ve enerji üretimi. *Erciyes Üniversitesi Fen Bilimleri Enstitüsü Fen Bilimleri Dergisi*, *26*(3), 240-247.

Guney, T. (2019). Renewable energy, non-renewable energy and sustainable development. *International Journal of Sustainable Development & World Ecology*, *26*(5), 389-397.

GWEC, (2022). Global Wind Report 2022, http://files.gwec.net/register?file=/files/GWR2017.pdf . [Accessed 15 01 2022].

IRENA (2022), International Renewable Energy Agency , Renewable Capacity Statistics 2022, https://irena.org/publications/2022/Apr/Renewable-Capacity-Statistics-2022 [Accessed 02 09 2022].

İlkiliç, C. (2012). Wind energy and assessment of wind energy potential in Turkey. *Renewable and Sustainable Energy Reviews*, *16*(2), 1165-1173.

Kahraman, B. (2018). Development Of A Real-Tıme Meteorologıcal Data Monıtorıng System For Solar Energy Plants: Master Thesis, Ege University, 120s.

Kapluhan, E (2014). Enerji Coğrafyası Açısından Bir İnceleme: Biyokütle Enerjisinin Dünyadaki Ve Türkiye'deki Kullanım Durumu. *Marmara Coğrafya Dergisi*, (30).

Karaguc, B. (2013). Geothermal Energy Potentıal And Economıc Impacts Of The Provınce Of Balıkesir: Master Thesis, Balıkesir University, 137s.

Kaygusuz, K. & Türker, M. F. (2002). Biomass energy potential in Turkey. *Renewable Energy*, *26*(4), 661-678.

Law No. 5539, (2006). Republic of Turkey Ministry of Energy and Natural Resources, 2006. Law No. 5539, http://www.resmigazete.gov.tr/eskiler/2006/07/20060718-2.htm [Accessed 17 02 2022].

Law No. 6446, (2013). Republic of Turkey Ministry of Energy and Natural Resources, 2013. Law No. 6446, http://www.resmigazete.gov.tr/eskiler/2013/03/20130330-14.htm [Accessed 16 02 2022].

Law5346, (2005). Republic of Turkey Ministry of Energy and Natural Resources, 2005. Law No. 5346, http://www.resmigazete.gov.tr/eskiler/2005/05/20050518-1.htm [Accessed 16 02 2019].

Malysheva, R., & Shlyamina, A. (2022). Overview of the Legal Framework for the Regulation of Greenhouse Gases in the Russian Federation. *KnE Social Sciences*, 172-177.

MEF (2019), Ministry of Environment and Forestry, Forest biomass situation for renewable energy in Turkey (in Turkish), MEF, Ankara.

NREA, (2010). Republic of Turkey Ministry of Energy and Natural Resources, 2005. Law No. 5346-29/12/2010-6094/2md., [Accessed 16 02 2019].http://www.resmigazete.gov.tr/eskiler/2005/05/20050518-1.htm.

NREA, (2011). Republic of Turkey Ministry of Energy and Natural Resources, 2011. Official Gazette: 28097, [Accessed 16 02 2019]. http://www.yegm.gov.tr/duyurular_haberler/document/en_yon_27_10_2011.pdf .

NREA, (2013). Republic of Turkey Ministry of Energy and Natural Resources, Law of Electricity Market. [Accessed 16 02 2019]. http://www.yegm.gov.tr/document/20180102M1_2018.pdf .

PDE24, (2018). Electricity in the 2024 Brazilian Energy Plan. [Accessed 08 02 2019]. http://www.mme.gov.br// .

Qiu, S., Lei, T., Wu, J., & Bi, S. (2021). Energy demand and supply planning of China through 2060. *Energy*, *234*, 121193.

RIST Long-Term Scenarios for Decarbonizing Japan (2017) https://www.wwf.or.jp/activities/activity/464.html , Accessed 20th Jun 2021.

RTMENR, (2005). Republic of Turkey Ministry of Energy and Natural Resources, 2005. Law No. 5346. [Accessed 16 02 2019]. http://www.resmigazete.gov.tr/eskiler/2005/05/20050518-1.htm .

RTMENR, (2007). Republic of Turkey Ministry of Energy and Natural Resources, 2007. Law No. 5686. [Accessed 16 02 2019]. http://www.resmigazete.gov.tr/eskiler/2007/06/20070613-1.htm .

Serteller, N. F. O. (2017). Examination and Comparison of Nuclear Energy with other Available Energy Sources for Electricity Production in Turkey. *International Journal of Humanities and Social Science Research*, *3*, 38-42.

Singh, U., Rizwan, M., Malik, H., & García Márquez, F. P. (2022). Wind energy scenario, success and initiatives towards renewable energy in India—A review. *Energies*, *15*(6), 2291.

Stastica Dierks (2022). https://www.statista.com/statistics/893590/wind-energy-generation-turkey/ . [Accessed 28 02 2022].

Stastica, (2022). [Accessed 15 01 2021]. https://www.statista.com/statistics/449827/co2-emissions-turkey/

Sweden Renewable Energy (SRE) 2019. Energy use in Sweden. [accessed 2019 May 24]. https://sweden.se/society/energy-use-in-sweden/ .

TEIAS, (2022). Turkish electricity transmission corporation (TEIAS) - Turkey Electricity Generation Capacity (2003–2021). Ankara; 2022.

TMMOB, (2009). Jeotermal Kongresi Bildiriler Kitabı, Aralık 2009.

TNREP, (2012). Republic of Turkey Ministry of Energy and Natural Resources, Turkey's Nation Renewable Energy Plan. [Accessed 16 02 2019]. https://kusip.gov.tr/kusip/yonetici/tematikAlanEkGoster.htm?id=75

WCRP, (2018). WEF Global Risks Report 2018 published. [Accessed 15 01 2019]. https://www.wcrp-climate.org/ .

WindMap, (2022). Republic of Turkey Ministry of Energy and Natural Resources, Turkey wind map http://www.yegm.gov.tr/YEKrepa/REPA-duyuru_01.html [Accessed 28 02 2022].

CHAPTER 6

THE USE OF AFYON-İSCEHİSAR (DOKIMEION) WHITE MARBLE FOR SCULPTURE AND ARCHITECTURAL MATERIALS IN ANCIENT TIMES

Mustafa Yavuz ÇELİK[1]

1 Prof. Dr.ORCID: 0000-0002-9695-7370 Afyon Kocatepe University, Afyon Vocational School, Department of Marble Technology, 03100, Afyonkarahisar, Turkey.

1. INTRODUCTION

The word "marble" reproduces from the Greek "marmaros" and means shine. The current meaning of marble includes all kinds of natural stones with high decorative properties in the stone industry. Petrographically, marble is a carbonate rock transformed due to regional or contact metamorphism. Pure marbles, which contain more than 95% calcite, are usually white. It may contain small amounts of quartz, feldspar, mica, chlorite, and other minerals (Mrozek-Wysocka 2014). Marbles are usually found in the crystalline complex where igneous and regionally metamorphosed rocks. Turkey has many large complex crystal structures that are contained in different colors of marble. Some of these marbles have been produced since ancient times. Nearly all-important antiquity statuary, monumental, religious, and important buildings are made of marble, for this reason, only the trade of marble was common in ancient times (Herz 1988).

Many of the cultural heritages (important buildings and monuments from ancient times) are made of natural stone. Different civilizations used natural stones for decorative purposes in architectural elements, floor and wall facings, sculptures, and sarcophagi in ancient times. Marble has been an important material used in monumental, religious, and important buildings, especially for decorative purposes since ancient times. The most important reason for this preference was especially its aesthetic and technical features. Due to these properties, the high requisition for marble in ancient times triggered the opening of quarries in the Mediterranean region, especially in Italy, Greece, and Western Anatolia (Mrozek-Wysocka 2014; Moropoulou et al. 2019).

In ancient times, vast quantities of marble blocks were produced from Greece and western Anatolia quarries to construct important buildings and monuments. Important marble quarries operated in Greece during these periods can be counted as Thasos, Paros, Naxos, Athens, and Doliana. The important marble quarries west of Turkey are Proconnesus (Marmara Island), Ephesus, and Dokimeion (Iscehisar-Afyon). The marble quarries operated in this period were not limited to these; it is known that many marble quarries with smaller capacities were operated in the Aegean region (Rapp 2009). While the source of ancient marble quarries in Turkey is generally the Menderes Massif (except Proconnesus), there needs to be more information about the quarries in other massifs. The outermost part of the Menderes Massif (200 x 300 km NE-SW) is formed by marbles and low-grade metamorphic schists beneath them. The Menderes Massif contains Denizli, Dokimeion (Afyon), Aphrodisias (Aydın), and Mylasa (Milas) antique marble quarries (Herz 1988).

Dokimeion (İscehisar) marble quarries, which are important marble

sources of both ancient times and today, still maintain their importance. Approximately 24 marble quarries are operated in the İscehisar-Afyon site (Çelik and Sabah 2008). The İscehisar-Afyon marble quarries have been the focus of attention of many researchers because the traces of ancient stone cuts from the Roman period are still visible, and the presence of many semi-worked artifacts. After the first studies that were started in the 1920s, studies have been conducted on the semi-worked architectural pieces (architrave, cornice, column, pedestal, frieze, capital) and sculptural materials in the Dokimeion marble quarries, and various artifacts (extensively sculpture and sarcophagi) made from these marbles (Waelkens 1985).

Until today, there has been too much research on the Dokimeion white marble, and this number is increasing amount of. Some of these studies are related to marble quarry management and stone quarrying in ancient times. Albustanlıoğlu (2002) and Fant (1989) investigated the Dokimeion marble quarries' operation and export organization in the Roman period. Scientific studies on İscehisar marble quarries have focused on the region's geology, economy, environmental problems, and evaluation of marble waste. For example, Çelik and Sabah (2008) investigated the geotechnical properties of İscehisar marble deposits and the impact of quarry and factory marble wastes on groundwater and the environment.

There are many architectural artifacts, sarcophagi, and sculptures exhibited in museums in Anatolia and many Mediterranean countries. Many researchers examined the artifacts made of İscehisar marbles exhibited in museums in Mediterranean countries. These studies have been conducted on subjects such as the archaeometry study, determination of the origin, petrographical, mineralogical, and geochemical properties of the Dokimeion white marble. Some researchers, such as Hall and Waelkens (1982), Topbaş (1987), Attanasio et al. (2011), Pensabene et al. (2012a), Çalik-Ross (2013), and Bruno et al. (2015) have worked on this topic. Bağcı (2020) has determined the petrographic, mineralogical, and geochemical features of İscehisar marbles. Çelik and Sert (2020) examined the Pavonazzetto marble (Dokimeion), and they specified its importance in ancient times, and to be a source of global heritage stone source. Also, some researchers refer to the stable isotope composition of the Dokimeion white marble (Cramer 2004; Poretti et al. 2017; Prochaska and Attanasio 2022).

The inscriptions of the abandoned marble artifacts in the İscehisar marble quarries gave important clues about the working order and production in the quarry. Some researchers such as Fant (1984), Herrmann and Tykot (2009), and Lubotsky (2017) have worked on this subject. Albustanlıoğlu (2013) examined the production of the Dokimeion marble quarries during the Roman Imperial period and the architectural materials and semi-worked blocks abandoned in the quarry. Researchers studied the

abandoned marble blocks and semi-worked artifacts in the İscehisar marble quarries. Fant (1985) reported that four unfinished sarcophagus lids, made of fine-grained white marble were found in the Docimium quarry in İscehisar. Fant (1988a) stated that two sculptures and some architectural artifacts were found in the Docimium quarry in İscehisar.

Many researchers have studied some marbles' physical and mechanical properties, including Afyon white marbles. Ozguven and Ozçelik (2014) examined the physical and mechanical properties of some Turkish natural building stones. Çelik and Sert (2021) examined the importance of Pavonazzetto marble (Dokimeion) in ancient times and investigated its durability with salt crystallization and freeze-thaw tests.

The present work was performed to introduce the Docimian white marble (Dokimeion-Phrygia/Iscehisar-Turkey), which was widely used in statues and sarcophagi in antiquity, and represents an important ancient white marble. One of the primary purposes of such scientific studies is to determine the authenticity of ancient objects, including precious marble sculptures. In such cases, petrographic and mineralogical examinations of marble materials and chemical analysis methods are generally used. These analyses also help determine the origin of the raw material and whether the marble objects are fake or antique copies of an original work. For this purpose, this study focused on three topics. Firstly, in this paper, Docimian white marble, widely used in Western Anatolia and Mediterranean regions in ancient times, was characterized using chemical, optical, scanning electron microscopy, and XRD. In the next part, the phases of Docimian white marble were investigated starting from the quarry to the final usage area. These procedures contained the transport of architectural materials, sculpture, and sarcophagi produced and worked from the quarry, and its usage in monumental, religious, and important constructions of the Romans. In the next section, examples of architectural materials, sculptures, and sarcophagi, made of Docimian white marble exhibited in museums, in Anatolia and many Mediterranean countries were given.

2. MATERIAL AND METHODS

2.1. Material

The İscehisar-Afyon area is known as an extensive marble area in Turkey. Dokimeion marble quarries are located 25 km northeast of Afyonkarahisar and approximately 1.5 km south of today's Iscehisar city (Fig. 1). The İscehisar marble deposit area is in two sections. It consists of marble quarries, Dangic hill of 500×1300 m^2, and Bacakale areas of 1000x4500 m^2. Dokimeion marbles, which have been in operation for an ancient time, have a thickness of 100 m at Dangic hill and 260 m at the Bacakale section (Çelik and Sabah 2008).

İscehisar (Dokimeion) marble quarries have been working for thousands of years. Two types of stone were extracted in Dokimeion quarries in ancient times. In addition to the fine-grained and translucent white marble, generally preferred in the construction of sarcophagi and statues, another type of marble with purple veins called pavonazzetto was also produced. These marbles are well known in Turkey and throughout the world. Some of these marble types, also well known in the world markets, are characteristic of their white, violet, sugar, tiger skin, and gray colors. Fine-grained and pure white marble whose trade name is Afyon white marble was investigated in this study. Four samples were taken from İscehisar marble quarries for the characterization of Afyon white marble. Typical samples were selected for use in chemical and mineralogical-petrographic analysis techniques.

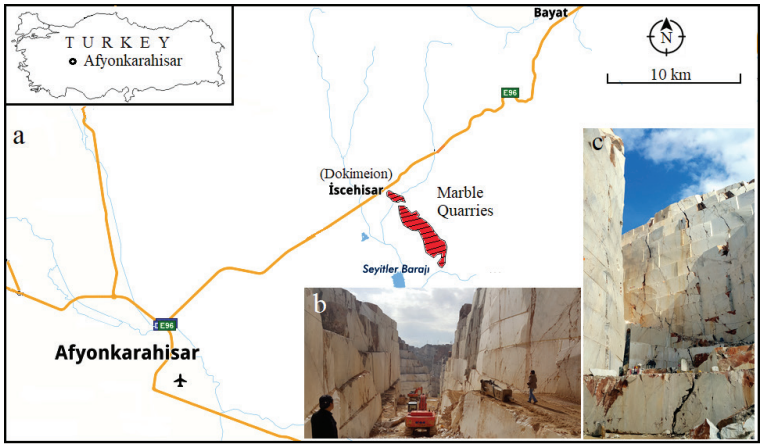

Figure 1. *The geographical location of İscehisar (Dokimeion) marble quarries (a) and view of modern marble quarry (b, c).*

İscehisar (Dokimeion) marbles are geologically divided into three units, considering their different grain sizes, colors, and minerals (Fig. 2). Afyon gray and tiger skin marbles form the lower units, Afyon sugar. Afyon white marbles form the central unit, and Afyon Violet marbles form the upper unit. The gray marbles in the lower unit are light gray and have a homogeneous appearance. It is a type of marble commonly found in many regional marble quarries. Afyon white marbles are the most homogeneous marbles in the marble zone. The central unit, whose dominant color is white, is composed of fine calcite minerals. Although it is more known, white marbles have fewer reserves than others. Medium-grained marble with delicate golden yellow veins is known as Afyon Sugar, which offers a different appearance than white marble. Afyon violet-colored marbles are

commonly found in the center of the marble zone. Purple, green, yellow, and violet colors are seen in these marbles (Sümer et al. 1997; Bağcı 2020; Çelik ve Sert 2020).

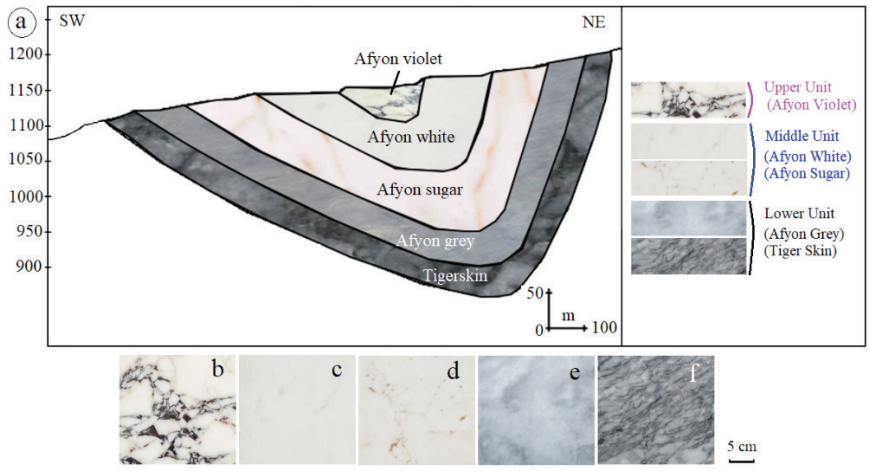

Figure 2. *Generalized geological cross-section (a) of the İscehisar (Dokimeion) marble area and trade names of the extracted marbles: Afyon violet (Pavonazzetto) (b), Afyon white (c), sugar (d), grey (e), and tiger skin (f) (Sümer et al. 1997).*

2.2. Methods

Chemical and mineralogical-petrographic (optical microscopy, maximum grain size (MGS) values, XRD, SEM) analyses were performed on Docimian (Afyon) white marble for material characterization. Two white marble samples from the Afyon-İscehisar marble quarry were analyzed for chemical content (major and trace elements). Whole-rock analyses were conducted at Acme Analytical Laboratories Ltd. (Vancouver, Canada). The determination of major and trace elements was determined by ICP analysis following lithium metaborate fusion of a 5 g white marble sample.

Determination of petrographic features such as primary mineral composition, structure, texture, and maximum grain size of calcite of the tested marble was performed with the help of optical microscopic analysis. The technique of optical microscopy was conducted using a Nikon Eclipse 2V100POL optical microscope mounted with a Nikon camera. MGS values were measured on images collected through a Nikon video camera using the Clemex Vision Lite software.

XRD (X-ray diffraction) analyses of the mineralogical compound of the Docimian (Afyon) white samples were carried out on powders from the

whole samples using a Shimadzu XRD- 6000 X-ray diffractometer housed at the laboratories of the Technology Application and Research Centre (TUAM), Afyon Kocatepe University. Powder diffraction patterns were obtained under the following conditions: Cu Kα X-ray (1.544 Å) with 30 kV, 30 mA energy, and scanned from 2 to 70° 2θ angle.

SEM-EDX (Scanning electron microscopy coupled with energy-dispersive X-ray spectroscopy) is a powerful device used to examine the material surfaces, and it gives useful information about the specimen microstructure with high resolution (Cardell et al. 2002). Scanning electron microscope (SEM) techniques were used to characterize the microstructure of carbon-coated Docimian white marble samples. SEM analysis was performed using an LEO 1430 VP model using an energy-dispersive X-ray spectrometer (EDS) equipped.

3. EXPERIMENTAL INVESTIGATION AND RESULTS

3.1. Physico-mechanical properties

The average physico-mechanical properties of Docimian white marble according to oguzmermer.com (2020) are given in Table 1. Docimian white marble's physico-mechanical properties were the apparent density of 2730 kg/m^3, low total porosity of approximately 0.7%, low water absorption by weight of 0.02%, the uniaxial compressive strength of 70 MPa, and compressive strength after frost 59 MPa.

Table 1. *Summary of some physico-mechanical properties of Docimian white marble (oguzmermer.com 2020).*

Tests	value
Density (real) (kg/m^3)	2730
Open porosity (%)	0.20
Total porosity (%)	0.70
Water absorption by weight (%)	0.02
Uniaxial compressive strength (MPa)	70.00
Flexural strength (MPa)	15.00
Compressive strength after frost (MPa)	59.00
Average abrasion resistance (cm^3/50 cm^2)	25.40

3.2. Analysis of chemical composition

Table 2 shows the oxides and major elements of the Docimian white marble obtained from ICP analyses, whereas Table 3 presents the concentrations of trace and rare-earth elements (REE) elements of the tested marbles. The concentration of CaO was determined as 55.35 and 56.08 wt%,

and MgO concentration of 0.14 and 0.49 wt% for the Docimian white marbles. Chemical analysis results are in agreement with XRD and SEM analyses proving the absence of dolomite minerals. The SiO_2 concentration ratios were determined as 0.53 and 1,08 wt% which can be associated with the presence of quartz minerals in the Docimian white marble. Some rare elements such as Na, Al, and Si represent silicate minerals. In this study, rare earth elements (REE) were found in trace concentrations in the Docimian white marble samples. Major elements (Fe, Ca, Na, Mg, Al, K, Ti, P, and S) were distributed as percentage concentrations in the Docimian white marble. According to chemical analyses, it was determined that the mean concentration of major element data is as follows, respectively; Ca as 37.09–39.12%, Na as 0.007–0.072%, Mg as 0.08–0.3%, Al as 0.01–0.36%, K as <0.01–0.05%, Ti as <0.001–0.007%, and Fe as <0.01–0.03% ranges.

Table 2. *Major element concentrations in wt % of oxide, total carbon (TOT/C), and sulfur (TOT/S) ratio in total content and ignition loss of the Docimian white marble.*

Component (wt%)	AB-1	AG-1	AK-1	AS-1	AS-2
SiO_2	0.98	0.53	1.08	0.58	0.53
Al_2O_3	0.12	0.06	0.65	0.18	0.17
Fe_2O_3	0.13	< 0.04	0.06	0.05	0.05
MgO	0.14	0.15	0.16	0.49	0.49
CaO	55.35	55.86	55.98	56.08	55.93
K_2O	< 0.02	< 0.02	0.07	0.04	0.04
Na_2O	< 0.01	< 0.01	< 0.01	0.05	0.02
TiO_2	< 0.01	< 0.01	0.02	< 0.01	< 0.01
MnO	0.01	0.01	< 0.01	< 0.01	< 0.01
P_2O_5	0.03	< 0.01	0.09	< 0.01	< 0.01
Cr_2O_3	< 0.001	< 0.001	< 0.001	0.002	0.004
LOI	42.8	42.9	41.5	42.1	42.3
TOT/C	12.42	12.53	12.42	12.75	12.64
TOT/S	0.03	0.02	0.01	< 0.01	0.02

Data on the abundances of trace and rare-earth elements (REE) are useful for geochemical investigations of natural stones. Isotopic and trace element analyses are used to accurately determine the origin of marbles. For this purpose, past studies mainly focused on rare and Sr elements (Mandi et al. 1995; Matthews 1997). Research to determine the origin of marbles has focused on elements that can replace Ca in the crystal lattice of $CaCO_3$. According to the principle of having a similar ionic radius, the elements that best replace Ca are Fe, Sr, Mn, and Mg (Attanasio et al. 2011). For this reason, these elements have been used by many researchers in the ancient

marble's provenance determination. For example, Attasino et al. (2011) reported the results of the strontium (Sr) analysis of the Docimian white marble between 67 and 311 ppm, average of 134 ppm. The notable match between the strontium (Sr) data (between 68 to 109 ppm) and the data of this study is clear. However, compared to the higher, and in a wide range, Mn (32 to 182 ppm) element data reported by Attasino et al. (2011), lower Mn data (between 15 to 74 ppm) were identified in this study. Furthermore, Sr and Mn data determined by various researchers for Dokimeion white marble data are as follows, respectively; Poretti et al. (2017) on average 123.62 ppm and 118.75 ppm; Moens et al. (1987) on average 95 ppm and 25.5 ppm, Bruno et al. (2015) Sr data on Dokimeion white marble as 85,8 ppm, Columbu et al. (2014) as 100 ppm, and Attanasio et al. (2013) as 99.7 ppm identified in their study. These Sr results approximately confirmed the data of the current study.

Table 3. *Geochemical (trace and REE) concentrations in ppm of the typical sample of Docimian white marble.*

Element		AB-1	AG-1	AK-1	AS-1	AS-2	Element		AB-1	AG-1	AK-1	AS-1	AS-2
Mg	%	0.08	0.09	0.1	0.28	0.3	Cu	ppm	1	0.5	<0.1	<0.1	0.9
Na	%	0.007	0.059	0.054	0.072	0.071	Ag	ppm	<0.1	<0.1	<0.1	<0.1	<0.1
Al	%	0.02	0.01	0.36	0.09	0.15	Mo	ppm	<0.1	<0.1	0.1	0.1	0.1
Ti	%	<0.001	0.003	0.007	0.003	0.001	Pb	ppm	0.7	0.5	0.7	0.4	0.9
K	%	<0.01	<0.01	0.05	0.03	0.03	Ba	ppm	3	3	7	6	9
Fe	%	0.02	<0.01	0.01	<0.01	0.03	Zn	ppm	1	1	1	<1	2
Ca	%	38.43	39.12	37.09	37.54	38.92	Cr	ppm	0.8	0.4	1.6	0.1	1.3
S	%	<0.1	<0.1	<0.1	<0.1	<0.1	Ni	ppm	<0.1	3.5	1.8	1.5	1.8
P	%	0.009	0.003	0.025	0.001	0.001	La	ppm	0,2	0,4	1,2	1,3	1,1
As	ppm	3	4	2	3	3	Ce	ppm	<1	<1	2	1	1
Mn	ppm	74	68	34	15	42	Y	ppm	0.3	2	1.1	1	1.3
Cd	ppm	<0.1	0.1	0.1	0.1	0.1	Zr	ppm	0.1	0.9	1.9	0.9	1.3
W	ppm	<0.1	<0.1	<0.1	<0.1	<0.1	Ta	ppm	<0.1	<0.1	<0.1	<0.1	<0.1
Au	ppm	<0.1	<0.1	<0.1	<0.1	<0.1	Be	ppm	<1	<1	<1	<1	<1
Th	ppm	<0.1	<0.1	0.3	0.1	0.1	Nb	ppm	<0.1	<0.1	0.4	0.1	0.1
Sr	ppm	76	68	73	103	109	Sn	ppm	<0.1	<0.1	0.1	<0.1	<0.1
U	ppm	0.1	0.1	0.1	0.1	0.2	Li	ppm	0.1	0.1	3.3	0.2	0.3
Sb	ppm	1.5	3.9	1.6	1.5	1.5	Sc	ppm	<1	<1	1	<1	1
Bi	ppm	<0.1	<0.1	<0.1	<0.1	<0.1	Hf	ppm	<0.1	<0.1	0.1	<0.1	<0.1
V	ppm	<1	1	<1	3	6	Rb	ppm	0.2	0.1	1.1	0.8	1.2
Co	ppm	<1	<1	<1	<1	<1							

3.3. Petrographic - mineralogic analysis

3.3.1. Polarizing optical microscope analysis

Thin section investigations of the marbles provide important information about the calcite grain boundaries. Straight grain boundaries are formed depending on the long-term balance of metamorphism conditions. The sutured boundaries in interlocking crystals formed by pressure occur under short metamorphism conditions (Gorgoni et al. 2002). Particular attention should be paid to the petrographic features that enable the description of the marbles. These petrographic parameters are of maximum grain size (MGS), textures, and grain boundary shape. Thin sections used in polarized microscope observations are made from selected four-piece Docimian white marble samples. Docimian white marble is generally composed of calcite minerals with polysynthetic twinning. Docimian white marble has calcite minerals with variable grain size and irregularly sutured boundaries. Calcite crystals have a heteroblastic texture (Fig. 4).

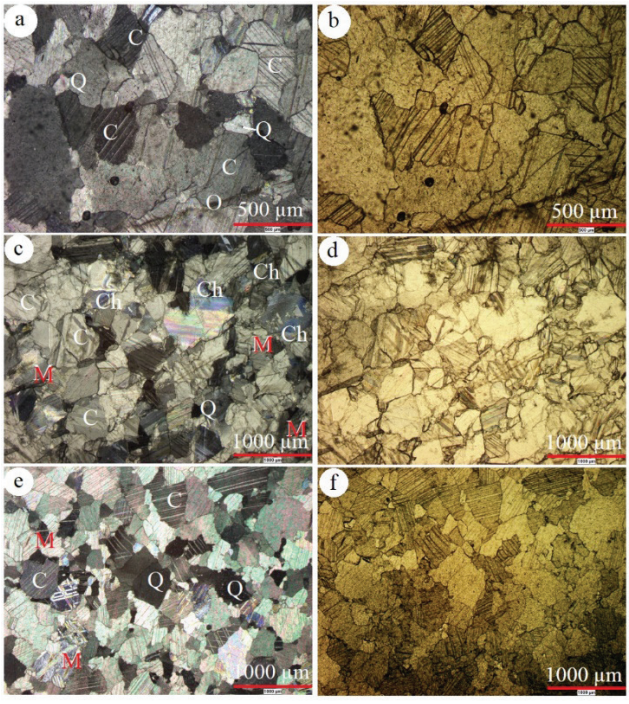

Figure 4. *Petrographic features of Docimian white marble under a polarizing microscope (XPL-cross-polarized light: a, c, e); (PPL-plane-polarized light: b, d, f). (C: calcite, Q: quartz, Ch: chloride, M: muscovite, O: opaque mineral)*

MGS (maximum grain size) is one of the most frequently used parameters, especially in ancient marble characterization studies. The grain size measurements of the calcite grains forming the Docimian white marble were measured in 6 different thin sections with a polarizing microscope. Maximum grain size (MGS) data measured from thin sections are given in Table 4. 56, 161 243, 263, 255, and 175 calcite grains were measured in each of the 6 measurements from thin sections, respectively. A wide range of MGS was measured on the Docimian white marble ranging from 18.5 to 1009.5 μm in length. The largest grain sizes measured in each measurement were 679.1, 702.4, 1009.5, 717.4, 757.6, 759.6, and 770.9 μm, and the smallest particle sizes were 33.5, 27.9, 37.8, 48.1, 18.5, 45.1, and 35.2 μm, respectively. According to the measurement results, the mean grain sizes were 242.2, 284.1, 210.7, 218.1, 207.8, 282.2, and 240.9 μm in each measurement, respectively.

According to the size of the calcite grains that make up the marble, marbles are classified as fine-grained (<2 mm), medium-grained (2–5 mm), and coarse-grained (>5 mm) (Antonelli and Lazzarini 2015; Ahmad 2018). Alternatively, marble calcite grain boundaries can be classified as curved, straight, sutured, and embayed according to their shape (Spry 1969; Ahmad 2018). The average grain size of the calcite crystals forming the Docimian white marble was measured between 18.5–1009.5 μm. The tested white marble samples are all fine-grained calcitic marbles.

Table 4. *MGS values of calcite grains measured in the Docimian white marbles (DWM).*

Sample	Count	Min	Max	Mean
DWM-1	56	33.5	679.1	242.2
DWM-2	161	27.9	702.4	284.1
DWM-3	243	37.8	1009.5	210.7
DWM-4	263	48.1	717.4	218.1
DWM-5	255	18.5	757.6	207.8
DWM-6	175	45.1	759.6	282.2
Mean	1153 (total)	35.2	770.9	240.9

Among the petrographic and mineralogical features used in the description of marbles, maximum grain size (MGS) is of great importance. For this reason, many researchers have conducted studies on this subject. In some of these studies, the maximum grain size data were reported for Dokimeion white marble (Table 5). For example, in the Docimian white marble, Bruno et al. (2015) measured MGS between 500 to 1500 μm, while Antonelli and Lazzarini (2015) measured MGS between 300 to 2100 μm.

Table 5. *Maximum grain size (MGS) mean values of Docimian white marble were reported by researchers in the literature.*

Determined by	Min (μm)	Max (μm)	Mean (μm)
Bruno et al. (2015)	600	1500	1100
Bruno et al. (2015)	500	1400	800
Bruno et al. (2015)	600	1200	800
Antonelli and Lazzarini (2015)	300	2100	
Attasino et al. (2006)	500	1500	860
Attasino et al. (2011)	240	860	
Attasino et al. (2011)	280	1080	
Attasino et al. (2011)	250	830	
Attasino et al. (2011)	150	770	
This study	35.2	770.9	240.9

3.3.2. X-ray diffraction analysis

The accessory minerals may not be observed in thin section examinations made from a small piece that does not represent the whole marble sample. Therefore, a detailed description of the mineral composition of marble should be based not only on microscopic observations (petrographic and SEM) but also on X-ray diffraction analysis. The X-ray diffraction method was used to determine the basic and accessory minerals of Docimian white marble. Mineralogic analysis via XRD showed that the major mineral phase in Docimian white marble is calcite (Fig. 5). Dolomite not be identified. Therefore, Docimian white marble was calcitic marble, not dolomitic marble. Other mineralogical components and impurities are also present. They are mainly quartz and mica (muscovite) minerals.

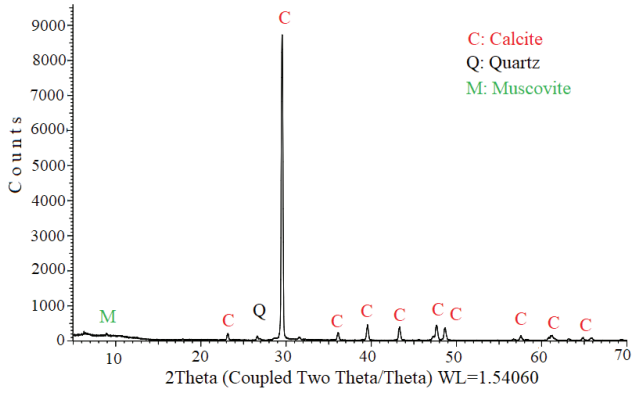

Figure 5. *XRD patterns of the Docimian white marble*

3.3.3. SEM analysis

SEM-EDX (Scanning electron microscopy coupled with Energy-dispersive X-ray spectroscopy) is a powerful device used to examine the material surfaces and gives useful information about the specimen microstructure with high resolution (Cardell et al. 2002). The Docimian white marble samples were investigated using SEM-EDS to identify their calcite minerals boundaries, pores between crystals, and microstructure. According to SEM-EDX observations, Docimian white marble consists of calcite united with each other in a granular texture. Among the calcite minerals, a few elongated mica minerals (muscovite) have been observed (Fig. 5).

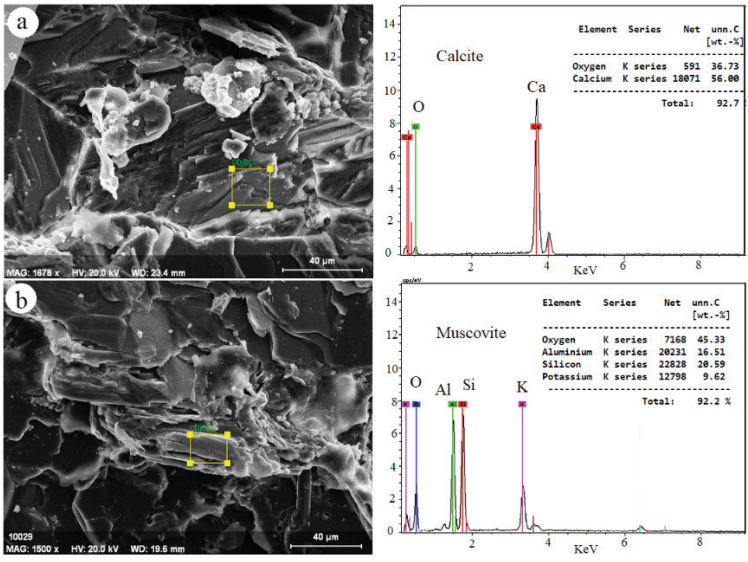

Figure 5. *SEM images and EDX analysis of calcite (a) and muscovite (b) mineral in Docimian white marble.*

4. PRODUCTION AND DISTRIBUTION OF DOCIMIAN WHITE MARBLE IN ANCIENT TIMES

4.1. Docimian white marble quarry in ancient times

Docimian marble known as Phrygium marble, Phrygian marble, or Synnadic (modern Şuhut) marble, a famous fine-grained white marble in ancient times was extracted from the ancient Dokimeion or Docimium, in central Phrygia, Asia Minor (Koch, 2001). Dokimeion (İscehisar) marble quarry was undoubtedly a famous and important quarry area in the ancient Roman world and, still supplies most of the marble utilized in modern Turkey (Attanasio 2003). Röder (1971) expressed quarrying operations were

intensified at the Bacakale section in the Dokimeion marble quarry. Quarry operations have caused a pit of 200 m in length, 80–110 m in width, and 40–5 m in depth in ancient times.

Röder (1971) has offered the pavonazzetto marble was extracted from this quarry and was employed mainly for constructions decreed by the Emperors that reigned during the middle of the II century AD. It was determined that there were 350 quarry inscriptions on Dokimeion's famous colored marble pavonazzetto blocks. Interestingly, the very high-quality white marble blocks, which were also worked by the Romans at Docimium, were not marked with similar inscriptions (Fant 1988b). The Docimium quarries own and run by an imperial bureau, as is obvious from inscriptions that testify to the organization of the quarrying (Fant 1989; Drew-Bear 1994; Hirt 2010). Considering that Pavonazzetto marble was extracted with Roman Imperial bureau ingenuity in these inscriptions and that information about them was included in the abandoned marble blocks, it can be concluded that there was no official intervention in white marble production (Waelkens 2019).

Modern quarry workers look for ancient quarries to find quality marble reserves. The presence of modern quarrying everywhere in Turkey threatens the preservation of ancient marble quarries as archaeological sites. Unfortunately, much of the evidence for ancient quarrying has been lost over time, and this situation is also valid for İscehisar-Afyon (Dokimeion) quarry site. İscehisar–Afyon marble quarries were intensively operated during the early Roman Empire and are still active today. The importance of the İscehisar–Afyon quarries is because traces of ancient stone cuts (Fig. 6) from the Roman periods are still visible and much half-worked material evidence is found.

Archaeological investigations of the İscehisar–Afyon (Dokimeion) quarries have yielded a large corpus of material testifying to their long activity in ancient times. Semi-worked sculptures, as well as architectural materials abandoned during the Roman Empire, have contributed much to the scholarly understanding of how ancient craftsmen worked with the marble blocks in the quarry (Fant 1989; Attanasio 2003). Nowadays, many semi-worked artifacts of all types and sizes made of Docimian white marble from the ancient quarries and abandoned on the site are exhibited in the İscehisar streets (Fig. 7). Fant (1985) reported that four unfinished sarcophagus lids were found in the quarries at Dokimeion (İscehisar) in central Phrygia. These finds have shown that the Dokimeion (İscehisar) quarries produced not only the well–known pavonazzetto but also high-quality white marble.

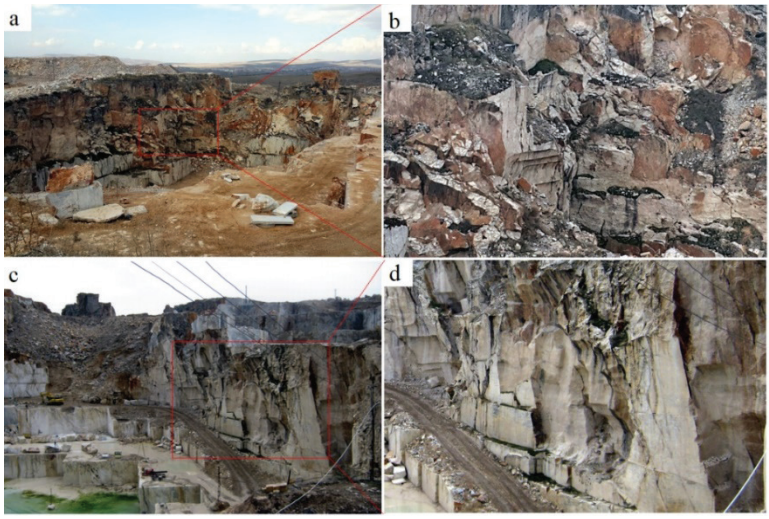

Figure 6. *The view of the ancient stone cut marks and details of the Docimian white marble quarry in İscehisar (ancient Dokimeion) (Çelik and Sert 2020).*

4.2. Distribution of Docimian white marble in ancient times

White marble was usually employed as building materials and colored stones for decoration. The systematic organization of quarrying and trade was not fully developed until the times of the Roman Empire when quarries became Imperial property. However, techniques for lifting and controlling the up-and-down transport were developed much earlier, and huge blocks of marble were moved long distances from the quarries to the construction sites (Freccero 2015). Construction in marble was an expensive business with transport costs sometimes many times greater than the quarrying costs, and this remained true in the Roman period (Burford 1960; Dodge 1988). The ancient Romans built an excellent system of roads, and it included a network of long-distance roads, primarily for military and administrative purposes, but that, nevertheless also served commercial transport (Berechman 2003). Indeed, Waelkens (1982) stated that the columnar sarcophagi were distributed along roads leading from Dokimeion to the north, west, and south coasts of Anatolia. (Hirt 2010) reported that Docimian marble was probably transported via Synnada (modern Şuhut), Apameia (modern Dinar), and Laodicea, down the Maeander to Tralles (modern Aydın), and then to the Port of Ephesos (Fig. 8). Waelkens (2019) stated that both pavonazzetto columns and blocks and sarcophagi in white Docimian marble must have traveled along the same roads. Thus, the marble blocks came down from the mountains to the seaside via a route ending at Ephesos where it would be loaded on ships headed for Rome.

Figure 7. *Antique architectural materials made in Docimian white marble, exhibited on the streets of İscehisar, extracted from the ancient Dokimeion marble quarry.*

Figure 8. *Docimian marbles transportation way map in the Dokimeion-Ephesus route during the Roman Empire (modified from Waelkens 1982; map source: Åhlfeldt 2020).*

Semi-worked architectural pieces and sculptural materials such as white marble blocks and sarcophagi were known to be transported to Rome from Northern Italy, Asia Minor, and Greece (Russell 2015). The marble blocks to be moved were often very large, heavy, and sometimes delicate. However, these blocks had to be moved to their final destination. The distances to be traveled were quite problematic, either by land or by sea transport. The transportation of marble produced from stone quarries, which are located at great distances was based on ship transportation in ancient times. The most important evidence, proving the export of Docimian marble from

the quarry to all of the Mediterranean area, is many shipwrecks with stone cargoes detected on different coasts.

Five ancient shipwrecks have been found in the sea off Croton, in southern Italy, each carrying marble cargo composed of massive blocks, column shafts, and smaller artifacts. Two of the ships (marble carriers) are located in the bay of Punta Scifo and, therefore, are identified as the Punta Scifo A and Punta Scifo B shipwrecks (Rice 2016). It was determined that the shipwreck came from Asia Minor and all the marble artifacts it carried were the origin of Proconnesus and Dokimeion quarries. The most likely point of departure was either Ephesus or Miletus. Therefore, the Punta Scifo A shipwreck may represent archaeological evidence to connect quarried marbles to their destination. This example is very important in the process of supply, transportation, and final use of the Dokimeion quarry materials (Bartoli 2008). Numerous marble products were raised from the Punta Scifo A shipwreck. Six of these marble artifacts exhibited at the Caputi Square (Croton) and Naval Museum (Capo Colonna) are different from the others. According to Pensabene (1978), these six marble artifacts (three bases and three Ionic capitals) came from Docimium, but they are not pavonazzetto marble. It is a whiter type of stone called White Synnadic (Fig. 9).

5. Use of the Docimian white marble in ancient times

While the numerous white marble quarries in Phrygia supplied local (Central Anatolia) city centers, the pavonazzetto quarried at Dokimeion, were extracted in whole quantities for the Mediterranean region markets. Production at these quarries reached a peak during the early to mid-second century AD. In Bacakale-Dokimeion, the largest quarry at the site, pavonazzetto was extracted in vast quantities. In the Dokimeion quarries (Bacakale), white marble was also quarried and extensively used in ancient times. Smaller adjacent quarries in the Dokimeion site exploited the less highly valued white marble, which was available in large blocks and was used to produce gravestones, sculptures, sarcophagi, and great columns (Fant 1985; Lazzarini et al. 1985). Waelkens (2019) reported that most of the products of the workshop were high-status sarcophagi made for the upper strata of society, particularly in Italy and the eastern Mediterranean (above all Asia Minor). He points out at the same time that lesser-skilled craftsmen also produced simpler tombstones and small statuary for the middle classes of a regional market. The white marble used by the Docimian sarcophagus workshop may be exploited locally from the fifth century BC on. A group of very early Hellenistic grave stelae (the late fourth century BC) from the vicinity of Dokimeion (Sülümenli, Synnada, and Dokimeion proper) is seemingly made of Docimian marble as well. By the third

quarter of the first century BC, it was already exported to Italy for large sculpture (Thonemann 2013; Waelkens 2019).

5.1. Use of the Docimian white marble as an architectural material in ancient times

Since the first century AD, Docimian white marble has been used in many buildings and monumental structures as architectural materials (architrave, cornice, column, pedestal, frieze, capital, and floor slab) in different parts of Anatolia. The famous luxury marble products from the Dokimeion quarries were extensively exported to the Rome and Mediterranean region in the second and third centuries. However, Docimian white marble has more regional use in Late Antiquity. Most of the products of the Dokimeion workshop in Late Antiquity were intended for local outlets in the western part of Central Anatolia. Like pavonazzetto marble and white marble sarcophagi, Corinthian pilaster capitals from Dokimeion are distributed across West Anatolia and the Mediterranean region (Kramer 1994; Niewöhner 2013).

The Corinthian capitals of the Zeus Temple at Aizanoi (Kütahya, Turkey) were carved from Docimian white marble, the chief material of high-quality stone masonry in central Anatolia (Jes 2002; Niewöhner 2013). Corinthian pilaster capitals and cladding in white marble abound at Sagalassos were imported from a workshop at Dokimeion from the second century AD on (modern Ağlasun, Burdur-Turkey) (Waelkens 2019; Waelkens et al. 2019). The demand for white and gray marble in Sagalassos was satisfied with the Docimian marble quarry (Corremans et al. 2009). A large number of Corinthian capitals, made of white Docimian marble are registered in the inventory of various country museums. Some of these are the: Corinthian capital with an eagle on the abacus beside the propylon of South Baths (Perge), the Corinthianizing capital in the South Severan Nymphaeum (Perge), Corinthian capital (Istanbul Archaeological Museum), Corinthianizing pilaster capital with Silenus (Museum of Fine Arts, Boston) (Herrmann and Tykot 2009). The marble trade also to the eastern Mediterranean area, including Jordan, thrived due to its extensive use in construction. Al-Bashaireh and David (2015) reported that there was a Corinthian capital made of white Dokimeion marble next to artifacts mostly of Proconnesos origin at ancient Gadara (Jordan).

Figure 9. *The bases (a, b) and Ionic capitals (c, d) are made of Dokimeion white marble extracted from the Punta Scifo A shipwreck (Bartoli 2008).*

Bruno et al. (1999) reported that in the Baths of Caracalla (Rome, Italy) most of the white marble was Prokonnesian and Pentelic but a few blocks of Luna and Docimian marble were also identified. Samples taken from a white marble architrave in Tauriana (Palmi, Italy) were determined to be of Docimium origin (Luca et al. 2020). Inherently, wall and floor veneer in the form of slabs can be transported to a construction site rather easily than columns. For this reason, Docimian white marble was used as the floor and wall covering in important monumental buildings in Anatolia and many Roman city centers. Corremans et al. (2009) reported that at Sagalassos, although local stone was preferred for mosaic floors, the large majority of the materials used for the polychrome opus sectile floor panels of the Imperial Baths and its wall revetment was imported from the Dokimeion quarries. The white marble used in the Heliocaminus Baths (Hadrian's Villa) come from Carrara quarries (Italy), but it was determined that the walls covering the Heliocaminus room (outside the swimming pool) came from the Dokimeion (İscehisar, Afyon, Turkey) quarries (Salvatori et al. 1988; Columbu et al. 2014). Ricca et al. (2015) reported that a detailed and multidisciplinary study was conducted on white marble taken from the submerged archaeological site of Baia (Naples, Italy). According to this multidisciplinary study, Dokimion white marble was also among the different varieties of marble used in the floor covering of this ancient Roman city. The fruit garland frieze of the temple of the emperor cult at Pessinus (modern Ballıhisar, Eskişehir, Southwestern Galatia) demonstrates that Docimian white marble was used in Anatolian monumental architecture (Devreker et al. 1995; Waelkens 2019).

5.2. Use of the Docimian white marble as sarcophagus in ancient times

Three main centers were identified in the production of the sarcophagus in the Roman Imperial period. These are Rome city, the capital of the Empire Athens, the important center of the Classical age, and the Dokimeion (İscehisar, Afyon) marble workshop in Phrygia. Apart from these three centers, there are sarcophagus workshops, but these have produced relatively low-quality or fewer works (Koch 1993). The use of sarcophagi has a long past in particular regions in Asia Minor. During the Roman imperial ages, the major production center of Asiatic sarcophagi was Dokimeion in Phrygia. The Dokimeion workshop specialized in large-scale sarcophagi with a colonnade's architectural form. These sarcophagi called the Dokimeion Colonnades type were decorated with high relief on all four sides, and fluted columns occurred around all four sides. Male and female figures are placed in arched niches separated in the inter-columniations, and a doorway motif occurs on one side. Other cities in Asia Minor also produced large quantities of sarcophagi, and some followed this architectural format (Awan 2000). Waelkens (2019) pointed out that the Docimian sarcophagus workshop produced not only so-called columnar sarcophagi but also various other types belonging to the so-called Hauptgruppe (main group) of Anatolian sarcophagi such as Pamphylian garland sarcophagi.

At least 10,000 Roman sarcophagi have survived, with fragments possibly representing as many as 20,000 (Elsner et al. 2010). Approximately 500 items of sarcophagi produced at Dokimeion in various stylistic types, including garland, figured-frieze, and columnar sarcophagi, have survived to date. Two hundred and thirty examples survive of the columnar sarcophagi, making it the most commonly produced type from the Dokimeion workshop (Pierucci 2017). There are approximately 105 fully or mostly preserved chests and approximately 700 fragments of marble sarcophagus chests and lids in Aphrodisias (the ancient city of Caria-Asia Minor). The columnar sarcophagi are approximately 215 in total (15 fully preserved chests or front panels and ca. 200 fragments from chests) (Öğüş 2014). In Aphrodisias, 27 extant items of the sarcophagus were found referring to the Dokimeion sarcophagus made of Phrygian marble in terms of form and decoration, but they have differed from the Dokimeion sarcophagus in a few respects (Öğüş 2018).

Dokimeion marble is found in many architectural monuments in the Mediterranean region, but the sarcophagi are also found at sites where Dokimeion marble is absent from buildings. One of the best of the best known of which is a luxury columnar sarcophagus exported to regions in Anatolia and the Mediterranean region. The most characteristic example of

this type of sarcophagus is the Sidamara sarcophagus (found in the village of Ambar, approximately 100 km south-east of Konya-Turkey) on exhibition at the Istanbul Archeology Museum (Fig. 10-a) (Niewöhner 2013). The Antakya sarcophagus is one example of the Dokimeion columnar sarcophagi, found in Antakya, Turkey in 1993, and is now exhibited in the Hatay Museum (Fig. 10-b). Garland sarcophagus (Baltimore Walters Art Museum) must have been produced in a specific workshop operating near the ancient Dokimeion quarry in Phrygia in Asia Minor. It was excavated from the Licinian tomb in Rome in 1885. It shows that this sarcophagus found in Rome was produced in the Dokimeion in Phrygia in Asia Minor and then exported to the city of Rome (Fig. 10-c). The Pamphylian (Achilles) sarcophagus was exhibited at the Museum of Art (Rhode Island) (Fig. 10-d), and the Rapolla sarcophagus was exposed at the Melfi National Museum (Italy) (Fig. 10-e). It became clear that the Heracles sarcophagus (235 cm long, 112 cm wide, and 3-ton weight) was seized in Geneva Custom in 2012, it was abducted from Perge (Antalya) in the 1960s. It was later seen at customs clearance in Switzerland in Geneva in 2010. After seven years of negotiations, it was in 2017 when the Turkish government could, fortunately, succeed in getting the Herakles sarcophagus back to Turkey and transferring it to the Antalya Archaeological Museum (Fig. 10-f).

Exhibited in Turkey and other countries museums and identified as made of Docimian marble, many sarcophagi listed by Waelkens (2019) and Waelkens et al. (2019). These sarcophagi are a garland sarcophagus from Side (Antalya Museum), a garland sarcophagus from Perge (Antalya Museum), a garland sarcophagus from Konya (Konya Museum), a garland sarcophagus from Ikonion (Konya Museum), garland sarcophagus from Synnada (Afyon Museum), garland sarcophagus from Apamea (Afyon Museum), frieze sarcophagus from Yalvaç (Yalvaç Museum), frieze sarcophagus (Dodekathlos of Heracles) from Caesarea Cappadocia (Kayseri Museum), columnar sarcophagus (Labors of Heracles) from Perge (Antalya Museum), the columnar sarcophagus (Dodekathlos of Heracles) from Perge (Antalya Museum), garland sarcophagus from Rome (Vatican Museum, Belvedere), columnar sarcophagus from Athens (British Museum), the columnar sarcophagus from Rome (twelve labors of Hercules) (Roma Villa Borghese Museum), columnar sarcophagus (Hunting sarcophagi) from Xanthus (British Museum), and columnar sarcophagus from Rome (Rome Torlonia Collection).

5.2. Use of the Docimian white marble as sculpture in ancient times

The two major categories of Roman sculpture are portraiture and relief sculpture although there is an overlap between the two types since some

portraits were executed in relief and some reliefs include distinctive portraits. There are three other major categories of Roman sculpture. The first is Roman idealizing sculpture, which represents divinities, mythological figures, heroes, and athletes with generic features. The Roman decorative sculpture was also produced in abundance and included such items as candelabra and table support used in civic, religious, and domestic contexts. Examples of the third category, minor arts, are not strictly speaking sculptures, and they must therefore be evaluated with monumental sculpture (Kleiner 1992)

Figure 10. *The examples of the Dokimeion type sarcophagus. Sidamara sarcophagus (İstanbul Archeology Museum) (Anon 1 2020) (a), Antakya sarcophagus (Antakya Archaeological Museum) (Anon 2 2020) (b), Garland sarcophagus (Baltimore Walters Art Museum) (Anon 3 2020) (c), Pamphylian (Achilles) sarcophagus (Museum of Art-Rhode Island) (Anon 4 2020) (d), Rapolla sarcophagus (Melfi National Museum, Italy) (Anon 5 2020) (e), Heracles sarcophagus (Antalya Archaeological Museum) (Waelkens 2019) (f).*

There are many sculptures and sculpture pieces made of Dokimeion white marble in Anatolia, which was the source of marble and museums in many countries of the world. Although there was original confusion between similar fine-grained marbles in the past, today a precise definition can be made with advanced analysis methods. Tyche-Fortuna goddess sculpture was carved of Docimian white marble, it extracted from Cremna

(present-day near Bucak, Turkey) in Pisidia, and it has been exhibited in the Museum of Fine Arts, Boston (Fig. 11-a). Again, in the same museum, various statues and busts made of Docimian white marble-like Votive relief to the god Mên, Hunter with the dog, Hygieia, the goddess of Health and Hypnos (Fig. 11-b), Portrait head of Emperor Domitian, and Head of Alexander the Great are exhibited. In the Sleeping Ariadne (Cleopatra) sculpture, the head and the lower part of the body are also carved in Dokimeion marble, housed in the Vatican Museums in Vatican City, it is a Roman Hadrianic copy of a Hellenistic sculpture. The Sleeping Ariadne (Cleopatra) sculpture was a famous sculpture of Antiquity. The figures of a sculpture were identified as Heracles and Telephos, unearthed during the construction of Eskişehir, Seyitgazi municipality building in 1987. The sculpture was carved from white marble, which was most probably extracted from the nearby Docimium quarries (Fig. 11-c) (Akkan 2005; Çalik-Ross 2013).

Bruno et al. (2015) indicated that the fine-grained and uniformly white or slightly honey-colored marble of the Sperlonga sculpture groups is now definitely proven to be Docimium marble from the Phrygian quarries of İscehisar. Sperlonga sculptures Polyphemos, Sculpture of Scylla attacking Odysseus ship, and Pasquino Groups, Theft of the Palladium sculpture group, and Ganymede sculpture were discovered in 1957 at the Grotto of Tiberius in Sperlonga (Italy) (Fig. 11-d). The National Museum of Archaeology of Sperlonga was opened to house these interesting sculptures in 1963. Lapuente et al. (2012) indicated that the analytical results confirm that different classical white marbles (Afyon, Pentelic, Paros, and dolomitic Thasos) were used for sculpturing purposes at Villa Adriana (Tivoli, Italy). Attanasio et al. (2011) pointed out that the trace element composition (especially Sr and Fe) could distinguish Dokimeion and Göktepe marbles perfectly and stated that the Dying Gaul sculpture (Capitoline Museum, Rome) was made of Dokimeion marbles (Fig. 11-e). Çelik (2019) reported that a naked sculpture of Aphrodite, probably made of Dokimeion white marble (with fine-grained), was found at the North Bath of the ancient city of Perge (Antalya, Turkey) during the excavation season in 2015. The Aphrodite sculpture exhibits in the Antalya Archaeological Museum. Pensabene et al. (2012b) indicated some sculptures in Hadrian's Villa (Tivoli, Italy) such as the head of Hadrian of Lunense, the Amazons, Hermes, and most likely the sculpture of Ares are made of Dokimeion white marble.

Figure 11. *Sculpture samples carved from Docimian white marble: Tyche-Fortuna goddess sculpture (Museum of Fine Arts, Boston, USA) (Anon 6 2020) (a), Hygieia, goddess of Health and Hypnos sculpture (Museum of Fine Arts, Boston) (Anon 7 2020) (b), Heracles and Telephos sculpture (Eti Archaeological Museum, Eskişehir, Turkey) (Akkan 2005) (c), Sculpture of Scylla attacking Odysseus ship (The National Museum of Archaeology of Sperlonga, Italy) (Platts 2006) (d), Dying Gaul sculpture (Capitoline Museum, Rome, Italy) (Anon 8 2020) (e).*

6. DISCUSSION AND CONCLUSIONS

During the past decades, several scientific methods have been used to determine the provenance of ancient marble. Archaeometry studies of ancient marbles require the collaboration of experts in various interdisciplinary fields (i.e., archaeology, architecture, art history, conservation, archaeometry, mineralogy, petrography, and geochemistry). Researching materials such as architectural pieces, sculptures, and sarcophagi made of ancient marble is also important in terms of revealing the preferences of ancient craftsmen and artists. Also, one of the tasks of archaeometry is to verify the origin of the marble material used to make various objects and sculptures found in museums and other archaeological collections by petrographic and geochemical studies.

Docimian white marble is composed of calcite crystals with an average grain size between 18.5 to 1009.5 μm. Calcite crystals exhibit a typical heteroblastic texture with clear evidence of stress in a strained fabric. Calcite crystals show sutured boundaries. Boundary grain shapes are mostly embayed, and curved and straight ones can be recognized. Moreover, calcite crystals in the white marbles with perfect cleavages exhibit polysynthetic twinning. According to the data obtained by polarizing optical microscope analysis, Docimian white marble is in the class of fine-grained calcite marbles.

In the Dokimeion quarries, besides the famous-colored marble pavonazzetto of the ancient period, fine-grained white marble type was also produced. White marbles were the most popular stone material for architectural pieces, sarcophagi, and sculptural products during ancient times. The workshops in Dokimeion in Phrygia produced several hundred sarcophagi that were then exported throughout Asia Minor and other regions in the Roman empire. Dokimeion quarries were not only a prominent source of marble for statuary, columns, and decorative building elements but even more so for the wall and floor veneer in ancient times.

In general, it shows that the minor and trace element concentrations and granulometric (Maximum Grain Size measurement) data obtained in this study can contribute significantly to the archaeometry description of Docimian white marble. Docimian white marble artifacts have an important position in historical and cultural buildings and monuments in all countries. The information obtained after the characterization studies are critical in new architectural and restoration projects where Docimian white marble will be used as a decorative stone. It is considered that the benefits of current work will contribute to the practical repair of the Docimian white marble artifacts in future conservation and intervention strategies.

REFERENCES

Åhlfeldt J (2020) Digital Atlas of the Roman Empire. Centre for Digital Humanities University of Gothenburg, Sweden. http://imperium.ahlfeldt.se/Accessed 1 November 2020

Ahmad A (2018) Archaeometric and provenance study of archaeological marble from Gadara and Gerasa in Jordan. Appl Phys A 124, 514 https://doi.org/10.1007/s00339-018-1940-7

Akkan RB (2005). The type of Herakles in Phrygia bye the help of Herakles statues which are protects in Eskişehir, Kütahya and Afyon (in Turkish). MSc Thesis. Anadolu University

Al-Bashaireh K, David L (2015) Dettman geochemical analyses and provenance determination of white marble samples from Churches in North Jordan. Bulletin of the American Schools of Oriental Research, 374:49–59

Albustanlıoğlu T (2002) Dokimeion mermer ocaklarının işletme ve ihracat organizasyonu (in Turkish). Anadolu Medeniyetleri Müzesi 2001 Yıllığı (16):276–294

Albustanlıoğlu T (2013) Inscriptions at the Roman Imperial quarry and some unique samples. Journal of History Culture and Art Research 2(4):55-77 (in Turkish) https://doi.org/10.7596/taksad.v2i4.209

Anon 1 (2020) https://www.facebook.com/turklandtravelagency/photos/pcb.507422523363986/5074 22380030667 Accessed 5 November 2020

Anon 2 (2020) https://www.picuki.com/media/2064556382916568735 Accessed 3 November 2020

Anon 3 (2020) https://commons.wikimedia.org/wiki/File:Roman_-_Garland_Sarcophagus_-_Walters_2329.jpg Accessed 6 November 2020

Anon 4 (2020) https://risdmuseum.org/art-design/collection/sarcophagus-coffin-21074 Accessed 6 November 2020

Anon 5 (2020) https://media-cdn.tripadvisor.com/media/photo-s/1a/4b/d7/24/sarcofago-di-rapolla.jpg Accessed 6 November 2020

Anon 6 (2020) https://collections.mfa.org/objects/151190 Accessed 8 November 2020

Anon 7 (2020) https://collections.mfa.org/internal/media/ dispatcher/915118/preview Accessed 8 November 2020

Anon 8 (2020) https://www.nga.gov/content/dam/ngaweb/exhibitions/pdfs/2013/dyinggaulfinalbrochure.pdf Accessed 8 November 2020

Antonelli F, Lazzarini L (2015) An updated petrographic and isotopic reference database for white marbles used in antiquity. Rend Fis Acc Lincei 26:399–413 https://doi.org/10.1007/s12210-015-0423-4

Attanasio D (2003) Ancient White Marbles. Analysis and Identification by Para-

magnetic Resonance Spectroscopy. L'Erma di Bretschneider, Rome

Attanasio D, Brilli M, Ogle N (2006) The Isotopic Signature of Classical Marbles. L'Erma di Bretschneider, Rome

Attanasio D, Bruno M, Prochaska W (2011) The Docimian marble of the Ludovisi and Capitoline Gauls and other replicas of the Pergamene Dedications. American Journal of Archaeology 115(4):575–587 https://doi.org/10.3764/aja.115.4.0575

Attanasio D, Bruno M, Prochaska W, Yavuz AB (2013) The Asiatic marbles of the Hadrian's Villa at Tivoli. Journal of Archaeological Science 40:4358–4368 https://doi.org/10.1016/j.jas.2013.06.032

Awan HT (2000) Roman Sarcophagi. In Heilbrunn Timeline of Art History. New York: The Metropolitan Museum of Art. http://www.metmuseum.org/toah/hd/rsar/hd_rsar.htm Accessed 5 November 2020

Bağcı M (2020) Mineralogical, petrographic, and geochemical characterization of colored İscehisar marbles (Afyonkarahisar, W-Turkey). Turkish J Earth Sci 29:946–975 https://doi.org/10.3906/yer-2001-20

Bartoli DG (2008) Marble transport in the time of the Severans: a new analysis of the Punta Scifo A shipwreck at Croton, Italy, Doctor of Philosophy, Texas A&M University

Berechman J (2003) Transportation-economic aspects of Roman highway development: the case of Via Appia. Transportation Research Part A 37:453–478 https://doi.org/10.1016/S0965-8564(02)00056-3

Bruno M, Gorgoni C, Pallante P (1999) I marmi dell'Arco di Settimio Severo: composizione strutturale, volumetria e analisi archeometriche, in P. Pensabene and C. Panella (eds), Arco di Costantino tra archeologia e archeometria (Studia Archeologica 100) Rome, 157–69

Bruno M, Attanasio D, Prochaska W (2015) The Dokimeion marble sculptures of the Grotto of Tiberius at Sperlonga. American Journal of Archaeology 119(3):375–394 https://doi.org/10.3764/aja.119.3.0375

Burford A (1960) Transport in Classical Antiquity. The Economic History Review 13(1):1–18 https://doi.org/10.2307/2591403

Cardell C, Yebra A, Van Grieken R (2002) Applying digital image processing to SEM-EDS and BSE images to determine and quantify porosity and salts with depth in porous media. Microchim Acta 140(1–2):9–14 https://doi.org/10.1007/s006040200063

Columbu S, Antonelli F, Lezzerini M, Miriello D, Adembri B, Blanco A (2014) Provenance of marbles used in the Heliocaminus Baths of Hadrian's Villa (Tivoli, Italy). Journal of Archaeological Science 49:332–342 https://doi.org/10.1016/j.jas.2014.05.026

Corremans M, Degryse P, Wielgosz D, Waelkens M (2009) The import and the use of white marble and coloured stone for wall and floor revetment at

Sagalassos. Interdisciplinary Studies on Ancient Stone Proceedings of the IX Association for the Study of Marbles and Other Stones in Antiquity (ASMOSIA) Conference (Tarragona 2009) 38–51

Cramer T (2004) Multivariate Herkunftsanalyse von Marmor auf petrografischer und geochemischer Basis - Das Beispiel kleinasiatischer archaischer, hellenistischer und römischer Marmorobjekte der Berliner Antikensammlung und ihre Zuordnung zu mediterranen und anatolischen Marmorlagerstätten. Dissertation Berlin, http://nbnresolving. de/urn:nbn:de:kobv:83-opus-7426.

Çalik-Ross A (2013) The statue group of Herakles and Telephos from Seyitgazi in Phrygia. Bulletin of the Institute of Classical Studies, 56(104):171–179 https://doi.org/10.1111/j.2041-5370.2013.tb02561.x

Çelik A (2019) Titus Flavius Clemens Pelopidianus' Aphrodite from Perge. Anadolu/Anatolia 45:1–32

Çelik MY, Sabah E (2008) Geological and technical characterisation of İscehisar (Afyon-Turkey) marble deposits and the impact of marble waste on environmental pollution. Journal of Environmental Management 87(1):106–116 https://doi.org/10.1016/j.jenvman.2007.01.004

Çelik MY, Sert M (2020) The importance of "Pavonazzetto marble" (Dokimeion-Phrygia/İscehisar-Turkey) since ancient times and its properties as a global heritage stone resource. Environ Earth Sci (2020) 79:201 https://doi.org/10.1007/s12665-020-08943-2

Çelik MY, Sert M (2021) Afyon Menekşe mermerinin Roma döneminden günümüze önemi, karakterizasyonu ve laboratuvar yaşlandırma (tuz kristalleşmesi ve donma-çözülme) testleriyle dayanıklılığın değerlendirilmesi (in Turkish). Gazi Üniversitesi Politeknik Dergisi 24 (3) 785 - 796 https://doi.org/10.2339/politeknik.673694

Devreker J, Thoen H, Vermeulen F (1995) The imperial sanctuary at Pessinus and its predecessors: a revision, Anatolia Antiqua 3:125–144 https://doi.org/10.3406/anata.1995.1180

Dodge H (1988) Decorative stones for architecture in the Roman Empire. Oxford Journal of Archaeology 7(1):65–80 https://doi.org/10.1111/j.1468-0092.1988.tb00168.x

Drew-Bear T (1994) Nouvelles inscriptions de Dokimeion. MEFRA 106:747–844 https://doi.org/10.3406/mefr.1994.1862

Elsner J, Huskinson J, Davies G (2010) Life, Death and Representation: Some New Work on Roman Sarcophagi ("Before Sarcophagi"). 29. Berlin: Walter De Gruyter. 21–55

Fant JC (1984) Seven unedited quarry inscriptions from Docimium (İscehisar, Turkey). Zeitschrift für Papyrologie und Epigraphik 54:171–182

Fant JC (1985) Four unfinished sarcophagus lids at Docimium and the Roman

Imperial quarry system in Phrygia. American Journal of Archaeology 89:665–662

Fant JC (1988a) New sculptural and architectural finds from Docimium. Department of Anthropology and Classical Studies. Paper 117

Fant JC (1988b) Ancient marble quarrying and trade: papers from a colloquium held at the Annual Meeting of the Archaeological Institute of America, San Antonio, Texas, 1986, edited by Fant JC (B.A.R. international series 453). Oxford: British Archaeological Reports

Fant JC (1989) Cavum antrum Phrygiae. The Organization and Operations of the Roman Imperial Marble Quarries in Phrygia. BAR International Series 482. Oxford: Oxford University Press

Freccero A (2015) Marble Trade in Antiquity: Looking at Labraunda. Antiqua/ Eski Anadolu XXIII, 2015, 11–54

Gorgoni C, Lazzarini L, Pallante P, Turi B (2002) An updated and detailed mineropetrographic and C-O stable isotopic reference database for the main Mediterranean marbles used in antiquity. In: J.J. Herrmann, N. Herz, R. Newman (eds.), ASMOSIA V, Interdisciplinary Studies on Ancient Stone. London: 115–131.

Hall A, Waelkens M (1982) Two Dokimeian sculptors in Iconium. Anatolian Studies 32:151–155

Herrmann JJ, Tykot RH (2009) Some products from the Dokimeion quarries: Craters, tables, capitals, and statues, Asmosia VII, ed. Y. Maniatis, Athens, pp. 59–75.

Herz N (1988) Geology of Greece and Turkey: Potential Marble Source Regions. In: Herz N., Waelkens M. (eds) Classical Marble: Geochemistry, Technology, Trade. NATO ASI Series (Series E: Applied Sciences), vol 153. Springer, Dordrecht.

Hirt AM (2010) Imperial Mines and Quarries in the Roman World: Organizational Aspects, 27 BC-AD 235. Oxford: Oxford University Press

Jes K (2002) Die neue Stadt. Aizanoi in der frühen Kaiserzeit, in Patris und Imperium. Kulturelle und politische Identität in den Städten der römischen Provinzen Kleinasiens in der fruhen Kaiserzeit, ed. C. Berns, H. von Hesburg, L. Vandeput and M. Waelkens. Leuven: 49–62

Kleiner DEE (1992) Roman Sculpture. New Haven: Yale University Press

Koch G (1993) Sarkophage der römischen Kaiserzeit. Wissenschaftliche Buchgesellschaft, Darmstadt

Koch G (2001) Sarkophage DerRömischen Kaiserzeit, Roma İmparatorluk Dönemi Lahitleri, (in Turkish), Çev. Z. Zühre İlkgelen, Arkeoloji ve Sanat Yayınları, İstanbul

Kramer J (1994) Korinthische Pilasterkapitelle in Kleinasien und Konstantinopel. Antike und spätantike Werkstattgruppen. Tubingen

Lapuente MP, León P, Nogales T, Royo H, Preite Martinez M, Blanc PH (2012) White sculptural materials from Villa Adriana: Study of provenance. In Interdisciplinary Studies on Ancient Stone, Proceedings of the IX ASMOSIA Conference, Tarragona, Spain, 8–13 June 2009; Garcia, M.A.G., Lapuente, P., Rodà, I., Eds.; Arqueologia Clàssica: Tarragona, Spain, 364–375

Lazzarini L, Moschini G, Xusheng H, Waelkens M. (1985) New light on some Phrygian marble quarries through a petrological study and the evaluation of Ca/Sr ratio. in P. Pensabene (ed.), Marmi antichi: problemi d'impiego, di restauro e d'identificazione (Studi Miscellanei 26). Rome, 41–46

Lubotsky A (2017) The Phrygian inscription from Dokimeion and its meter, in: I. Hajnal–D. Kölligan – K. Zipser (eds.), Miscellanea Indogermanica. Festschrift für José Luis García Ramón zum 65. Geburtstag, Innsbruck, 427–431

Luca RD, Barca D, Bloise A, Dominici R, Lezzerini M, Sica M, Miriello D (2020) Provenance of white marbles from the Roman City of Tauriana (Palmi, Reggio Calabria, Italy). Minerals, 10, 297 https://doi.org/10.3390/min10040297

Mandi V, Vassiliou A, Maniatis Y, Grimanis AP (1995) An evaluation of the contribution of trace elements to the determination of marble provenance. In: Maniatis Y, Herz N, Basiakos Y (eds) ASMOSIA III, the study of marble and other stones used in antiquity. Archetype Publications Ltd, London, 207–212

Matthews KJ (1997) The Establishment of a database of neutron activation analyses of white marbles. Archaeometry 39:321–32 https://doi.org/10.1111/j.1475-4754.1997.tb00809.x

Moens L, Roos P, De Rudder J, De Paepe P, Van Hende J, Waelkens M (1987) Identification of archaeologically interesting white marbles by instrumental neutron activation analysis (INAA) and petrography: Comparison between samples from Afyon and Upk (Turkey), Journal of Trace and Microprobe Techniques, 5:101–114

Moropoulou A, Delegou ET, Apostolopoulou M, Kolaiti A, Papatrechas C, Economou G, Mavrogonatos C (2019) The white marbles of the Tomb of Christ in Jerusalem: characterization and provenance, Sustainability 11:2495 https://doi.org/10.3390/su11092495

Mrozek-Wysocka M (2014) Ancient marbles: Provenance determination by archaeometric study. In Geoscience in Archaeometry. Methods and Case Studies; Michalska, D., Szczepaniak, M., Eds.; Wydawnictwo Naukowe Bogucki: Poznan, Poland, 99–122

Niewöhner P (2013) Phrygian marble and stonemasonry as markers of regional distinctiveness in Late Antiquity. In P. Thonemann (Ed.), Roman Phrygia: Culture and Society (Greek Culture in the Roman World, 215-248). Cambridge: Cambridge University Press. doi:10.1017/CBO9781139381574.011

oguzmermer.com (2020) http://www.oguzmermer.com/katalog/ Accessed 21 November 2020

Ozguven A, Ozçelik Y (2014) Effects of high temperature on physico-mechanical properties of Turkish natural building stones. Engineering Geology 183:127–136 https://doi.org/10.1016/j.enggeo.2014.10.006

Öğüş E (2014) Columnar Sarcophagi from Aphrodisias: Elite emulation in the Greek East. American Journal of Archaeology 118(1):113–136

Öğüş E (2018) Columnar Sarcophagi from Aphrodisias. Reichert Verlag, Wiesbaden

Pensabene P (1978) A cargo of marble shipwrecked at Punta Scifo near Crotone (Italy). IJNA 7:105–18 https://doi.org/10.1111/j.1095-9270.1978.tb01055.x

Pensabene P, Antonelli F, Lazzarini L, Cancelliere S. (2012a) Archaeometric analyses of white marbles from Hadrian's Villa (Tivoli, Italy) and the use of Pentelic and Dokymaean Marbles in the statuary of the so-called Canopus, In Interdisciplinary Studies on Ancient Stone Proceedings of the IX Association for the Study of Marbles and Other Stones in Antiquity (ASMOSIA) Conference, Tarragona 2009, A. G. Garcia-M., P. L. Mercadal, I. R. de Llanza (Eds.), Institut Català d'Arqueologia Clàssica, Tarragona, 104-108

Pensabene P, Antonelli F, Lazzarini L, Cancelliere S (2012b) Provenance of marble sculptures and artifacts from the so-called Canopus and other buildings of "Villa Adriana" (Hadrian's villa–Tivoli, Italy). J Archaeol Sci 39:1331–1337 https://doi.org/10.1016/j.jas.2012.01.015

Pierucci A (2017) The biography of a Dokimeion columnar sarcophagus fragment. MVSE 51, 25-44, Ed. Jane Biers, Annual of the Museum of Art and Archaeology, University of Missouri

Platts, HFML (2006) Art, architecture and landscape in 'villa' residences of Italy from c. 1st B.C. to c. 2nd A.D. Doctor of Philosophy, University of Bristol

Poretti G, Brilli M, De Vito C, Conte AM, Borghi A, Günther D, Zanetti A (2017) New considerations on trace elements for quarry provenance investigation of ancient white marbles. Journal of Cultural Heritage 28:16–26. https://doi.org/10.1016/j.culher.2017.04.008

Prochaska W, Attanasio D (2022) The challenge of a successful discrimination of ancient marbles (part III): A databank for Aphrodisias, Carrara, Dokimeion, Göktepe, Hymettos, Parian Lychnites and Pentelikon. Journal of Archaeological Science: Reports 45, 103582. https://doi.org/10.1016/j.jasrep.2022.103582

Rapp G (2009) Building, Monumental, and Statuary Materials. In: Archaeomineralogy. Natural Science in Archaeology. Springer, Berlin, Heidelberg. https://doi.org/10.1007/978-3-540-78594-1_11

Ricca M, Belfiore CM, Ruffolo SA, Barca D, De Buergo MA, Crisci GM, La Russa MF (2015) Multi-analytical approach applied to the provenance study

of marbles used as covering slabs in the archaeological submerged site of Baia (Naples, Italy): The case of the "Villa con ingresso a protiro". Appl Surf Sci 357:1369–1379 https://doi.org/10.1016/j.apsusc.2015.10.002

Rice C (2016) Shipwreck cargoes in the Western Mediterranean and the organization of Roman maritime trade. Journal of Roman Archaeology 29:165–192 https://doi.org/10.1017/S1047759400072093

Röder J (1971) Marmor Phrygium; Die Antiken Marmorbrüche von İscehisar in Westanatolien. JDL 86:253–312

Russell B (2015) Transport and Distribution, in E. A. Friedland, M. G. Sobocinski and E. K. Gazda (eds.), The Oxford Handbook of Roman Sculpture (Oxford) 189–206

Salvatori A, Trucchi D, Guidobaldi F (1988) The marbles used in the decorations of Hadrian's Villa at Tivoli. In: Classical Marble: Geochemistry, Technology, Trade. Lucca

Spry A (1969) Metamorphic Textures. Oxford, Pergamon Press, 350 p.

Sümer EÖ, AÜ Tolluoğlu, Y Erkan (1997) Importance of geologic data in marble production and three-dimensional modelling of Afyon İscehisar marbles (In Turkish), Turkish 2nd Marble Symposium Proceedings Book, Afyon, 35–43

Thonemann P (2013) Phrygia: an anarchist history, 950 BC - AD 100, bk.: P. Thonemann (ed.), Roman Phrygia. Culture and Society, Cambridge, 24–74 https://doi.org/10.1017/CBO9781139381574.002

Topbaş A (1987) Un sarcophage D'apamée de Phrygie. Revue Archéologique, Nouvelle Série, 2:361–374

Waelkens M (1982) Dokimeion. Die Werkstatt der repräsentativen kleinasiatischen Sarkophage. Chronologie und Typologie ihrer Produktion,Archäologische Forschungen 11, Berlin

Waelkens M (1985) From a Phrygian quarry. The provenance of the statues of the Dacian Prisoners in Trajan's Forum at Rome. AJA 89: 641–653.

Waelkens M (2019) The sarcophagus workshop of Dokimeion. In: The Book of International Symposium on Burial Customs in Anatolia during the Hellenistic and Roman Periods. Bilgin Kültür Sanat, Ankara. 537–580.

Waelkens M, Baumer LE, Demirel M (2019) The Heracles Sarcophagus from Geneva. Workshop, Date, Provenance and Iconography. Deutsches Archäologisches Institut, Abteilung Istanbul

CHAPTER 7

BIOENGINEERING APPROACHES TO ENHANCE STABILITY OF NUCLEIC ACID THERAPEUTICS

Ebru KIRMIZIAY[1]
Ceren ÖĞÜTÇÜ[2]
Hüseyin Saygın PORTAKAL[3]

1 Izmir University of Economics, Genetics and Bioengineering ORCID ID: 0000-0002-6054-3141
2 Izmir University of Economics, Genetics and Bioengineering ORCID ID: 0000-0002-8039-2053
3 Research Assistant, Izmir University of Economics, Genetics and Bioengineering ORCID ID: 0000-0002-3582-4152

1. Introduction

Our era has witnessed great advancements in the treatment of various diseases causing worldwide deaths. To date, while treatment approach- es based on the design and synthesis of chemical ligands have been developed, the discovery of nucleic acid therapeutics with distinct mechanisms has opened a new gate in health sciences (Sridharan & Gogtay, 2016). Today, a great amount of bioengineering efforts are aiming to design efficient nucleic acid therapeutics in both ribonucleic acid (RNA) and deoxyribonucleic acid (DNA) chemistry.

Considering the central dogma phenomenon, three methods named as knock-in describing the targeted expression of genes (Porteus, 2016), knock-down silencing the gene at mRNA level (Porteus, 2016), and knock-out silencing the gene at genomic level (Zuo et al., 2017) have been developed by manipulating of various natural mechanisms. In this scope, natural post-transcriptional regulation mechanisms such as RNA interference (RNAi) (Setten, Rossi, & Han, 2019), and Ribozymes which are special RNA molecules having catalytic activity (Müller, Appel, Balke, Hieronymus, & Nübel, 2016) are manipulated as knock down approaches. Furthermore, other engineered nucleic acid therapeutics such as aptamers (Adachi & Nakamura, 2019), antisense oligonucleotides (ASO) (Rinaldi & Wood, 2018), and deoxyribozymes (Grimpe, 2011) are designed and utilized to inhibit expression of the genes in mRNA level. In addition, gene editing at the genomic level has taken a great step with the discovery of CRISPR/Cas systems which are natural immune mechanisms of microorganisms against viruses (Yuanyuan Xu & Li, 2020). Besides that designing a reprogrammable gene editing system based on the manipulation of CRISPR/Cas mechanism has brought the Nobel Prize to its own inventors, it has become a greatly effective tool for genome editing with its high specificity and efficiency (Portakal, 2023). In addition, while vaccination processes are targeting to introduce antigen molecules to the immune system, DNA and mRNA vaccines are recently developed vaccination approaches (Leitner, Ying, & Restifo, 2007). In particular, mRNA vaccines have come into prominence in the fight with Covid-19 pandemic (Fang et al., 2022).

Despite the efficiency of nucleic acid therapeutics there are many intracellular and extracellular biological barriers that are able to limit the half-life of these therapeutic agents. For instance, recognition as foreign by reticuloendothelial system (RES) and other cells of immunity, exonuclease enzymes and high concentration of salt, sugar, and other ingredients in blood circulation, epithelial and endothelial cell layers such as blood brain barrier (BBB), extracellular matrix structures, undesired electrostatic interactions between negatively charged therapeutics and cell membrane

and nuclear membrane, acidic conditions and digestive enzyme content of endosome vesicles, and cytoskeleton structures are affecting the stability and delivery efficiencies of such therapeutic molecules (Dowdy, 2017; Kulkarni et al., 2021; Mollé, Smyth, Yuen, & Johnston, 2022). Considering these biological barriers, many bioengineering approaches aiming to protect nucleic acid therapeutics such as chemical modifications (Fàbrega, Aviñó, & Eritja, 2022), designing the nucleic acids with secondary structures (Jain, Polak, & Hud, 2003), usage of xeno nucleic acids (XNA) (Duffy, Arangundy-franklin, & Holliger, 2020), and encapsulation with viral or non-viral delivery agents (Pamukcı, Portakal, & Eroğlu, 2018) have been developed over few years. While great advancements in this research area have been recorded to date, many other bioengineering and biotechnological studies are going on to enhance the stabilities and delivery efficiencies of nucleic acid therapeutics. As such, nucleic acid therapeutics based treatment approaches' working principles, biological barriers that are encountered, the strategies targeting to overcome these obstacles, and recent advancements are discussed in this chapter.

2. Therapeutic Approaches Using Nucleic Acid Molecules

2.1. RNA interference (RNAi)

RNA interference (RNAi) is a natural post transcriptional regulation mechanism promoted for the expression level adjustment of the mRNA products (Ha, 2019). Fundamentally, microRNA (miRNA) molecules are small non-coding RNAs which may target mRNA molecules sequence specifically. Once to be synthesized, pri-miRNAs are processed by the Drosha-DGCR8 complex in the nucleus and pre-miRNAs are released to cytoplasm through Exportin 5 (XPO5) nucleus membrane protein. The secondary structures of the released pre-miRNA molecules are cleaved by DICER enzyme and while the sense strand leaves the duplex, the antisense strand of the miRNA molecule is loaded into RNA-induced silencing (RISC) complex. Target mRNAs are recognized by this strand sequence specifically and digested by the Argonaute-2 (AGO2) component of the RISC complex. Thus, protein coding mRNAs are silenced and translation is blocked (Agrawal et al., 2003). Today, this natural mechanism is manipulated as a gene knock-down approach (Mocellin & Provenzano, 2004). As such, mainly two nucleic acid therapeutics which are short-hairpin RNA (shRNA) (Sheng, Flood, & Xie, 2020) and silencing RNA (siRNA) (Dana et al., 2017) are designed with bioengineering applications. While siRNAs are 20-25 bp long double stranded RNAs (dsRNA), they are delivered to cytoplasm of cells directly and processed by DICER enzymes. Once to be processed, while passenger strand leaves the duplex, guide strand containing the sequence that is able to recognize target mRNA is loaded into RISC complex, and expression of the gene is silenced through

cleavage of its mRNA product by AGO2 (Friedrich & Aigner, 2022). However, synthesizing of shRNA initiates in the nucleus since that it's delivered by plasmid vectors. Synthesized pri-shRNAs are processed by DROSHA, and pre-shRNAs are exported to cytoplasm through XPO5. Within cytoplasm, it's cleaved by DICER enzyme and its antisense strand is loaded into the RISC complex once to be unwound. Thus, target mRNA is digested and gene silencing is accomplished (Moore, Guthrie, Huang, & Taxman, 2010). Many therapeutics based on RNAi mechanisms are recently designed, synthesized, and utilized for various genetic disorders with sufficient efficiency (Paul et al., 2022).

2.2. CRISPR/Cas9

Discovery of repetitive sequences in the genome of high salt tolerant Haloferax mediterranei archea isolated from Santa Pola coasts of Spain in 1993 has become one of milestones in the biotechnological research areas (Mojica, Juez, & Rodriguez-Valera, 1993). While this sequences have been named as clustered regularly interspaced palindromic repeats (CRISPR), it's also revealed that this repetitive sequences might be found in the genome of several infecting organisms such as Mycobacterium tuberculosis, Clostridium difficile, Yersinia pestis (McAllister & Sorg, 2021; Pourcel, Salvignol, & Vergnaud, 2005; Wei et al., 2019) etc. Further researches have put forward that CRISPR sequences has an immune function for prokaryotes against infecting organisms along with a special CRISPR associated (Cas) enzyme (Barrangou & Marraffini, 2014). Primarily this mechanism is based on; i) adaptation: processing of infecting organisms' genome by Cas enzymes and to integrate the fragments into host genome, ii) expression: producing of non-coding guide RNA (gRNA) composed of two distinct RNA molecules which are trans-activating crispr RNA (tracrRNA) and crispr RNA (crRNA) as well as Cas enzymes from Cas and CRISPR genes flanked with spacer regions, iii) interference: recognition and digestion of the infecting organisms' genome in second infection by gRNA loaded into Cas enzyme having cleavage activity (Sorek, Lawrence, & Wiedenheft, 2013). Intriguing sequence specifically recognition of DNA chemistry has forced the scientist to develop a genome editing tool based on the manipulation of CRISPR/Cas system. Therefore, to develop a CRISPR/Cas system based reprogrammable system for gene editing has powerfully impacted the biotechnological advancements and has brought Chemistry Nobel Prize to Jennifer Doudna and her colleague Emmanualle Charpentier in 2020 (Portakal, 2023). As a knock-out approach of CRISPR/Cas9 is aiming to create a double strand break (DSB) over the host genome of genetically disordered cells (Li et al., 2020). In this scope, an engineered gRNA with the name of single guide RNA (sgRNA) targeting the genetic sequence adjacent to protospacer adjacent motif (PAM sequence – NGG

for Staphylococcus pyogenes Cas 9 (SpCas9)) is designed and delivered with Cas9 enzyme (Allen, Rosenberg, & Hendel, 2021). Once to create DSBs over host genome by targeting with sgRNA loaded Cas9, it's repaired with natural repair mechanisms which are non-homologous end joining (NHEJ) or homology directed repair (HDR) (Hsu, Lander, & Zhang, 2014). Principally, NHEJ repairs DSBs by insertion or deletion of few bases, yet HDR requires template oligonucleotides designed with homology arms (Chang, Pannunzio, Adachi, & Lieber, 2017; Davis & Maizels, 2014). The impressive efficiency and specificity of the CRISPR/Cas9 system have the most attention of many genetic engineering researches. Furthermore, many novel gene silencing approaches using distinct Cas enzyme derivatives such as dead Cas9 (dCas9) that has no cleavage activity (Saifaldeen, Al-Ansari, Ramotar, & Aouida, 2020) or Cas13 that is able to recognize RNA chemistry (Kick, von Wrisberg, Runtsch, & Schneider, 2022) have been developed and investigated over many years. In addition, lots of therapeutic agents based on CRISPR/Cas9 have been designed for various genetic disorders and intriguing advancements have been accomplished. For instance, He and his colleagues have knock out CCR5 receptor of an embryo in 2018, and the individual who named as CRISPR Baby has been protected against human immunodeficiency virus (HIV) infection (Schmidt et al., 2020).

2.3. Aptamers

One of the most significant parameters acting a role in interactions between biomolecules is their secondary and tertiary structures. Aptamers are 20-100 bp long oligonucleotides that might have binding affinity to several biomolecules such as proteins, lipids, metabolites, carbohydrates, nucleic acids (Guan & Zhang, 2020) etc. While these single stranded oligonucleotides might be found in DNA or RNA chemistries, the sequence of aptamers is the main parameter defining secondary and tertiary structures (K. Wang, Wang, Ma, Li, & Zhang, 2023). Due to many advantages such as high binding affinity, specificity, efficiency, low immunogenicity, low toxicity, and low cost for production, aptamers are evaluated as more preferable than antibody therapeutics (Keefe, Pai, & Ellington, 2010). As of the discovery of Systematic Evolution of Ligands by Exponential Enrichment (SELEX) technique in 1990, aptamer production has made great progress (Yixin Xu et al., 2021). SELEX technique includes the following steps; i) incubation of an aptamer library with target molecule as positive selection, ii) collection the bound aptamers and incubation with nonspecific molecule as negative selection, iii) the amplification of unbound aptamer with polymerase chain reaction (PCR), iv) to repeat the cycle up to 15-20 rounds in order to select the best aptamer structures (Zhuo et al., 2017). Today, aptamer therapeutics have broad spectrum of

usage in disorders from cancer, neurodegenerative diseases, autoimmune disorders to infection diseases (Dixit, Sawant, & Khan, 2020).

2.4. Deoxyribozymes and Ribozymes

Contrary to abundance of protein enzymes within metabolic processes, various nucleic acid molecules might have catalytic activities as well. As such, Ribozymes, which are RNA molecules having catalytic activity has been discovered in the 1980s (Sankaran, 2012). As in the RNAi natural mechanism, Ribozymes are utilized as post transcriptional expression regulation by cells. The expression adjustment properties of Ribozymes are based on the sequence specifically recognition and cleavage of protein coding mRNAs (Janzen et al., 2020). In addition, many other biological functions of Ribozymes such as RNA splicing, viral replication, and tRNA synthesis have been revealed over many years. While the catalytic profiles of Ribozymes are sourced from their special secondary and tertiary structures, various Ribozyme types such as hammerhead, VS Ribozyme, Hairpin Ribozyme have been designed and their efficiency for the treatment of several diseases have been analyzed to date (Weinberg, Weinberg, & Hammann, 2019). Besides, Deoxyribozymes are artificial catalytic biomolecules in DNA chemistry (Silverman, 2016). Similarly, Deoxyribozymes might have RNA cleavage activity as well as the functions such as DNA ligation, phosphorylation, glycosylation, adenylation, and degradation (Baum & Silverman, 2008). These engineered catalysts have found a significant role in the development of several therapeutics for various disorders (Murphy et al., 2008).

2.5. Antisense Oligonucleotides (ASO)

Antisense therapy is an efficient knock-down approach and it's based on to silence protein coding mRNA molecules by targeting with engineered single stranded antisense oligonucleotides (ASO) (Crooke, Liang, Baker, & Crooke, 2021). These short oligonucleotides could recognize the target mRNA molecules sequence specifically and block their expression (Fusco et al., 2019). The silencing of target mRNA might be carried out through steric blockage, cleavage by requiring RNAse H enzyme, and modulation of exon content via RNA splicing mechanism (Gagliardi & Ashizawa, 2021). Today, ASOs take a significant place in the treatment of various genetic disorders. For instance, Milasen, Fomivirsen, Morpholino, Volanesorsen, Mipomersen, Inotersen, and Nusinersen ASOs have been approved by Food and Drug Administration (FDA) in the treatment of Batten disease, Cytomegalovirus retinitis infection, Duchenne Muscular Dystrophy, Familial Chylomicronaemia Syndrome, Familial Hypercholesterolemia, Hereditary Transthyretin-mediated Amyloidosis, and Spinal Muscular Atrophy diseases, respectively (Gopi, Dhanaraju, & Dhanaraju, 2022).

2.6. mRNA and DNA Vaccines

The immune system is one of the most complicated body systems of mammalian species and it provides defense mechanisms against various infections and genetically disordered cells. The working principle of this system is based on the signaling cascades between different types of immune cells after the recognition of foreign molecules (Cota & Midwinter, 2015). Terminologically, the foreign molecules belonging to living organisms are named as antigen and vaccination processes aiming to activate the immune system against targets are carried out through to introduce related antigens (Pollard & Bijker, 2021). DNA and mRNA vaccines are one of the most promising techniques that are performed to produce the antigen proteins (Leitner, Ying, & Restifo, 1999). The working principle of DNA vaccines is based on: i) delivery of DNA molecules which is responsible for antigen production, ii) transcription of its mRNA in nucleus, iii) expression of antigen protein and recognition of it by immune system cells (Lopes, Vandermeulen, & Préat, 2019). In addition, mRNA vaccines' working principle is composed of the steps; i) production of antigen producing mRNAs through in vitro transcription method, ii) delivery of mRNA molecules to human body, iii) expression of antigen and to develop immune response via recognition (Chaudhary, Weissman, & Whitehead, 2021). Besides the efficiencies of both techniques have been investigated and proven over many years, in particular, mRNA vaccines have impacted our lives in Covid-19 outbreak that has caused a huge amount of worldwide deaths. Today, mankind has taken a great step in the fighting against SARS-Cov-2 virus by the help of mRNA vaccine technology (Cosentino & Marino, 2022).

3. Biological Limitations

Delivery of nucleic acid therapeutics are limited with various extracellular and intracellular biological barriers (Figure 1). One of the most significant barriers that limit the transfer of nucleic acids to the target region of the body consists of anatomical structures such as epithelial and endothelial cells. For instance, the blood brain barrier (BBB) which is composed of tightly attached endothelial cells limits the delivery of nucleic acid therapeutics to brain tissue (Yang, Gao, Liu, Pang, & Qi, 2017). In addition, even in RNA or DNA chemistry, nucleic acid molecules might be degraded once to be recognized as foreign by reticuloendothelial system (RES) and distinct cell types of immune system (Yona & Gordon, 2015). Besides, extracellular matrix (ECM) including collagen produced by fibroblasts and high interstitial fluid pressure (IFP) could limit the transportation of nucleic acid therapeutics to the target cells (Poltavets, Kochetkova, Pitson, & Samuel, 2018). Apart from these limitations, while high salt, sugar, plasma and serum protein concentrations are able

to nucleic acid agglomeration, these therapeutic molecules might also be degraded by exonuclease enzymes found in blood circulation (Sajid, Moazzam, Tiwari, Kato, & Cho, 2020).

Due to the fact that both nucleic acid molecules and cell membrane are negatively charged because of the phosphate and mucin groups in their chemical structures, respectively, undesired electrostatic interactions inhibit the delivery of nucleic acids to cells (Ghavimi & Pourhossein, 2014). Over many years this obstacle is tried to be overcome with cellular uptake mechanisms such as endocytosis. However, once the endocytosis, nucleic acids are uptaken within endosome vesicles having high concentration of digestive enzymes and low pH conditions. These parameters are also affecting the half-life of nucleic acid therapeutics (Du Rietz, Hedlund, Wilhelmson, Nordenfelt, & Wittrup, 2020). In addition, even after to release of nucleic acids to cytoplasm, they encounter with structural protein network named as the cytoskeleton matrix. While this protein network limits the RNA therapeutics to reach target molecules, nuclear membrane which has similar structure with cell membrane is another barrier limiting the DNA therapeutics to reach nucleus in order to be transcribed (Tatiparti, Sau, Kashaw, & Iyer, 2017). In light of this information, to develop effective methods enhancing stability and delivery efficiency of nucleic acid therapeutics has become one of the main efforts of bioengineering research areas.

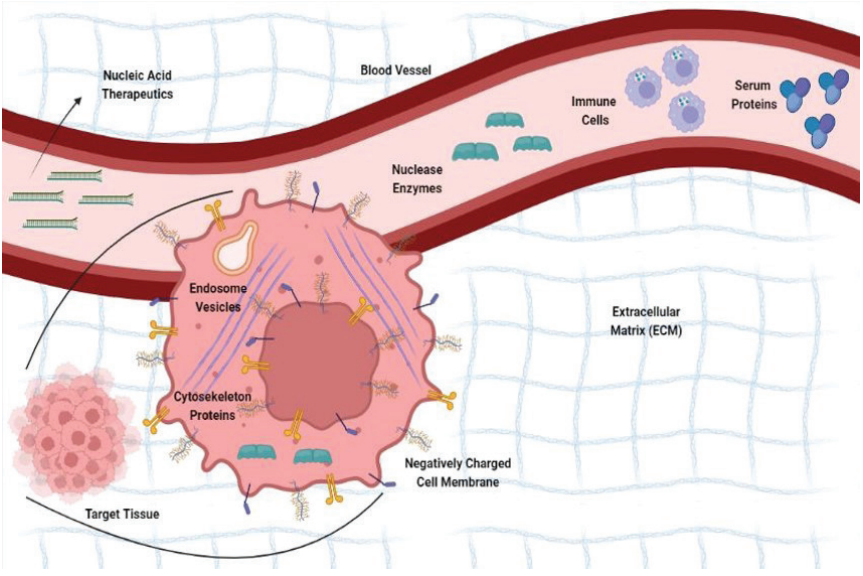

Figure 1. The biological barriers that are able to limit the efficiencies of nucleic acid therapeutic agents.

4. Novel Engineering Approaches to Overcome Biological Limitations

4.1. Chemical Functionalization of Nucleic Acid Therapeutics

The development of novel bioengineering techniques suggesting therapeutic approaches to various diseases and biomolecules has also greatly impacted recent treatment methods. Biomolecule identification and quantification are now crucial due to their relationship with the diseases' stages. For instance, proteins considered cancer markers are found in larger quantities in the plasma of cancer patients and thus they might be identifiable at low levels to increase survival rates through early detection and prompt treatment (D. H. Park & Lee, 2015; Saha, Agasti, Kim, Li, & Rotello, 2012). ELISA and PCR are two common procedures mostly performed to detect biomolecules for disease diagnosis. However, low sensitivity and selectivity, extended procedure times, low throughput, high costs, and a requirement for complex devices are some of the fundamental drawbacks of these techniques (Hosseini, Vázquez-Villegas, Rito-Palomares, & Martinez-Chapa, 2018; Wassenegger, 2001). Therefore, throughout the years, effective probes for detecting biomolecules have been developed by bioengineers using nanoparticles made of various metallic, ceramic, and semiconducting materials with the aim of chemically or physically modifying the biomolecules in terms of surface properties, conductivity, chemical activity, or solubility (Gupta & Gupta, 2005; Sink, Lochmann, & Fecteau, 2008). Therefore, techniques on nanoparticles and biomolecules based on therapeutic intervention with the chemical or physical function of the substance, called functionalization, require bioengineering to increase the stability of the substance used. From this perspective, various studies can be shown as examples of functionalization.

For instance, Mirkin and his colleagues carried out a study aiming for DNA – gold-nanoparticles conjugation functionalization in 1996. In this study, DNA oligonucleotides with thiol groups are attached to the surfaces of gold particles. By leveraging the specificity of DNA contacts to drive the interactions between particles of varied sizes and compositions, Mirkin's method made it feasible to customize the optical, electrical, and structural characteristics of the colloidal aggregates. During the study, NaCl treatment was applied to rule out electrostatic repulsion between DNA strands to increase stability and enhance DNA functionalization, or changes were made on pH to obtain ideal thiolated DNA (Burns, Butler, Moran, & Whitesides, 1991; Mirkin, Letsinger, Mucic, & Storhoff, 1996).

Apart from functionalization with gold nanoparticles, functionalization with silver nanoparticles (AgNP) has also attracted attention. However, AgNPs, which are observed as comparable to AuNPs since they have few

disadvantages. One of these disadvantages is that silver undergoes oxidation by reaction with oxygen-containing fluids. The other drawback is that AgNPs' poor colloidal stability prevents DNA conjugation, which prolongs the synthesis process (Park, Joo, Kim, & Lee, 2012). Several anchoring groups were created and employed to change the DNA strands at one of their terminal ends in order to increase the conjugation effectiveness of the DNA strands and the AgNP surface (Z. Zhang et al., 2011). Triple cyclic disulfides were the first multiple anchoring units designed for DNA-AgNP conjugation, and they improved the conjugates' stability and their capacity to endure severe ionic conditions. Afterwards, as an anchoring group, phosphorothioates were used, offering improved salt and thermal stability (Pal, Sharma, Yan, & Liu, 2009). Ultimately, AgNPs were functionalized with DNA through the use of dual thiol units, which produced several times the reproducibility of mono-thiolated AgNPs (Liu et al., 2013).

Expeditious and simple conjugation of AuNPs with DNA has been achieved using a commercial non-ionic amphiphilic polymer, in order not to use convoluted anchoring methods (Zu & Gao, 2009). In highly ionic circumstances, AgNPs with an FSN layer were likewise quickly coupled with monothiol DNA in 4 hours. A biopolymer was used to obtain high AgNP stability, and a method of lowering pH was suggested for rapid DNA-AgNP conjugation (Zheng, Li, & Deng, 2012). The conjugates displayed great stability in phosphate buffer and hybridized with their corresponding DNA- AgNPs, demonstrating their potential as useful nanoprobes. This pH-control method allowed dense and rapid DNA loading on AgNP surfaces (Zhang, Servos, & Liu, 2012). These advancements have revealed that functionalization is an engineering approach which is used for various therapeutic purposes, such as nucleic acid delivery, and water-soluble drug delivery, necessary for biomolecules and nanoparticles such as DNA that are in contact with each other or are being studied in this direction. The further studies on the chemical modifications of nucleic acid therapeutics will also demonstrate the efficiencies of developed bioengineering approaches.

4.2. Xeno Nucleic Acids (XNAs)

One of the most significant recent biological engineering achievements in the history of science is Xeno Nucleic Acids (XNA). While these synthetic nucleic acids have been designed in 2009 as the first time, they exhibit quite similarity with DNA and RNA molecules. XNAs are synthetic biopolymers involved in the storage and processing of genetic information. Since the components of XNAs are not encountered in nature, they are required to be synthesized *in vitro* with the essential enzymatic mechanisms supported from the cells (Herdewijn & Marliere, 2009).

Considering the biological limitations encountered in nucleic acid based therapies, unmodified DNA/RNA molecules are digested by nuclease enzymes and they are inactivated when they are delivered to the cells. Furthermore, unaltered nucleic acids have a low binding ability to the target, necessitating large concentrations that might have negative side effects. Thus, it is believed that chemical changes are crucial for the creation of functional nucleic acid agents, and these reasons lead scientists to design and produce XNAs (Munagala et al., 2021; Sharma, Rungta, & Prasad, 2014). Phosphodiester linkage, a nucleobase, and a sugar moiety are the three subunits that make up a nucleotide. Any of these subunits can be subject to chemical changes (McKenzie, El-Khoury, Thorpe, Damha, & Hollenstein, 2021). However, particularly, chemical changes in the sugar moiety of nucleic acid analogs create xeno-nucleic acids (XNAs) (Herdewijn & Marliere, 2009). Through changing the innate characteristics of native DNA/RNA, XNAs have become a family of nucleic acid equivalents with sugar group modification (Wang, Li, Chu, & Lo, 2022), considerably expanded the uses of nucleic acids in biotechnology and nanomedicine (Herdewijn & Marliere, 2009). 2'-OMe (2′-Omethyl), one of the most well studied examples of such sugar modifications, is an RNA formed by adding methyl to the 2'-hydroxy of ribose (Kawasaki et al., 1993). As for the biomedical applicatios, 2'-OMe RNA has been used in the treatment of age-related macular degeneration so far, and this modification has increased RNAi activity and serum stability (Gragoudas, E. S., Adamis, A. P., Cunningham, E. T., Jr, Feinsod, M., Guyer, 2004). In addition, it is an engineering product that has been demonstrated by Jackson et al. as a potential solution for reducing the unwanted off-target side effects of siRNA drugs (Jackson et al., 2006).

2′-deoxy-2′-fluoro (2'-F) RNA is another commonly used example obtained by replacing the 2′-hydroxyl on sugar with fluorine (Kawasaki et al., 1993). 2′-F RNA has been extensively exploited in gene regulation and aptamer synthesis, due to its potent affinity for binding to the target RNA, high thermal stability, and capacity to suppress innate immunological responses. It is also known that 2'-F modified siRNAs' nuclease stability has increased (Khvorova & Watts, 2017). 2'-OMe and 2'-F RNA samples are two of the most common samples in both clinical and research development. Apart from these, there are other synthesized XNA samples whose chemical structures are illustrated in Figure 2 (Wang, Li, Chu, & Lo, 2022). In the light of those information, it is revealed that XNA is a biological engineering method and product that might affect the efficiencies of nucleic acid therapeutics and the treatments at various molecular points, such as off-target side effects, immune responses, nuclease stability, thermal stability, and is extremely convenient for further engineering developments.

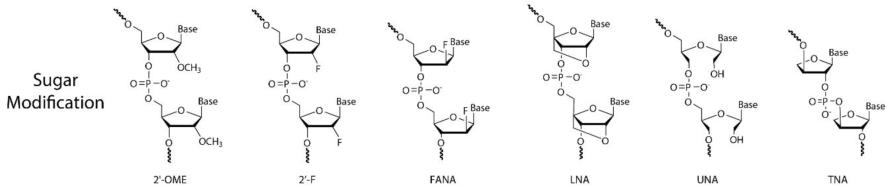

Figure 2. Sugar moiety modification examples of XNAs. 2'-OME: 2'-O-methyl RNA; 2'-F: 2'-deoxy-2'-fluoro RNA; FANA: 2'-deoxy-2'-fluoroarabinonucleic acid; LNA: locked nucleic acid; UNA: unlocked nucleic acid; TNA: threose nucleic acid.

4.3. Designing Nucleic Acid Therapeutics with Secondary Structures

DNA biopolymers are composed of nucleotide residues which are cytosine (C), guanine (G), adenosine (A), and thymine (T). The human genome consists of 20% C, 20% G, 30% A, and 30% T. However, the structure of RNA contains uracil (U) instead of thymine (T). While the DNA strands composed of nucleotides interact with one another via hydrogen bonds, guanines bind to cytosines with three hydrogen bonds and adenines bind to thymines or uracils with totally two hydrogen bonds(Minchin & Lodge, 2019). The base pairing has a critical function in the process of understanding DNA and structures. DNA has two polynucleotide chains which make a double helix, similarly, RNA has only one relatively short polynucleotide chain which makes a single helix. Two polynucleotide chains are coiled into a double helix to generate the secondary structure of DNA. The two chains of the helix often run antiparallel to one another and are typically read from 5' to 3'. All of the bases on one strand complete all of the bases on another strand so that the amount of A-T and G-C is always equal to each other. The double helix involves major and minor grooves. (Krueger & Kool, n.d.)

Torque and external forces are enforced on double-stranded DNA (dsDNA) and RNA (dsRNA) for elucidating the mechanical characteristics and conformational transitions of these fundamental biological building blocks. Nucleic acid helices behave like elastic rods when forces and torque are applied, and identify the stiffness of twisting, bending, and stretching. Unexpectedly, RNA shortens is observed when it is unwound, whereas DNA lengthens (Lipferta et al., 2014). Stem-loop structures in single-stranded DNA or RNA (ssDNA and ssRNA) are created through an intramolecular base pairing between the complementary sequences of a single nucleic acid strand. These intramolecular interactions may create a special motif named as a hairpin. A properly constructed stem-loop oligonucleotide probe would open in the presence of sequences that are

complementary to the loop sequence. This property enables the creation of numerous biosensors for the real-time detection of unlabelled biomolecule targets, including proteins and nucleic acids (Farahani, Behmanesh, & Ranjbar, 2020). As another secondary structure pseudoknots are created via two base-paired stems (S1 and S2) and at least two single-stranded loops (Peselis & Serganov, 2014). Finally, G-quadruplexes (G4s) are one of the most significant secondary structures of nucleic acids. G-quadruplexes are globularly folded, noncanonical, four-stranded structures that are produced in guanine-rich nucleic acid sequences and are easily synthesized under physiologically relevant conditions. While 3% of the human genome is composed of protein-coding sequences, many noncanonical secondary structures are observed in both coding and noncoding regions. The biological functions of G4s are based on their locations such as human telomeres, oncogene promoter regions, replication initiation sites, and the 5′ and 3′ untranslated region (UTR) of mRNA. As such, G4s might have crucial biological functions such as regulation of gene transcription, translation, replication, and genomic stability (Yang, 2019). The possible secondary structures of nucleic acid molecules are illustrated in Figure 3.

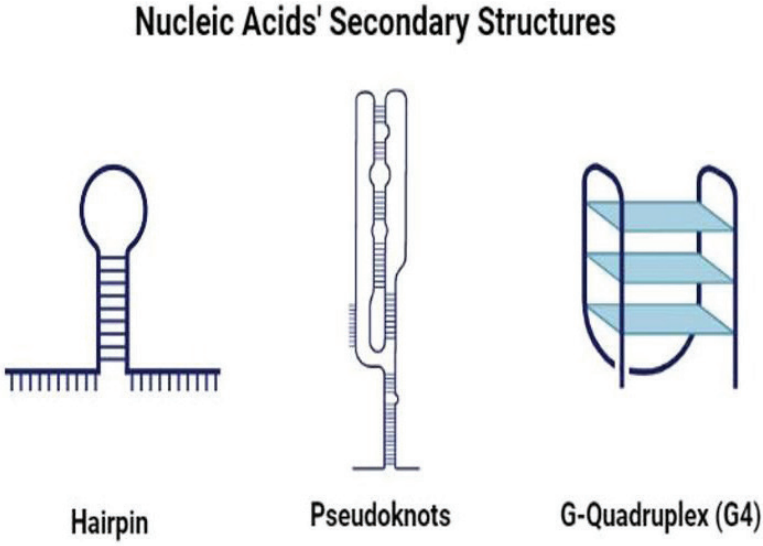

Figure 3. The illustrations of nucleic acids' secondary structures created via hydrogen bond interactions.

It's demonstrated in the literature that these aforementioned secondary structures have quite stability comparing the double helix or single-stranded forms of nucleic acids. Considering these phenomena, designing the nucleic acid therapeutics with those secondary structures

might protect them against nuclease enzymes, agglomeration through interactions with serum proteins, and low pH conditions of endosome vesicles. Due to the fact that designing nucleic acid therapeutics with such secondary structures is quite promising, the analysis of the stability and creation of convenient design is rather significant. As such, there are available tools such as SHAPE that might predict the dynamics and free energy alterations of the nucleic acids' secondary structures. In particular, the SHAPE computes the kinetics of folding, thermodynamics, and model visualization (Low & Weeks, 2010). In addition, RDNAnalyzer is another tool that can analyze the secondary structures of nucleic acids. Particularly, it utilizes the Nussinov dynamic programming algorithm and has a broad interval to analyze sequences. Since various interactions have a significant role in the formation of hairpins, pseudoknots, and double helices in nucleic acids, shape and structure are crucial for biomolecular function likewise producing novel pharmaceutics and taking knowledge about genetic diseases. Recent modern and physical techniques such as Nuclear Magnetic Resonance (NMR) – characterization of physical and chemical properties, and X-Ray Crystallography are considerably extent expensive and time-consuming. Therefore, the discovery and produce novel techniques are assessed as quite promising in the design of nucleic acid therapeutics (Afzal, Shahid, Shehzadi, Nadeem, & Husnain, 2012).

4.4. Nano Level Delivery Vectors

To date, the biological limitations encountered in nucleic acid delivery processes have forced scientists to develop delivery vectors that might overcome the barriers. The dynamically evolving area of the nano-level delivery system uses novel materials and nanometer-scale characteristics to generate delivery vectors that are efficient in carrying genetic material into a range of different cell types. The new delivery vectors' innovative physicochemical characteristics can be leveraged to overcome the difficulties currently associated with delivering nucleic acids both in vitro and in vivo. Despite novel breakthroughs in characterization methods and the synthesis of nanostructures, designing highly effective and non-toxic delivery systems still face several challenges (Garcia-Guerra, Dunwell, & Trigueros, 2018). A reliable, effective, targeted, and non-pathogenic method of delivering gene therapy materials is tried to be designed and produced. Due to their biocompatibility with various physicochemical characteristics, nanomaterials for nucleic acid delivery offer an extraordinary chance to overcome these disadvantages due to the fact that they can easily be functionalized with any sort of biomolecules/ moieties for selective targeting.

Today, the general design principles of nucleic acid delivery nanoparticles, their remarkable capabilities, and the structure-function

interactions of these nanomaterials with biological systems, including damaged cells and tissues are discussed. Therefore, nano-level viral vectors and non-viral vectors are recently designed and produced to overcome biological limitations (Figure 4). For instance, nucleic acid therapeutics encapsulated delivery vectors are produced with various biomaterials such as polymers, lipids, inorganic compounds, and composites of these materials. Furthermore, while the envelope of viral organisms is used as delivery vectors as well, the nano-level biomaterial-based vectors provide a controlled release of therapeutics. Importantly, the nanoscale level of the delivery system establishes biocompatibility, non-toxicity, and adequate compatibleness. In this scope, the design of gene delivery vectors exhibit significant advantages such as high transfection efficiencies and low cytotoxicity.

4.4.1. Viral Vectors

Due to their convenient infecting mechanisms, viral organisms are used to deliver nucleic acid therapeutics today. These viral vectors are derived from adenovirus (AV), adeno-associated virus (AAV), retrovirus (RV), and lentivirus (LV) that provide high transfection efficiency, and ease to produce, yet low cargo capacity. However, since those viral organisms are recognized as foreign by the immune system, they could activate a strong immune response. Apart from their immunogenicity, they exhibit toxicity causing them to kill somatic and non-disordered cells. Furthermore, the production of viral vectors that encapsulate nucleic acid therapeutics requires the production of various plasmids encoding gag, pol, rev, and tat genes as well as the related sequences flanked with LTR regions. Once to produce these plasmids, viral vectors are produced by isolation from in vitro applications once to transfect special cell lines such as HEK-293T. Although the efficiencies of viral vectors are assessed as quite adequate for in vitro studies, such those drawbacks may limit their usage of in vivo applications. As such, many bioengineering, material engineering, and chemical engineering scientists have focused on producing other nano-level delivery agents designed by non-viral materials (Bulcha, Wang, Ma, Tai, & Gao, 2021).

4.4.2. Non-Viral Vectors

Comparing the viral vectors, non-viral vectors that are produced with biomaterials such as lipids, polymers, and inorganic materials exhibit strong advantages. For instance, the design and production of such those materials are based on chemical reactions, and they enable functionalization which might enhance the transfection efficiency and specificity for the target cells. In addition, they have low toxicity and immunogenicity since they are not recognized as foreign by the immune system. Furthermore, the

tunable size of these kinds of delivery agents makes them quite convenient to use in passive targeting that is aiming to transfer the loads through tiny gaps between endothelial cells. Since that nano-level vectors produced with non viral compounds are not the target of nuclease enzymes and serum proteins, they might protect the loaded therapeutic agents against these limitations. Furthermore, such delivery agents have quite a stability in various storage conditions and do not lose their ingredients for a great time interval. Besides all, since that biomaterials are biodegradable and biocompatible materials, once to deliver their load they do not accumulate within the host body without any toxicity. In addition, since such those carriers might be produced with high stability against harsh conditions, they could deliver their load without degradation within low pH endosome vesicles and positively charged nanocarriers may act as proton sponges and provide controlled release of the therapeutic agents. However, the low load capacity and low transfection efficiency of these nanoparticles might limit the efficiency of the treatment approach based on the usage of nucleic acids. Numerous studies that are carried out by bioengineers, chemical engineers, and material engineers are still going on to enhance the transfection efficiency of these nano-level non-viral vectors. In addition, the impact of this approach has been highlighted in the Covid-19 pandemic since those mRNA vaccines against SARS-Cov-2 are generally encapsulated and delivered to human bodies through the nanoparticles produced in the light of these techniques (Dizaj, Jafari, & Khosroushahi, 2014).

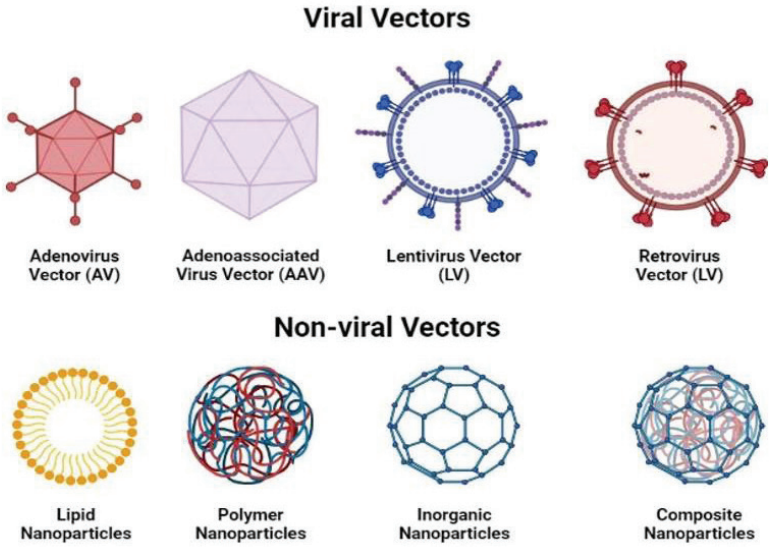

Figure 4. Illustrations of nano-level delivery vectors for nucleic acid therapeutics.

5. Conclusion

One of the most significant progresses that have been made in health sciences from the last decades is production of novel therapeutic agents in nucleic acid chemistry. While these approaches might be performed with the agents in both DNA and RNA chemistry, in general, they are based on manipulation of natural mechanisms by synthetic products. Today, knock-in aiming to express a gene within a cell, knock-down silencing a gene in mRNA level, and knock-out silencing a gene in genomic level methods are efficiently carried out with these novel approaches. However, although these biotechnological therapeutic agent products have high performance according to their target, yet they encounter various macro and micro level biological barriers which are able to affect their stabilities and delivery efficiencies. As such, many novel bioengineering approaches such as usage of xeno nucleic acids (XNA), designing the molecules with secondary structures, chemical modifications, and production of viral and non-viral delivery agents have been developed over a few years. While the efficiencies of this approach have been demonstrated with a great number of studies, this area is also providing collaborative researches to various engineering subclasses such as bioengineering, chemical engineering, material engineering, etc. In this scope, the working principles of the treatment approaches based on nucleic acid therapeutics, the biological barriers that are limiting the stability and delivery of these molecules, the novel strategies aiming to overcome related obstacles, and recent advancements in this area are discussed in this chapter in order to provide broad spectrum of information to engineering scientists intending to study to enhance nucleic acid therapeutics' stability.

Acknowledgement

The figures in the chapter were created with BioRender.com

REFERENCES

Adachi, T., & Nakamura, Y. (2019). Aptamers : A Review of Their Chemical Properties. *Molecules*, *24*, 4229. Retrieved from https://doi.org/10.3390/molecules24234229

Afzal, M., Shahid, A. A., Shehzadi, A., Nadeem, S., & Husnain, T. (2012). Software RDNAnalyzer: A tool for DNA secondary structure prediction and sequence analysis Abbreviations: RDNAnalyzer (Random DNA Analyser), GUI: Graphical user interface, XAML (Extensible Application Markup Language). *Print) Bioinformation*, *8*(14), 687.

Agrawal, N., Dasaradhi, P. V. N., Mohmmed, A., Malhotra, P., Bhatnagar, R. K., & Mukherjee, S. K. (2003). RNA Interference: Biology, Mechanism, and Applications. *Microbiology and Molecular Biology Reviews*, *67*(4), 657–685. https://doi.org/10.1128/mmbr.67.4.657-685.2003

Allen, D., Rosenberg, M., & Hendel, A. (2021). Using Synthetically Engineered Guide RNAs to Enhance CRISPR Genome Editing Systems in Mammalian Cells. *Frontiers in Genome Editing*, *2*(January), 1–16. https://doi.org/10.3389/fgeed.2020.617910

Barrangou, R., & Marraffini, L. A. (2014). CRISPR-cas systems: Prokaryotes upgrade to adaptive immunity. *Molecular Cell*, *54*(2), 234–244. https://doi.org/10.1016/j.molcel.2014.03.011

Baum, D. A., & Silverman, S. K. (2008). Deoxyribozymes: Useful DNA catalysts in vitro and in vivo. *Cellular and Molecular Life Sciences*, *65*(14), 2156–2174. https://doi.org/10.1007/s00018-008-8029-y

Bulcha, J. T., Wang, Y., Ma, H., Tai, P. W. L., & Gao, G. (2021, December 1). Viral vector platforms within the gene therapy landscape. *Signal Transduction and Targeted Therapy*, Vol. 6. Springer Nature. https://doi.org/10.1038/s41392-021-00487-6

Burns, J. A., Butler, J. C., Moran, J., & Whitesides, G. M. (1991). Selective Reduction of Disulfides by Tris(2-carboxyethyl)phosphine. *Journal of Organic Chemistry*, *56*(8), 2648–2650. https://doi.org/10.1021/jo00008a014

Chang, H. H. Y., Pannunzio, N. R., Adachi, N., & Lieber, M. R. (2017). Non-homologous DNA end joining and alternative pathways to double-strand break repair. *Nature Reviews Molecular Cell Biology*, *18*(8), 495–506. https://doi.org/10.1038/nrm.2017.48

Chapter 8: THE ROLE OF CRISPR/CAS SYSTEMS IN HEALTH SCIENCES AND RECENT ADVANCEMENTS. (2023). (January).

Chaudhary, N., Weissman, D., & Whitehead, K. A. (2021). mRNA vaccines for infectious diseases: principles, delivery and clinical translation. *Nature Reviews Drug Discovery*, *20*(11), 817–838. https://doi.org/10.1038/s41573-021-00283-5

Cosentino, M., & Marino, F. (2022). Understanding the Pharmacology of

COVID-19 mRNA Vaccines: Playing Dice with the Spike? *International Journal of Molecular Sciences*, *23*(18). https://doi.org/10.3390/ijms231810881

Cota, A. M., & Midwinter, M. J. (2015). The immune system. *Anaesthesia and Intensive Care Medicine*, *16*(7), 353–355. https://doi.org/10.1016/j.mpaic.2015.04.006

Crooke, S. T., Liang, X. H., Baker, B. F., & Crooke, R. M. (2021). Antisense technology: A review. *Journal of Biological Chemistry*, *296*, 100416. https://doi.org/10.1016/j.jbc.2021.100416

Dana, H., Chalbatani, G. M., Mahmoodzadeh, H., Karimloo, R., Rezaiean, O., Moradzadeh, A., … Gharagouzlo, E. (2017). *Molecular Mechanisms and Biological Functions of siRNA*. *13*(2), 48–57.

Davis, L., & Maizels, N. (2014). Homology-directed repair of DNA nicks via pathways distinct from canonical double-strand break repair. *Proceedings of the National Academy of Sciences of the United States of America*, *111*(10), 1–9. https://doi.org/10.1073/pnas.1400236111

DIXIT, N., SAWANT, G., & KHAN, H. (2020). a Review on Aptamers in Gene Therapy and Their Applications. *International Journal of Pharmacy and Pharmaceutical Sciences*, *12*(12), 16–21. https://doi.org/10.22159/ijpps.2020v12i12.39241

Dizaj, S. M., Jafari, S., & Khosroushahi, A. Y. (2014). A sight on the current nanoparticle-based gene delivery vectors. *Nanoscale Research Letters*, Vol. 9, pp. 1–9. Springer New York LLC. https://doi.org/10.1186/1556-276X-9-252

Dowdy, S. F. (2017). Overcoming cellular barriers for RNA therapeutics. *Nature Biotechnology*, *35*(3), 222–229. https://doi.org/10.1038/nbt.3802

Du Rietz, H., Hedlund, H., Wilhelmson, S., Nordenfelt, P., & Wittrup, A. (2020). Imaging small molecule-induced endosomal escape of siRNA. *Nature Communications*, *11*(1). https://doi.org/10.1038/s41467-020-15300-1

Duffy, K., Arangundy-franklin, S., & Holliger, P. (2020). *Modified nucleic acids : replication , evolution , and next-generation therapeutics*. 1–14.

Fàbrega, C., Aviñó, A., & Eritja, R. (2022). Chemical Modifications in Nucleic Acids for Therapeutic and Diagnostic Applications. *Chemical Record*, *22*(4). https://doi.org/10.1002/tcr.202100270

Farahani, N., Behmanesh, M., & Ranjbar, B. (2020). Evaluation of Rationally Designed Label-free Stem-loop DNA Probe Opening in the Presence of miR-21 by Circular Dichroism and Fluorescence Techniques. *Scientific Reports*, *10*(1). https://doi.org/10.1038/s41598-020-60157-5

Fang, E., Liu, X., Li, M., Zhang, Z., Song, L., Zhu, B., … Li, Y. (2022). Advances in COVID-19 mRNA vaccine development. *Signal Transduction and Targeted Therapy*, *7*(1), 1–31. https://doi.org/10.1038/s41392-022-00950-y

Friedrich, M., & Aigner, A. (2022). Therapeutic siRNA: State-of-the-Art and Future Perspectives. *BioDrugs*, *36*(5), 549–571. https://doi.org/10.1007/s40259-022-00549-3

Fusco, D. Di, Dinallo, V., Marafini, I., Figliuzzi, M. M., Romano, B., & Monteleone, G. (2019). Antisense oligonucleotide: Basic concepts and therapeutic application in inflammatory bowel disease. *Frontiers in Pharmacology*, *10*(MAR). https://doi.org/10.3389/fphar.2019.00305

Gagliardi, M., & Ashizawa, A. T. (2021). The challenges and strategies of antisense oligonucleotide drug delivery. *Biomedicines*, *9*(4). https://doi.org/10.3390/biomedicines9040433

Garcia-Guerra, A., Dunwell, T. L., & Trigueros, S. (2018). Nano-Scale Gene Delivery Systems: Current Technology, Obstacles, and Future Directions. *Current Medicinal Chemistry*, *25*(21), 2448–2464. https://doi.org/10.2174/0929867325666180108100723

Ghavimi, R., & Pourhossein, M. (2014). Limitations of clinical application of siRNA delivery based on non-viral vectors. *Journal of Isfahan Medical School*, *32*(272), 34–48.

Gopi, C., Dhanaraju, M. D., & Dhanaraju, K. (2022). Antisense oligonucleotides: recent progress in the treatment of various diseases. *Beni-Suef University Journal of Basic and Applied Sciences*, *11*(1). https://doi.org/10.1186/s43088-022-00202-6

Gragoudas, E. S., Adamis, A. P., Cunningham, E. T., Jr, Feinsod, M., Guyer, D. R. (2004). Pegaptanib for neovascular age-related macular degeneration. *The New England Journal of Medicine, 351*(27), 2805–2816. https://doi.org/10.1093/med/9780190050726.003.0039

Grimpe, B. (2011). Deoxyribozymes: New Therapeutics to Treat Central Nervous System Disorders. *Frontiers in Molecular Neuroscience*, *4*(September), 1–5. https://doi.org/10.3389/fnmol.2011.00025

Guan, B., & Zhang, X. (2020). Aptamers as versatile ligands for biomedical and pharmaceutical applications. *International Journal of Nanomedicine*, *15*, 1059–1071. https://doi.org/10.2147/IJN.S237544

Gupta, A. K., & Gupta, M. (2005). Synthesis and surface engineering of iron oxide nanoparticles for biomedical applications. *Biomaterials*, *26*(18), 3995–4021. https://doi.org/10.1016/j.biomaterials.2004.10.012

Ha, M. (2019). Mechanism of RNA interference discovered. *Nature Research 2019*, *296*(December), 2019.

Herdewijn, P., & Marliere, P. (2009). Toward Safe Genetically Modified Organisms through the Chemical Diversification of Nucleic Acids. *Chemistry & Biodiversity*, *6*(6), 201791–201808. https://doi.org/10.1002/9780470977873.ch9

Hosseini, S., Vázquez-Villegas, P., Rito-Palomares, M., & Martinez-Chapa, S.

O. (2018). Advantages, Disadvantages and modifications of conventional ELISA. In *SpringerBriefs in Applied Sciences and Technology*. Singapore: Springer. https://doi.org/10.1007/978-981-10-6766-2_5

Hsu, P. D., Lander, E. S., & Zhang, F. (2014). Development and applications of CRISPR-Cas9 for genome engineering. *Cell*, *157*(6), 1262–1278. https://doi.org/10.1016/j.cell.2014.05.010

Jackson, A. L., Burchard, J., Leake, D., Reynolds, A., Schelter, J., Guo, J., … Linsley, P. S. (2006). Position-specific chemical modification of siRNAs reduces "off-target" transcript silencing. *Rna*, *12*(7), 1197–1205. https://doi.org/10.1261/rna.30706

Jain, S. S., Polak, M., & Hud, N. V. (2003). Controlling nucleic acid secondary structure by intercalation: Effects of DNA strand length on coralyne-driven duplex disproportionation. *Nucleic Acids Research*, *31*(15), 4608–4615. https://doi.org/10.1093/nar/gkg648

Janzen, E., Janzen, E., Blanco, C., Peng, H., Kenchel, J., Kenchel, J., … Chen, I. A. (2020). Promiscuous Ribozymes and Their Proposed Role in Prebiotic Evolution. *Chemical Reviews*, *120*(11), 4879–4897. https://doi.org/10.1021/acs.chemrev.9b00620

Kawasaki, A. M., Casper, M. D., Freier, S. M., Lesnik, E. A., Zounes, M. C., Cummins, L. L., … Dan Cook, P. (1993). Uniformly Modified 2′-Deoxy-2′-fluoro Phosphorothioate Oligonucleotides as Nuclease-Resistant Antisense Compounds with High Affinity and Specificity for RNA Targets. *Journal of Medicinal Chemistry*, *36*(7), 831–841. https://doi.org/10.1021/jm00059a007

Keefe, A. D., Pai, S., & Ellington, A. (2010). Aptamers as therapeutics. *Nature Reviews Drug Discovery*, *9*(7), 537–550. https://doi.org/10.1038/nrd3141

Khvorova, A., & Watts, J. K. (2017). The chemical evolution of oligonucleotide therapies of clinical utility. *Nature Biotechnology*, *35*(3), 238–248. https://doi.org/10.1038/nbt.3765

Kick, L. M., von Wrisberg, M. K., Runtsch, L. S., & Schneider, S. (2022). Structure and mechanism of the RNA dependent RNase Cas13a from Rhodobacter capsulatus. *Communications Biology*, *5*(1), 1–9. https://doi.org/10.1038/s42003-022-03025-4

Krueger, A. T., & Kool, E. T. (n.d.). *Model Systems for Understanding DNA Base Pairing*.

Kulkarni, J. A., Witzigmann, D., Thomson, S. B., Chen, S., Leavitt, B. R., Cullis, P. R., & van der Meel, R. (2021). The current landscape of nucleic acid therapeutics. *Nature Nanotechnology*, *16*(6), 630–643. https://doi.org/10.1038/s41565-021-00898-0

Leitner, W. W., Ying, H., & Restifo, N. P. (1999). DNA and RNA-based vaccines: Principles, progress and prospects. *Vaccine*, *18*(9–10), 765–777. https://doi.org/10.1016/S0264-410X(99)00271-6

Li, H., Yang, Y., Hong, W., Huang, M., Wu, M., & Zhao, X. (2020). Applications of genome editing technology in the targeted therapy of human diseases: mechanisms, advances and prospects. *Signal Transduction and Targeted Therapy*, *5*(1). https://doi.org/10.1038/s41392-019-0089-y

Lipferta, J., Skinnera, G. M., Keegstraa, J. M., Hensgensa, T., Jagera, T., Dulina, D., … Dekker, N. H. (2014). Double-stranded RNA under force and torque: Similarities to and striking differences from double-stranded DNA. *Proceedings of the National Academy of Sciences of the United States of America*, *111*(43), 15408–15413. https://doi.org/10.1073/pnas.1407197111

Liu, M., Wang, Z., Zong, S., Zhang, R., Zhu, D., Xu, S., … Cui, Y. (2013). SERS-based DNA detection in aqueous solutions using oligonucleotide- modified Ag nanoprisms and gold nanoparticles. *Analytical and Bioanalytical Chemistry*, *405*(18), 6131–6136. https://doi.org/10.1007/s00216-013-7016-9

Lopes, A., Vandermeulen, G., & Préat, V. (2019). Cancer DNA vaccines: current preclinical and clinical developments and future perspectives. *Journal of Experimental and Clinical Cancer Research*, *38*(1), 1–24. https://doi.org/10.1186/s13046-019-1154-7

Low, J. T., & Weeks, K. M. (2010). SHAPE-directed RNA secondary structure prediction. *Methods*, *52*(2), 150–158. https://doi.org/10.1016/J.YMETH.2010.06.007

Manuscript, A. (2007). *DNA and RNA vaccines - progress and prospects*. *18*, 765–777.

McAllister, K. N., & Sorg, J. A. (2021). CRISPR genome editing systems in the genus clostridium: A timely advancement. *Journal of Bacteriology*, *201*(16). https://doi.org/10.1128/JB.00219-19

McKenzie, L. K., El-Khoury, R., Thorpe, J. D., Damha, M. J., & Hollenstein, M. (2021). Recent progress in non-native nucleic acid modifications. *Chemical Society Reviews*, *50*(8), 5126–5164. https://doi.org/10.1039/d0cs01430c

Minchin, S., & Lodge, J. (2019). Understanding biochemistry: Structure and function of nucleic acids. *Essays in Biochemistry*, Vol. 63, pp. 433–456. Portland Press Ltd. https://doi.org/10.1042/EBC20180038

Mirkin, C. A., Letsinger, R. L., Mucic, R. C., & Storhoff, J. J. (1996). A DNA-based method for rationally assembling nanoparticles into macroscopic materials. *Nature*, Vol. 382, pp. 607–609. https://doi.org/10.1038/382607a0

Mocellin, S., & Provenzano, M. (2004). RNA interference: Learning gene knockdown from cell physiology. *Journal of Translational Medicine*, *2*, 1–6. https://doi.org/10.1186/1479-5876-2-39

Mojica, F. J. M., Juez, G., & Rodriguez-Valera, F. (1993). Transcription at different salinities of Haloferax mediterranei sequences adjacent to partially modified PstI sites. *Molecular Microbiology*, *9*(3), 613–621. https://doi.org/10.1111/j.1365-2958.1993.tb01721.x

Mollé, L. M., Smyth, C. H., Yuen, D., & Johnston, A. P. R. (2022). Nanoparticles for vaccine and gene therapy: Overcoming the barriers to nucleic acid delivery. *Wiley Interdisciplinary Reviews: Nanomedicine and Nanobiotechnology*, *14*(6), 1–38. https://doi.org/10.1002/wnan.1809

Moore, C. B., Guthrie, E. H., Huang, M. T. H., & Taxman, D. J. (2010). Short hairpin RNA (shRNA): design, delivery, and assessment of gene knockdown. *Methods in Molecular Biology (Clifton, N.J.)*, *629*(2), 141–158. https://doi.org/10.1007/978-1-60761-657-3_10

Müller, S., Appel, B., Balke, D., Hieronymus, R., & Nübel, C. (2016). *Thirty-five years of research into ribozymes and nucleic acid catalysis : where do we stand today ? [version 1 ; referees : 2 approved] Referee Status : 5*(0), 1–11. https://doi.org/10.12688/f1000research.8601.1

Munagala, R., Aqil, F., Jeyabalan, J., Kandimalla, R., Wallen, M., Tyagi, N., … Gupta, R. C. (2021). Exosome-mediated delivery of RNA and DNA for gene therapy. *Cancer Letters*, *505*(December 2020), 58–72. https://doi.org/10.1016/j.canlet.2021.02.011

Murphy, T. M., Berzano, M., Cotter, D. M., Mcevoy, S. E., Thomas, K. a, & Whelan, K. F. (2008). *The Journal of the American Society of Parasitologists*. *94*(4), 1043–1052. https://doi.org/10.1016/j.echo.2007.11.008

Pal, S., Sharma, J., Yan, H., & Liu, Y. (2009). Stable silver nanoparticle-DNA conjugates for directed self-assembly of core-satellite silver-gold nanoclusters. *Chemical Communications*, (40), 6059–6061. https://doi.org/10.1039/b911069k

Pamukcı, A., Portakal, H., & Eroğlu, E. (2018). TERAPÖTİKMoleküllerin Aktariminda KullanilanYeniNesilBiyomalzemeler. *Erzincan Üniversitesi Fen Bilimleri Enstitüsü Dergisi*, *11*(3), 524–542. https://doi.org/10.18185/erzifbed.339405

Park, D. H., & Lee, J. S. (2015). Functionalized nanoparticle probes for protein detection. *Electronic Materials Letters*, *11*(3), 336–345. https://doi.org/10.1007/s13391-014-4383-0

Park, H. G., Joo, J. H., Kim, H. G., & Lee, J. S. (2012). Shape-dependent reversible assembly properties of polyvalent DNA-silver nanocube conjugates. *Journal of Physical Chemistry C*, *116*(3), 2278–2284. https://doi.org/10.1021/jp210732u

Paul, A., Muralidharan, A., Biswas, A., Kamath, B. V., Joseph, A., & Alex, A. T. (2022). siRNA therapeutics and its challenges: Recent advances in effective delivery for cancer therapy. *OpenNano*, *7*(March), 100063. https://doi.org/10.1016/j.onano.2022.100063

Peselis, A., & Serganov, A. (2014, November 1). Structure and function of pseudoknots involved in gene expression control. *Wiley Interdisciplinary Reviews. RNA*, Vol. 5, pp. 803–822. https://doi.org/10.1002/wrna.1247

Pollard, A. J., & Bijker, E. M. (2021). A guide to vaccinology: from basic principles to new developments. *Nature Reviews Immunology*, *21*(2), 83–100. https://doi.org/10.1038/s41577-020-00479-7

Poltavets, V., Kochetkova, M., Pitson, S. M., & Samuel, M. S. (2018). The role of the extracellular matrix and its molecular and cellular regulators in cancer cell plasticity. *Frontiers in Oncology*, *8*(OCT), 1–19. https://doi.org/10.3389/fonc.2018.00431

Porteus, M. H. (2016). Knock-in editing: It functionally corrects! *Blood*, *127*(21), 2507–2509. https://doi.org/10.1182/blood-2016-03-703181

Pourcel, C., Salvignol, G., & Vergnaud, G. (2005). CRISPR elements in Yersinia pestis acquire new repeats by preferential uptake of bacteriophage DNA, and provide additional tools for evolutionary studies. *Microbiology*, *151*(3), 653–663. https://doi.org/10.1099/mic.0.27437-0

Rinaldi, C., & Wood, M. J. A. (2018). Antisense oligonucleotides: The next frontier for treatment of neurological disorders. *Nature Reviews Neurology*, *14*(1), 9–22. https://doi.org/10.1038/nrneurol.2017.148

Saha, K., Agasti, S. S., Kim, C., Li, X. N., & Rotello, V. M. (2012). Gold Nanoparticles in Chemical and Biological Sensing. *Chemical Reviews*, *112*(5), 2739–2779. https://doi.org/10.1021/cr2001178

Saifaldeen, M., Al-Ansari, D. E., Ramotar, D., & Aouida, M. (2020). CRISPR FokI Dead Cas9 System: Principles and Applications in Genome Engineering. *Cells*, *9*(11). https://doi.org/10.3390/cells9112518

Sajid, M. I., Moazzam, M., Tiwari, R. K., Kato, S., & Cho, K. Y. (2020). Overcoming barriers for siRNA therapeutics: From bench to bedside. *Pharmaceuticals*, *13*(10), 1–25. https://doi.org/10.3390/ph13100294

Sankaran, N. (2012). How the discovery of ribozymes cast RNA in the roles of both chicken and egg in origin-of-life theories. *Studies in History and Philosophy of Science Part C :Studies in History and Philosophy of Biological and Biomedical Sciences*, *43*(4), 741–750. https://doi.org/10.1016/j.shpsc.2012.06.002

Schmidt, J. K., Strelchenko, N., Park, M. A., Kim, Y. H., Mean, K. D., Schotzko, M. L., … Slukvin, I. I. (2020). Genome editing of CCR5 by CRISPR-Cas9 in Mauritian cynomolgus macaque embryos. *Scientific Reports*, *10*(1), 1–12. https://doi.org/10.1038/s41598-020-75295-z

Setten, R. L., Rossi, J. J., & Han, S. ping. (2019). The current state and future directions of RNAi-based therapeutics. *Nature Reviews Drug Discovery*, *18*(6), 421–446. https://doi.org/10.1038/s41573-019-0017-4

Sharma, V. K., Rungta, P., & Prasad, A. K. (2014). Nucleic acid therapeutics: Basic concepts and recent developments. *RSC Advances*, *4*(32), 16618–16631. https://doi.org/10.1039/c3ra47841f

Sheng, P., Flood, K. A., & Xie, M. (2020). Short Hairpin RNAs for Strand-Spe-

cific Small Interfering RNA Production. *Frontiers in Bioengineering and Biotechnology*, *8*(August), 1–8. https://doi.org/10.3389/fbioe.2020.00940

Silverman, S. K. (2016). Catalytic DNA: Scope, Applications, and Biochemistry of Deoxyribozymes. *Trends in Biochemical Sciences*, *41*(7), 595–609. https://doi.org/10.1016/j.tibs.2016.04.010

Sink, T. D., Lochmann, R. T., & Fecteau, K. A. (2008). Validation, use, and disadvantages of enzyme-linked immunosorbent assay kits for detection of cortisol in channel catfish, largemouth bass, red pacu, and golden shiners. *Fish Physiology and Biochemistry*, *34*(1), 95–101. https://doi.org/10.1007/s10695-007-9150-9

Sorek, R., Lawrence, C. M., & Wiedenheft, B. (2013). CRISPR-mediated adaptive immune systems in bacteria and archaea. *Annual Review of Biochemistry*, *82*(February), 237–266. https://doi.org/10.1146/annurev-biochem-072911-172315

Sridharan, K., & Gogtay, N. J. (2016). Therapeutic nucleic acids: current clinical status. *British Journal of Clinical Pharmacology*, 659–672. https://doi.org/10.1111/bcp.12987

Tatiparti, K., Sau, S., Kashaw, S. K., & Iyer, A. K. (2017). siRNA delivery strategies: A comprehensive review of recent developments. *Nanomaterials*, *7*(4), 1–17. https://doi.org/10.3390/nano7040077

Wang, F., Li, P., Chu, H. C., & Lo, P. K. (2022a). Nucleic Acids and Their Analogues for Biomedical Applications. *Biosensors*, *12*(3), 93. https://doi.org/10.3390/bios12020093

Wang, F., Li, P., Chu, H. C., & Lo, P. K. (2022b). Nucleic Acids and Their Analogues for Biomedical Applications. *Biosensors*, *12*(2), 93. https://doi.org/10.3390/bios12020093

Wang, K., Wang, M., Ma, T., Li, W., & Zhang, H. (2023). Review on the Selection of Aptamers and Application in Paper-Based Sensors. *Biosensors*, *13*(1). https://doi.org/10.3390/bios13010039

Wassenegger, M. (2001). Advantages and disadvantages of using PCR techniques to characterize transgenic plants. *Applied Biochemistry and Biotechnology - Part B Molecular Biotechnology*, *17*(1), 73–82. https://doi.org/10.1385/MB:17:1:73

Wei, J., Lu, N., Li, Z., Wu, X., Jiang, T., Xu, L., … Guo, S. (2019). The Mycobacterium tuberculosis CRISPR-Associated Cas1 Involves Persistence and Tolerance to Anti-Tubercular Drugs. *BioMed Research International*, *2019*. https://doi.org/10.1155/2019/7861695

Weinberg, C. E., Weinberg, Z., & Hammann, C. (2019). Novel ribozymes: discovery, catalytic mechanisms, and the quest to understand biological function. *Nucleic Acids Research*, *47*(18), 9480–9494. https://doi.org/10.1093/nar/gkz737

Xu, Yixin, Jiang, X., Zhou, Y., Ma, M., Wang, M., & Ying, B. (2021). Systematic Evolution of Ligands by Exponential Enrichment Technologies and Aptamer-Based Applications: Recent Progress and Challenges in Precision Medicine of Infectious Diseases. *Frontiers in Bioengineering and Biotechnology*, *9*(August), 1–13. https://doi.org/10.3389/fbioe.2021.704077

Xu, Yuanyuan, & Li, Z. (2020). CRISPR-Cas systems: Overview, innovations and applications in human disease research and gene therapy. *Computational and Structural Biotechnology Journal*, *18*, 2401–2415. https://doi.org/10.1016/j.csbj.2020.08.031

Yang, D. (2019). G-Quadruplex DNA and RNA. In *Methods in Molecular Biology* (Vol. 2035, pp. 1–24). Humana Press Inc. https://doi.org/10.1007/978-1-4939-9666-7_1

Yang, Z. Z., Gao, W., Liu, Y. J., Pang, N., & Qi, X. R. (2017). Delivering siRNA and chemotherapeutic molecules across BBB and BTB for intracranial glioblastoma therapy. *Molecular Pharmaceutics*, *14*(4), 1012–1022. https://doi.org/10.1021/acs.molpharmaceut.6b00819

Yona, S., & Gordon, S. (2015). From the reticuloendothelial to mononuclear phagocyte system - The unaccounted years. *Frontiers in Immunology*, *6*(JUL), 1–7. https://doi.org/10.3389/fimmu.2015.00328

Zhang, X., Servos, M. R., & Liu, J. (2012). Fast pH-assisted functionalization of silver nanoparticles with monothiolated DNA. *Chemical Communications*, *48*(81), 10114–10116. https://doi.org/10.1039/c2cc35008d

Zhang, Z., Wen, Y., Ma, Y., Luo, J., Jiang, L., & Song, Y. (2011). Mixed DNA-functionalized nanoparticle probes for surface-enhanced Raman scattering-based multiplex DNA detection. *Chemical Communications*, *47*(26), 7407–7409. https://doi.org/10.1039/c1cc11062d

Zheng, Y., Li, Y., & Deng, Z. (2012). Silver nanoparticle-DNA bionanoconjugates bearing a discrete number of DNA ligands. *Chemical Communications*, *48*(49), 6160–6162. https://doi.org/10.1039/c2cc32338a

Zhuo, Z., Yu, Y., Wang, M., Li, J., Zhang, Z., Liu, J., … Zhang, B. (2017). Recent advances in SELEX technology and aptamer applications in biomedicine. *International Journal of Molecular Sciences*, *18*(10), 1–19. https://doi.org/10.3390/ijms18102142

Zu, Y., & Gao, Z. (2009). Facile and controllable loading of single-stranded DNA on gold nanoparticles. *Analytical Chemistry*, *81*(20), 8523–8528. https://doi.org/10.1021/ac901459v

Zuo, E., Cai, Y. J., Li, K., Wei, Y., Wang, B. A., Sun, Y., … Yang, H. (2017). One-step generation of complete gene knockout mice and monkeys by CRISPR/Cas9-mediated gene editing with multiple sgRNAs. *Cell Research*, *27*(7), 933–945. https://doi.org/10.1038/cr.2017.81

CHAPTER 8

A STUDY ON CRYOGENIC IMPACT ENERGY IN MGALSI TERNARY ALLOY

Bünyamin ÇIÇEK[1]
Tuna AYDOĞMUŞ[2]

1 Dr., Hitit University, Corum, Türkiye, https://orcid.org/0000-0002-6603-7178
2 Dr., Hitit University, Corum, Türkiye, https://orcid.org/0000-0002-8736-2949

1. Introduction

Magnesium (Mg) element is a metal that has been frequently found in the literature in recent years. It takes place in all studies where lightness is an important variable. The density of the Mg element is 1.7 g/cm^3. The fact that it has such a low density is the most prominent feature of its preference in studies. Therefore, Mg metal is almost 75% lighter than iron (Fe) when densities are compared. However, as with all elements, it has very low mechanical and corrosive resistance in its pure state. For this reason, it should be used as an alloy (Savitsky & Baton, 1952; Zeytin, 1999; Furuya vd., 2000; Mordike & Ebert, 2001; Kainer & Von Buch, 2003).

Mg element, like other metals, cannot meet many expected properties in its pure state. In this process, alloys can be obtained with additional metals added to the Mg element. Alloys can generally be applied within the framework of Hume-Rothery rules. In the case of Mg alloying, it is most successfully used with metals such as aluminum (Al), zinc (Zn), silicon (Si) and calcium (Ca). Mg alloys formed by the addition of other elements gain serious improvements in many parameters. For example, a Mg alloy supported with Al and Zn can give successful results in terms of mechanical and corrosiveness. A Mg alloy produced by the addition of Ca can show increased biocompatibility. In addition to these elements, many metals and rare earth elements give many properties to Mg metal (Froes vd., 1998; Friedrich & Schumann, 2001; Menahem Bamberger & Dehm, 2008; Jiang vd., 2011).

Mg alloys are not named according to the names of the elements, but with the abbreviations specified in the standard. This nomenclature consists of letters and numbers. A notation is used with the letter A for Al, Z for Zn, X for Ca and S for Si. Afterwards, the figures that indicate the weight % ratio are listed. For example, it is stated that while there is 9% Al by weight in the AS92 alloy, there is 2% Si (Jiang vd., 2011; Sun & Ahlatci, 2011; Xu vd., 2011; Kulkarni vd., 2012).

The mechanical, corrosive, bio, physical and tribological properties of Mg alloys are among the many cited studies in the literature. For this reason, serious projects are being produced every day on the different properties of this light element. Many production methods such as welding, coating, spraying, melting, casting and rolling of Mg alloys are frequently used. In casting systems, which is the main production method, Mg alloys can only be produced with special equipment. High oxygen affinity is the most dangerous element for Mg alloy in all production methods (Menahem Bamberger & Dehm, 2008; Zheng vd., 2011; M Bamberger, 2013).

For this reason, Mg alloys are produced in almost all production methods in a vacuum or a controlled atmosphere. In general, oxygen-free pro-

duction can be made in environments supported by an inert gas such as argon (Ar) and helium (He). Except for inert gases, it is used in passive gases such as SF6 that are heavier than air and have di-electric properties. The solidification process after production is also an important factor for Mg metal. Thus, even with controlled cooling, Mg alloys are subjected to homogenization (long time at low temperature) annealing in many studies. Thus, residual stresses in the structure during production can be eliminated. As described here, after a difficult and costly production process, Mg alloys can be used under service conditions (Mordike & Ebert, 2001; Sun & Ahlatci, 2011; Cao vd., 2015; L. Liu vd., 2015; Vander Voort, 2015; Zhu vd., 2021; Singh & Sehgal, 2022).

Numerous alloys are being developed for Mg metal with different elements at a newly designed rate. However, basic tests such as microstructure characterization, mechanical values, corrosive resistance and hardness of the new alloy developed should yield good results. Apart from basic properties, some alloys are rarely tested for creep values and cryogenic results. However, with such tests, the desired end product is reached (Çiçek & Sun, 2012; Cao vd., 2015; Chen vd., 2018; Korgiopoulos vd., 2021; Z. Liu vd., 2021).

In this section, the results of a non-standard Mg alloy developed with the mentioned literature in a cryogenic experiment are discussed. Al and Si elements were added to Mg metal in the developed alloy. Produced and homogenized by alloy casting method. The samples obtained were crushed in the notched impact test (Charpy) at a low temperature of -80°C (193°K) in methanol. In this study, the state of possible phases between Mg-Al and Mg-Si was investigated. Afterwards, it is aimed to bring a low temperature test result of this alloy produced to the literature. With this experiment, the results on cryogenic impact energy, which has very little data in the literature, are discussed under the title of Mg alloys.

2. Materials manufacturing and test methods

The Mg alloy casting method produces it. Casting was made in an atmosphere protected and SF6 gas environment, in an oven where product can be taken from the bottom. Pure Mg ingots charged into the graphite crucible reached 750°C. Then, Al12Si ingots were added from the product addition section to the furnace. 80% Mg and 20% Al12Si by weight were used. Gas flow was provided during melting. The liquid metal was transferred to the lower mold by waiting for 10 minutes at 750°C. The casting mold made of 1.4140 quality steel is heated up to 300°C in order to prevent sudden cooling effects. The casting was made into a mold at 300°C. It was then allowed to free cool to room temperature. The samples, which were removed from the mold in the form of Ø25 mm rods, were subjected to

homogenization annealing at 400°C for 12 hours. During homogenization, a conventional oven without atmosphere control was used. After 12 hours, it was allowed to free cool to room temperature. Conventional metallographic processes for characterization and analysis prepared the alloy. FEI / Quanta 450 FEG scanning electron microscope (SEM) was used for characterization. Elemental analysis was performed on Rigaku brand X-ray Fluorescence (XRF) device. In addition, the phase fraction was analyzed with image processing logic over the obtained microstructure images. Image-J program was used as image processing program.

The samples obtained after casting and homogenization processes were processed in cnc milling for impact energy test (Charpy). In order to increase the surface roughness quality, all surfaces were cleaned with 1200 mesh sandpaper before notching. Sample dimensions are given in Figure 1. EN ISO 148-2-2017 standard was taken into account in sample and notch dimensions (ISO, 2017). The samples were prepared as square prisms on the CNC milling machine. Sample notches were prepared with the NSM201B brand device.

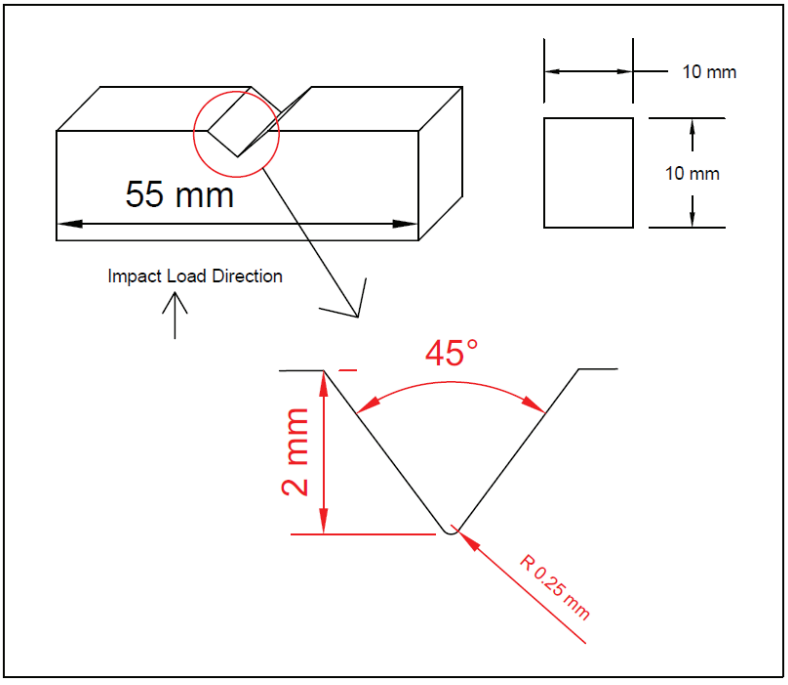

Figure 1. Charpy test specimen details

Crushing was done with TE brand TRJBW-300 model 300 J pendulum. The cracking process is applied in charpy type. For the crushing process, the

samples were cooled to -80°C (193°K) with a "Jinan Testing" brand "DWC-80" model cooler in methanol and kept at this temperature for 5 minutes. It is used as coupled to the coolant crushing device. The material taken from the cooling chamber was broken in less than 5 seconds as stated in the relevant standard article (EN ISO 148-2, item: 8.4) (ISO, 2017). Experiments were made in the form of service procurement in Sıla Kalite-Türkiye company. The crushing and cooling unit is shown in Figure 2.

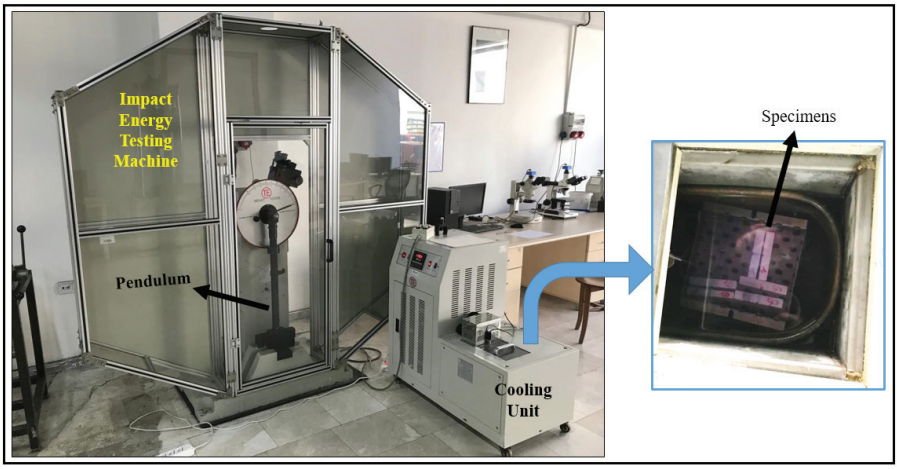

Figure 2. Impact Energy Testing Module

The samples obtained after crushing were washed with methanol at room temperature and taken into macro examination. Surface analysis was performed from the fracture zone.

3. Results and Discussions

MgAlSi alloy was first taken into XRF analysis and elemental analysis rates are given in Table 1. The Mg level was measured as 81.04 ± 0.61% in the alloy formed with 80% Mg and 20% Al12Si ingots by weight. Al ratio is at the level of 17.01 ± 0.25 %. The Si ratio is approximately 2.32 ± 0.19 %. Elements that are less than 0.1% due to the impurity rate of the ingots were not taken into consideration. The values in the Table 1 are given as the average of 3 measurements. Deviations were calculated based on the measurements.

Table 1. XRF analyses results

Elements	Mg %wt	Al %wt	Si %wt
MgAlSi	81.04 ± 0.61	17.01 ± 0.25	% 2.32 ± 0.19

The microstructure images obtained in the SEM examination, which was first applied to MgAlSi alloys, are shown in Figure 3 at low and high magnification. The substructure observed in the microstructure is α-Mg. The lighter colored helical network structure is the intermetallic Mg17Al12 phase. As it is observed at high magnification (2000x), this phase is formed as eutectic, while it is observed as a pre-eutectic structure (Lamellar structure) at the intermediate boundaries. Prismatic diagonal structures that are attached to or independently of the intermetallic phases are Mg_2Si particles. These phase definitions are confirmed by our past work (Çiçek & Sun, 2012; Çiçek vd., 2013; Cicek vd., 2020). The main purpose at this stage is to discuss the cryogenic results of the alloy rather than the phase fraction.

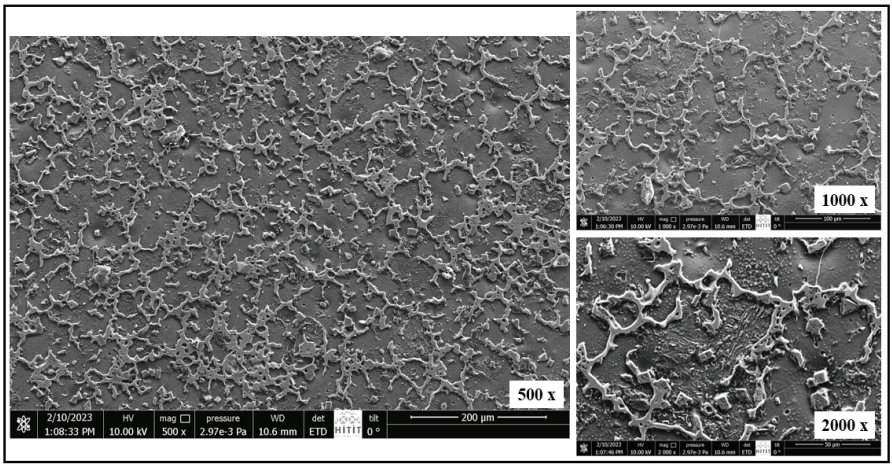

Figure 3. Microstructures of the alloy at different magnifications

The fraction of intermetallic structures observed in the microstructure obtained from MgAlSi alloy is important. As it is known, intermetallic structures are called secondary β phase. Mg, excluding the amount that forms compounds with Al and Si, is indicated as α. With this result, the α / β ratio can be traced (Sun & Ahlatci, 2011; Kulkarni vd., 2012; Çiçek vd., 2013). For this reason, the secondary β phase ratio was calculated as 32.68% in the image processing process (Figure 4). As a result, this process examines the cryogenic properties of an alloy containing up to 32% of intermetallic structure. This phase fraction can be used in the comparison process.

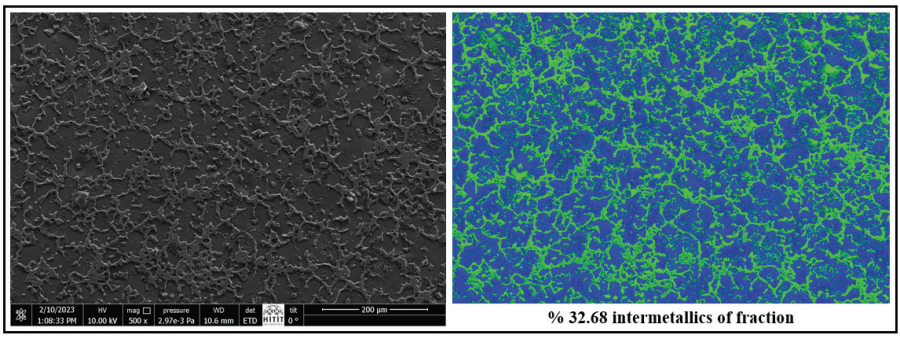

Figure 4. Image processing analyses of microstructure

MgAlSi alloy, which was examined as cryogenic, was subjected to -80°C (193°K) crushing process. The specimens fractured in Charpy style under 300 J pendulum exhibited the impact energies given in Table 2. The process was followed in 8 samples in total.

Table 2. Impact energy for specimens and average value

Specimens	Impact Energy (-80°C) (193°K) Joule	Avg. Impact Energy Joule
1	2.585	**2.3895** - 0.4065 + 0.5605
2	1.983	
3	2.828	
4	2.950	
5	2.222	
6	1.983	
7	2.222	
8	2.343	

According to the values given in the Table 2, the MgAlSi alloy was able to produce an average of 2.3895 J impact energy in the cryogenic environment at a temperature of -80°C (193°K). In the impact energy test applied as 8mm x 10mm after the notch depth (2mm), 80-mm^2 area was exposed to a sudden load from the pendulum. Thus, when the total average impact energy is proportioned to the surface area (2.3895 / 80-mm^2), a value of 0.029 J/mm^2 is calculated. In a study by Desai et al, the impact energy of AlSi10Mg alloy was determined at the level of 0.03-0.05 J/mm^2 at cryogenic temperatures (Desai vd., 2016). Based on this, the MgAlSi ternary alloy structure in this study gave similar results with the literature.

The samples obtained after the impact energy measurement applied in Charpy style are given in Figure 5.

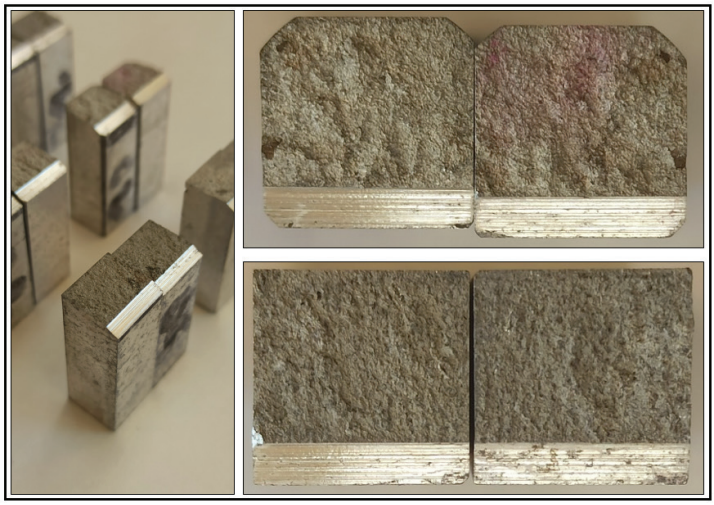

Figure 5. Fracture surfaces macro images for random specimens

According to the fractions observed on the fractured surfaces, the samples after casting and homogenization showed similar structures. No casting defects such as gas void, inclusion or segregation were detected in the samples due to the casting process. A brittle fracture occurred when the surfaces were followed.

It is a known process that light alloys subjected to sudden impact loads at low temperatures can exhibit brittle fracture (Zheng vd., 2011; Polmear vd., 2017). In this study, the brittle fracture fractography revealed by the examination of the surfaces can be explained in this way.

It is known that applications using light alloys based on Mg or Al are increasing day by day. Light alloys, which we encounter at all stages such as biomaterials, tribological products, mechanical values and corrosive environment, can give successful results at room temperature. (Zheng vd., 2011; Agarwal vd., 2016; Desai vd., 2016). In this study, the impact energy of a light alloy at a cryogenic temperature was defined.

4. General Conclusions

An alloy of Mg metal formed with Al and Si was produced in this study. The produced alloy was subjected to the notch breaking test in accordance with the relevant standard (EN ISO 148-2) according to the Charpy style at a cryogenic temperature. As a result of experiments and investigations, the following general conclusions were reached.

a. Mg metal was prepared with Al12Si ingot alloy and successfully produced in an atmosphere-controlled furnace.

b. As a result of elemental analysis and microstructure characterization of MgAlSi ternary alloy, similar results were obtained in the literature. Intermetallic Mg-Al phase and Mg-Si phases in the form of particles were detected in the microstructure.

c. Impact notch test was performed at the relevant standard conditions at a cryogenic temperature (-80°C / 193°K) and an impact energy of 0.03 J/mm^2 was obtained.

Thus, a new experiment and conclusion process on the cryogenic properties of Mg alloys has been added to the literature.

Acknowledgement

We would like to thank TÜV Sıla Kalite A.Ş. for supporting the preparation of this study.

REFERENCES

Agarwal, S., Curtin, J., Duffy, B., & Jaiswal, S. (2016). Biodegradable magnesium alloys for orthopaedic applications: A review on corrosion, biocompatibility and surface modifications. *Mater Sci Eng C, 68*, 948-963. doi:https://doi.org/10.1016/j.msec.2016.06.020

Bamberger, M. (2013). Structural refinement of cast magnesium alloys. *Materials Science and Technology, 17*(1), 15-24. doi:https://doi.org/10.1179/026708301101509061

Bamberger, M., & Dehm, G. (2008). Trends in the development of new Mg alloys. *Annu. Rev. Mater. Res., 38*, 505-533. doi:https://doi.org/10.1146/annurev.matsci.020408.133717

Cao, F., Shi, Z., Song, G.-L., Liu, M., Dargusch, M. S., & Atrens, A. (2015). Influence of hot rolling on the corrosion behavior of several Mg–X alloys. *Corros. Sci., 90*, 176-191. doi:10.1016/j.corsci.2014.10.012

Chen, J., Tan, L., Yu, X., Etim, I. P., Ibrahim, M., & Yang, K. (2018). Mechanical properties of magnesium alloys for medical application: A review. *J. Mech. Behav. Biomed. Mater., 87*, 68-79.

Cicek, B., Aydogmus, T., & Sun, Y. (2020). A basic study on artificial aging in Mg-10Al12Si+ 1Pb alloy. *Materials Research Express, 7*(1), 016588. doi:https://doi.org/10.1088/2053-1591/ab66f2

Çiçek, B., Ahlatçı, H., & Sun, Y. (2013). Wear behaviours of Pb added Mg–Al–Si composites reinforced with in situ Mg2 Si particles. *Materials & Design, 50*, 929-935. doi:https://doi.org/10.1016/j.matdes.2013.03.097

Çiçek, B., & Sun, Y. (2012). A study on the mechanical and corrosion properties of lead added magnesium alloys. *MATER DESIGN, 37*, 369-372. doi:https://doi.org/10.1016/j.matdes.2012.01.029

Desai, R. S., Joshi, A. G., & BV, S. K. (2016). Study on influence of cryogenic treatment on mechanical properties of alsi10mg alloy. *International Journal of Research in Engineering and Technology, 5*(33), 53-56.

Friedrich, H., & Schumann, S. (2001). Research for a "new age of magnesium" in the automotive industry. *Journal of Materials Processing Technology, 117*(3), 276. doi:https://doi.org/10.1016/S0924-0136(01)00780-4

Froes, F., Eliezer, D., & Aghion, E. (1998). The science, technology, and applications of magnesium. *The Journal of The Minerals, Metals & Materials Society (TMS), 50*(9), 30-34. doi:https://doi.org/10.1007/s11837-998-0411-6

Furuya, H., Kogiso, N., Matunaga, S., & Senda, K. (2000). *Applications of magnesium alloys for aerospace structure systems.* Paper presented at the Materials Science Forum.

ISO, I. S. O. (2017). EN ISO 148-2 - Metallic materials — Charpy pendulum impact test — Part 1: Test method. CH-1214 Vernier, Geneva, Switzerland: ISO.

Jiang, Y., Tang, G., Shek, C., & Liu, W. (2011). Microstructure and texture evolution of the cold-rolled AZ91 magnesium alloy strip under electropulsing treatment. *Journal of alloys and compounds, 509*(11), 4308-4313.

Kainer, K., & Von Buch, F. (2003). The current state of technology and potential for further development of magnesium applications. *J. Magnes. Alloy.*, 1-22. doi:https://doi.org/10.1002/3527602046.ch1

Korgiopoulos, K., Langelier, B., & Pekguleryuz, M. (2021). Mg17Al12 Phase Refinement and the Improved Mechanical Performance of Mg-6Al alloy with trace Erbium Addition. *Materials Science and Engineering: A*, 141075. doi:https://doi.org/10.1016/j.msea.2021.141075

Kulkarni, R. R., Prabhu, N., Hodgson, P. D., & Kashyap, B. P. (2012). Phase dissolution of γ-Mg 17 Al 12 during homogenization of as-cast AZ80 Magnesium alloy and its effect on room temperature mechanical properties *Magnesium Technology 2012* (pp. 543-548): Springer.

Liu, L., Chen, X., Pan, F., Wang, Z., Liu, W., Cao, P., Yan, T., & Xu, X. (2015). Effect of Y and Ce additions on microstructure and mechanical properties of Mg–Zn–Zr alloys. *Mater. Sci. Eng. A, 644*, 247-253. doi:10.1016/j.msea.2015.07.065

Liu, Z., Sato, N., Gao, W., Yubuta, K., Kawamoto, N., Mitome, M., Kurashima, K., Owada, Y., Nagase, K., & Lee, C.-H. (2021). Demonstration of ultrahigh thermoelectric efficiency of 7.3% in Mg3Sb2/MgAgSb module for low-temperature energy harvesting. *Joule, 5*(5), 1196-1208.

Mordike, B., & Ebert, T. (2001). Magnesium: properties-applications-potential. *Mater Sci Eng A, 302*(1), 37-45. doi:https://doi.org/10.1016/S0921-5093(00)01351-4

Polmear, I., StJohn, D., Nie, J.-F., & Qian, M. (2017). *Light alloys: metallurgy of the light metals*: Butterworth-Heinemann.

Savitsky, E., & Baton, V. (1952). Mechanical properties of alloys of the magnesium—cadmium system. *Russian Chemical Bulletin, 1*(3), 383-387. doi:https://doi.org/10.1007/BF01171984

Singh, K., & Sehgal, A. K. (2022). Evaluation of characteristics of friction stir welded Mg-Al-Zn magnesium alloy. *Materials Today: Proceedings*.

Sun, Y., & Ahlatci, H. (2011). Mechanical and wear behaviors of Al–12Si–XMg composites reinforced with in situ Mg2Si particles. *Materials & Design, 32*(5), 2983-2987. doi:https://doi.org/10.1016/j.matdes.2011.01.009

Vander Voort, G. (2015). Metallography of Magnesium and its Alloys. *Buehler Tech-Notes, 4*(2).

Xu, C. X., Ju, H., & Zhou, Y. (2011). *Effect of Ca on Microstructure and Properties of Mg-Al-Si Alloys.* Paper presented at the Advanced Materials Research.

Zeytin, H. (1999). *Magnesium Alloys: Application and Future in Automotive Industry*. Paper presented at the International Casting Congree, Ankara, Türkiye.

Zheng, B., Ertorer, O., Li, Y., Zhou, Y., Mathaudhu, S. N., Tsao, C. Y., & Lavernia, E. J. (2011). High strength, nano-structured Mg–Al–Zn alloy. *Materials Science and Engineering: A, 528*(4-5), 2180-2191.

Zhu, L., Qiu, F., Zou, Q., Han, X., Shu, S.-L., Yang, H.-Y., & Jiang, Q.-C. (2021). Multiscale design of α-Al, eutectic silicon and Mg2Si phases in Al-Si-Mg alloy manipulated by in situ nanosized crystals. *Materials Science and Engineering: A, 802*, 140627. doi:https://doi.org/10.1016/j.msea.2020.140627

CHAPTER 9

TURKEY'S RENEWABLE ENERGY POLICIES IN DEVELOPMENT PLANS, LAWS AND REGULATIONS

Fatih Selim BAYRAKTAR[1], Ramazan KÖSE[2]

1 Research Assistant, Mechanical Engineering, Simav Faculty of Technology, Kütahya Dumlupınar University, Kütahya, Turkey, ORCID: 0000-0002-8672-3511

2 Prof. Dr., Mechanical Engineering, Engineering Faculty, Kütahya Dumlupınar University, Kütahya, Turkey, ORCID: 0000-0001-6041-6591

1. INTRODUCTION

Energy and its sustainability are among the most important problems that human beings need to solve. Population growth, the desire for a luxurious life, financial gain, mobility and communication, and the increasing number of people reaching materials and technology to meet these needs have brought with it the increasing energy demand and intense efforts to meet this demand.

Energy is one of the factors that reflect the social, cultural and economic development of a country. In the absence of domestic technology; If the energy supply is based on imported energy sources rather than domestic and renewable energy sources, energy may harm rather than contribute to social and economic development. Due to intense foreign dependency, increasing energy bills, disruptions and problems in energy supply, energy can become a source of problems for the security of the country and one of the most important obstacles to development and independence. Due to such reasons, it is necessary to work intensively to first define, design, construct, develop and then implement domestic and national energy policies and programs that aim to protect and develop the interests of the society.

In this study, first, the political steps taken to support renewable energy in our country are explained. Then, to understand the effectiveness of the steps taken and to make comparisons, the energy production data in Turkey and in the world between the years 2005-2021 were examined. In the conclusion and recommendations section, a general evaluation has been made and suggestions have been made to make renewable energy more effective in Turkey.

2. RENEWABLE ENERGY POLICIES IN TURKEY

2.1. Development Plans

Table 1: Renewable Energy in Development Plans.

Dev. Plan	Sections on Renewable Energy
1st D. P. 1963-1967 (Devlet Planlama Teşkilatı [DPT], 1963)	- Only in the 2/h subsection of the Measures Subsection, it was requested to test biogas facilities near state farms in areas with agricultural centers.
2nd D. P. 1968-1972 (DPT, 1967)	- Renewable energy was not mentioned.
3rd D. P. 1973-1977 (DPT, 1972)	- To correct the thermal/hydraulic balance deteriorated against hydraulics planned. - Geothermal, one of the renewable energy sources, will start to be used in Turkey.
4th D. P. 1979-1983 (DPT, 1979)	- The share of hydraulic energy production in total energy production remained at 12.8% despite the Keban Dam. - Research and development studies for the utilize of alternative sources and solar energy have gained great importance in this plan.

5th D. P. 1985-1989 (DPT, 1984)	- The share of hydraulic energy was expected to increase to 20 percent. - In the long term, it will be possible to focus on hydraulic resources to overcome the electricity energy bottleneck. - While prioritizing reliable and cheap sources in increasing energy production, necessary initiatives will be supported to benefit from new and especially renewable energy sources (especially solar, geothermal and biogas). - State will closely monitor the developments in the world regarding research and practice on the mixed Solar-Water Power.
6th D. P. 1990-1994 (DPT, 1989)	- Necessary measures will be taken to benefit from renewable energy sources such as geothermal and solar energy, especially hydraulic energy, to a greater extent.
7th D. P. 1996-2000 (DPT, 1995)	- One of the most important developments in energy production is observed in hydraulic energy, - The use of renewable energy resources will be emphasized.
8th D. P. 2001-2005 (DPT, 2000)	- Considering the aim of protecting nature, measures will be taken to develop and expand new and renewable energy sources and to have a larger share in consumption. Thus, it will be ensured that the energy potential of country is used at the highest level by adding renewable energy resources as well as domestic fossil resources.
9th D. P. 2007-2013 (DPT, 2006)	- To increase the share of electrical energy generation based on renewable energy sources in total electricity production, the Law No. 5346 on the Use of Renewable Energy Sources in Electricity Generation was passed into law. - Work on the Energy Efficiency Law was completed, but it was not enacted until the date of the development plan report.
10th D. P. 2014-2018 (Kalkınma Bakanlığı, 2013)	- It is stated that to increase the share of renewable energy resources in energy production is important to make more use of domestic resources. - To increase energy supply security renewable energy production continued to be supported. - 38 new geothermal fields have been discovered. - The contribution of renewable energy to the country's economics will be raised by increasing the locality rates and domestic production capacity in renewable energy production devices, and unique technologies will be developed. - Karapınar Energy Specialized Industrial Zone was established. - To ensure energy supply security, the incentive system for electricity production from renewable energy sources was developed and domestic equipment manufacturing was supported. - Essential actions will be taken in the operation of integrating renewable energy sources into the interconnected system without jeopardizing the security and sustainability of the energy transmission and distribution system.

11th D. P. 2019-2023 (Cumhurbaşkanlığı Strateji ve Bütçe Başkanlığı, 2019)	- The ratio of renewable energy in total electricity production raised from 28.9% to 32.5% between 2013 and 2018. - Tenders for Wind and Solar Renewable Energy Resource Areas (YEKA) with a total capacity of 2,000 MW were held to utilize renewable energy sources effectively and efficiently and to produce domestically the equipment used in production facilities. - Efforts to support renewable energy production continued to increase energy supply security. - New investment models will be implemented through mechanisms that will include the use of technology transfer, R&D, domestic equipment and public procurement in the field of renewable energy. - The ratio of renewable energy-based electricity generation in the total will be raised, and the necessary investments and planning will be made for the safe inclusion of renewable energy into the interconnected grid. - Required assistance activities will be implemented in the process of connecting renewable energy generation facilities to transmission and distribution lines. - In order for companies to meet their own electricity needs, unlicensed solar power generation plant and wind power generation plant applications will be made more widespread. - Exploration, production and R&D works for high-potential domestic energy resources such as geothermal will be increased to use domestic resources more.

2.2. Laws

Table 2: Renewable Energy in Laws.

Law No. and Name	**Considerations on Renewable Energy**
Law No. 5346: Use of Renewable Energy Resources for the Purpose of Electricity Generation Law - *Yenilenebilir Enerji Kaynaklarının Elektrik Enerjisi Üretimi Amaçlı Kullanımına İlişkin Kanun* (Resmi Gazete, 2005a) **Date:** 10.05.2005 **Official Gazette No.:** 25819	It aims to improve the production of electrical energy from renewable energy, to increase the diversity of these resources, to bring renewable energy sources to the financial system in an economical, reliable and high quality manner, to protect the environment and to evaluate wastes for this purpose, to reduce greenhouse gas emissions and to make necessary developments for the manufacturing sector to achieve these goals. In the sub-heading of the law: - Identification, Protection and Use of Renewable Energy Resource Areas and Certification of Electric Energy Obtained from Renewable Resources - Procedures and Principles to be Assigned in Electricity Production from Renewable Energy Sources - Implementation Principles Regarding the Investment Period frameworks of such subjects were determined.

Law No. 5627: Energy Efficiency Law – *Enerji Verimliliği Kanunu* (Resmi Gazete, 2007) **Date:** 02.05.2007 **Official Gazette No.:** 26510	It is an important law in terms of renewable energy, as it covers the principles and procedures to be applied for the utilization of renewable energy sources, as well as for the purposes of raising energy awareness throughout the country; improving and supporting energy efficiency in electricity production facilities, residences, industrial enterprises, transportation, energy generation, transmission, distribution and consumption stages, transmission and distribution networks.
Law No. 6094: Amending the Law on the Use of Renewable Energy Resources for the Purpose of Electricity Generation - *Yenilenebilir Enerji Kaynaklarının Elektrik Enerjisi Üretimi Amaçlı Kullanımına İlişkin Kanunda Değişiklik Yapılmasına Dair Kanun* (Resmi Gazete, 2011a) **Date:** 08.01.2011 **Official Gazette No.:** 27809	The 10-year prices for the generation license holders to be supported within the scope of the RES Support Mechanism described in the Law No. 5346 are determined in Table I (Table 4). Real persons and legal entities producing electrical energy from renewable energy from renewable energy sources will also be able to benefit from the same prices if they supply the electrical energy they generate above their demands to the distribution system. The relevant distribution company has to purchase this electrical energy. For companies that generate electricity from renewable energy sources managed by licensed legal entities using domestically produced mechanical and/or electromechanical components, the prices in Table II (Table 4) are added to the prices in Table I (Table 3).
Law No. 6122: Approval of the Status of the International Renewable Energy Agency Law - *Uluslararası Yenilenebilir Enerji Ajansının Statüsünün Onaylanmasının Uygun Bulunduğuna Dair Kanun* (Resmi Gazete, 2011b) **Date:** 10.03.2011 **Official Gazette No.:** 27870	With this law, it was found appropriate to approve the "Status of the International Renewable Energy Agency" passed into law in Bonn on January 26, 2009.
Law No. 6446: Electricity Market Law - *Elektrik Piyasası Kanunu* (Resmi Gazete, 2013a) **Date:** 30.03.2013 **Official Gazette No.:** 28603	In this law, a regulation was made regarding the licensing of production facilities that use renewable energy sources installed on building surfaces. Unlicensed operation of generation facilities based on renewable energy resources with an installed capacity of up to 1 MW or energy production plants based on renewable energy resources with the same production and consumption, which use all of the energy they produce without giving it to the distribution or transmission system, are allowed to operate without a license.

Table 3. Table No. I Specified in Law No. 6094 (Resmi Gazete, 2011a).

Table No. I (YEKDEM Base Prices)	
Production Facility Type Based on Renewable Energy Source	**Prices (ABD dollar cent/kWh)**
a. Hydroelectric production facility	7,3
b. Wind energy production facility	7,3
c. Geothermal energy production facility	10,5
d. Biomass production facility (including landfill gas)	13,3
e. Solar energy production facility	13,3

Table 4. *Table No. II Specified in Law No. 6094 (Resmi Gazete, 2011a).*

Table No. II (Domestic Production)		
Facility Type	**Domestic Manufacturing**	**Domestic Production Additives (ABD dollar cent/kWh)**
A- Hydroelectric production facility	1. Turbine	1,3
	2. Generator and power electronics	1,0
B- Wind energy production facility	1. Blade	0,8
	2. Generator and power electronics	1,0
	3. Turbine tower	0,6
	4. All mechanical parts in rotor and nacelle groups (Except for the payments made for the blade group, generator and power electronics.)	1,3
C-PV solar power production facility	1. PV panel integration and solar structural mechanics fabrication	0,8
	2. PV modules	1,3
	3. PV module cells	3,5
	4. Invertor	0,6
	5. PV module focusers	0,5
D-CSP based production facility	1. Radiation collection tube	2,4
	2. Reflective surface	0,6
	3. Sun tracking system	0,6
	4. Mechanical parts of the heat energy storage system	1,3
	5. Mechanical parts of tower receivers	2,4
	6. Stirling motor	1,3
	7. Panel integration and solar panel structural mechanics	0,6
E- Biomass production facility	1. Fluidized bed steam boiler	0,8
	2. Liquid or gas fueled steam boiler	0,4
	3. Gasification and gas cleaning group	0,6
	4. Steam or gas turbine	2,0
	5. Internal combustion engine or stirling engine	0,9
	6. Generator and power electronics	0,5
	7. Cogeneration system	0,4
F- Geothermal energy production facility	1. Steam or gas turbine	1,3
	2. Generator and power electronics	0,7
	3. Steam injector or vacuum compressor	0,7

2.3. Regulations

Table 5: Renewable Energy in Regulations [18-27].

Regulation Name	**Considerations on Renewable Energy**
Regulation on Procedures and Principles Regarding Certification of Renewable Energy Source - *Yenilenebilir Enerji Kaynak Belgesi Verilmesine İlişkin Usul ve Esaslar Hakkında Yönetmelik* (Resmi Gazete, 2005b) **Date:** 01.10.2005 / **O.G. No.:**25956	It is aimed to determine the procedures and principles in the process of issuing a renewable energy resource certificate to the licensed legal entities that produce from renewable energy resources.
Regulation on Domestic Manufacturing of Parts Used in Facilities Producing Electrical Energy from Renewable Energy Sources - *Yenilenebilir Enerji Kaynaklarından Elektrik Enerjisi Üreten Tesislerde Kullanılan Aksamın Yurt İçinde İmalatı Hakkında Yönetmelik* (Resmi Gazete, 2011c) **Date:** 19.06.2011 / **O.G. No.:**27969 Arrangements Made: **Date:** 26.07.2012 / **O.G. No.:**28365 **Date:** 04.09.2013 / **O.G. No.:**28755 **Date:** 09.06.2017 / **O.G. No.:**30091 **Date:** 28.07.2017 / **O.G. No.:**30137	The components used in the power plants producing electrical energy from renewable energy sources and manufactured domestically together with their integrating parts are allowed to be used for the Purpose of Electricity Generation of Renewable Energy Resources Law. It is aimed to determine the procedures and principles regarding the determination, certification and supervision of the additional price according to the Schedule II in the annex of the related Law.
Regulation on Solar Energy Based Electricity Generation Facilities – *Güneş Enerjisine Dayalı Elektrik Üretim Tesisleri Hakkında Yönetmelik* (Resmi Gazete, 2011d) **Date:** 19.06.2011 / **O.G. No.:**27969 Arrangements Made: **Date:** 09.01.2020 / **O.G. No.:**31003	It regulates the procedures and principles regarding the check of the generation amounts of electricity produced in power plants that generate electricity from solar energy or where solar energy and another energy source are used as a hybrid.

Regulation on Increasing Efficiency in the Use of Energy Resources and Energy - *Enerji Kaynaklarının Ve Enerjinin Kullanımında Verimliliğin Artırılmasına Dair Yönetmelik* (Resmi Gazete, 2011e) **Date:** 27.10.2011 / **O.G. No.:**28097 Arrangements Made: **Date:** 06.07.2022 / **O.G. No.:**31888	It is aimed to regulate the procedures and principles for improving efficiency in the utilization of energy resources, to use energy effectively, to ligthening the burden of energy costs on the economy and to preserve the environment. In the definition of project on-site generation component (PYÜB-Proje yerinde üretim bileşeni) in the regulation: A new field definition has been made for the use of renewable energy by using the expression of electricity production systems based on renewable energy sources established to provide a part of the energy need of the industrial enterprise. In addition, it is stated in the regulation that public institutions and organizations that carry out and/or support R&D projects give priority to projects on hydrogen production techniques that can be economical by using renewable energy sources and provide promotion and technical support.
Regulation on Certification and Support of Renewable Energy Resources - *Yenilenebilir Enerji Kaynaklarının Belgelendirilmesi ve Desteklenmesine İlişkin Yönetmelik* (Resmi Gazete, 2013b) **Date:** 01.10.2013 / **O.G. No.:**28782 Arrangements Made: **Date:** 29.04.2016 / **O.G. No.:**29698 **Date:** 28.10.2016 / **O.G. No.:**29871 **Date:** 23.02.2017 / **O.G. No.:**29988 **Date:** 11.05.2017 / **O.G. No.:**30063 **Date:** 21.04.2018 / **O.G. No.:**30398 **Date:** 09.10.2018 / **O.G. No.:**30650 **Date:** 23.08.2019 / **O.G. No.:**30867 **Date:** 08.03.2020 / **O.G. No.:**31062 **Date:** 28.07.2020 / **O.G. No.:**31199 **Date:** 07.08.2020 / **O.G. No.:**31206 **Date:** 14.11.2020 / **O.G. No.:**31304 **Date:** 09.05.2021 / **O.G. No.:**31479 **Date:** 19.08.2021 / **O.G. No.:**31573 **Date:** 10.02.2022 / **O.G. No.:**31746 **Date:** 01.03.2022 / **O.G. No.:**31765	Encouragement of electricity generation based on renewable energy resources and establishment of the YEK Support Mechanism (YEKDEM) to be operated within the scope of the Law on the Use of Renewable Energy Resources for Electricity Generation, dated 10.05.2005 and numbered 5346, and issuing the Renewable Energy Resources Certificate for production plants based on renewable energy resources to legal entities holding generation licenses. It covers the procedures and principles regarding the authorities and duties, rights and responsibilities of legal and real persons in the certification process.

Regulation on the Procedures and Principles Regarding the Determination, Grading, Protection and Use of Renewable Energy Resource Areas for Electric Energy Production - *Elektrik Enerjisi Üretimine Yönelik Yenilenebilir Enerji Kaynak Alanlarının Belirlenmesi, Derecelendirilmesi, Korunması Ve Kullanılmasına İlişkin Usul ve Esaslara Dair Yönetmelik* (Resmi Gazete, 2013c) **Date:** 27.11.2013 / **O.G. No.:**28834	It is aimed to regulate the procedures and principles regarding the determination, protection, grading and use of renewable energy resource areas suitable for electricity production in public and national treasury lands.
The Regulation on Electrical Engineering Services for the Generation of Electrical Energy from Renewable Energy Sources of the TMMOB – EMO - *Türk Mühendis ve Mimar Odaları Birliği Elektrik Mühendisleri Odası Yenilenebilir Enerji Kaynaklarından Elektrik Enerjisi Üretimine Ait Elektrik Mühendisliği Hizmetleri Yönetmeliği* (Resmi Gazete, 2015) **Date:** 28.02.2015 / **O.G. No.:**29281 Arrangements Made: **Date:** 23.02.2019 / **O.G. No.:**30695	The purpose of the regulation; to define the engineering services related to the production of electrical energy from renewable energy resources, to regulate the duties, authorities and responsibilities of the engineers who will carry out these services and to regulate the procedures and principles regarding the supervision of these services.
Regulation on Supporting Domestic Parts Used in Facilities Producing Electricity from Renewable Energy Sources - *Yenilenebilir Enerji Kaynaklarından Elektrik Enerjisi Üreten Tesislerde Kullanılan Yerli Aksamın Desteklenmesi Hakkında Yönetmelik* (Resmi Gazete, 2016a) **Date:** 24.06.2016 / **O.G. No.:**29752 Arrangements Made: **Date:** 20.09.2019 / **O.G. No.:**30894 **Date:** 28.05.2020 / **O.G. No.:**31138 **Date:** 10.12.2020 / **O.G. No.:**31330 **Date:** 09.04.2021 / **O.G. No.:**31449	The purpose of this regulation; regarding the conditions of application of the additional price according to the Schedule II in the annex of the Law No. 5346 and the determination, certification and inspection of the additional price amount to be applied within the scope of each application determining the principles and procedures.
Renewable Energy Source Areas Regulation - *Yenilenebilir Enerji Kaynak Alanları Yönetmeliği* (Resmi Gazete, 2016b) **Date:** 09.10.2016 / **O.G. No.:**29852 Arrangements Made: **Date:** 11.04.2017 / **O.G. No.:**30035 **Date:** 31.12.2019 / **O.G. No.:**30995 **Date:** 09.04.2021 / **O.G. No.:**31449	The purpose of the regulation; to utilize renewable energy resources effectively and efficiently by creating YEKA (Yenilenebilir Enerji Kaynak Alanları) in public and national treasury immovables and to produce or supply the high-tech components used in electrical power production plants based on renewable energy sources in the country.

Renewable Energy Source Guarantee Certificate Regulation in the Electricity Market - *Elektrik Piyasasında Yenilenebilir Enerji Kaynak Garanti Belgesi Yönetmeliği* (Resmi Gazete, 2020) **Date:** 14.11.2020 / **O.G. No.:**31304 Arrangements Made: **Date:** 21.05.2021 / **O.G. No.:**31487	The purpose of this regulation; To encourage the utilization of renewable energy sources in electricity production and consumption and to protect the environment, providing the opportunity to track and prove that a certain amount or ratio of electrical energy provided to consumers by licensed legal entities is generated from renewable energy sources, providing certification to consumers of electrical energy generated from renewable energy sources, to regulate the procedures and principles regarding the foundation of the energy resource guarantee system and the objective and transparent operation of this system.

3. ENERGY GENERATION STATUS IN TURKEY

Electricity production increased by approximately 100% in this period, while electricity production from renewable energy increased by 184.2%. The share of renewable energy in our country's electricity production increased from 24.7% to 35% between 2005-2021. The share of electricity production from renewable energy was low in 2021, as the generation of hydroelectric installed power was severely affected by the decrease in precipitation. In 2020, this rate was 42.4%.

Table 6. *Distribution of Turkey's electricity generation by primary sources over the years (ELDER, 2022).*

PRIMARY ENERGY SOURCES		ELECTRITY GENERATION (TWh)				
		2005	2010	2015	2020	2021
FOSSIL FUELS	COAL	43.07	55.05	76.17	105.81	111.48
	NAT. GAS	70.97	98.14	99.22	70.93	99.19
	OTHER	8.02	2.18	2.22	0.32	0.32
RENEW. SOURCES	HYDRO	39.66	51.8	67.15	78.09	53.05
	SOLAR	0	0	0.19	10.95	13.21
	WIND	0.06	2.92	11.65	24.83	29.14
	OTHER	0.23	1.13	5.18	15.76	18.14
TOTAL		162.01	211.22	261.78	306.69	324.53

4. ENERGY GENERATION STATUS IN THE WORLD

Electricity production increased by approximately 54,2% in this period, while electricity production from renewable energy increased by 142.2%. The share of renewable energy in worlds' electricity production increased from 17.7% to 27.9% between 2005-2021.

Table 7. Distribution of the worlds' electricity generation by primary sources over the years (BP, 2022).

PRIMARY ENERGY SOURCES		ELECTRITY GENERATION (TWh)				
		2005	2010	2015	2020	2021
FOSSIL FUELS	COAL	7357,7	8634,3	9406,5	9439,3	10244
	NAT. GAS	3762,7	4888,4	5622,2	6371,7	6518,5
	OTHER	4069,8	3868,2	3747,7	3585,7	3772,8
RENEW. SOURCES	HYDRO	2911,3	3429,2	3878,4	4346	4273,8
	SOLAR	4,2	33,6	254,7	846,2	1032,5
	WIND	104,6	346,4	831,3	1596,4	1861,9
	OTHER	255,1	380,8	551,1	703,9	762,8
TOTAL		18465,4	21581,3	24292	26889,2	28466,3

The share of renewable energy in Turkey has increased from 24% to 35%, and its share in total energy has increased by 1.42 times. The increase in renewable energy in the world increased from 17.7% to 27.9% between 2005-2021, and its share in total energy increased 1.58 times. Thus, in the same time period, our country did not gain enough momentum to evaluate its potential by showing an increase below the average increase of the world.

5. CONCLUSIONS

Turkey pays huge sums for fossil fuel imports every year. While exports were 254.2 billion dollars in 2022, imports were 364.6 billion dollars. According to these values, the foreign trade deficit is at the level of 110.2 billion dollars. Turkey paid 97.14 billion $ for energy imports in 2022 (İMMİR, 2023). The use of renewable energy sources in electricity production will have positive effects on Turkey's foreign trade balances. The multiplier effect on parameters such as employment, exports and national income may reinforce these effects. The World Bank also states that renewable energy technologies are far ahead of fossil fuels and nuclear energy in the amount of work created per unit electricity produced.

The main pillars of Turkey's energy policy have been determined as environmental protection and development, and sustainable development. The energy needed must be produced in uninterrupted, high quality, reliable and economic conditions, considering the environmental effects. Turkey's emphasis on fossil fuels in energy resources is contrary to environmental policies. To keep the balance between answering the energy demand for the progress of the country and the environmental impacts arising from it, studies should be carried out to coordinate energy policies and environmental policies.

Despite its positive aspects, there are certain reasons why the use of renewable energy sources is not at the expected and desired level both in the world and in our country. The most important of them are; The existence of a market based on fossil fuels and the effects of established interest relations in this market, insufficient R&D studies due to insufficient incentives, the low level of competition in the market for these expensive and technology-developing resources, infrastructure inadequacies, political instability and low level of determination can be counted.

The main starting point to be adopted in solving many problems (financing, technological, educational, etc.) in front of renewable energy development and accelerating investments in renewable energy sources is that the relevant units of the state and political powers have a systematic and scientific approach to the issue. In addition, the work of the relevant persons, institutions and organizations for the future of renewable energy resources should be supported with a political will; A renewable energy policy should be established and implemented as soon as possible, in accordance with the realities of the country and international developments, considering all the economic, social, political and environmental dimensions of the issue.

While forming energy politics and selecting sources for energy generation, the costs of the chosen sources to the community, in another words, the social costs should also be considered. If the costs caused by the damages caused by fossil fuels to the environment and society (external costs) are considered in cost calculations, it will be understood that non-renewable energy technologies would be more expensive than renewables (IRENA, 2016). In this context, societal (external) costs must be considered for renewable energy sources to reach the position they deserve in Turkey. The energy market, which sees social costs as a competitive component, will be fairer. In such a market, which will provide more competitive opportunities, where clean energy is used more, renewable resources will be picked firstly in energy generation. In this regard, it is necessary to contain the environmental aspect in the researches to be carried out to form the most favorable energy policy to provide the energy need of Turkey on the long view and to produce plans agreeable for this policy.

6. SUGGESTIONS

To put the renewable energy sector on strong foundations in the development process and to create healthy policies, some suggestions can be listed as follows;

I. Turkey should primarily employ renewable energy resources in its geography with high potential (Benli, 2013) in terms of diversifying ener-

gy sources and assuring security of supply.

II. As a result of the highly active politics in Turkey, the constant change of energy-related projects and targets hinders the healthy and rapid progress of developments in the sector. For such reasons, long-term preparation of energy programs is required and it is essential to ensure its continuity.

III. In order to increase the interest in alternative energy investments, interest rates should be reduced in loan financing provided to investors by public and private banks.

IV. Sufficient public awareness about renewable energy resources in Turkey has not been achieved yet [IEA, 2021; Irmak, Ayaz, Gok & Sahin, 2014]. In order to raise awareness of the public, studies and projects should be started in cooperation with the public and private sector constituents.

V. There are many incentive mechanisms to improve the utilize of renewable energy sources in our country (YEKA, YEKDEM etc.). New and more comprehensive incentive systems should be implemented to attract investors with applications such as subsidies, tax exemptions and tax refunds.

VI. Projects that are envisaged to be performed in the energy sector, especially renewable energy resources in Turkey, sometimes encounter difficulties of varying degrees. To avoid possible bottlenecks in the system, existing laws and regulations should be developed as soon as possible and rearranged in accordance with the needs of the sector.

VII. Although our country has the ability and potential to manufacture the equipment used in renewable energy with domestic production, it pays significant amounts for the import of these devices. Due to this import, there is a loss of foreign exchange and the progress of domestic production and industry is negatively affected. Although Law No. 6094 encourages domestic technology products, more political and economic support is needed.

VIII. In the process of full membership to the EU, Turkey has started legislation harmonization in the alternative energy sector, and regulations need to be implemented quickly to gain functionality. In addition, bureaucratic obstacles (Kalkınma Bakanlığı, 2019) that foreign energy investors have to overcome in terms of its contribution to Our country's economy should be resolved.

IX. The energy demands of public establishments should be met with renewable energy sources, so that the energy need of public establishments will be met with clean energy and will set an example for the society.

X. The potential of renewable energy resources in Our country should be determined in a healthier way, R&D studies should be carried out on how to use this potential, and there should be government support for these studies to be carried out.

XI. Policies and targets should be consistent and long-term so that they can develop renewable energy industries regionally and increase employment.

XII. The developments in the world on renewable energy technologies should be followed, studies and researches to be conducted within the country should be encouraged.

REFERENCES

Benli, H. (2013). Potential of renewable energy in electrical energy production and sustainable energy development of Turkey: Performance and policies. *Renewable Energy*, 50, 33-46.

BP, Statistical Review (2022). *Statistical Review of World Energy – all data, 1965-2021*. Retrieved from https://www.bp.com/en/global/corporate/energy-economics/statistical-review-of-world-energy/downloads.html

ELDER (Elektrik Dağıtım Hizmetleri Derneği - Association of Electricity Distribution System Operators) (2022). *2022 Presidential Annual Program Energy Sector Summary Report*. Retrieved from https://www.elder.org.tr/Content/files/a4cfa306-6d2a-44ff-920d-2f2b55741b18.pdf

IEA (2021). Turkey 2021, Energy Policy Review. Retrieved from https://iea.blob.core.windows.net/assets/cc499a7b-b72a-466c-88de-d792a9daff44/Turkey_2021_Energy_Policy_Review.pdf

IRENA, A Renewable Energy Roadmap (Remap). (2016). *The true cost of fossil fuels: Saving on the externalities of air pollution and climate change*. Retrieved from https://www.irena.org/-/media/files/irena/agency/publication/2016/irena_remap_externality_brief_2016.pdf

Irmak, E., Ayaz, M. S., Gok, S. G., & Sahin, A. B. (2014). A survey on public awareness towards renewable energy in Turkey. In *3rd International Conference on Renewable Energy Research and Applications, ICRERA 2014*, 932-937.

İstanbul Maden ve Metaller İhracatçı Birlikleri (İMMİR) (2023). *Ekonomik ve ihracat verileri bülteni Ocak 2023*. Retrieved from https://immib.org.tr/files/kio/Ekonomi%20ve%20İhracat%20Bülteni-Ocak%202023.pdf

Law No. 5346 on the Use of Renewable Energy Resources for the Purpose of Electricity Generation. (2005a, 10 May). Official Gazette (Resmi Gazete) (No.: 25819). Retrieved from https://www.resmigazete.gov.tr/eskiler/2005/05/20050518-1.htm

Law No. 5627 on Energy Efficiency. (2007, 18 April). Official Gazette (Resmi Gazete) (No.: 26510). Retrieved from https://www.resmigazete.gov.tr/eskiler/2007/05/20070502-2.htm

Law No. 6094 Amending the Law on the Use of Renewable Energy Resources for the Purpose of Electricity Generation. (2011a, 8 January). Official Gazette (Resmi Gazete) (No.: 27809). Retrieved from https://www.resmigazete.gov.tr/eskiler/2011/01/20110108-3.htm

Law No. 6122 Approving the Status of the International Renewable Energy Agency. (2011b, 22 February). Official Gazette (Resmi Gazete) (No.: 27870). Retrieved from https://www.resmigazete.gov.tr/eskiler/2011/03/20110310-26.htm

Law No. 6446 on Electricity Market. (2013a, 30 March). Official Gazette (Resmi

Gazete) (No.: 28603). Retrieved from https://www.resmigazete.gov.tr/eskiler/2013/03/20130330-14.htm

Regulation on Certification and Support of Renewable Energy Resources. (2013b, 1 October). Official Gazette (Resmi Gazete) (No.: 28782). Retrieved from https://www.resmigazete.gov.tr/eskiler/2013/10/20131001-4.htm

Regulation on Domestic Manufacturing of Parts Used in Facilities Producing Electrical Energy from Renewable Energy Sources. (2011c, 19 June). Official Gazette (Resmi Gazete) (No.: 27969). Retrieved from https://www.resmigazete.gov.tr/eskiler/2011/06/20110619-5.htm

Regulation on Increasing Efficiency in the Use of Energy Resources and Energy. (2011e, 27 October). Official Gazette (Resmi Gazete) (No.: 28097). Retrieved from https://www.resmigazete.gov.tr/eskiler/2011/10/20111027-5.htm

Regulation on the Procedures and Principles Regarding the Determination, Grading, Protection and Use of Renewable Energy Resource Areas for Electric Energy Production. (2013c, 27 November). Official Gazette (Resmi Gazete) (No.: 28834). Retrieved from https://www.resmigazete.gov.tr/eskiler/2013/11/20131127-6.htm

Regulation on Procedures and Principles Regarding Issuance of Renewable Energy Source Certificate. (2005b, 4 October). Official Gazette (Resmi Gazete) (No.: 25956). Retrieved from https://www.resmigazete.gov.tr/eskiler/2005/10/20051004-3.htm

Regulation on Solar Energy Based Electricity Generation Facilities. (2011d, 19 June). Official Gazette (Resmi Gazete) (No.: 27969). Retrieved from https://www.resmigazete.gov.tr/eskiler/2011/06/20110619-4.htm

Regulation on Supporting Domestic Parts Used in Facilities Producing Electricity from Renewable Energy Sources. (2016a, 24 June). Official Gazette (Resmi Gazete) (No.: 29752). Retrieved from https://www.resmigazete.gov.tr/eskiler/2016/06/20160624-1.htm

Renewable Energy Source Areas Regulation. (2016b, 9 October). Official Gazette (Resmi Gazete) (No.: 29852). Retrieved from https://www.resmigazete.gov.tr/eskiler/2016/10/20161009-1.htm

Renewable Energy Source Guarantee Certificate Regulation in the Electricity Market. (2020, 14 November). Official Gazette (Resmi Gazete) (No.: 31304). Retrieved from https://www.resmigazete.gov.tr/eskiler/2020/11/20201114-2.htm

T. C. Ministry of Development (Kalkınma Bakanlığı), Özel İhtisas Komisyonu Raporu. (2018). İş ve yatırım ortamının iyileştirilmesi. Retrieved from https://www.sbb.gov.tr/wp-content/uploads/2020/04/IsYatirimOrtamininIyilestirilmesiOzelIhtisasKomisyonuRaporu.pdf

T. C. Ministry of Development (Kalkınma Bakanlığı) Tenth Development Plan 2014-2018, Prime Ministry State Printing House (December, 2013). Re-

trieved from https://www.sbb.gov.tr/wp-content/uploads/2022/08/Onuncu_Kalkinma_Plani-2014-2018.pdf Access Date: 03/10/2022.

T. C. Presidential Strategy and Budget Department (Cumhurbaşkanlığı Strateji ve Bütçe Başkanlığı) Eleventh Development Plan 2019-2023, Prime Ministry State Printing House (July, 2019). Retrieved from https://www.sbb.gov.tr/wp-content/uploads/2022/07/On_Birinci_Kalkinma_Plani-2019-2023.pdf Access Date: 03/10/2022.

T. C. Prime Ministry State Planning Organization (Devlet Planlama Teşkilatı – DPT) Development Plan (First Five Years) 1963-1967, Prime Ministry State Printing House (January, 1963). Retrieved from https://www.sbb.gov.tr/wp-content/uploads/2022/07/Kalkinma_Plani_Birinci_Bes_Yillik_1963-1967.pdf Access Date: 03/10/2022.

T. C. Prime Ministry State Planning Organization (DPT) Second Five-Year Development Plan 1968-1972, Prime Ministry State Printing House (July, 1967). Retrieved from https://www.sbb.gov.tr/wp-content/uploads/2022/07/Ikinci_Bes_Kalkinma_Plani-1968-1972.pdf Access Date: 03/10/2022.

T. C. Prime Ministry State Planning Organization (DPT) New Strategy and Development Plan Third Five Years 1973-1977, Prime Ministry State Printing House (October, 1972). Retrieved from https://www.sbb.gov.tr/wp-content/uploads/2022/08/Yeni-Strateji-ve-Kalkinma-Plani_Ucuncu-Bes-Yil_1973_1977.pdf Access Date: 03/10/2022.

T. C. Prime Ministry State Planning Organization (DPT) Fourth Five-Year Development Plan 1979-1983, Prime Ministry State Printing House (April, 1979). Retrieved from https://www.sbb.gov.tr/wp-content/uploads/2022/08/Dorduncu-Bes-Yillik-Kalkinma-Plani_1979_1983.pdf Access Date: 03/10/2022.

T. C. Prime Ministry State Planning Organization (DPT) Fifth Five-Year Development Plan 1985-1989, Prime Ministry State Printing House (July, 1984). Retrieved from https://www.sbb.gov.tr/wp-content/uploads/2022/08/Besinci-Bes-Yillik-Kalkinma-Plani-1985-1989.pdf Access Date: 03/10/2022.

T. C. Prime Ministry State Planning Organization (DPT) Sixth Five-Year Development Plan 1990-1994, Prime Ministry State Printing House (June, 1989). Retrieved from https://www.sbb.gov.tr/wp-content/uploads/2022/07/Altinci_Bes_Yillik_Kalkinma_Plani-1990-1994.pdf Access Date: 03/10/2022.

T. C. Prime Ministry State Planning Organization (DPT) Seventh Five-Year Development Plan 1996-2000, Prime Ministry State Printing House (July, 1995). Retrieved from https://www.sbb.gov.tr/wp-content/uploads/2022/07/Yedinci_Bes_Yillik_Kalkinma_Plani-1996-2000.pdf Access Date: 03/10/2022.

T. C. Prime Ministry State Planning Organization (DPT) Long Term Strategy and Eighth Five-Year Development Plan 2001-2005, Prime Ministry State Printing House (June, 2000). Retrieved from:https://www.sbb.gov.tr/wp-content/uploads/2022/07/Uzun_Vadeli_Strateji_ve_Sekizinci_Bes_Yillik_Kalkinma_Plani-2001-2005.pdf Access Date: 03/10/2022.

T. C. Prime Ministry State Planning Organization (DPT) Ninth Development Plan 2007-2013, Prime Ministry State Printing House (July, 2006). Retrieved from https://www.sbb.gov.tr/wp-content/uploads/2022/07/Dokuzuncu_Kalkinma_Plani-2007-2013.pdf Access Date: 03/10/2022.

Union of Chambers of Turkish Engineers and Architects Chamber of Electrical Engineers Regulation on Electrical Engineering Services for Electricity Production from Renewable Energy Sources. (2015, 28 February). Official Gazette (Resmi Gazete) (No.: 29281). Retrieved from https://www.resmigazete.gov.tr/eskiler/2015/02/20150228-20.htm

CHAPTER 10

INDUSTRY 5.0: A STUDY ON SUPPORTING TECHNOLOGY SYSTEMS, APPLICATIONS, AND FUTURE DIRECTIONS

A. F. M. Shahen SHAH[1],
Muhammet Ali KARABULUT[2]

1 Asst. Prof. Dr. Yildiz Technical University ORCID: 0000-0002-3133-6557
2 Asst. Prof. Dr. Kafkas University ORCID: 0000-0002-2080-5485

1. Introduction

Next-generation wireless networks that are intelligent, resilient, and dependable are expected to serve as a technological enabler for meeting the various communication and computation needs of Industry 5.0 services and applications (Ji, 2021), which are built on the foundation of three key concepts: sustainability, resilience, and human-centered industry (Maddikunta, 2021). Increased manufacturing output while fewer interruptions and disaster situations are examples of resilience. Sustainability primarily tackles environmental issues, such as energy conservation and resource recycling. Human interests and requirements are put at the center of the manufacturing process, including customization and computer contact, according to the human-centric strategy.

The industrial sector is focused on mitigating negative effects to successfully handle trash and lessen its effects on the ecology in response to the fast rise in environmental contamination brought on by Industry 2.0. Nothing about Industry 4.0 protects the earth. The next industrial transformation has thus been sparked by the need for a technical answer to provide production processes that are pollution-free (Nahavandi, 2019). By decreasing garbage production through the bioeconomy, which creates a pollution-free atmosphere, Industry 5.0 guarantees the viability of society. With the help of technology that allows machines to share and work alongside humans, the fifth industrial revolution (Industry 5.0) has placed a strong emphasis on intelligent manufacturing. With the help of robots and the return of people to manufacturing halls, Industry 5.0 is employing human intellect and ingenuity in intelligent processes. Without worrying about their jobs, people will cooperate and share with the machines, creating value-added services.

By combining several technologies, including artificial intelligence (AI), cloud computing, Internet of Things (IoT), cognitive computing, and cyber-physical systems (CPSs), the Industry 4.0 standard has completely transformed the industrial sector. Making the industrial sector "smart" by linking machinery and other devices that can communicate with one another and manage one another throughout their lifetimes is the primary idea behind Industry 4.0 (Xu, 2020; Li, 2018). Process mechanization is given top precedence in Industry 4.0, which reduces the need for human involvement in the production procedure (Lasi, 2014; Priya, 2021). Industry 4.0 aims to increase overall performance and output by implementing machine learning (ML) to provide understanding between devices and apps (Azeem, 2021; Zhang, 2020). Industry 5.0 is currently being intended as a way to combine strong, clever, and precise technology with the distinctive ingenuity of human specialists. Many technological futurists think that Industry 5.0 will give production one more personal touch (Nahavandi,

2019). Industry 5.0 is anticipated to bring together humans' critical, rational reasoning and highly precise robots. Another significant accumulation of Industry 5.0 is mass customization, which allows consumers to choose individualized and customizable goods based on their preferences and requirements. Industry 5.0 will enable flexibility between robots and humans, greatly boost production productivity, and enable accountability for engagement and ongoing tracking activities. The goal of the partnership between people and robots is to quickly boost output. By giving boring, repetitious tasks to robots or machines and thinking-intensive responsibilities to people, Industry 5.0 can improve the standard of output.

Table 1. *Distinction between this survey and other survey papers.*

Ref.	Enabling Technologies	Impact of 6G	Applications	Future Opportunities	Challenges
(Long, 2020)	X	X	√	X	X
(Al Faruqi, 2019)	X	X	√	X	√
(Ozdemir, 2018)	√	X	√	X	X
(Sachsenmeier, 2016)	X	X	√	X	X
(El Far, 2021)	X	X	X	√	√
Our Survey	√	√	√	√	√

The distinction between this survey and other survey publications is further explained in Table 1. In this study, enabling technology systems, applications and future directions on Industry 5.0 are reviewed. Following is a list of the contributions this study provides. Descriptions of Industry 5.0 are provided based on the existing literatures, which aids in developing a comprehensive concept of Industry 5.0 from various angles. The features of Industry 5.0 compared to previous industrial revolutions are discussed. Industry 5.0-related projects, goods, and groups that create guidelines were investigated. A general basic level of information was given about 6G, which emerged with the Industry 5.0 revolution. Accordingly, the wide uses and objectives are explained. Despite numerous research and development initiatives, Industry 5.0 faces a number of difficulties and issues. The potential research directions are also highlighted for implementation of Industry 5.0.

The remainder of the paper is structured as follows: Section 2 outlines the vision of Industry 5.0. Section 3 presents uses and effective tools in

Industry 5.0. Key Enablers of Industry 4.0 and Industry 5.0 are discussed in Section 4. Discussion, future opportunities and challenges are presented in Section 5. Lastly, Section 6 provides the conclusions.

2. The Rise of Industry 5.0 Vision

The Industry 4.0 is currently taking place. German government listed this project as one of its upcoming initiatives in its 2010 "High-Tech Strategy 2020" action plan. The final goal was to increase automation in smart production and implement automated management with a focus on mass production, as was done during the earlier three industrial revolutions (Tange, 2020). The use of the cutting-edge supporting technologies of the corresponding era, for example, the introduction of various ICT technologies enables the transition from the electronics-based Industry 3.0 to the goal of Industry 4.0 (Aceto, 2019), is one of the major distinctions between different revolutions. Thus, by improving the effectiveness and intelligence of production and robotic processes, Industry 4.0's digital transformation reshapes today's sectors (Chen, 2020). The next industrial transformation, or Industry 5.0, has recently come under discussion in academics and among scholars as a natural progression of the current Industry 4.0 model.

While mass production with minimal waste and increased productivity was a key element of Industry 4.0, Industry 5.0 strives for mass-customized production with zero waste, minimal expense, as well as maximum precision (Yetis, 2020). The idea of Industry 5.0 has yet to fully develop, through examines, for instance, the different meanings and findings made about the Industry 5.0 strategy by eminent industry scholars and practitioners. All pertinent Industry 5.0 ideas place a strong emphasis on the coexistence of humans and robots in order to build an intelligent society in which cobots (robots) handle the less creative aspects of invention and humans handle the more creative ones. In this respect, the European Commission (EC) created the future plans to supplement the industry 5.0 vision with resilience, human-centeredness, and sustainable methods (Industry 5.0, 2023; Industry 5.0, 2021). The next industrial transformation can be realized by enabling people freedom in conjunction with objectives of mass-customization in efficient supply chains, such as flexibility and expandable product variations. This has beneficial effects and advantages for various societal sectors. Figure 1 shows a brief history of industry revolution.

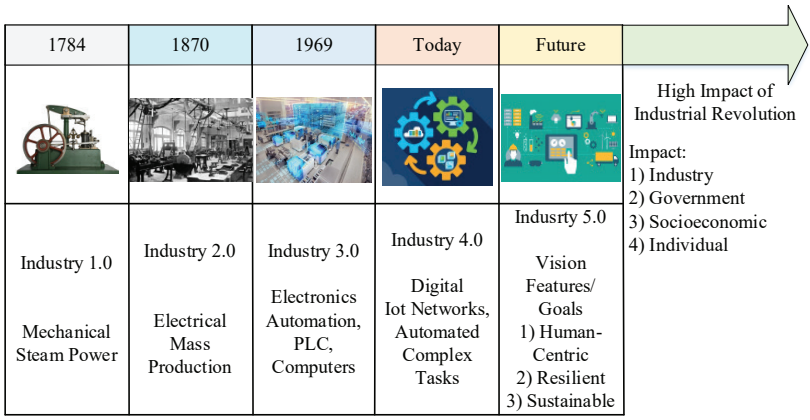

Figure 1. *A brief history of industry revolution.*

Future industries must contribute to the development of solutions for pressing societal issues, such as: 1) preserving the environment and natural resources and combating climate change (sustainability); 2) adopting circular production models; 3) developing enabling ICT technologies; and 4) revising energy consumption regulations to ensure the effective use of natural resources in the event of external shocks, such as the Covid-19 pandemic (human-centric value). The 17 Sustainable Development Goals (SDG) or Global Goals stated in Agenda 2030 of the United Nations (UN) must be realized and enabled by Industry 5.0 vision components (UN, 2017).

By combining both established and cutting-edge methods and technologies, FoFs in Industry 5.0 can offer creative answers to impending social problems. Notably, significant developments in a number of emerging technologies, such as robotics (Xiloyannis, 2021), Industry Internet of Things (IIoT) (Mahmood, 2022), computer vision (Janai, 2020), big data analytics and computation technologies (Ma, 2021), B5G wireless networks (Huang, 2021), and AI (Du, 2020), have made it possible for new industrial applications to be developed that are both vertical and horizontal.

3. Uses and Effective Tools in Industry 5.0

With the integration of cognitive skills and creativity, a number of supporting technological trends, including EC, big data analytics, IoE, cobots, blockchain, and 6G can help sectors boost production and deliver tailored goods more rapidly. Industry 5.0 is an improved production paradigm with an emphasis on interplay between robots and people thanks to these supporting technologies. Intelligent robots are put together to cooperate with people, making human powers more efficient and incredibly simple for both individuals and small companies to manage than ever before. In this part, supporting technologies for Industry 5.0 are briefly discussed.

3.1. Edge computing (EC)

Due to the IoT's rapid growth and the abundance of cloud services, a novel concept known as EC, which permits data processing at network peripheral, has been introduced. EC can be very helpful in the shift to Industry 4.0 as well as in the upcoming Industry 5.0. Expectations for delay expenses, energy life restrictions, reaction time standards, data security, as well as privacy can all be met by EC (Pham, 2020). EC reduces transmission costs and ensures that applications are effective even in distant locations. Furthermore, EC can manage data without transferring it to a public cloud, reducing security worries for crucial Industry 5.0 activities.

3.2. 6G and beyond

6G will eventually be able to provide Industry 5.0 with substantial value-added services. A very dense network of thousands or millions of sensors, cars, and hardware components makes it challenging to construct radio infrastructure. It won't be feasible to satisfy the quickly rising broadband needs due to the robust development of smart infrastructure and prospective apps with existing networks (like 4G and 5G networks) (Shah, 2022; Shah, 2021). The Industry 5.0 transformation can offer improved delay and support high-quality services, as well as comprehensive IoT infrastructure and incorporated AI powers, thanks to the use of 6G and beyond. By supplying intelligent frequency management, mobile EC driven by AI, and intelligent mobility, 6G networks aid in the efficient and effective improvement of application performance in Industry 5.0 applications (Chowdhury, 2020). The requirements of an intelligent information society, which can deliver ultrahigh data speeds, ultra-low delay, ultra-high dependability, high energy economy, traffic capacity, etc., are anticipated to be met by 6G networks for Industry 5.0 apps.

3.3. Cobots

Recent advancements in automation and robotics have made working with computers increasingly important. Due to the incredibly quick advancements in AI and smart technology, it is clear that all devices with computing capabilities have become more intelligent and have introduced a new technology called cobots. Collaborative robots are those created specifically to work alongside humans. Through this collaboration, human skills are improved and made easier than ever for individuals and small companies to automate. Cobots have a lot to give in Industry 5.0. Robots can accomplish their intended task when working with people, which enables them to deliver mass-produced, individualized goods to consumers quickly and accurately. Cobots can be personalized in many ways in Industry 5.0, such as by offering medical services, smart apps that effectively

outline a patient's healthy lifestyle, and medical needs to develop a completely unique health-fitness regimen (Simoes, 2020).

3.3. Internet of Everything (IoE)

IoE is a network of connections between individuals, systems, organizations, and physical objects. Industry 5.0 applications can benefit greatly from IoE by opening up new options (Li, 2021). IoE's developments in Industry 5.0 have the potential to bring about new features, improve user encounters, and benefit sectors and countries. The importance of IoE in Industry 5.0, increasing consumer satisfaction and trust, and generating customized experiences utilizing data produced by IoE. By removing communication route obstacles and lowering delay, IoE use in Industry 5.0 offers a chance to reduce running expenses.

3.4. Blockchain

Industry 5.0 could be greatly improved by blockchain technology. In Industry 5.0, centralized administration of a significant number of diverse linked devices is a key task. By allowing dispersed confidence, blockchain can be used to create autonomous and distributed administration systems. Secure peer-to-peer contact using blockchain technology offers an unchangeable database for keeping documents (Prabadevi, 2021). Also, a segmented and dispersed strategy using blockchains can provide a better degree of security for data and activities. Blockchain technology can also be used to allow data collecting and getting.

3.5. Big Data

Big data is currently a hot topic of debate in both academics and business. It symbolizes a big and varied collection of data gathered from all kinds of sources. Big Data technologies like AI, ML, social networking, data integration, data mining, and so forth are used in many data analysis methods (Mitra, 2021). Industry 5.0 often places a lot of emphasis on big data analytics. Big Data Insights can be utilized by some businesses in Industry 5.0 to better understand customer behavior, which can then be utilized to maximize product pricing, concentrate on enhancing production productivity, and assist in lowering administrative costs. Big data analytics can be utilized to make decisions in real-time to enhance industry competitive advantage with a focus on providing recommendations on prediction results for important events in Industry 5.0 applications.

4. Key Enablers of Industry 4.0 and Industry 5.0

Numerous helpful studies about new technologies that make up Industry 4.0, their debut, and their advantages are currently available. A distinct

understanding of how Industry 4.0 affects business models and groups is sought after by the studies that have surfaced from the literature (Ibarra, 2018). However, it is noted that less work has been put into studying the function of people in the future industry, suitable organizing models, methods for creating long-term value, and social impacts (Tirabeni, 2019). Long-term progress depends on these interconnected elements in terms of sustainability-related problems, technology, people, and their jobs.

Industry 4.0 focused on all newly developed technologies in terms of technology. But as a result of Industry 5.0, some new technologies are getting more attention from researchers, while others are losing their appeal. Again, the growing interest in HMI and AI demonstrates that more emphasis is being placed on using technology as an assist to the routine duties performed by human workers. Due to the widespread adoption of the 5G wireless network in modern society, the Industrial Internet of Things has emerged as a key area of technological study.

6. Discussion, Future Opportunities and Challenges

The majority of sectors, including biological sciences, retail, manufacturing, health care, textiles, medicine, and banking, have embraced Industry 5.0 as a result of its development.

Time-space barriers can be removed in 6G with the aid of AI and holographic communication, allowing for the effective optimization of productivity as long as there is an ultra-low delay communication network. By offering high data rates in interior settings, visible light communication is another potential technology that can satisfy the needs of the healthcare industry. Additionally, the vast quantity of patient medical information needs to be extremely private and properly segmented. All of these situations can be satisfactorily addressed by 6G technologies, which can guarantee stable communication. The Internet of Bio-Nano-Things and the Internet of Nano-Things are thought to be IoT for the future of healthcare, according to current study.

The state-of-the-art indicates that by embracing supporting technical trends like EC, big data analytics, IoE, cobots, blockchain, and 6G, Industry 5.0 plays a major part in a diversity of uses. All of these supporting technologies combine brain abilities and invention to help businesses produce more goods and distribute tailored goods more rapidly.

6.1. Discussion

Industry 5.0 and its merger with AI, IoT, and Big Data were the subject of a research that was published in (Leong, 2020). They propose constructing riskier and more intricate hyper-connected networks, which have the

potential to shape the future of many industries, including the use of digital drugs to track actual drug adherence. In many digital settings, big data accumulations will gain from AI, IoT, as well as Industry 5.0. Additionally, (Javaid, 2020) showed the potential uses of Industry 5.0 in coronavirus disease (COVID) for patient-specific treatment and diagnostics. In order to assist COVID epidemic, they have utilized Industry 5.0 technologies like holography, 4D images, robotic robots, videoconferencing, and smart inhalers. In order to address the issues related to the COVID pandemic's effects, they suggested that Industry 5.0 take on some of the significant challenges (such as patient tracking, automatic personalized treatment, supply chain optimization, raising awareness, digital medicine, drug manufacturing, and crowd monitoring). Furthermore, in the post-COVID period, development of cobot, CHIPBOT (implanted circuits in COVID patients), and CURBOT (currency and bankless systems) can be used for mobile purchases, kidnapping tracing, patient surveillance, and treatment.

A value-sensitive architecture for smart workplaces was suggested in (Longo, 2020). The promise of Industry 5.0 in human-machine symbiosis-based future industry is discussed. Additionally, industrial systems engineering offered answers to the machine's social repercussions on human employees and demonstrated how value-based design reduces problems associated with the application of the symbiosis Industry 5.0. To meet requirements of IoT and Industry 5.0, the managers should have a greater grasp of the innovation ecosystem, business strategy, and design thinking, according to ultimate innovation management paradigm established in (Aslam, 2020). However, the research does not discuss how the structure and safety measures will be implemented once they are integrated with corporate operations.

Better traffic control solutions are still in demand, but Industry 5.0 can significantly progress the industry by combining computer intelligence, human intelligence, and 5G networks with other technologies. When creating a cleverer driverless car, Industry 5.0 can incorporate sophisticated technologies to facilitate communication and teamwork. In addition, the cloth business will gain more from this change by being able to offer clients more customized outfits. Fiber computing (Sherburne, 2020) can be used by Industry 5.0 to create more specialized goods, which will subsequently result in more environmentally friendly cloth production. In order to service clients more personally, Industry 5.0 has a broad variety of uses in almost all fields.

6.2. Challenges

Through the use of a cognitively empowered production process, Industry 5.0 can allow the most individualized client services. Some of the

possible execution issues covered in this part must be resolved for smooth services. Security is one of the possible difficulties. The security risk in diverse data processing and employing cloud services for variegated user and corporate data management must be double-checked as we progress towards more digitalized calculation. While providing customers with tailored and more accurate services, privacy-preserving data interactions, privacy in data gathering, and social problems must also be taken into consideration. The return of human labor to the manufacturing floor may be successful, but there must be effective training provided for both parties in order to address real problems and ensure that human and computer intellect coexist peacefully. By combining human-robot co-working with specialized customer assistance, the issues related to ramping up the users and the production processes must be taken into consideration. In order to prevent possible disadvantages and detrimental social effects on the acceptance of AI, ethical considerations must also be made.

It is essential to create reciprocal confidence in the ecosystem by authenticating the enormous variety of various stakeholders, including IoT nodes, computers, cloud nodes, communication nodes, and joint partner nodes. The Industry 5.0 verification methods should be lightweight to be deployed with IoT nodes, adaptable to link billions of devices, and quantum resistant to withstand uses of quantum computing in the future.

Privacy is a crucial prerequisite for Industry 5.0 apps because the entire ecosystem relies on costly intellectual property, expensive production inputs, and membership administration. To link machinery and people, creators and other partners, and to share tracking and control information, data is transferred over the Internet in Industry 5.0. In order to maintain the confidence of the cloud production environment, such data must not be accessible to malevolent Internet users.

When the system's workload varies constantly, scalability can be described in terms of the system's resilience, adaptability, and reactivity. Scalability in Industry 5.0 refers to a system's efficiency under various working circumstances, regardless of whether there are more or fewer hyperconnected systems present in the network. Industry 5.0 is designed to link and converse with a variety of systems from other companies as well as a variety of people. Scalability is one of the characteristics of Industry 5.0, which is an improvement of Industry 4.0, but it poses a greater challenge when making robots or other machines and people a partner by sharing their task. Using service level signs that have been verified in accordance with the service level goals stated in service level agreements, the scaling can be monitored. This is a crucial issue because non-deterministic development of companies, equipment, and people is another element. Technology providers in the Industry 5.0 ecosystem must be able

to provide service at any capacity, adaptable enough to extend and grow, and provide a low-latency reaction without any data processing delays in order to guarantee scaling. The many inquiries received from the adaptable cloud and dynamic peripheral servers must be processed by AI-based cobots without any unforeseen delays.

To tackle any technology, societal, and management problems, uniformity and regulatory policies must be implemented because a competent worker in Industry 5.0 is anticipated to give a high-value job in production. A competent workforce is imparted by taking into account a variety of management, employee, corporate culture, management infrastructure, and standard policy issues. Inadequate teachers and budgetary limitations make it difficult for people who work alongside cobots to receive the appropriate training, which is the main skill space challenge. By the time Industry 5.0 is completely implemented, there will be a greater need for qualified workers, and the use of new technologies will increase as well. This will necessitate sufficient training for both potential teachers and students. This might encourage public-private collaborations. Reforming the legal framework will also be required. The educated personnel can also support corporate success.

Laws and rules are a key prerequisite for any industrial revolution's complete acceptance. Although there are generally accessible standards for technology, innovation policy, and industry policies, the more particular standard for this new age needs to be implemented. Different rules relating to both the human and cobot must be developed as Industry 5.0 seeks to bring back the human labor force to share and work alongside cobots and clever machines. Without appropriate rules and laws, a number of problems could develop in this co-production setting. Cobots must be distinguished from other machines, such as drones, by regulations that are implemented. Additionally, laws promoting the use of cobots, AI, and other robots in the industrial sector should be developed for more accurate forecasts and advanced coproduction. The implementation will be completed more quickly and will be easier to handle with better laws, regulations, standards, and rules.

7. Conclusion

In this paper, an overview of Industry 5.0's enabling technologies and possible uses is provided. This survey is started by defining a few Industry 5.0 ideas from the viewpoints of the scholarly and business groups. The study on the key supporting technologies of Industry 5.0 was then followed by a discussion on some of the possible uses of Industry 5.0, including digital healthcare, supply chain management, cloud manufacturing, industrial production, etc. The Industry 5.0 transformation and the 6G cellular con-

nectivity revolution will change how the world looks in the future. Industry 5.0 is an idea created to consistently align the productivity of people and robots in the workplace. Industry 5.0, made possible by a variety of new apps and enabling technologies, is anticipated to boost industrial output and client happiness. A number of difficulties and unresolved problems are also discussed that need to be addressed in order to fully actualize the idea of Industry 5.0 in the near future, including privacy, security, human-robot collaboration in a workplace, scaling, and specialized labor.

REFERENCES

Ji, B., et al., (2021). A survey of computational intelligence for 6g: Key technologies, applications and trends, IEEE Transactions on Industrial Informatics, 17(10), 7145–7154.

Maddikunta, P. K. R., et al., (2021). Industry 5.0: A survey on enabling technologies and potential applications, Journal of Industrial Information Integration, 100257.

Nahavandi, S., (2019). Industry 5.0 – a human-centric solution, Sustainability, 11(16), 4371.

Xu, L.D., (2020). The contribution of systems science to industry 4.0, Syst. Res. Behav. Sci., 37(4), 618–631.

Li, L., (2018). China's manufacturing locus in 2025: With a comparison of ''made-inchina 2025" and ''industry 4.0", Technol. Forecast. Soc. Change, 13, 66–74.

Lasi, H., et. al., (2014). Industry 4.0, Bus. Inf. Syst. Eng., 6(4), 239–242.

Priya, V. I., et. al., (2021). Robust attack detection approach for IIoT using ensemble classifier, Comput. Mater. Contin., 66(3), 2457–2470.

Azeem, M., et. al., (2021). Symbiotic relationship between machine learning and industry 4.0: A review, J. Ind. Integr. Manag., 2130002.

Zhang, C., et. al., (2020). A review of research relevant to the emerging industry trends: Industry 4.0, IoT, blockchain, and business analytics, J. Ind. Integr. Manag., 5(1), 165–180.

Longo, F., et. al., (2020). Value-oriented and ethical technology engineering in industry 5.0: a human-centric perspective for the design of the factory of the future, Appl. Sci., 10(12), 4182.

Al Faruqi, U., (2019). Future service in industry 5.0, J. Sist. Cerdas, 2(1), 67–79.

Özdemir, V., et. al., (2018). Birth of industry 5.0: Making sense of big data with artificial intelligence, ''the internet of things" and next-generation technology policy, Omics: J. Integr. Biol. 22(1), 65–76.

Sachsenmeier, P., (2016). Industry 5.0-the relevance and implications of bionics and synthetic biology, Engineering, 2(2), 225–229.

El Far, O.A., et. al., (2021). Prospects of industry 5.0 in algae: Customization of production and new advance technology for clean bioenergy generation, Energy Convers. Manag.: X 10 100048.

Tange, K., et al., (2020). A systematic survey of industrial internet of things security: Requirements and fog computing opportunities, IEEE Communications Surveys & Tutorials, 22(4), 2489–2520.

Aceto, G., et. al., (2019). A survey on information and communication technologies for industry 4.0: State-of-the-art, taxonomies, perspectives, and challenges, IEEE Communications Surveys & Tutorials, 21(4), 3467–3501.

Chen, K.-C., et al., (2020). Wireless networked multirobot systems in smart factories, Proceedings of the IEEE, 109(4), 468–494.

Yetiş, H., et al., (2020). Optimization of mass customization process using quantum-inspired evolutionary algorithm in industry 4.0, IEEE International Symposium on Systems Engineering, 1–5.

"Industry 5.0, a transformative vision for Europe," Jan 2022, accessed on: Mar. 14, 2023. [Online]. Available: ec.europa.eu/info/publications/industry-50-transformativevision-europe en

"Industry 5.0," Jan 2021, accessed on: Mar. 14, 2023. [Online]. Available: ec.europa.eu/info/publications/industry-50 en

U. Nations, Work of the Statistical Commission pertaining to the 2030 Agenda for Sustainable Development, July 2017, accessed on: Mar. 16, 2022. [Online]. Available: undocs.org/A/RES/71/313

Xiloyannis, M., et al., (2021). Soft robotic suits: State of the art, core technologies, and open challenges, IEEE Transactions on Robotics, 1–20.

Mahmood, A., et al., (2022). Industrial IoT in 5G-and-beyond networks: Vision, architecture, and design trends, IEEE Trans. Ind Informat., 18(6), 4122–4137.

Janai, J., et al., (2020). Computer vision for autonomous vehicles: Problems, datasets and state of the art, Foundations and Trends® in Computer Graphics and Vision, 12(1), 1–308.

Ma, J., et al., (2021). Multitask learning for visual question answering, IEEE Transactions on Neural Networks and Learning Systems, 1–15.

Huang, Y., et al., (2021). True-data testbed for 5G/B5G intelligent network, Intelligent and Converged Networks, 2(2), 133–149.

Du, A., et al., (2021). Cracau: Byzantine machine learning meets industrial edge computing in industry 5.0, IEEE Transactions on Industrial Informatics, 1–1.

Pham, Q.-V., et al., (2020). A survey of multi-access edge computing in 5G and beyond: Fundamentals, technology integration, and state-of-the-art, IEEE Access, 8, 116974–117017.

Shah, A. F. M. S, (2022). A Survey From 1G to 5G Including the Advent of 6G: Architectures, Multiple Access Techniques, and Emerging Technologies, IEEE 12th Annual Computing and Communication Workshop and Conference (CCWC), Las Vegas, NV, USA, 1117-1123.

Shah, A. F. M. S., et al., (2021). Survey and Performance Evaluation of Multiple Access Schemes for Next-Generation Wireless Communication Systems, IEEE Access, 9, 113428-113442.

Chowdhury, M.Z., et al., (2020). 6G wireless communication systems: Applications, requirements, technologies, challenges, and research directions, IEEE Open J. Commun. Soc. 1, 957–975.

Simões, A.C., et al., (2020). Factors influencing the intention of managers to adopt collaborative robots (cobots) in manufacturing organizations, J. Eng. Technol. Manag. 57, 101574.

Li, X., et al., (2021). A review of internet of things – resource allocation, IEEE Internet Things J. 8(11), 8657–8666.

Prabadevi, B., et. al., (2021). Toward blockchain for edge-of-things: A new paradigm, opportunities, and future directions, IEEE Internet Things Mag.

Mitra, A., (2021). On the capabilities of cellular automata-based MapReduce model in industry 4.0, J. Ind. Inf. Integr. 21 100195.

Ibarra, D., et. al., (2018). Business Model Innovation through Industry 4.0: A Review. Procedia Manuf. 2018, 22, 4–10.

Tirabeni, L., et. al., (2019). How Can Organisations and Business Models Lead to a More Sustainable Society? A Framework from a Systematic Review of the Industry 4.0. Sustainability, 11, 6363.

Leong, Y.K., et. al., (2020). Significance of industry 5.0, in: P.L. Show, K.W. Chew, T.C. Ling (Eds.), The Prospect of Industry 5.0 in Biomanufacturing, CRC Press, 1–20.

Javaid, M., et. al., (2020). Industry 5.0: Potential applications in covid-19, J. Ind. Integr. Manag. 2050022.

Longo, F., et. al., (2020). Value-oriented and ethical technology engineering in industry 5.0: a human-centric perspective for the design of the factory of the future, Appl. Sci. 10(12), 4182.

Aslam, F., et. al., (2020). Innovation in the era of IoT and industry 5.0: Absolute innovation management (AIM) framework, Information, 11(2), 124.

Sherburne, C., (2020). Textile industry 5.0? Fiber computing coming soon to a fabric near you, AATCC Rev. 20(6), 25–30.

CHAPTER 11

THE INVESTIGATION OF CAPILLARY WATER ABSORPTION ON UNTREATED AND TREATED POROUS NATURAL BUILDING STONES UNDER DIFFERENT WATER CONDITIONS

Mustafa Yavuz ÇELİK[1]

1 Prof. Dr. ORCID: 0000-0002-9695-7370 Afyon Kocatepe University, Afyon Vocational School, Department of Marble Technology, 03100, Afyonkarahisar, Turkey.

1. INTRODUCTION

One of the most important reasons for using natural building blocks by all civilizations for thousands of years is that they can withstand atmospheric effects. Volcanic rocks such as trachyte, basalt, andesite, and tuff have been used in most of the historical structures that have survived in the Afyonkarahisar region. These building stones were used to construct many historical and monumental structures (fountains, bridges, caravanserais, baths, and mosques) that have survived to the present day in the Afyonkarahisar region. Additionally, many churches, tombs, and settlement areas are carved into easily excavated tuff rocks in the Ayazini region. These historical structures are damaged over time because the tuffs are very porous and have a high-water absorption capacity (Figure 1).

The natural building stone may cause weathering problems on exposure to rain and chemical pollutants in the air. The weathering of stones is a complex process, usually caused by atmospheric effects (sunlight, rain, wind, and freeze/thaw). All these weathering types are associated with the pore system of the stone and, therefore, the presence of absorbed water. Salt crystallization, one of the most effective decay factors, results in the stress of volume expansion in the crystal phase when the saline solutions absorbed or contained in the stone reach the degree of saturation within the pores. Thus, the deterioration process begins (Rodriguez-Navarro and Doehne 1999; Cnudde et al. 2004). Deterioration in historical buildings can be more destructive due to capillary water absorption, which allows salt water to penetrate the building stones. It is known that the most destructive salts that cause damage to historical buildings are sodium chloride and sodium sulfate, which can be found in the water absorbed by the material (Rodriguez-Navarro and Doehne 1999; Benavente et al. 2001). It is considered that the factor that causes the building blocks to break down over time is the stress that occurs due to the crystallization of salts within the pores (Clifton 1980).

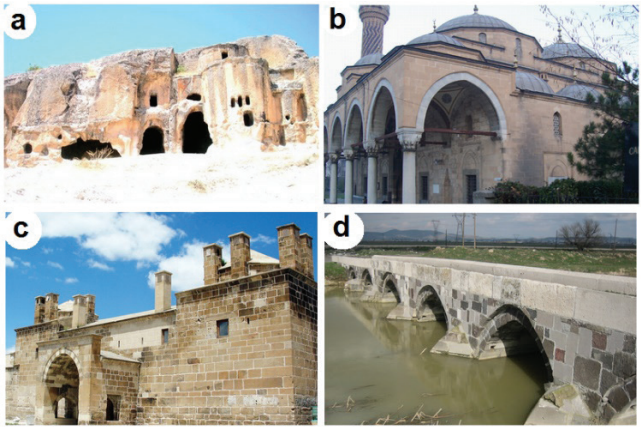

Figure 1. *Examples of historical buildings made of tuff and andesite in the Afyonkarahisar region. The Ayazini church was built in the 9th century and is carved inside of a rock mountain, located in the Ayazini district (a), İmaret Mosque was built in 1477, located in the Afyonkarahisar (b), Doger Caravansarie was built in the 15th century, located in the İhsaniye, Afyonkarahisar (c), Altı Göz Bridge was built before 1209, located in the Afyonkarahisar (d).*

The presence of water in stones has caused damage to many historic buildings and monuments. Water can reach the building from the pores in the stone in several ways. Capillary water uptake is the most important water penetration mechanism for building materials. The capillary capillarity effect of the water on the ground is a phenomenon that occurs spontaneously in nature due to surface tension. Here, the water moves higher than its current level. These absorbed waters from the beginning of the decomposition process (Chen et al. 2004). Deterioration events have revealed the necessity of preserving the stones in historical buildings. The amount of water absorption must be reduced to slow the degradation of building stones. Water repellents have been developed to reduce the risks of moisture-related damage and extend the life of monuments (Tsakalof et al. 2007).

Many authors in previous works reported the relationship between the pore size distribution and its effects on the degradation of stone. Open porosity is important for describing the water uptake behavior of natural stones. Many researchers have examined the porosity diameter, and petrographic and structural properties of natural stones, all of which are very important for capillary water absorption. Hoffmann and Niesel (1992), investigated the relationship of porosity to the weathering of stones. Nicholson (2001), studied the importance of porosity structure in the decay mechanism of five different limestones. Şengün et al. (2014), examined

the capillary water absorption coefficients of 118 different natural stones and identified other rock properties.

Many studies on natural building stones focus on capillary water absorption. The first theoretical studies on the capillary behavior of water in porous media were made by Washburn (1921). Mosquera et al. (2000), using three different granites, found capillary water absorption coefficients as 0.24, 0.89, and 1.24 $kg/m^2s^{0.5}$. Capillary index studies with two different methods (relative and absolute) were carried out by Peruzzi et al. (2003). Karoglou et al. (2005), examined the water absorption characteristics of the different building materials, including four building stones, two bricks, and six plaster. Moreno et al. (2006), investigated the deterioration of granites which are caused by salt pollution with rising water absorption. Ioannou et al. (2009) investigated the capillary rise behavior of limestone samples using different liquids. They have reported that large-diameter porosities have reduced capillary water absorption capacity according to small-diameter porosities. Vazquez et al. (2010) stated that capillary water absorption and ultrasound wave velocities in granites are related to crack properties. Al-Naddaf (2011) examined the potential for capillary water absorption in sandstones and examined the formation of salt crystals in sandstones.

Tomašić et al. (2014) studied capillary water absorption potential in dynamic waters. They have reported in two different limestones that the structural properties of the stone can increase or decrease the capillary water absorption. Juhász et al. (2014) investigated the movement of microorganisms in porous limestone, together with capillary water absorption. Also suggested a capillary water sorption classification in travertine. Çelik and Kaçmaz (2016) studied the dynamic and static capillary water absorption capacities of andesite and tuffs. Karagiannis et al. (2016) examined the capillary water absorption of the building blocks at different temperatures and reported a relationship between them. Çelik and Ylmaz (2018) studied the impact of various aqueous (acidic, salty, and static) ambiances on the capacity of porous building stones to absorb water through capillary action. Çelik et al. (2019) examined the impact of temperature on time-dependent water absorption in Ayazini (Afyonkarahisar) tuffs. Karagiannis et al. (2019) examined the impact of dynamic environmental conditions.

Volcanic rocks such as andesite and tuff were used as building blocks in the Roman, Seljuk, and Ottoman periods. In the Afyonkarahisar (Turkey) region, numerous structures are built from andesite and tuff from these periods. These building stones are still used as local construction materials in Afyonkarahisar. Many historical buildings' interior and exterior surfaces deteriorate due to the water and moisture absorbed by the capillary, and the ornaments with high artistic value are significantly damaged. Figure 2 shows that the building stone is damaged due to capillary water uptake

and degradation. In historical buildings, the capillary water absorption capacities of the building materials to be used should be known to reduce and eliminate (restore) the damages caused by capillary water absorption and to choose the appropriate material for the new buildings to be built. Studies to be conducted to protect cultural heritage depend on the water absorption and salt crystallization performance of porous building stones. In this study, characterization studies were conducted on selected stones, including the determination of the physico-mechanical, chemical, mineralogical-petrographic, and pore properties of the abundant porous andesite and tuffs used as building stones. Capillary water absorption capacities were determined to evaluate stone resistance in pure water and saltwater environments, depending on capillary water absorption potentials. In cases where it is determined that the elements that destroy natural stones are water containing dissolved salts infiltrating from the surface, and these cannot be prevented by other means, surface protection is applied with chemical substances. This study conducted experimental studies on the applied and non-applied samples with water-repellent chemicals. Thus, it will be possible to reveal the relationship between capillary water absorption in historical buildings and building materials, as well as data on the capillary water absorption potential of the materials to be selected for new buildings to be built in the region.

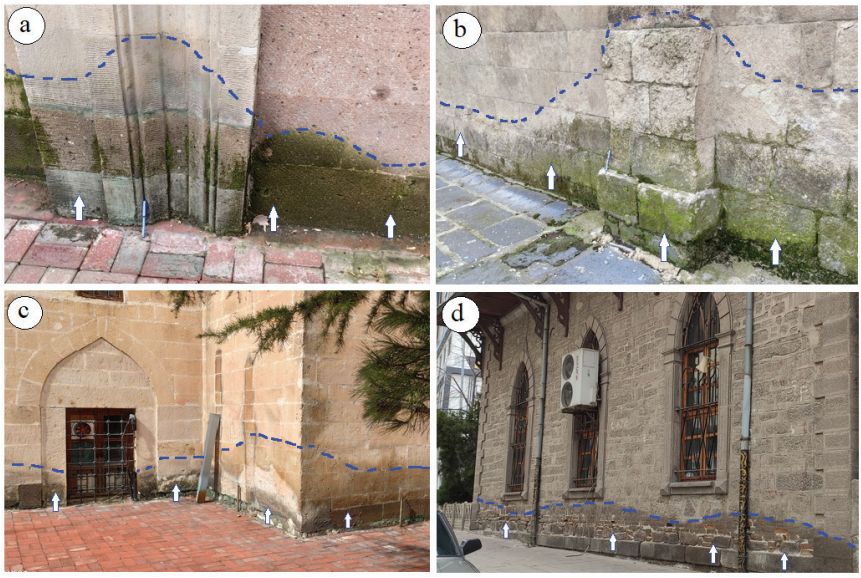

Figure 2. *Photos of the decayed due to water absorption of the capillary in the historic buildings constructed using tuff and andesite. With the water rising from the ground the color of the stone is darkened, and excessive humidity increases the formation of degradation on the wall.*

2. MATERIAL AND METHODS

2.1. Materials

The samples of andesite and tuff stone used in this study were obtained from the quarries around Afyonkarahisar, Turkey. These selected stones have been used as building stones in historical buildings in the region. The quarries which the stones are taken from are active. The map showing the locations where the samples are taken is given in Figure 3. A sufficient number of samples of cubic shape (70×70×70 mm) was prepared from each building stone sample for use in the experiments.

Salty water was prepared with the NaCl salt (halite) in the capillary water absorption experiments. In experiments, it was used as a commercial water repellent, a solvent-based protective for natural stones. Solvent-based water-repellent materials can penetrate more deeply than water-based ones. The water-repellent surface coating was applied to the stone surface with a brush in two consecutive steps, with an interval of 24 h. 48 h waited for the polymerization process.

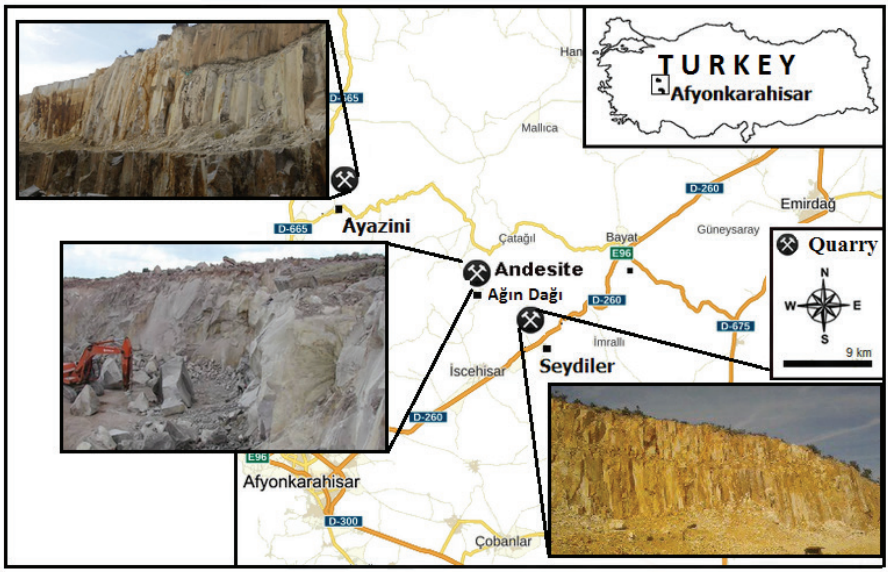

Figure 3. *Location map of the quarries where the examined building stones were produced.*

2.2. Methods

A polarized optical microscope, X-ray diffraction (XRD), and scanning electron microscope (SEM) were used for determining the miner-

alogical and petrographic characteristics of the tested stones. Polarized light optical microscopy is the basic tool in use in petrography. Polarizing microscopy provides for the study of stone's textural, mineralogical, and grain information. For this purpose, two of each sample thin section of the tested stones were used in this study. The investigation was performed by using a Leica DM 2500P optical microscope equipped with a digital camera. The X-ray powder diffraction (XRD-Panalytical X-pert MRD) method was used to further specification the mineralogical composition. The Scanning Electron Microscope (SEM) was used to access further details of the texture and petrographical features of assessing magnified images. During the preparation of samples, each sample was covered by a thin carbon film. SEM examinations were performed with the LEO 1430-VP device.

The porous system properties of the voids and their volume and size are strongly related to the decay of the building stones. Mercury injection or intrusion porosimetry, saturation in liquids, and gas adsorption are the most known methods in characterizing porous system characteristics. The mercury Intrusion Porosimetry (MIP) principle is that a non-wetting liquid with a contact angle greater than 90º will only intrude capillaries under pressure (Abell et al. 1999). This research method is widely used to characterize the porosity of building blocks and to evaluate the degree of degradation. In the experiments, the pore size distributions of all three samples were determined using AutoPore IV 9500 V1.09 mercury Porosimetry.

The physical and mechanical properties of natural stones have crucial importance when stones are used for buildings. Therefore, laboratory studies are indispensable to investigate the stone properties for use purposes. Building stones, particularly andesite, and tuff, are significant in the building materials of Afyonkarahisar's historic building. Physical and mechanical tests/experiments have been conducted to determine properties such as density, water absorption, porosity, P-wave velocity, and uniaxial compressive strength of these building stones used in the experiments. These tests were carried out according to the TS EN standards specified in Table 1. In the experiments, six pieces of 70x70x70 mm samples were used for each type of stone. The P-wave velocity measurements of the stones were carried out by Proceq Pundit Lab ultrasonic testing device (P-wave) by TS EN 14579 standard (54 kHz).

Table 1 *The related TS EN standards used in tests*

Tests	Related standards
Density (real) (kg/m^3)	TS EN 1936 (2010)
Absorption by weight (%)	TS EN 13755 (2009)
Total porosity (%)	TS EN 1936 (2010)
P-wave velocity (km/s)	TS EN 14579 (2006)
Uniaxial compressive strength (MPa)	TS EN 1926 (2007)
Water absorption coefficient by capillarity	TS EN 1925 (2000)

The capillary water absorption test was carried out according to the TS EN 1925 standard. For this experiment, the base of the building stone samples was immersed in water at a depth of 3 ± 1 mm. The time intervals in the capillary water absorption experiments were selected to be 1, 3, 5, 10, 15, 30, 60, 480 (8 h), 1440 (24 h), and 2880 min (48 h). At each time interval, the samples were removed from the water, and droplets were removed from the surface using a dry cloth. Then, each sample was weighed to a precision of 0.01 gr, and the amounts of water absorbed according to the time interval were determined (Figure 4). In the protection of tested building stone samples, water-repellent products were coated on all surfaces, and capillary water absorption experiments were repeated simultaneously. All experiments were performed on two different liquids, normal and salty. A 14% NaCl solution by weight was prepared for the experiments. The results were plotted as water absorption content against the square root of time (in minutes). The coefficient of capillary water absorption (C) is calculated from equation 1:

$$C = \frac{m_i - m_d}{A.\sqrt{t_i}} \quad (1)$$

m_i: successive masses of the specimen during testing, (g)

m_d: weight of the dry sample, (g)

A: area of the side immersed in water, (m^2)

t_i: time (s)

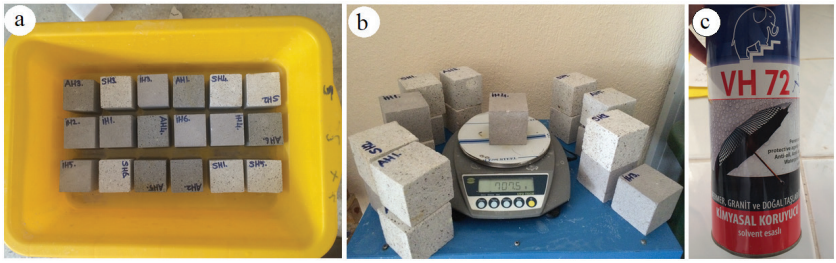

Figure 4. *View of the tested building stone samples in water absorption capillarity experiment (a), determination of weights of samples (b), water repellent used in experiments (c).*

3. EXPERIMENTAL INVESTIGATION AND RESULTS

3.1. Petrography and mineralogy

Polarized light microscope analysis

Polarized microscopy studies were conducted to determine the mineralogical composition and textural properties of andesite and tuffs. Andesites have a matrix composed of glassy microlites from fine-grained plagioclase. Plagioclase, hornblende, pyroxene, and biotite phenocrysts were observed in the matrix. In pyroxene minerals, fractures, and cracks are very obvious. Biotite and hornblende are seen as dark-colored minerals. Hornblende showed signs of disintegration. Because of the investigations, it was determined that the andesitic composition of the rock was observed in the pinkish-reddish color hornblende and the alteration in biotite. It has been determined that Ayazini tuffs are vitrified, porphyric, and vesicular textures. In the Ayazini tuff samples, volcanic glass (pumice) fragments and quartz and feldspar minerals were observed in varying proportions. The feldspars are usually plagioclase crystals—the vitric components observed as glass splinters and pumice fragments. The pumice fragments are characterized by spongiform texture and occasionally transformed into clay minerals. The thin section of the Seydiler tuffs contained phenocrysts scattered irregularly in the matrix consisting of volcanic glass. Feldspar, quartz, and hornblende were detected as the main minerals. The rock fragments were observed in the rock. Pumice is very large in the tuffs, and it is observed that the grain size is small and elliptical. The tuffs are generally defined as crystalline vitric tuffs. (Figure 5).

SEM analysis

Scanning electron microscopy (SEM) has been used to determine micro-morphological features and clay minerals that are not observed in thin

sections of the samples of andesite and tuffs. Feldspar (plagioclase-albite), quartz, biotite, and clay minerals are observed in SEM (Scanning Electron Microscopy) analysis of the samples of andesite and tuff (Figure 6). Crystals of quartz in Ayazini tuff are observed as hexagonal shapes. SEM analysis revealed smectite clay minerals on plagioclase minerals. The formation of clay minerals shows that volcanic glass (pumice) and feldspar are weathered.

X-ray diffraction analysis

The results of the XRD analysis of andesite and tuff samples are shown in Figure 7. As a result of XRD analysis, feldspar (andesine, sanidine), montmorillonite, and tridymite minerals were detected in andesite (Figure. 6a). In tuffs, quartz, feldspar, illite, hornblende, and cristobalite minerals were determined (Figure. 6b, c). The presence of clay minerals such as montmorillonite and illite shows that volcanic glass components and feldspar are weathered. In the XRD graph, the elevation of $2\theta = 0°$ in the andesite, $2\theta = 20°$ and $2\theta = 15°$ in the tuffs supports the presence of amorphous material (volcanic glass).

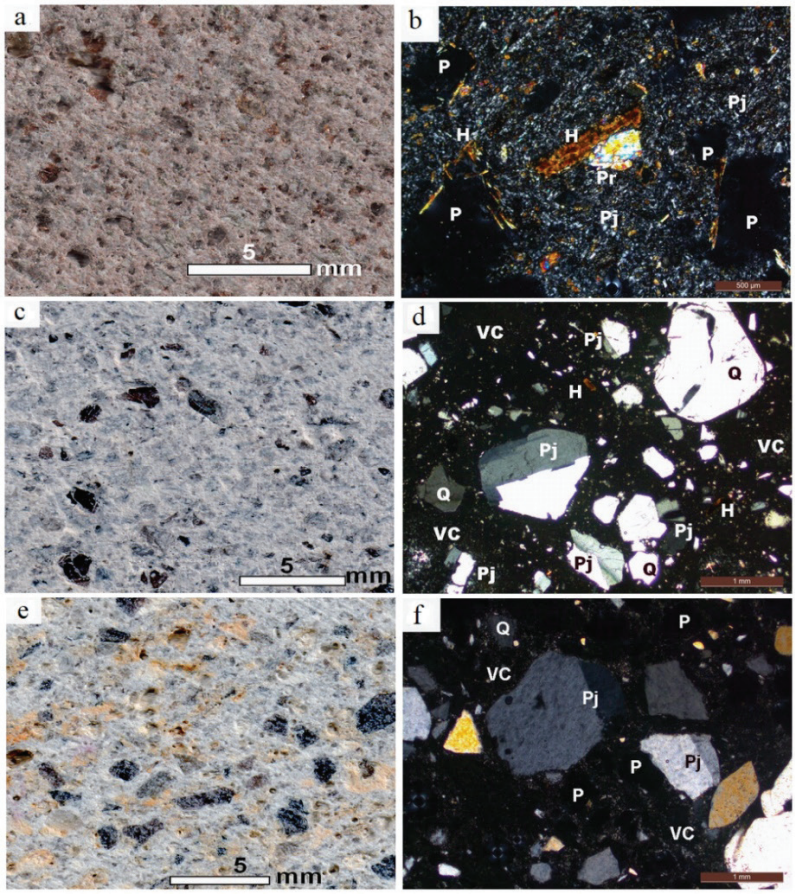

Figure 5. *Surface and thin section view of the tested stones used in the experiments. İscehisar andesite (a, b) Ayazini tuff (c, d) and Seydiler tuff (e, f). Q: quartz, Pj: plagioclase, H: hornblende, VC: volcanic glass, P: pore.*

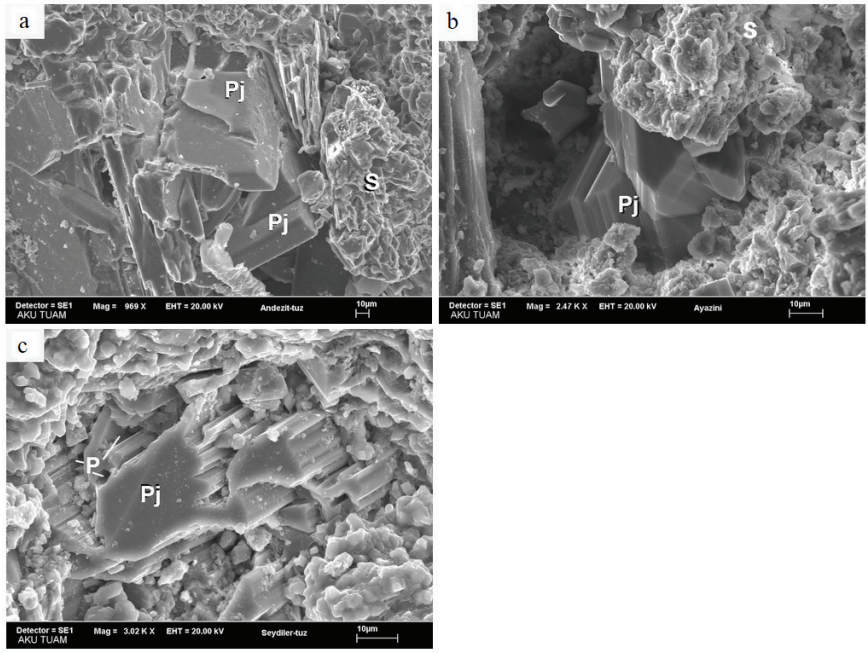

Figure 6. *SEM micrograph of the İscehisar andesite (a) Ayazini tuff (b), and Seydiler tuff (c).*

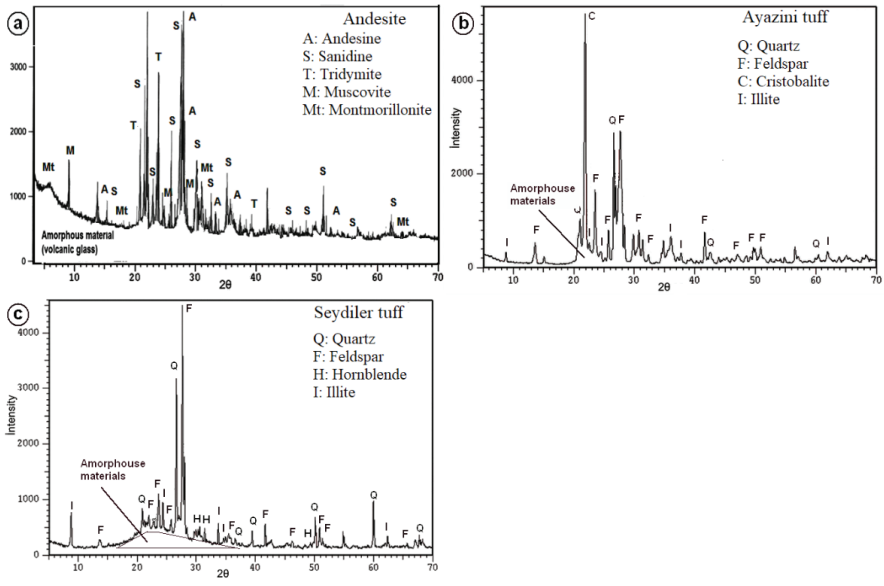

Figure 7. *XRD plots showing the mineral peaks of the İscehisar andesite (a) Ayazini tuff (b), and Seydiler tuff (c).*

3.2. Pore-size distribution

Porosities are classified by their size according to Klopfer (1985): microporosity (<0.1 μm), meso porosity (0,1 μm - 1 mm), and macro porosity (> 1 mm). Capillary water absorption is practically related to porosities between 0.1 μm and 1 mm in diameter. As porosity diameters decrease in rocks, the capillarity property increases. Macro porosities are larger than 1 mm in diameter and allow more water to move within the material. The Mercury porosimetry method is widely used in determining the pore-size distribution of building stones. The results obtained in the experiment of tested stone with the mercury porosimetry are given in Table 2. In the tested stone, the average pore diameter was measured as 0.0764, 0.4274, and 0.0643 μm in the andesite, Ayazini, and Seydiler tuffs, respectively.

Table 2. *Pore size distribution experiment characteristics of andesite and tuffs (Contact angle: 130 °C, Hg surface tension: 485 dynes/cm, Evacuation pressure: 100 μmHg, Mercury filling pressure: 0.52 psia).*

	Andesite	Ayazini tuff	Seydiler tuff
Total Intrusion Volume (mL/g)	0.0965	0.1362	0.0564
Total Pore Area (m^2/g)	5.054	1.275	3.509
Median Pore Diameter (Volume) (nm)	2225.4	2335.6	185.7
Median Pore Diameter (Area) (nm)	12.5	73.0	30.7
Average Pore Diameter (4V/A) (nm)	76.4	427.4	64.3
Bulk Density at 0.52 psia (g/mL)	2.0198	1.7311	2.2083
Apparent (skeletal) Density (g/mL)	2.5088	2.2651	2.5225
Porosity (%)	19.4925	23.5781	12.4548
Stem Volume Used (%)	67	29	37

The percentages of the pore size distribution of İscehisar andesite, Ayazini tuff, and Seyitler tuff according to Klopfer's (1985) classification are given in Table 3. The pores between 1 μm and 1 mm, which increase the capillary water absorption of the building blocks, are known as "capillary pores." Macro pores (>1 mm) ensure the circulation of the absorbed liquid (Siegesmund and Dürrast 2011). According to mercury porosimetry results, it has been determined that most of the Andesite pores are in the range of 0.1 to 10 μm. For andesite, those with pore size distribution ratios less than 0.1 μm were 21.68%; those between 0.1 and 1 μm were determined as 10.69%, and those larger than 1 μm were determined as 67.62%. Ayazini tuff exhibits pore size distribution from 0.01 μm to 100 μm. Most of the pores have a pore size between 0.1 and 10 μm. For Ayazini tuff, those with pore size distribution ratios less than 0.1 μm were 4,76%; those between 0.1 and 1 μm were determined as 16,17%, and those larger than

1 μm were determined as 79,07%. The Seydiler tuff has pore sizes ranging from 0.1 μm to 4 μm. For Seydiler tuff, those with pore size distribution ratios less than 0.1 μm were 17,2%; those between 0.1 and 1 μm were determined as 16,88%, and those larger than 1 μm were determined as 65,92%. According to the results of the mercury porosimetry in the Seydiler tuffs, it was determined that approximately 82% of the pores were greater than 0.1 μm.

Table 3. *Pore size distribution of İscehisar andesite, Ayazini tuff, and Seydiler tuff tested according to Klopfer's (1985) classification*

	Pore size distribution (%)		
	micro pores (<0,1 μm)	meso pores (0,1-1 μm)	macro pores (>1 μm)
İscehisar andeziti	21,68	10,69	67,62
Ayazini tüfü	4,76	16,17	79,07
Seydiler tüfü	17,2	16,88	65,92

All three porous building stones are seen to have a unimodal pore size distribution. The mercury porosimetry data show that the pore distribution shows that the predominant pore diameter generally ranges from 0.4 μm to 5 μm (Figure 8). This distribution is located in the meso porosity (0,1 μm - 1 mm) area in Klopfer's (1985) classification given above. The pore size distribution of İscehisar andesite varies between 0.01 μm and 200 μm. About 78% of these are in the class of capillary pores (0.1 μm to 1 mm). Due to this feature, İscehisar andesite is extremely sensitive to water absorption. This sensitivity shows that it is more sensitive to capillary water absorption events. However, the pores appear to be concentrated in size from 1 to 4 μm. The pores have a single peak distribution between 2 and 3 μm. The Ayazini tuff appears to have a pore size distribution between 0.02 and 200 μm. The Ayazini tuff exhibits a single peaked pore size distribution. The pores are concentrated between 1 and 5 μm. The Seydiler tuff has an essentially single peaked pore size distribution. In this peak, the pores are concentrated between 0.4 and 5 μm, while the presence of another smaller peak between 0.02 and 0.3 μm is also seen. Pore peaks appear at 3 μm and 0.1 μm points, respectively.

3.3. Physical and Mechanical Properties

To evaluate the quality of natural building stones, it is necessary to know their physical and mechanical properties. Parameters such as water absorption, density, porosity, and uniaxial compressive strength are related to strength. Low-density and high-porosity building stones usually have

low strength. Porosity is one of the most important factors for water absorption and permeability. High-porosity natural stone has a high-water absorption value. For each test, six of each building block sample were tested against the standards, and the results are presented in Table 4.

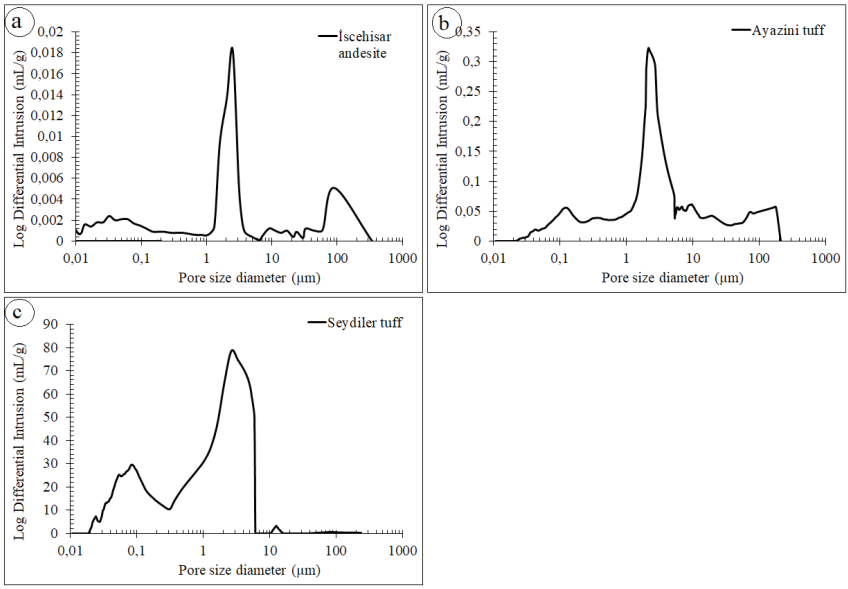

Figure 8. *Pore size distribution graphs of the tested İscehisar andesite, Ayazini tuff, and Seydiler tuff*

The Ayazini tuff has the lowest real density value, 2336 kg/m^3, while the values of the Seydiler tuff and the İscehisar andesite are 2369 and 2435 kg/m^3, respectively. The İscehisar andesite shows the highest real density. The İscehisar andesite has the lowest open porosity (9.00%) value, while the values of the Seydiler tuff and the Ayazini tuff are 12.18% and 30.94%, respectively. Water absorption values of building stones were directly proportional related to porosity. As expected, the Ayazini tuff has the highest porosity and maximum water absorption capacity. Another feature is that P-wave velocity is inversely related to porosity; in natural stone with much porosity, P-wave velocities are measured less. For this reason, the lowest P wave velocity is measured in Ayazini tuffs since it has the most porosity (1.16 km/s). The İscehisar andesite has the highest P-wave value (2.16 km/s). The İscehisar andesite shows the highest uniaxial compressive strength value as 91.24 MPa.

Table 4. *Physical and mechanical properties of İscehisar andesite, Ayazini tuff, and Seydiler tuff (Each experiment was performed with 6 samples and averaged)*

Tests	İscehisar Andesite			Ayazini Tuff			Seydiler Tuff		
	min	max	mean	min	max	mean	min	max	mean
Density (real) (kg/m^3)	2289	2546	2435	2123	2498	2336	2346	2523	2369
Water absorption by weight (%)	4.49	6.19	5.78	10.94	13.98	15.90	6.77	9.24	3.88
Open porosity (%)	7.68	9.80	9.00	30.07	31.87	30.94	9.77	14.41	12.18
Total porosity (%)	24.89	27.16	26.07	38.46	39.87	39.03	23.02	27.48	25.06
P-wave velocity (km/s)	2.08	2.26	2.16	1.06	1.32	1.16	1.09	1.32	1.92
Uniaxial compressive strength (MPa	86.65	106.98	91.24	14.54	19.98	16.06	57.05	65.24	61.45

3.4. Capillary Water Absorption

Environmental impacts have significant effects on the water absorption of natural building stones. Particularly porously, building stones are highly affected by these effects. Chemical protectors are used to reducing the water absorption properties of building stones used in historic buildings. This study determined capillarity and water absorption values of untreated and water-repellent chemical-treated samples by following TS EN 1925. The water absorption coefficients of the tested natural building stones are given in Table 5. A graph of the capillary water absorption of the untreated and treated tested stones is given in Figure 9. The capillary coefficient gives an idea of the water absorption kinetics due to capillary porosity and cracks in a stone. In other words, it expresses how quickly the stone can absorb water when it comes into contact with the water. According to the Washburn equation, the capillary coefficient is proportional to the square root of the water uptake time for a given surface in contact with water.

Table 5. *Capillary water absorption properties of İscehisar andesite, Ayazini tuff, and Seydiler tuff (Each experiment was performed with 6 samples and averaged) (T: treated, UT: untreated)*

Time	min	1	3	5	10	15	30	60	480	1440	2880
	$Sec^{0.5}$	7.75	13.42	17.32	24.49	30.00	42.43	60.00	169.71	293.94	415.69
		Capillary absorption (C) ($kg/m^2\ s^{0.5}$)									
İscehisar Andesite	Water (UT)	0.40	0.54	0.65	0.78	0.89	1.08	1.75	2.67	4.92	8.09
	Salty water (UT)	0.55	0.68	0.80	0.96	1.13	1.36	1.98	3.72	6.24	8.90
	Water (T)	0.03	0.04	0.06	0.07	0.09	0.11	0.15	0.42	0.82	1.79
	Salty water (T)	0.02	0.06	0.07	0.11	0.13	0.16	0.20	0.56	0.84	1.57
Ayazini Tuff	Water (UT)	5.22	7.76	10.35	14.23	17.35	18.25	18.55	18.62	18.78	19.34
	Salty water (UT)	3.26	6.45	9.67	13.28	17.65	19.83	20.05	20.14	20.40	21.04
	Water (T)	0.17	0.39	0.65	0.95	1.33	1.80	2.74	12.47	15.85	18.02
	Salty water (T)	0.05	0.13	0.22	0.34	0.50	0.80	1.28	5.96	10.62	15.65
Seydiler Tuff	Water (UT)	0.25	0.37	0.47	0.59	0.70	0.87	1.25	2.16	3.11	4.51
	Salty water (UT)	0.22	0.33	0.45	0.58	0.72	0.90	1.42	2.09	3.40	5.25
	Water (T)	0.04	0.05	0.06	0.09	0.12	0.14	0.19	0.53	1.02	1.91
	Salty water (T)	0.04	0.07	0.10	0.14	0.16	0.23	0.28	0.75	1.24	2.43

Rocks with high capillary porosity are generally expected to have a high-water absorption capacity. This means that it can absorb water faster through capillary water absorption. According to Graue et al. (2011), the capillary water absorption values are; low (<0.5 $kg/m^2s^{0.5}$), medium (0.5 - 3.0 $kg/m^2s^{0.5}$), and strong (>3.0 $kg/m^2s^{0.5}$) classified. Capillary data showed differences in İscehisar andesite, Ayazini tuff, and Seydiler tuff. According to this classification, all samples were evaluated to have high capillary water absorption capacity. This result can be attributed to the high porosity and capillary pore percentage determining capillary water uptake.

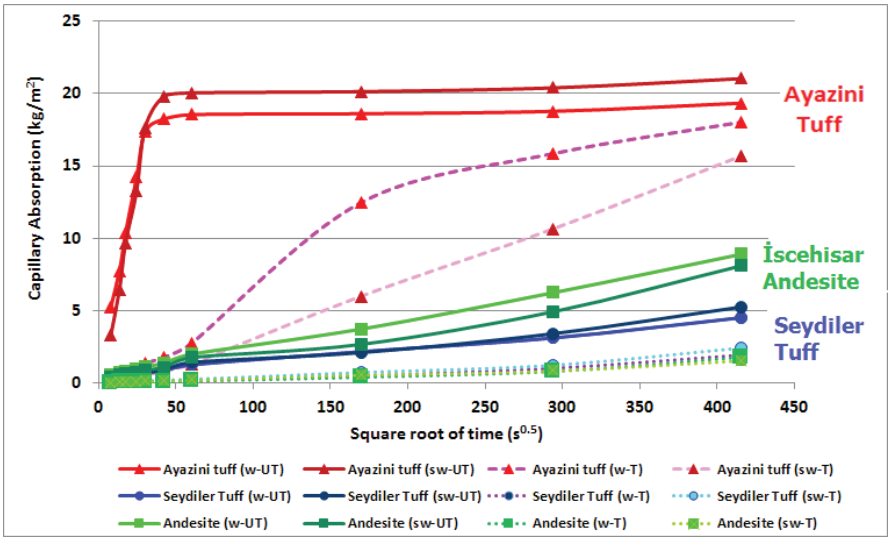

Figure 9. *Water absorption by capillarity for a tested stone sample before and after treatment (w-UT: water untreated, sw-UT: salty water untreated, w-T: water treated, sw-T: salty water treated).*

3.4.1. Capillary water absorption of Iscehisar andesite

In the normal and salty water conditions of the treated and untreated Iscehisar andesite, the determined capillary water absorption graph is given in Figure 10. The photographs of the water absorption levels in the experiment are shown in Figure 11. The water absorption values of the untreated andesite were determined as 8.09 kg/m^{2}s$^{0.5}$, and the salty water absorption values were determined as 8.90 kg/m^{2}s$^{0.5}$. The capillary absorption coefficient of the andesite is greater than 3 kg/m^{2}s$^{0.5}$, so it has strong capillary water absorption. Untreated andesite samples were not fully saturated in normal water conditions at the end of 2880 min in the capillary water absorption test. In salty water, almost complete saturation occurred at 2880 min. Treated andesite samples showed a significant decrease in the capillary water absorption test in normal and salty water at the end of 2880 min. The treated andesite's water absorption values were determined at 1.79 kg/m^{2}s$^{0.5}$, and the salty water absorption values were determined at 1.57 kg/m^{2}s$^{0.5}$.

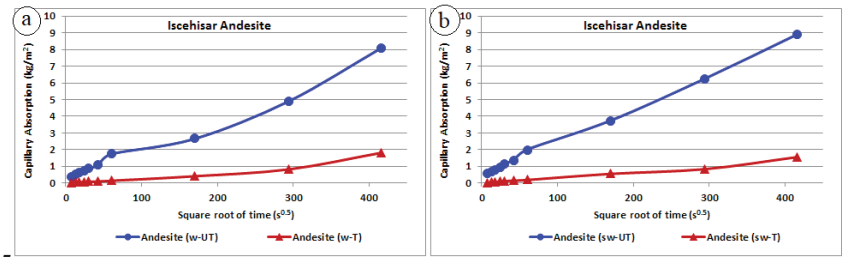

Figure 10. *Graph of capillary water absorption as a function of time for the untreated (a) and treated İscehisar andesite (b). (w-UT: normal water untreated, w-T: normal water treated, sw-UT: salty water untreated, sw-T: salty water treated)*

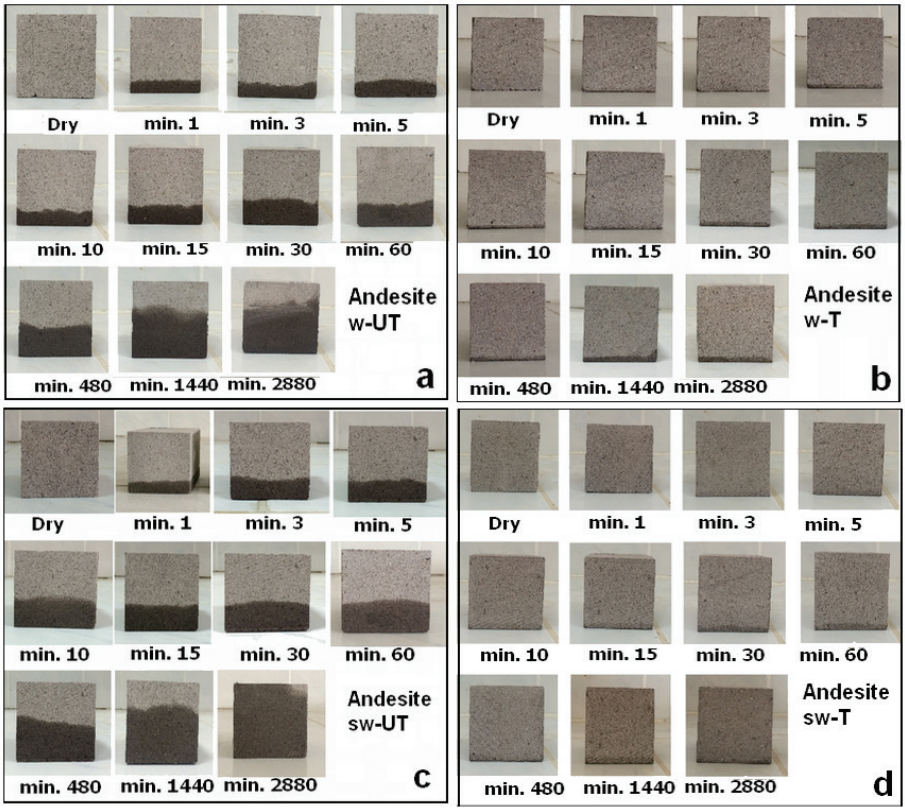

Figure 11. *Water absorption by capillarity levels views of untreated (a) and treated samples of İscehisar andesite (b). (w-UT: normal water untreated, w-T: normal water treated, sw-UT: salty water untreated, sw-T: salty water treated).*

3.4.2. Capillary water absorption of Ayazini tuff

In the normal and salty water conditions of the treated and untreated Ayazini tuff, the graph of determined capillary water absorption is given in Figure 12. The photographs of the water absorption levels are given in Figure 13. Untreated Ayazini tuff samples were fully saturated in normal water conditions after only 15 min in the capillary water absorption test. Likewise, in salt water, the saturation was almost complete after 15 min. According to the capillary water absorption of untreated Ayazini tuff data for water and salty water, the water uptake is 19.34 and 21.04 kg/m^{2}s$^{0.5}$. Similarly, the water absorption data of the treated samples are 18.02 and 15.65 kg/m^{2}s$^{0.5}$, respectively. The capillary absorption coefficient of the Ayazini tuff is greater than 3 kg/m^{2}s$^{0.5}$, so it has strong capillary water absorption. As can be inferred from examining the capillarity curves, treated samples decreased water uptake with the water repellent. Ayazini tuff has the most open porosity of the tested building stones (30.94%). The high capillary water absorption capacity of the Ayazini tuff can be explained by its capillary porosity of over 95%.

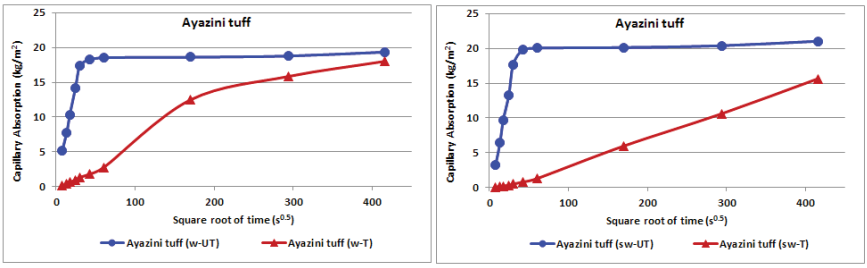

Figure 12. *Graph of capillary water absorption as a function of time for the untreated (a) and treated Ayazini tuff (b). (w-UT: normal water untreated, w-T: normal water treated, sw-UT: salty water untreated, sw-T: salty water treated)*

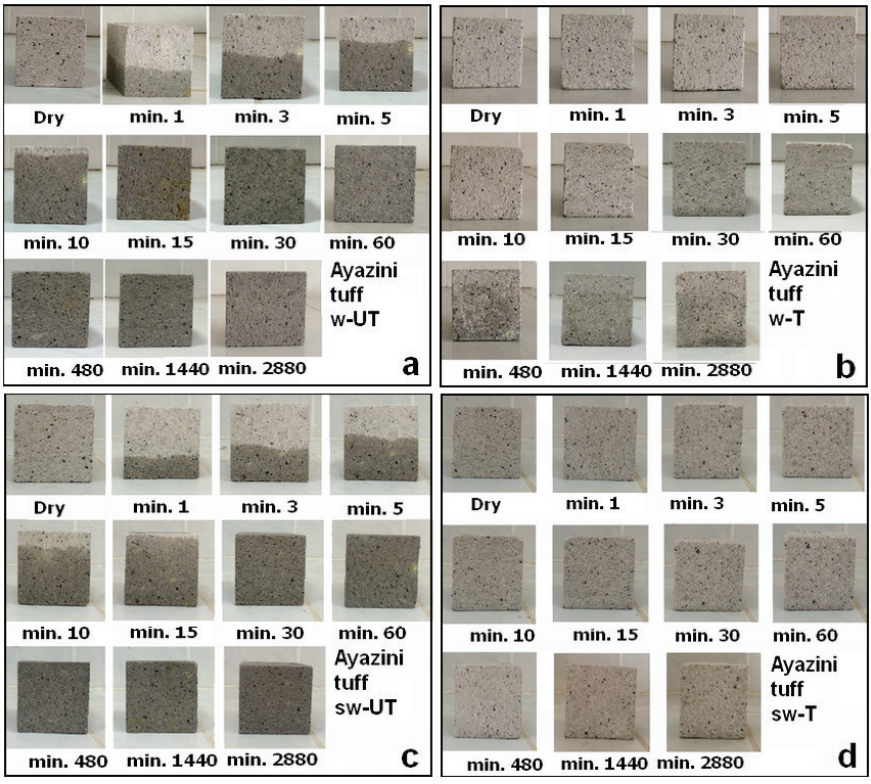

Figure 13. *Water absorption by capillarity levels views of untreated (a) and treated samples of Ayazini tuff (b) (w-UT: normal water untreated, w-T: normal water treated, sw-UT: salty water untreated, sw-T: salty water treated).*

3.4.3. Capillary water absorption of Seydiler tuff

In the normal and salty water conditions of the treated and untreated Seydiler tuff, the graph of determined capillary water absorption is given in Figure 14. The photographs of the water absorption levels are given in Figure 15. Untreated Seydiler tuff samples were not fully saturated in normal and salty water conditions at the end of 2880 min in the capillary water absorption test. This situation is because Seydiler tuff has the lowest open porosity ratio, and the pore size distribution is smaller than other tested stones. Here, more time will be needed to complete the capillary water uptake. Seydiler tuff showed at least a capillary water absorption coefficient within the tested building stones. Untreated Seydiler tuff data for normal and salty water, respectively, the water uptake is 4.51 and 5.25 kg/$m^2s^{0.5}$. Likewise, the water absorption data of the treated Seydiler tuff samples were 1.91 and 2.43 kg/$m^2s^{0.5}$, respectively. The capillary absorption coefficient of the Seydiler tuff is greater than 3 kg/$m^2s^{0.5}$, so it has strong

capillary water absorption. The water-repellent chemical reduced the water uptake in the processed Seydiler tuff samples.

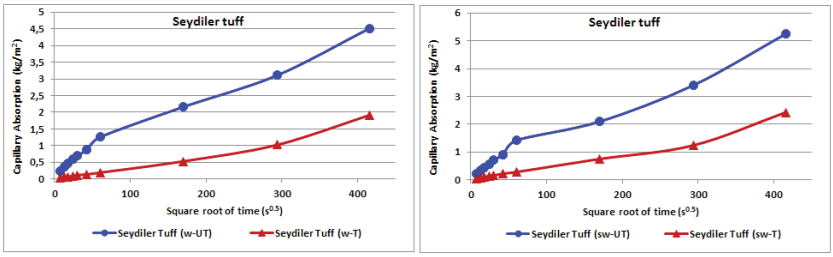

Figure 14. *Graph of capillary water absorption as a function of time for the untreated (a) and treated Seydiler tuff (b). (w-UT: normal water untreated, w-T: normal water treated, sw-UT: salty water untreated, sw-T: salty water treated)*

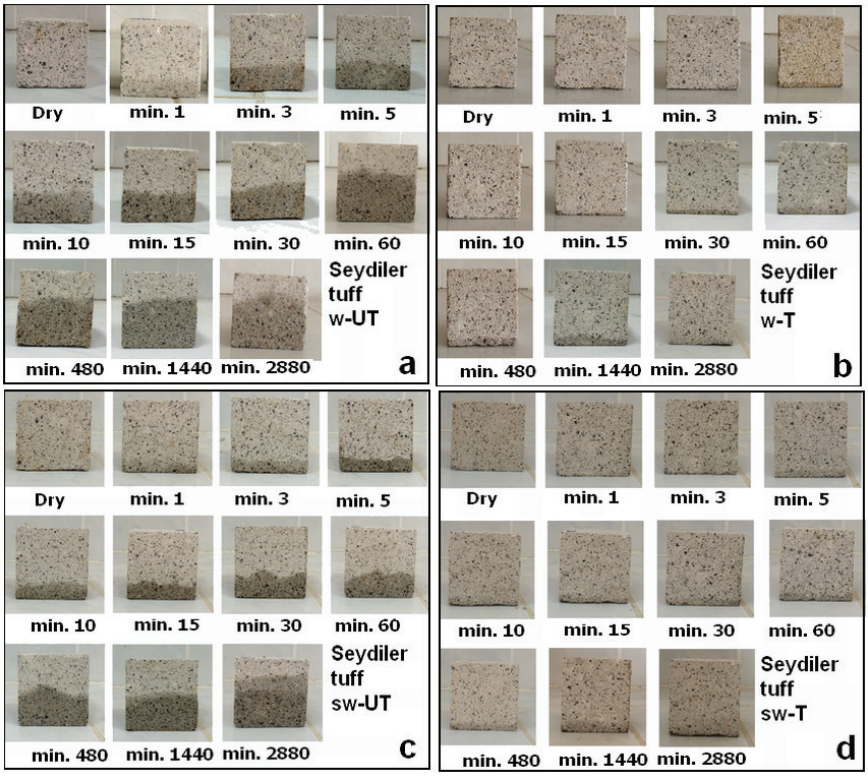

Figure 15. *Water absorption by capillarity levels views of untreated (a) and treated samples of Seydiler tuff (w-UT: normal water untreated, w-T: normal water treated, sw-UT: salty water untreated, sw-T: salty water treated).*

3.5. Resistances of surface protection treatments

For decades, surface protection treatment chemicals have been used successfully to protect buildings against moisture and consequent physical, chemical, and biological deterioration. The degradation of historic buildings in the urban area is mainly due to atmospheric effects. High porosity in connection with high water uptake has a high potential for damage to building stones. The best way to avoid deterioration is to prevent water penetration into the stone since water accumulation is mainly responsible for stone decay. Water repellents are surface protection materials that increase the contact angle between the water and the building stone surface. For this reason, water repellents reduce water penetration in building stones.

It was determined that all building block samples examined had high capillary water absorption values in both normal and saltwater conditions. Water absorption by capillarity coefficients for building stone samples before and after treatment was given in Figure 16. The main effect is to reduce normal and salty water penetration. Applying surface protection treatments decreases liquid water flow through the film formed on the surface of the samples, thus decreasing capillary water absorption and open porosity.

A solvent-based commercial water-repellent chemical was used in the experiments. The protective rate of the used water-repellent chemicals is shown in Figure 17. It has been determined that the effect of surface protection processes is more effective in andesite and Seydiler tuffs than in Ayazini tuff samples. The best protection rate in experiments was seen in the andesite samples. The capillary water absorption measured with the Iscehisar andesite sample decreases by about 77.87% in normal water conditions after surface treatments. Similarly, in salty water conditions, this ratio was 82.4%. The second-best protection rate was measured in the Seydiler tuff. The capillary water absorption measured with the Seydiler tuff sample is reduced by about 57.59% in normal water conditions after surface treatments. Similarly, this is 53.76% in saltwater conditions. Andesite and Seydiler tuff after the surface treatment process have a water uptake value its medium capillary absorption (0.5 to 3.0 kg/m2 s0.5). Experimental studies have shown that the water absorption rate decreases slightly if the Ayazini tuff is covered with chemical protectors. This ratio was measured at 6.84% in normal and 25.63% in salty water conditions. Even when applying surface treatment, Ayazini tuff is most probably exposed to deterioration because its porosity values are much higher than other tested stones. For this reason, it should be used with caution in areas with a lot of groundwater.

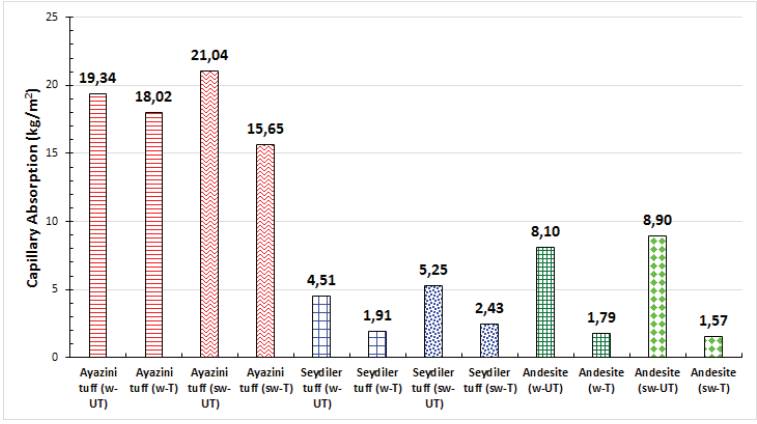

Figure 16. *Water absorption by capillarity for building stone samples before and after water-repellent treatment (w-UT: static water untreated, w-T: static water treated, sw-UT: salty water untreated, sw-T: salty water treated).*

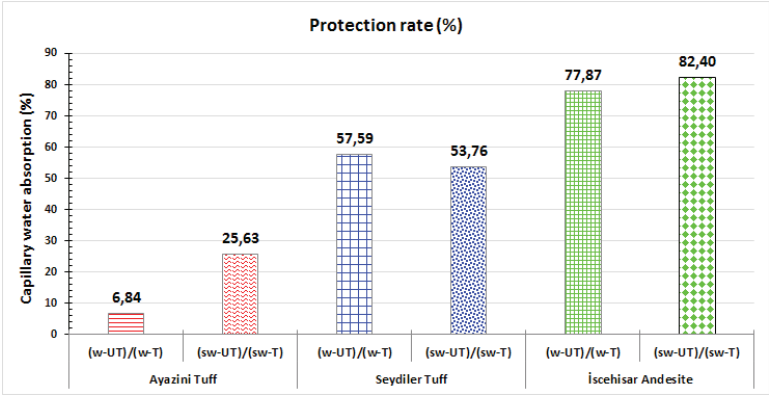

Figure 17. *Protective properties of the water-repellent chemical in terms of capillary water absorption.*

4. Conclusions

The main results of this study can be summarized as follows: Mineralogical-petrographic, mechanic-physical properties, and pore size distribution of the building stones were investigated for which the capillary water absorption test.

In capillary water absorption experiments, the water absorption coefficients of all tested untreated stones are greater than 3 $kg/m^2s^{0.5}$, so they have strong capillary water absorption. In normal and salty conditions, the water absorption coefficients of all tested untreated building stones vary from 4.51 to 21.04 $kg/m^2s^{0.5}$. In salt water, the water absorption coefficient is higher. The reason is that the salt ions increase the surface tension of the stone surface.

The durability and aesthetic appearance of natural building stones may be improved by covering them with water repellents due to reduced capillary water absorption. Control of open porosity and capillary water absorption helps evaluate the treatments given to the stone materials. The test results showed that the surface water repellent is efficient in cases where the water penetration mechanism is the capillary suction. The water-repellent material showed protection on all tested building stones. After the surface treatment process, andesite and Seydiler tuff have a water uptake value in the medium capillary absorption (0.5-3.0 $kg/m^2s^{0.5}$), while the capillary water absorption coefficients are significantly reduced. The andesite and Seydiler tuff present higher efficiency in decreasing water capillary action than the Ayazini tuff in water. According to laboratory test results: Ayazini tuff is not suitable for use as a building stone in the Afyonkarahisar area in a humid environment. For this reason, it is suggested that this stone should be preferred only for decorative cladding of the interior of buildings.

REFERENCES

Abell AB, Willis KL, Lange DA (1999) Mercury intrusion porosimetry and image analysis of cement-based materials. J Colloid Interface Sci 211:39-44

Al-Naddaf M (2011) Quantifying the influence of halite and sylvite crystallization on capillary water absorption coefficient of sandstone. J Am Inst Conservat 50:1, 1-13

Benavente D, Garcia Del Cura MA, Bernabe UA, Ordonez S (2001) Quantification of salt weathering in porous stones using an experimental continuous partial immersion method. Eng Geol 59:313–325

Chen TC, Yeung MR, Mori N (2004) Effect of water saturation on deterioration of welded tuff due to freeze–thaw action. Cold Regions Sci Technol 38:127–36

Clifton JR (1980) Stone consolidating materials - A status report. US Dep Commer Nat Bur Stand, NBS Tech Note 1118:46

Cnudde V, Cnudde JP, Dupuis C, Jacobs PJS (2004) X-ray micro-CT used for the localization of water repellents and consolidants inside natural building stones. Mater Charact 53:259–271

Çelik MY, Kaçmaz AU (2016) The investigation of static and dynamic capillary by water absorption in porous building stones under normal and salty water conditions. Environ Earth Sci February 2016, 75:307

Çelik MY, Yılmaz S (2018) Influence of the static, salty, acidic hydrous environments on the capillarity potential of the porously building stone. Journal of the Faculty of Engineering and Architecture of Gazi University 33(2):591-607.

Çelik MY, Arsoy Z, Sert M, Kahraman B (2019) Ayazini (Afyonkarahisar) tüflerinde sıcaklığın zamana bağlı su emme özelliğine etkisinin incelenmesi. (in Turkish) Proceedings of the 26th International Mining Congress and Exhibition of Turkey, IMCET 2019, Antalya, April 16–19, 1625–1634.

Graue B, Siegesmund S, Middendorf B (2011) Quality assessment of replacement stones for the Cologne Cathedral: mineralogical and petrophysical requirements. Environ Earth Sci 63:1799–1822

Hoffmann D, Niesel K (1992) Pore structure of rendering as a feature of its weathering – 7th International Congress on the Deterioration and Conservation of Stone, Lisbon, pp. 611-620

Ioannou I, Andreou A, Tsikouras B, Hatzipanagiotou K (2009) Application of the sharp front model to capillary absorption in a vuggy limestone. Eng Geol 105:20–23

Juhász P, Kopecskó K, Suhajda Á (2014) Analysis of capillary absorption properties of porous limestone material and its relation to the migration depth of bacteria in the absorbed biomineralizing compound, Per Pol Civil Eng Vol.

58/paper 7020:1–8

Karoglou M, Moropoulou A, Giakoumaki A. Krokida MK (2005) Capillary rise kinetics of some building materials. J Colloid Interface Sci. 284, 260–264

Karagiannis N, Karoglou M, Bakolas A, Moropoulou A (2016) Effect of temperature on water capillary rise coefficient of building materials. Build Environ 106:402-408

Karagiannis N, Karoglou M, Bakolas A, Krokida MK, Moropoulou A (2019) The influence of dynamic environmental conditions on capillary water uptake of building materials. J Build Phys 42(4):506.

Klopfer H (1985) Feuchte. In: Lutz P et al (eds) Lehrbuch der Bauphysik. Teubner, Stuttgart, pp 329–472

Moreno F, Vilela SAG, Antunes ÂSG, Alves CAS (2006) Capillary-rising salt pollution and granitic stone erosive decay in the parish church of Torre de Moncorvo (NE Portugal)-implications for conservation strategy. J. Cult. Herit 7:56–66

Mosquera MJ, Rivas T, Priet B, Silva B (2000) Capillary rise in granitic rocks: Interpretation of kinetics on the basis of pore structure. J Colloid Interface Sci 222:41-45

Nicholson DT (2001) Pore properties as indicators of breakdown mechanisms in experimentally weathered limestones. Earth Surf Proc Landf 26:819-838

Peruzzi R, Poli T, Toniolo L (2003) The experimental test for the evaluation of protective treatments: a critical survey of the 'capillary absorption index'. J Cult Herit 4:251–54

Rodriguez-Navarro C, Doehne E (1999) Salt weathering: influence of evaporation rate, supersaturation and crystallization pattern. Earth Surf Processes Landforms 24(3):191-209

Sengun N, Demirdag S, Akbay D, Ugur I, Altindag R, Akbulut A (2014) Investigation of the relationships between capillary water absorption coefficients and other rock properties of some natural stones. V. Global Stone Congress, 22-25 October 2014, Antalya/Türkiye

Siegesmund S, Dürrast H (2011) Physical and mechanical properties of rocks. In: Stone in architecture, 4th edition, Siegesmund S., Snethlage R. eds., Berlin: Springer, pp. 97–225.

Tomašić I; Lukić D, Peček N; Kršinić A (2011) Dynamics of capillary water absorption in natural stone. Bull Eng Geol Environ. 70:673–680

Tsakalof A, Manoudis P, Karapanagotis I, Chryssoulakis I, Panayiotou C (2007) Assessment of synthetic polymeric coatings for the protection and preservation of stone monuments. J Cult Herit 8:69–72

TS EN 1925 (2000) Natural stone test methods-Determination of water absorption coefficient by capillarity, Turkish Standards Institute, Ankara, Turkey, 10 pp

TS EN 1926 (2007) Natural stone test methods-determination of uniaxial compressive strength. Turkish Standards Institute, Ankara, Turkey, 19 pp

TS EN 1936 (2010) Natural stone test methods-determination of real density and apparent density and of total and open porosity. Turkish Standards Institute, Ankara, Turkey, 10 pp

TS EN 13755 (2009) Natural stone test methods-determination of water absorption at atmospheric pressure. Turkish Standards Institute, Ankara, Turkey, 10 pp

TS EN 14579 (2006) Natural stone test methods-determination of sound speed propagation. Turkish Standards Institute, Ankara, Turkey, 14 pp

Vázquez P, Alonso FJ, Esbert RM, Ordaz J (2010) Ornamental granites: Relationships between p-waves velocity, water capillary absorption and the crack network. Constr Build Mater 24:2536–2541

Washburn EW (1921) The Dynamics of Capillary Flow, Phys. Rev, 17,273–283

CHAPTER 12

THE PLACE OF SMALL ORGANIC MOLECULES IN FLUORESCENT SENSOR SYSTEMS

Merve ZURNACI[1]

1 Kastamonu University, Central Research Laboratory, Kastamonu, TURKEY Orcid id: https://orcid.org/0000-0002-2928-3492 e-mail: mzurnaci@kastamonu.edu.tr

Introduction

F. Goppelsröder described the first fluorescent chemosensor to measure aluminum ion (Al^{3+}) in 1867 (Czarnik, 1993). Upon this, a lot of research has been done on sensor technology and these researches have gained speed day by day. Most of these research are related to the materials as sensors and their application areas (Gambhire, Labhade, & Kale, n.d.). Among the materials as sensors, fluorescent organic materials draw attention with their strong emission properties and properties (Doan, Pitter, Kocher, Wilson, & Goodson, 2015; Zhu, Li, Zhu, & Huang, 2022). In particular, many fluorescent organic materials are designed for use in sensors (Dikmen, Turhan, Yaman, & Bütün, 2021; Lee, Kim, & Sessler, 2015; J. Wang, Yuan, Hu, Xu, & Xue, 2016).

Organic materials are often encountered in sensor technology as heterocyclic compounds (especially with the dense π conjugate system) (C. Wang, Dong, Hu, Liu, & Zhu, 2012). On the other hand, nitrogen-containing heterocycles come to the fore in sensor applications because they play an essential role in the preparation of transition metal complexes and change the electronic properties of the molecule based on the acidity of the –NH proton (Batista, Costa, & Raposo, 2014). Developed for various anions and cations, these organic materials have attracted great interest due to their applications in the environment, chemistry, biology and medicine (Shin, Teresa Gutierrez-Wing, & Choi, 2021). Designing a fluorescent sensor for a cation or anion requires an acceptor unit that interacts selectively with the cation or anion (Lee et al., 2015). Many small organic molecules have been designed for sensing, imaging and biomedical applications (Yang et al., 2022).

Photophysical properties (brightness, photostability, wavelength range), electrochemical properties and biochemical properties of organic compounds are important parameters in the sensor's design (Kiran, Hogan, James, & Wilson, 2011). Especially in the development of anion sensors, −NH and −OH groups are important in the formation of hydrogen/halogen bonds (Chudzinski, McClary, & Taylor, 2011). It is recognized molecularly through interaction with, In addition, the distance between −NH and −OH groups effectively changes the fluorescence (González-Ruiz et al., 2022).

Fluorescent sensors generally consist of 3 parts: a receptor (ionophore), a fluorophore (signal moiety) and a chelator (S, Sam, George, N, & Varghese, 2021)(Figure 1). The general skeletal structure of small organic molecules used in sensors is shown in Figure 2. The sensor properties of these molecules, derived by the binding of different groups, have been studied in detail in the literature (Cano, Alvarez, & Giraldo, 2019; Pesavento, Marchetti, De Maria, Zeni, & Cennamo, 2019).

In this study, I present an overview of the design of small organic molecules applied in detecting various analytes, including cations and anions. Application areas are mentioned by giving examples of small organic molecules. I hope this study will support the new thoughts to design a new organic material for detecting ions or metals in many technologies.

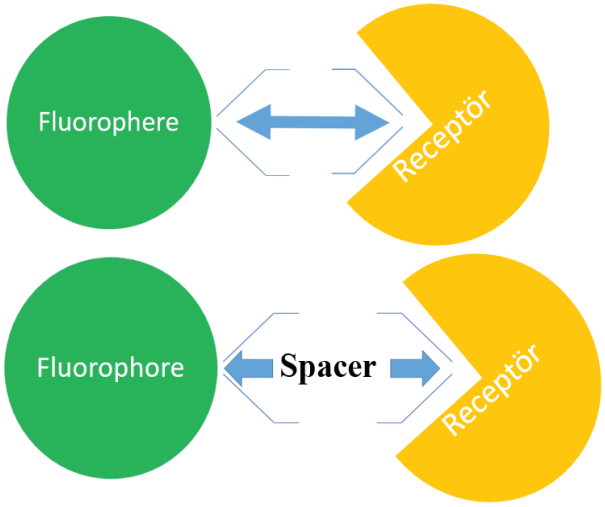

Figure 1. *Schematic representation of the receptor, fluorophore and spacer.*

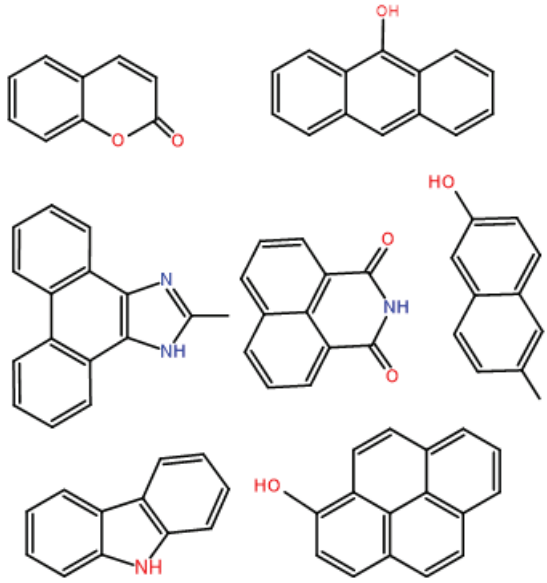

Figure 2. *Some of small organic molecule general skeleton structures for fluorescent sensors*

2. Types and Features of Fluorescent Sensors

Cation sensors

While many cations have important roles in the body, some cations contain heavy metals that harm human health (Jaishankar, Tseten, Anbalagan, Mathew, & Beeregowda, 2014). The design of new organic compounds is very important for the detection of such cations (Valeur & Leray, 2000). The small organic molecules that can act as sensors detect cations thanks to a fluorescent signal (intensity) (NAGANO, 2010). Many situations can be mentioned for fluorescence signals, such as quenching, enhancement, excimers, explexes, lifetimes and anisotropy (Pu, 2004).

Cation consists of sensors, connectors and signal units (Dongare & Gore, 2021). The binding unit (receptor) interacts with the analyte and causes specific changes. The electronic environment is caused by chemical changes, such as redox potential, or physically observable changes, such as color. These changes are reflected in the signaling unit. The sensors based on this approach are shown schematically in Figure 3.

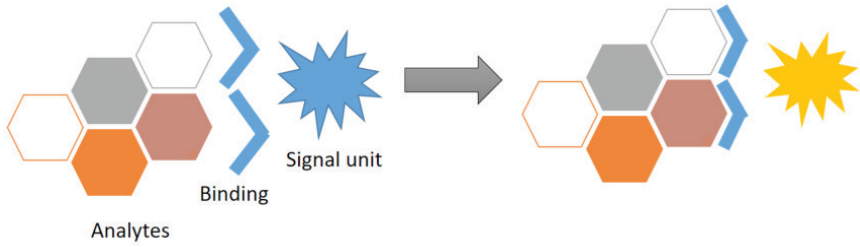

Analytes: Cation, anion or small molecule

Figure 3. *Schematic representation of sensor mechanism*

When the literature is examined, it is seen that chemo sensors exhibit much better selectivity towards Al^{3+}, Fe^{3+}, Cu^{2+}, Zn^{2+}, Ag^{+} and Cd^{2+} ions than other cations. Many reports examine heavy metal cations such as lead, arsenic and mercury due to their harmful and toxic effects on biological systems and the environment. Analytical methods such as flame photometry, atomic absorption spectrometry, ion-sensitive electrodes and inductive optic emission spectrophotometer are used to detect cations.

Among organic molecules, Schiff bases draw attention to detecting metallic cations, thanks to their easy and inexpensive synthesis methods and good coordination with metal ions. The Schiff bases have been designed as fluorescent sensors for the detection of various metal ions. Some

properties of the Schiff base (such as its structural configuration and binding capacity) affect the selectivity and high sensitivity of fluorescent sensors (Khan et al., 2021). Derivatives of Schiff bases used as fluorescent cation sensors are given in Figure 4.

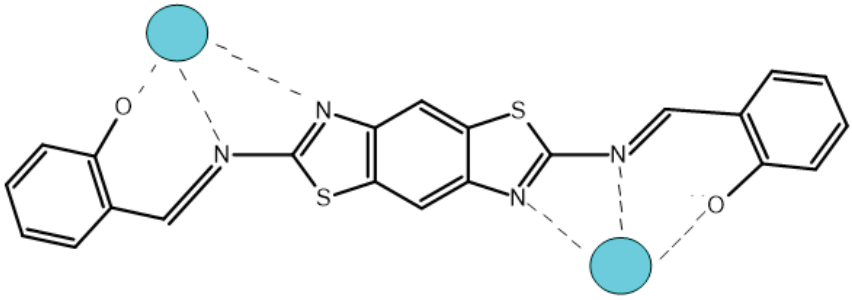

Figure 4. *Structure of Schiff base as fluorescent sensors*

Aluminum and iron are essential elements used in many different chemical processes. Excess of these elements causes toxic effects and some diseases. In excess of iron; such as anaemia, heart failure. In excess of aluminium, Alzheimer's and Parkinson's diseases occur. On the other hand, Cu^{2+} deficiency can cause coronary heart disease, and excess can cause harmful toxic effects on the environment and body. For these reasons, detecting Al^{3+}, Fe^{3+} and Cu^{2+} is necessary. In the literature, a new fluorescent sensor has been designed for the detection of Al^{3+} and Cu^{2+}, exhibiting fluorescence emission at 440-520 nm. This sensor detects Cu^{2+} in neutral aqueous medium; It can detect Al^{3+} in a slightly acidic aqueous medium. It has also been reported that it has been successfully used for the detection of Cu^{2+} and Al^{3+} ions in living cells. The molecular structure of the designed sensor is given in Figure 5. Moreover, anthracene-based small organic molecules as fluorescent sensors were used for the detection of Fe^{3+}. With the addition of Fe^{3+}, the fluorescence intensity in the aqueous buffer solution was considered (Figure 6).

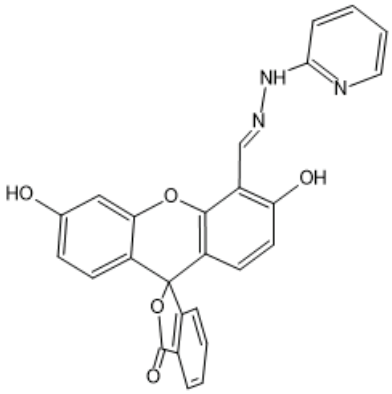

Figure 5. *Structure of organic molecule for the detection of* Cu^{2+} *and* Al^{3+}

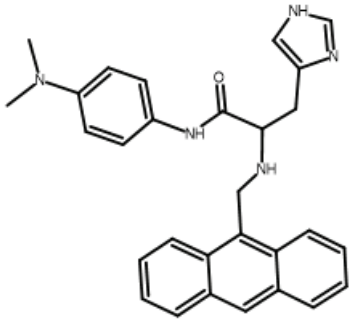

Figure 6. *The small organic molecule as fluorescent sensor for* Fe^{3+}

Quinoline or benzimidazole, derived from p-bond and nitrogen-containing heterocycles, are among the molecules used for interaction with the metal (cation). Quinoline can interact easily thanks to its strong fluorescence, easy production and nitrogen atoms in its structure. Benzimidazole is an electron-rich moiety. With these properties, a molecular derivative with a quinoline-benzimidazole skeleton can be used as a fluorescent sensor. These molecules took part in the sensor designed for Cu^{2+} detection. The structure of the designed hybrid molecule is given in Figure 7 (L. Liu et al., 2017).

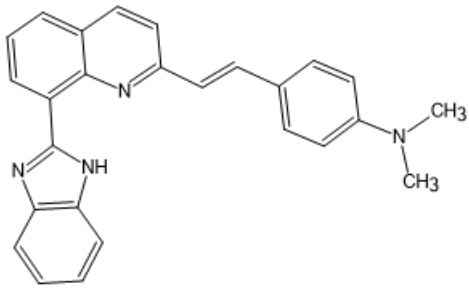

Figure 7. *Structure of quinoline-benzimidazole skeleton*

Anion sensors

Anions play fundamental roles in many biological and chemical processes (González-Ruiz et al., 2022; S et al., 2021). It is of great importance to developing new methods to detect anions. Sensing of anionic analytes of biological and environmental importance has recently become an area of focus (D. Wu et al., 2017). Especially in the last 25 years, the interest in small organic molecule anion sensors has been increasing and attracting the attention of researchers (Gale & Caltagirone, 2015).

The fluorophore recognizes the signal unit and receptor anions, which converts the data into an optical form. The anion binds to the receptor, the change in fluorescence properties occurs, this change is monitored. These changes are converted into an optical signal. Changes in the optical signal, such as increasing the intensity of fluorescence, changing or quenching of the stokes shift, are observed. Several signaling mechanisms can be mentioned for the fluorescent sensors (Dongare & Gore, 2021). For the interaction between anions and sensors, signaling mechanisms such as chelation-enhanced fluorescence (CHEF), photo-induced electron transfer (PET), light-induced-intramolecular/intermolecular charge transfer (ICT), and excited-state intramolecular proton transfer (ESIPT) are available (Dongare & Gore, 2021; Valeur & Leray, 2000) (Figure 8).

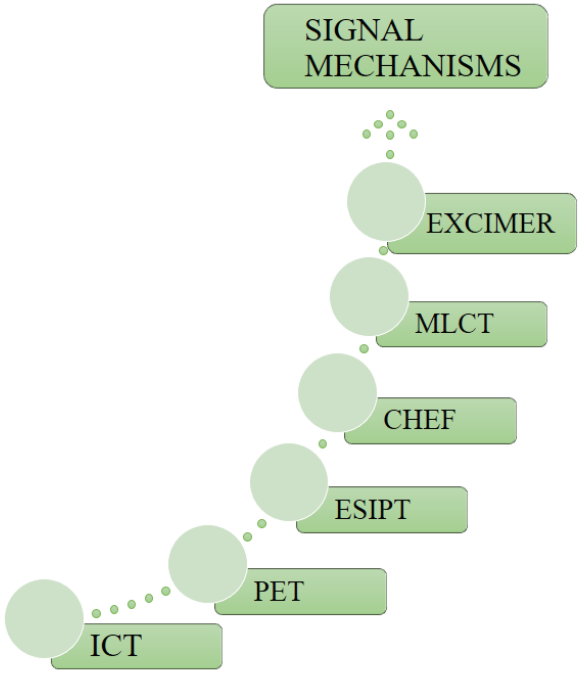

Figure 8. *Signal mechanism for fluorescent sensor systems*

Anions are difficult to detect compared to cations and some problems are encountered while designing (Beer & Gale, 2001). The use of positively charged acceptors and neutral ligands plays an important role in the design of anion sensors (S et al., 2021). An important parameter in designing an anion sensor is the hydrogen bond interaction (Dongare & Gore, 2021). With this method, fluorescent anion sensors with many small organic molecules (in which hydrogen bonding is active) have been synthesized (Gale & Caltagirone, 2015). For example, a molecule was designed by coupling thiourea to the naphthylimide structure and used as a fluorescent anion sensor (Gunnlaugsson, Kruger, Jensen, Pfeffer, & Hussey, 2003)(Figure 9).

Many fluorescent sensors used to detect of anions have been developed by deriving different organic molecules (Noushija, Shanmughan, Mohan, & Shanmugaraju, 2022). In general, many fluorescent sensors have been developed based on the fact that the −NH and −OH sensors in the structure contribute to the properties (Batista et al., 2014; Dongare & Gore, 2021). This section covers small organic molecule fluorescent sensors designed for the detection of anions such as F^-, Cl^-, CN^-.

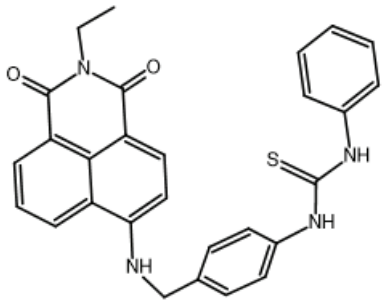

Figure 9. *Naphthylimide based fluorescent sensors*

Many sensors are designed to monitor fluorescence intensity changes for anions. Among these anions, molecules with superior fluorescence properties, such as coumarin and pyrene were synthesized for cyanide (Q. Wu et al., 2015). Cyanide anions were detected by hydrogen bond interaction. There was a clear change in color, fluorescence and absorption-emission spectrum. The coumarin-pyrene hybrid structure synthesized for CN^- detection is given in Figure 10.

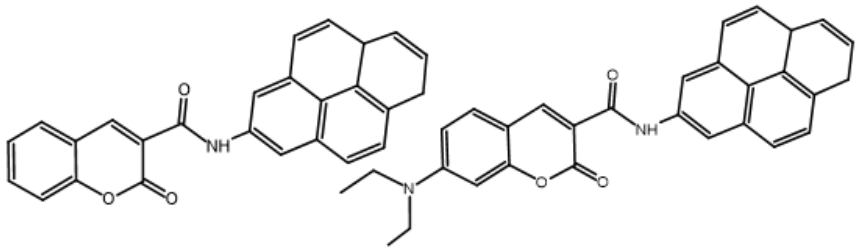

Figure 10. *Coumarin-pyrene hybrid structure for fluorescent sensors*

The use of carbazole and its derivatives as fluorescent anion sensors are in the literature (Bąk, Chabuda, Montes, Quesada, & Chmielewski, 2018; Zou et al., 2019). In the study conducted in 2022, carbazole-derived sensors were designed to detect F^-, Cl^-, Br^-, CN^-, Ac^- and OH^- anions (González-Ruiz et al., 2022)(Figure 11). Carbazole acted as a selective fluorescence chemosensor for fluoride and chloride. The increase in fluorescent emission intensity for fluoride and chloride anions is a result of specific interactions involving hydrogen bonds and intermolecular charge transfer of the solvent. The dose of fluoride, one of the important anions, can be dangerous for the body (Zhou, Zhang, & Yoon, 2014). The intake of the required amount of fluoride ions is beneficial for the teeth (Opydo-Szymaczek, Pawlaczyk-Kamieńska, & Borysewicz-Lewicka, 2022). The structure of the synthesized molecule for the detection of fluoride is presented in Figure 12 (Anjaneyulu, Kumar, Sankannavar, & Rao, 2012).

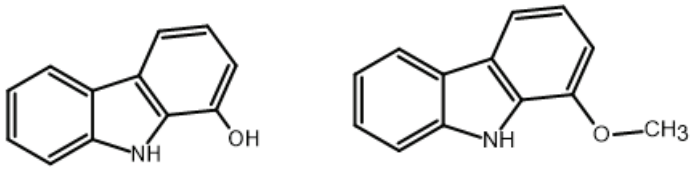

Figure 11. *Carbazole-derived fluorescent sensors*

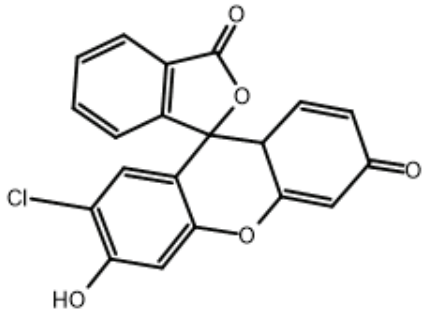

Figure 12. *Fluorescent sensors for detection of fluoride*

Among the anions, especially the chloride ion plays an important role in various stages of human biology and disease regulation (Bregestovski & Arosio, 2011; Salto et al., 2021). Cystic fibrosis, an inherited disease, is related to the chloride ion (Toh, Batchelor-McAuley, Tschulik, & Compton, 2013). Many organic molecules are available for the detection of chloride Figure 13 shows exemplary structures for these (Shao, Qiao, Lin, & Lin, 2009).

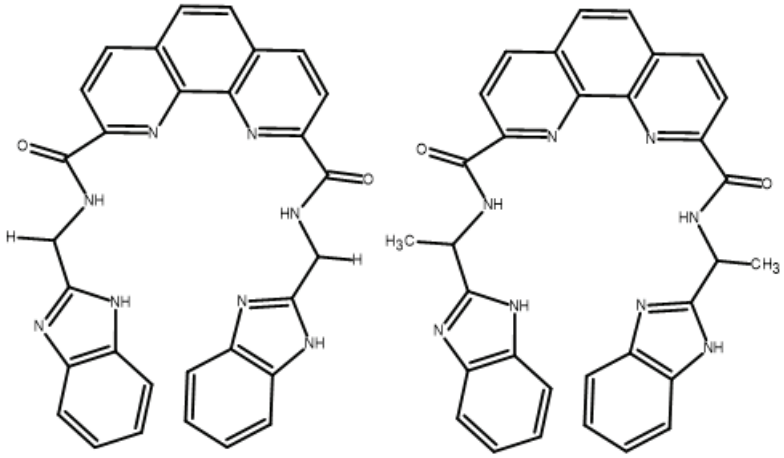

Figure 13. *Structures of for fluorescent anion sensors*

3. Applications and Advantages of Fluorescent Sensors

Especially small organic molecules carrying π-conjugated systems are promising structures for many applications such as dye-sensitized solar cells, OLEDs, OFETs, optical systems, opto-electronic devices and sensor technology (Ferreira, Costa, Gonçalves, Belsley, & Raposo, 2017; Frath, Massue, Ulrich, & Ziessel, 2014). In addition to these, it is also encountered in the fields of biology, medicine, biomedical, pharmacy, mining and environmental engineering. Among these applications, fluorescent sensors are of great interest for the detection of anions or cations due to their high sensitivity-selectivity and portable use in the literature (Chen, Xue, Gao, Yang, & Zang, 2020). Figure 14 shows the different application areas of fluorescent sensors. Thanks to the excellent fluorescent and electrochemical properties of these molecules, their use in these areas is increasing day by day.

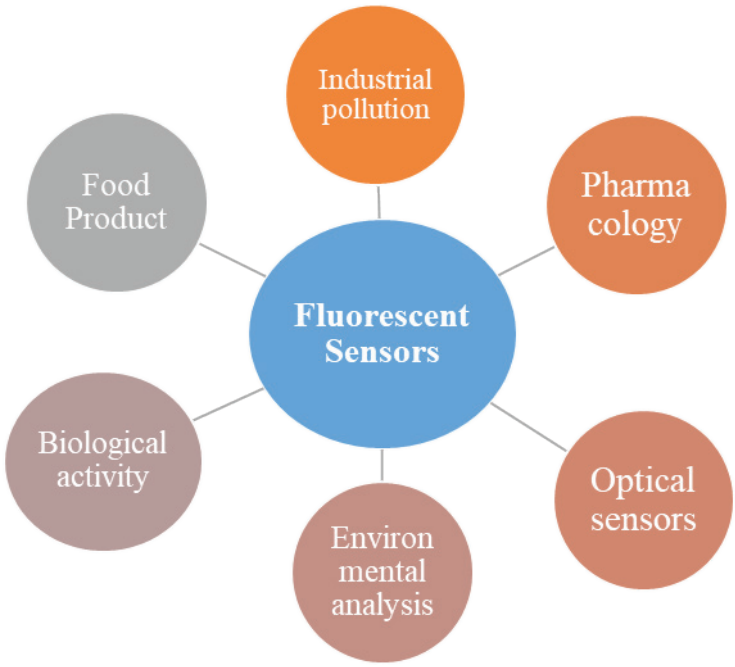

Figure 14. *Application areas of fluorescent sensors*

Due to the ease of use, high selectivity and sensitivity in fluorescence tests, fluorescent sensors have grown significantly and have become applicable in various fields over the past few years. In this topic, the applications of fluorescent sensors are briefly described. Using fluorescent sensors, toxic trace elements such as Cd^{2+}, As^{+2}, Cu^{3+}, Pb^{2+}, Hg^{2+}, Ni^{+} and Zn^{2+} can be detected (Rasheed et al., 2018). These toxic elements are located; It has many applications on food, drinking water and environmental wastes (Bowyer, Shen, & New, 2020; Rasheed et al., 2018). Fluorescent sensors for the copper(II) ion have been reported in the literature (Aksuner, Henden, Yilmaz, & Cukurovali, 2009). Copper is the third most abundant trace metal in the human body (S. Liu, Wang, & Han, 2017; Shi, Cui, Liu, & Pu, 2020). For applications in biological and environmental systems, their quantification is carried out using fluorescent sensors (Cheng et al., 2016).

Amy A. Bowyer and colleagues synthesized a series of molecules with fluorescent sensors for the detection of heavy metal ions in their study in 2019. They were able to classify these ions with almost 100% accuracy. With this sensor, it has been tried as a quantitative tool to accurately classify heavy metals in pool water and detect Pb^{2+}. This designed sensor has provided the advantage of obtaining comprehensive information about the environmental water source in advance. In their work, they derivatized the coumarin skeleton to enable the detection of different heavy metal ions.

The hydroxyl group in the structure of coumarin, the presence of donor electrons makes the structure fluorescent. Based on this feature, they developed a sensor that responds to different fluorescence responses. The structure of coumarin, which is the skeleton of the molecules they synthesized in their studies, is presented in Figure 15 (Bowyer et al., 2020).

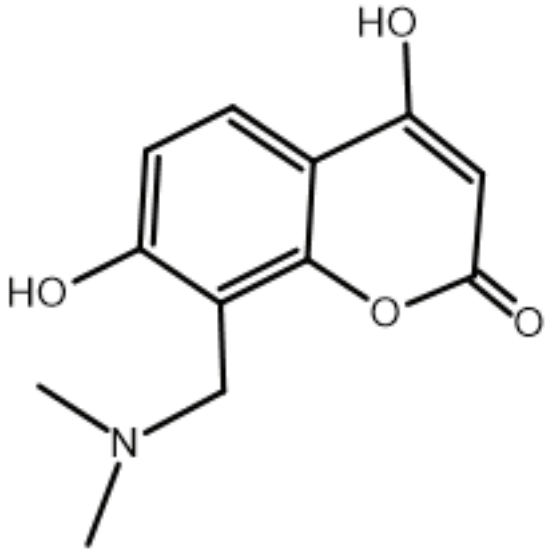

Figure 15. *Coumarin skeleton for fluorescent sensors in their study*

Fluorescent sensors can also be used in biological applications (Ai, 2014; Jo et al., 2016). The fluorescent sensor designed for the detection of the Zn^{2+} cation synthesized for use in biological applications is given in Figure 16. Genetically encoded sensors have been developed that can be used to detect redox biological processes. These sensors based on fluorescent proteins have reached wide applications in biology (Hirano, Kikuchi, Urano, Higuchi, & Nagano, 2000). In another study, a benzoxazole-based Zn^{2+} sensor was designed to be used in biological applications (Figure 17). The opening of the hydrogen bond as a result of the coordination of the molecule with Zn^{2+} caused a shift in emission and absorption. Based on this feature, they developed a Zn^{2+} sensor. They used this sensor to monitor changes in the amount of intracellular Zn^{2+} in fibroblast cells (Taki, Wolford, & O'Halloran, 2004).

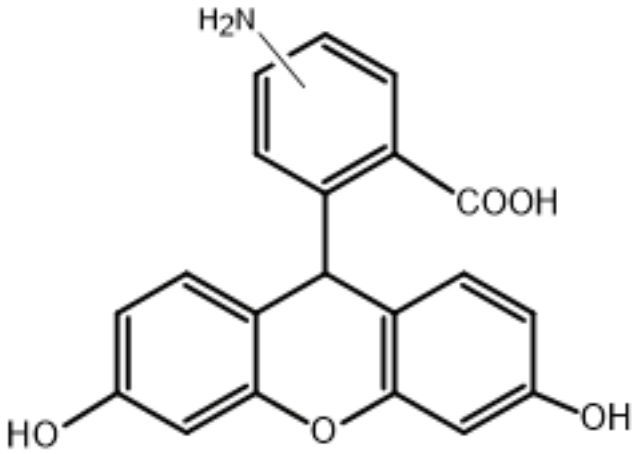

Figure 16. *Fluorescent sensor for Zn^{2+} cation in biological applications*

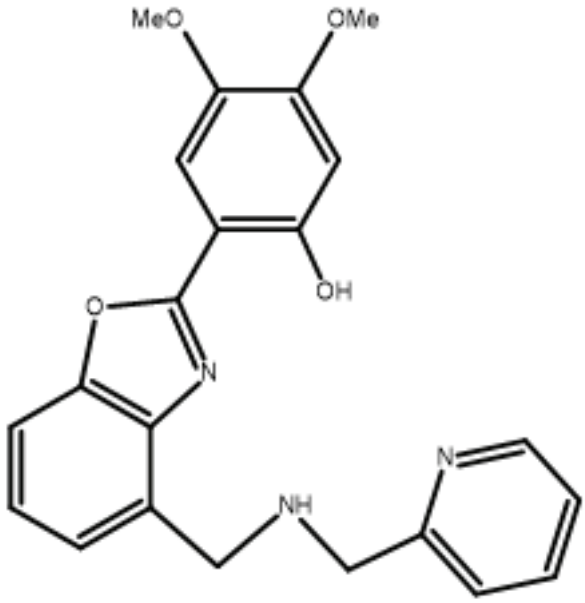

Figure 17. *Benzoxazole-based Zn^{2+} fluorescent sensor for biological applications*

5. Conclusion

This work provides an overview of small organic molecule-based fluorescent sensors used for the detection of cations, anions and various analytes. I have highlighted some examples of small organic molecules as fluorescent sensors. Afterward, I briefly summarized the application areas. I mentioned the importance of fluorescent sensors for detecting important analytes for the body and monitoring toxicants in samples such as environment food. This work will help new researchers do further studies on different small organic molecules.

The design and synthesis of small organic molecules will form a stepping for the design of new fluorescent sensors for cations and anions in the future. These molecules have led to the formation of small organic molecule-based sensors, offering a different perspective on organic synthesis. Interest in these sensors, sensitive and specific sensors, will increase day by day.

REFERENCES

Ai, H. (2014). Fluorescent Sensors for Biological Applications. *Sensors*, *14*(9), 17829–17831. https://doi.org/10.3390/s140917829

Aksuner, N., Henden, E., Yilmaz, I., & Cukurovali, A. (2009). A highly sensitive and selective fluorescent sensor for the determination of copper(II) based on a schiff base. *Dyes and Pigments*, *83*(2), 211–217. https://doi.org/10.1016/j.dyepig.2009.04.012

Anjaneyulu, L., Kumar, E. A., Sankannavar, R., & Rao, K. K. (2012). Defluoridation of Drinking Water and Rainwater Harvesting Using a Solar Still. *Industrial & Engineering Chemistry Research*, *51*(23), 8040–8048. https://doi.org/10.1021/ie201692q

Bąk, K. M., Chabuda, K., Montes, H., Quesada, R., & Chmielewski, M. J. (2018). 1,8-Diamidocarbazoles: an easily tuneable family of fluorescent anion sensors and transporters. *Organic & Biomolecular Chemistry*, *16*(28), 5188–5196. https://doi.org/10.1039/C8OB01031E

Batista, R. M. F., Costa, S. P. G., & Raposo, M. M. M. (2014). Selective colorimetric and fluorimetric detection of cyanide in aqueous solution using novel heterocyclic imidazo-anthraquinones. *Sensors and Actuators, B: Chemical*, *191*, 791–799. https://doi.org/10.1016/j.snb.2013.10.030

Beer, P. D., & Gale, P. A. (2001). Anion Recognition and Sensing: The State of the Art and Future Perspectives. *Angewandte Chemie International Edition*, *40*(3), 486–516. https://doi.org/10.1002/1521-3773(20010202)40:3<486::AID-ANIE486>3.0.CO;2-P

Bowyer, A. A., Shen, C., & New, E. J. (2020). A fluorescent three-sensor array for heavy metals in environmental water sources. *The Analyst*, *145*(4), 1195–1201. https://doi.org/10.1039/C9AN02182E

Bregestovski, P., & Arosio, D. (2011). *Green Fluorescent Protein-Based Chloride Ion Sensors for In Vivo Imaging*. https://doi.org/10.1007/4243_2011_27

Cano, D., Alvarez, L., & Giraldo, O. (2019). A DFT study of chemical sensors based on organic semiconductors (OSC) derived from 1− H − Borole. *Materials Research Express*, *6*(11), 115101. https://doi.org/10.1088/2053-1591/ab43f0

Chen, S., Xue, Z., Gao, N., Yang, X., & Zang, L. (2020). Perylene Diimide-Based Fluorescent and Colorimetric Sensors for Environmental Detection. *Sensors*, *20*(3), 917. https://doi.org/10.3390/s20030917

Cheng, D., Liu, X., Yang, H., Zhang, T., Han, A., & Zang, L. (2016). A Cu2+-Selective Probe Based on Phenanthro-Imidazole Derivative. *Sensors*, *17*(12), 35. https://doi.org/10.3390/s17010035

Chudzinski, M. G., McClary, C. A., & Taylor, M. S. (2011). Anion Receptors Composed of Hydrogen- and Halogen-Bond Donor Groups: Modulating Selectivity With Combinations of Distinct Noncovalent Interactions. *Jour-*

nal of the American Chemical Society, *133*(27), 10559–10567. https://doi.org/10.1021/ja202096f

Czarnik, A. W. (1993). *Supramolecular Chemistry, Fluorescence, and Sensing*. (1990), 1–9. https://doi.org/10.1021/bk-1993-0538.ch001

Dikmen, Z., Turhan, O., Yaman, M., & Bütün, V. (2021). An effective fluorescent optical sensor: Thiazolo-thiazole based dye exhibiting anion/cation sensitivities and acidochromism. *Journal of Photochemistry and Photobiology A: Chemistry*, *419*, 113456. https://doi.org/10.1016/j.jphotochem.2021.113456

Doan, P. H., Pitter, D. R. G., Kocher, A., Wilson, J. N., & Goodson, T. (2015). Two-Photon Spectroscopy as a New Sensitive Method for Determining the DNA Binding Mode of Fluorescent Nuclear Dyes. *Journal of the American Chemical Society*, *137*(29), 9198–9201. https://doi.org/10.1021/jacs.5b02674

Dongare, P. R., & Gore, A. H. (2021). Recent Advances in Colorimetric and Fluorescent Chemosensors for Ionic Species: Design, Principle and Optical Signalling Mechanism. *ChemistrySelect*, *6*(23), 5657–5669. https://doi.org/10.1002/slct.202101090

Ferreira, R. C. M., Costa, S. P. G., Gonçalves, H., Belsley, M., & Raposo, M. M. M. (2017). Fluorescent phenanthroimidazoles functionalized with heterocyclic spacers: Synthesis, optical chemosensory ability and two-photon absorption (TPA) properties. *New Journal of Chemistry*, *41*(21), 12866–12878. https://doi.org/10.1039/c7nj02113e

Frath, D., Massue, J., Ulrich, G., & Ziessel, R. (2014). Luminescent materials: Locking π-conjugated and heterocyclic ligands with boron(III). *Angewandte Chemie - International Edition*, *53*(9), 2290–2310. https://doi.org/10.1002/anie.201305554

Gale, P. A., & Caltagirone, C. (2015). Anion sensing by small molecules and molecular ensembles. *Chemical Society Reviews*, *44*(13), 4212–4227. https://doi.org/10.1039/C4CS00179F

Gambhire, M. S., Labhade, S. R., & Kale, R. R. (n.d.). *Fluorescent based chemosensors and its applications : A Review*. 1–6.

González-Ruiz, V., Cores, Á., Caja, M. M., Sridharan, V., Villacampa, M., Martín, M. A., … Menéndez, J. C. (2022). Fluorescence Sensors Based on Hydroxycarbazole for the Determination of Neurodegeneration-Related Halide Anions. *Biosensors*, *12*(3), 175. https://doi.org/10.3390/bios12030175

Gunnlaugsson, T., Kruger, P. E., Jensen, P., Pfeffer, F. M., & Hussey, G. M. (2003). Simple naphthalimide based anion sensors: deprotonation induced colour changes and CO2 fixation. *Tetrahedron Letters*, *44*(49), 8909–8913. https://doi.org/10.1016/j.tetlet.2003.09.148

Hirano, T., Kikuchi, K., Urano, Y., Higuchi, T., & Nagano, T. (2000). Highly Zinc-Selective Fluorescent Sensor Molecules Suitable for Biological Ap-

plications. *Journal of the American Chemical Society*, *122*(49), 12399–12400. https://doi.org/10.1021/ja002467f

Jaishankar, M., Tseten, T., Anbalagan, N., Mathew, B. B., & Beeregowda, K. N. (2014). Toxicity, mechanism and health effects of some heavy metals. *Interdisciplinary Toxicology*, *7*(2), 60–72. https://doi.org/10.2478/intox-2014-0009

Jo, T. G., Lee, J. J., Nam, E., Bok, K. H., Lim, M. H., & Kim, C. (2016). A highly selective fluorescent sensor for the detection of Al 3+ and CN − in aqueous solution: biological applications and DFT calculations. *New Journal of Chemistry*, *40*(10), 8918–8927. https://doi.org/10.1039/C6NJ01544A

Khan, S., Chen, X., Almahri, A., Allehyani, E. S., Alhumaydhi, F. A., Ibrahim, M. M., & Ali, S. (2021). Recent developments in fluorescent and colorimetric chemosensors based on schiff bases for metallic cations detection: A review. *Journal of Environmental Chemical Engineering*, *9*(6), 106381. https://doi.org/10.1016/j.jece.2021.106381

Kiran, R. V., Hogan, C. F., James, B. D., & Wilson, D. J. D. (2011). Photophysical and Electrochemical Properties of Phenanthroline-Based Bis-cyclometallated Iridium Complexes in Aqueous and Organic Media. *European Journal of Inorganic Chemistry*, *2011*(31), 4816–4825. https://doi.org/10.1002/ejic.201100639

Lee, M. H., Kim, J. S., & Sessler, J. L. (2015). Small molecule-based ratiometric fluorescence probes for cations, anions, and biomolecules. *Chemical Society Reviews*, *44*(13), 4185–4191. https://doi.org/10.1039/C4CS00280F

Liu, L., Dan, F., Liu, W., Lu, X., Han, Y., Xiao, S., & Lan, H. (2017). A high-contrast colorimetric and fluorescent probe for Cu2+ based on benzimidazole-quinoline. *Sensors and Actuators B: Chemical*, *247*, 445–450. https://doi.org/10.1016/j.snb.2017.03.069

Liu, S., Wang, Y.-M., & Han, J. (2017). Fluorescent chemosensors for copper(II) ion: Structure, mechanism and application. *Journal of Photochemistry and Photobiology C: Photochemistry Reviews*, *32*, 78–103. https://doi.org/10.1016/j.jphotochemrev.2017.06.002

NAGANO, T. (2010). Development of fluorescent probes for bioimaging applications. *Proceedings of the Japan Academy, Series B*, *86*(8), 837–847. https://doi.org/10.2183/pjab.86.837

Noushija, M. K., Shanmughan, A., Mohan, B., & Shanmugaraju, S. (2022). Selective Recognition and Reversible "Turn-Off" Fluorescence Sensing of Acetate (CH3COO−) Anion at Ppb Level Using a Simple Quinizarin Fluorescent Dye. *Chemistry*, *4*(4), 1407–1416. https://doi.org/10.3390/chemistry4040092

Opydo-Szymaczek, J., Pawlaczyk-Kamieńska, T., & Borysewicz-Lewicka, M. (2022). Fluoride Intake and Salivary Fluoride Retention after Using High-Fluoride Toothpaste Followed by Post-Brushing Water Rinsing and

Conventional (1400–1450 ppm) Fluoride Toothpastes Used without Rinsing. *International Journal of Environmental Research and Public Health*, *19*(20), 13235. https://doi.org/10.3390/ijerph192013235

Pesavento, M., Marchetti, S., De Maria, L., Zeni, L., & Cennamo, N. (2019). Sensing by Molecularly Imprinted Polymer: Evaluation of the Binding Properties with Different Techniques. *Sensors*, *19*(6), 1344. https://doi.org/10.3390/s19061344

Pu, L. (2004). Fluorescence of Organic Molecules in Chiral Recognition. *Chemical Reviews*, *104*(3), 1687–1716. https://doi.org/10.1021/cr030052h

Rasheed, T., Bilal, M., Nabeel, F., Iqbal, H. M. N., Li, C., & Zhou, Y. (2018). Fluorescent sensor based models for the detection of environmentally-related toxic heavy metals. *Science of The Total Environment*, *615*, 476–485. https://doi.org/10.1016/j.scitotenv.2017.09.126

S, K., Sam, B., George, L., N, S. Y., & Varghese, A. (2021). Fluorescein Based Fluorescence Sensors for the Selective Sensing of Various Analytes. *Journal of Fluorescence*, *31*(5), 1251–1276. https://doi.org/10.1007/s10895-021-02770-9

Salto, R., Giron, M. D., Puente-Muñoz, V., Vilchez, J. D., Espinar-Barranco, L., Valverde-Pozo, J., … Paredes, J. M. (2021). New Red-Emitting Chloride-Sensitive Fluorescent Protein with Biological Uses. *ACS Sensors*, *6*(7), 2563–2573. https://doi.org/10.1021/acssensors.1c00094

Shao, J., Qiao, Y., Lin, H., & Lin, H. (2009). Rational Design of Novel Benzimidazole-Based Sensor Molecules that Display Positive and Negative Fluorescence Responses to Anions. *Journal of Fluorescence*, *19*(1), 183–188. https://doi.org/10.1007/s10895-008-0400-8

Shi, F., Cui, S., Liu, H., & Pu, S. (2020). A high selective fluorescent sensor for Cu2+ in solution and test paper strips. *Dyes and Pigments*, *173*, 107914. https://doi.org/10.1016/j.dyepig.2019.107914

Shin, Y.-H., Teresa Gutierrez-Wing, M., & Choi, J.-W. (2021). Review—Recent Progress in Portable Fluorescence Sensors. *Journal of The Electrochemical Society*, *168*(1), 017502. https://doi.org/10.1149/1945-7111/abd494

Taki, M., Wolford, J. L., & O'Halloran, T. V. (2004). Emission Ratiometric Imaging of Intracellular Zinc: Design of a Benzoxazole Fluorescent Sensor and Its Application in Two-Photon Microscopy. *Journal of the American Chemical Society*, *126*(3), 712–713. https://doi.org/10.1021/ja039073j

Toh, H. S., Batchelor-McAuley, C., Tschulik, K., & Compton, R. G. (2013). Electrochemical detection of chloride levels in sweat using silver nanoparticles: a basis for the preliminary screening for cystic fibrosis. *The Analyst*, *138*(15), 4292. https://doi.org/10.1039/c3an00843f

Valeur, B., & Leray, I. (2000). Design principles of fluorescent molecular sensors for cation recognition. *Coordination Chemistry Reviews*, *205*(1), 3–40. https://doi.org/10.1016/s0010-8545(00)00246-0

Wang, C., Dong, H., Hu, W., Liu, Y., & Zhu, D. (2012). Semiconducting π-Conjugated Systems in Field-Effect Transistors: A Material Odyssey of Organic Electronics. *Chemical Reviews*, *112*(4), 2208–2267. https://doi.org/10.1021/cr100380z

Wang, J., Yuan, F., Hu, H.-M., Xu, B., & Xue, G.-L. (2016). A luminescent coordination polymer with potential active site for the sensing of metal cation, anion and nitrobenzene explosive. *Inorganic Chemistry Communications*, *71*, 19–22. https://doi.org/10.1016/j.inoche.2016.06.030

Wu, D., Sedgwick, A. C., Gunnlaugsson, T., Akkaya, E. U., Yoon, J., & James, T. D. (2017). Fluorescent chemosensors: the past, present and future. *Chemical Society Reviews*, *46*(23), 7105–7123. https://doi.org/10.1039/C7CS00240H

Wu, Q., Liu, Z., Cao, D., Guan, R., Wang, K., Shan, Y., … Ma, L. (2015). Coumarin amide derivatives as fluorescence chemosensors for cyanide anions. *Materials Chemistry and Physics*, *161*, 43–48. https://doi.org/10.1016/j.matchemphys.2015.04.048

Yang, Y., Gao, F., Wang, Y., Li, H., Zhang, J., Sun, Z., & Jiang, Y. (2022). Fluorescent Organic Small Molecule Probes for Bioimaging and Detection Applications. *Molecules*, *27*(23), 8421. https://doi.org/10.3390/molecules27238421

Zhou, Y., Zhang, J. F., & Yoon, J. (2014). Fluorescence and Colorimetric Chemosensors for Fluoride-Ion Detection. *Chemical Reviews*, *114*(10), 5511–5571. https://doi.org/10.1021/cr400352m

Zhu, H., Li, Q., Zhu, W., & Huang, F. (2022). Pillararenes as Versatile Building Blocks for Fluorescent Materials. *Accounts of Materials Research*, *3*(6), 658–668. https://doi.org/10.1021/accountsmr.2c00063

Zou, Q., Tao, F., Wu, H., Yu, W. W., Li, T., & Cui, Y. (2019). A new carbazole-based colorimetric and fluorescent sensor with aggregation induced emission for detection of cyanide anion. *Dyes and Pigments*, *164*, 165–173. https://doi.org/10.1016/j.dyepig.2019.01.023

CHAPTER 13

ADVANCED HYDROGEN PRODUCTION FROM BIOGAS: A COMPREHENSIVE OVERVIEW

Mehmet Ali BİBERCİ[1]

1 Assistant Prof. Dr. University of Çankırı Karatekin, Engineering Faculty, Department of Mechanical Engineering, m.alibiberci@karatekin.edu.tr, ORCID ID: 0000-0002-0328-9538

1. INTRODUCTION

Hydrogen has the potential to replace fossil fuels in a variety of applications, including transportation, heating, and power generation [1, 2]. However, vast majority of hydrogen produced today is derived from fossil fuels, mostly natural gas, via steam methane reforming [3]. This process is energy-intensive and emits substantial volumes of carbon dioxide, which contributes to global warming. Thus, it is necessary to find ecologically benign and more sustainable alternatives for hydrogen production [4]. Hydrogen is an energy carrier that can be utilized as a fuel in a variety of applications, including fuel cells, internal combustion engines, and industrial operations [5]. Hydrogen provides various advantages over traditional fuels, including zero emissions, high energy density, and adaptability [6]. However, hydrogen cannot be created from fundamental energy sources, such as fossil fuels or renewable energy. (In Figure 1) [7]. Hydrogen is typically produced from fossil fuels, such as natural gas, however this approach is not sustainable and releases greenhouse gases [8]. Therefore, the production of hydrogen from renewable sources, such as biogas, has been investigated as an option that is both sustainable and environmentally beneficial [9]. Producing hydrogen from biogas, a mixture of methane and carbon dioxide produced from organic waste such as agricultural and food waste, sewage sludge, and landfill gas, is one viable way [10]. Many technologies and processes, including biogas reforming, partial oxidation, and biological approaches, can convert biogas to hydrogen [11]. This paper focuses on biogas reforming, which is the most widely studied and commercially available method for hydrogen production from biogas.

Exploration of diverse renewable energy sources, such as biogas, has been spurred by the rising global demand for clean and sustainable energy [12]. Biogas is a mixture of gases created by the anaerobic digestion of organic materials like agricultural waste, food waste, and sewage sludge [13]. Biogas mainly consists of methane (CH_4) and carbon dioxide (CO_2), but it also contains trace amounts of other gases, such as hydrogen (H_2), nitrogen (N_2), and hydrogen sulfide (H_2S) [14]. Particularly in the transportation and industrial sectors, the production of hydrogen from biogas has attracted interest as a possible method of producing sustainable and environmentally friendly energy [15]. The aim of this book chapter is to provide a comprehensive overview of the recent advancements in biogas reforming to produce hydrogen. This chapter will discuss the various technologies available for hydrogen production from biogas, the advantages and disadvantages of each technology, and the future prospects of biogas reforming for hydrogen production.

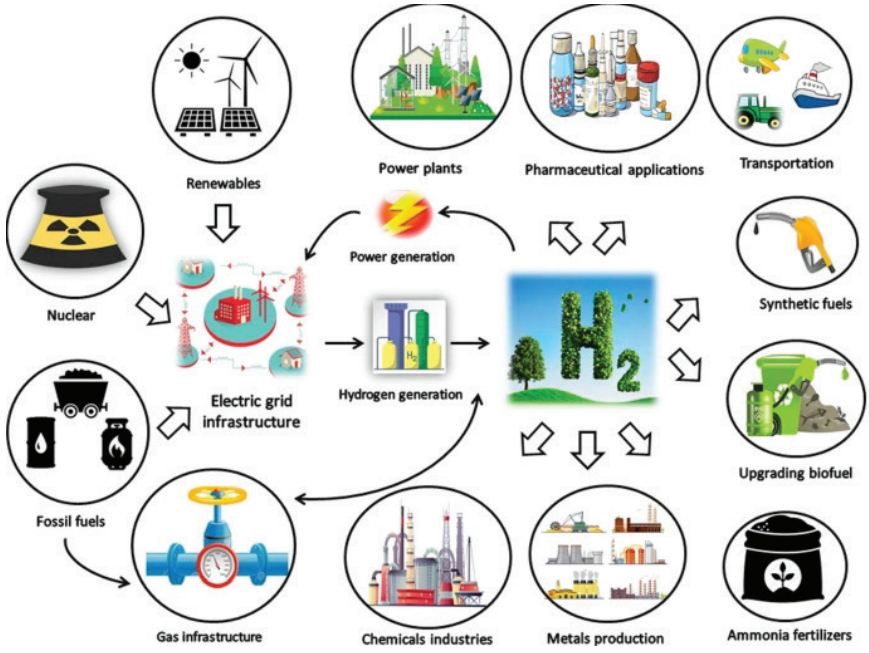

Figure 1. *Production methods and uses of hydrogen*

2. TECHNOLOGIES FOR BIOGAS REFORMING

Reforming biogas is the most studied and commercially available method for producing hydrogen from biogas [16]. Biogas reforming is a thermochemical process involving the reaction of biogas with steam or oxygen at elevated temperatures and pressures in the presence of a catalyst to create hydrogen and carbon dioxide [17]. Depending on the kind of reactants and the operating conditions, biogas reforming can be classified into three distinct types: steam reforming, partial oxidation, and autothermal reforming [18, 19]. Figure 2 shows the schematic of biogas reforming.

The most prevalent type of biogas reforming is steam reforming (SR), which includes the interaction of biogas with steam over a nickel-based catalyst at temperatures between 800 and 1000 °C and pressures between 10 and 40 bar [20]. The advantages of steam reforming over alternative biogas reforming methods are a high hydrogen production, minimal carbon dioxide emissions, and low cost [21]. However, the downsides of steam reforming include high energy consumption, catalyst deactivation, and the need for high-purity biogas [22].

Partial oxidation reforming (POR) is a type of biogas reforming that involves the reaction of biogas with oxygen or air at temperatures between 1000 and 1300°C and pressures between 10 and 30 bar over a noble met-

al-based catalyst [23]. Partial oxidation has several advantages over steam reforming, including lower energy usage, a higher rate of hydrogen production, and the possibility to use impure biogas [24]. However, partial oxidation has a number of problems, including excessive carbon dioxide emissions, catalyst deactivation, and explosion danger. [25].

Combining steam reforming and partial oxidation, autothermal reforming (ATR) is the reaction of biogas with a mixture of steam and oxygen over a dual-bed catalyst system at temperatures between 800 and 1000°C and pressures between 10 and 40 bar [26]. Autothermal reforming has several advantages over steam reforming and partial oxidation, including lower energy usage, a higher rate of hydrogen production, and the possibility to use impure biogas [27]. However, the downsides of autothermal reforming include higher carbon dioxide emissions than steam reforming and the danger of catalyst deactivation. [28].

In addition to conventional biogas reforming, there are also dry reforming and membrane reforming [29]. Dry reforming (DR) is the reaction of biogas and carbon dioxide that yields hydrogen and carbon monoxide [30], whereas membrane reforming combines reforming with hydrogen separation using a membrane reactor [31].

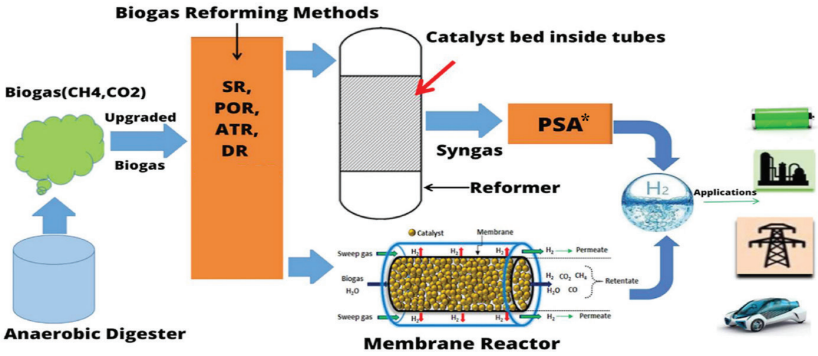

** Pressure Swing Adsorption (PSA)*

Figure 2. *The schematic of biogas reforming*

Due to its high potential and efficiency, hydrogen production from biogas reforming has emerged as a promising sustainable energy solution [32]. Typically, the production of hydrogen from biogas includes steam reforming or dry reforming. The widespread usage of steam reforming is owing to its great efficiency, low cost, and ease of operation [33]. However, recent attention has been drawn to dry reforming because to its capacity to create hydrogen with a smaller carbon footprint [34]. This study provides

an overview of the latest developments in hydrogen production from biogas reforming under the following headings.

2.1. Catalysts for Hydrogen Production

Catalysts are essential for the synthesis of hydrogen from biogas reforming [35]. Because to their high activity, low price, and resistance to carbon deposition, nickel-based catalysts are frequently utilized in the steam reforming process [36]. There are several types of catalysts, including metal-based, non-metal, and bimetallic catalysts [37].

Due to their great catalytic activity and low cost, metal-based catalysts such as nickel, cobalt, and iron have been researched extensively for biogas reforming [38]. However, carbon deposition causes deactivation of these catalysts, which can be alleviated by adding promoters or employing support materials [39]. Due to their high oxygen storage capacity and redox characteristics, non-metal catalysts like ceria-based catalysts have also showed potential for biogas reformation [40].

Bimetallic catalysts have also emerged as a promising strategy for enhancing biogas reforming catalytic performance [41]. These catalysts are more stable and selective than their monometallic counterparts [42]. In addition, bimetallic catalysts can lower the amount of precious metals needed for the reforming process [43].

Many research have studied the use of various catalysts for biogas reforming, including nickel-based catalysts supported on alumina, silica, and zeolites, among others. Wu et al. (2021) investigated the thermodynamics and experimental performance of a nickel-based catalyst supported on alumina for biogas reforming hydrogen generation. At 800°C, they discovered that the catalyst was highly active and stable, with a hydrogen yield of up to 63% [44]. Zitouni et al. (2021) studied the effect of operating conditions and catalyst type on biogas steam reforming hydrogen production and purity. The most effective catalyst was a nickel-based catalyst supported on alumina, with a hydrogen production of 77% at 800°C and a steam-to-carbon ratio of 3 [45]. Wang et al. (2017) provided a thorough summary of current developments in the development of catalysts for hydrogen production from biogas reforming. They explored the features, advantages, and disadvantages of a variety of catalysts, including nickel, cobalt, iron, and ruthenium-based catalysts. The study determined that nickel-based catalysts are the most effective catalysts for producing hydrogen from biogas reforming [46]. In a separate study, Pham et al. (2023) examined the use of nickel-based catalysts for biogas reforming to produce hydrogen [47]. The study discussed the effect of various factors, such as the catalyst composition, temperature, and pressure, on the performance

of nickel-based catalysts. The study concluded that nickel-based catalysts have great potential for hydrogen production from biogas reforming, and further research is required to optimize their performance.

In conclusion, the broad adoption of hydrogen as a sustainable energy carrier is contingent on the development of efficient and cost-effective catalysts for biogas reforming. Thus, this section provides an overview of the most recent advancements in catalyst design for biogas reforming and identifies the obstacles that must be overcome in order to achieve sustainable hydrogen generation from biogas.

2.2. Membrane Reactors for Hydrogen Production

Due to its capacity to separate hydrogen and carbon dioxide throughout the reaction, membrane reactors have emerged as a viable method for producing hydrogen from biogas reforming [48]. Combining chemical reactions and separation processes in a single unit, membrane reactors have emerged as a potential method for hydrogen synthesis from biogas [49]. This cutting-edge method permits the synthesis of hydrogen with excellent selectivity, purity, and efficiency [50]. Recent research have demonstrated that membrane reactors can improve the biogas usage efficiency for hydrogen production by overcoming the limits of conventional reforming techniques [51]. Membrane reactors provide numerous benefits, including a high hydrogen production, less carbon dioxide emissions, and cheap running costs. Much research has been conducted on the utilization of these reactors for many applications, including the production of hydrogen from biogas [52].

A number of research papers have focused on the utilization of membrane reactors for the production of hydrogen from biogas. For example, Wang et al. (2022) examined the performance of a Pd-Ag membrane reactor for the synthesis of hydrogen from biogas. The results demonstrated the reactor's high hydrogen purity and productivity, demonstrating its potential for industrial-scale hydrogen production [53]. Cai et al. (2021) assessed the performance of an oxygen-permeable mixed-conducting membrane reactor for hydrogen generation from biogas. The study demonstrated that the reactor's high hydrogen yield and low carbon dioxide emissions make it a potential technology for the production of clean energy [54]. In a separate research, Minutillo (2020) examined the evolution of membrane reactors for hydrogen production via biogas reforming in depth [55]. The study discussed the advantages and disadvantages of various types of membrane reactors, including palladium membranes, ceramic membranes, and polymer membranes. The study concluded that membrane reactors have the potential to enhance the performance of hydrogen production from biogas reforming, but further research is required to optimize the reactor design and performance.

The findings of these studies indicate that membrane reactors can play a vital role in hydrogen production from biogas, and there is a need for further research to optimize their performance. So, this book chapter will contribute to the development of efficient and sustainable hydrogen production technologies, which can have significant implications for the energy industry and the environment.

2.3. Integration of Renewable Energy with Biogas Reforming

The combination of renewable energy with biogas reforming has garnered attention due to its potential to improve the sustainability and efficiency of hydrogen generation. In the subject of energy systems, renewable energy integration has become a main point of study and development [56]. The integration of biogas reforming with renewable energy sources such as solar and wind power has received considerable interest because to the growing need for sustainable and environmentally friendly energy options [57]. Reforming biogas is the conversion of biogas into hydrogen-rich syngas, which can be utilized as a fuel in a variety of applications [58]. The combination of renewable energy and biogas reforming is a potential strategy for attaining sustainable energy production and lowering greenhouse gas emissions [59]. Intermittent nature of renewable energy sources makes their integration with biogas reformation difficult [60]. However, recent advances in energy storage technology and control systems have made it possible to combine biogas reforming with renewable energy sources [61].

Several research have examined the practicability and economic viability of integrating renewable energy with biogas reforming. Q. Zhao et al. (2021) examined the integration of solar photovoltaic (PV) systems with biogas reforming for hydrogen production. The study discovered that integrating solar PV systems with biogas reforming could result in substantial reductions in greenhouse gas emissions and lower energy prices [62]. J. Kim et al. (2022) investigated the feasibility of combining wind energy and biogas reforming for hydrogen generation. The study indicated that the combination of wind energy and biogas reforming could result in substantial reductions in carbon dioxide emissions and cheaper energy prices [63]. Cho et al. (2023) offered an in-depth analysis of the incorporation of renewable energy with biogas reforming for hydrogen production. The study examined the benefits and drawbacks of various renewable energy sources, such as solar and wind power, and their integration with biogas reforming. The study found that the integration of renewable energy with biogas reforming has the potential to significantly improve the sustainability and efficiency of hydrogen generation [64].

In addition, the integration of renewable energy and biogas reforming has the potential to enhance energy security by decreasing reliance on fossil fuels. Biogas reforming can employ waste biomass, such as agricultural wastes, to produce sustainable hydrogen, hence lowering reliance on natural gas as a hydrogen production source. Integration of renewable energy sources with biogas reforming may also result in the creation of new jobs in the renewable energy sector, so contributing to economic growth [65].

The combination of renewable energy with biogas reforming is a viable strategy for attaining sustainable energy production and minimizing greenhouse gas emissions, as stated in the conclusion. Current improvements in energy storage technology and control systems have made it possible to combine biogas reformation with renewable energy sources. Several studies have explored the feasibility and economic sustainability of integrating renewable energy with biogas reforming, and the results indicate substantial potential for reducing carbon emissions and lowering energy prices.

2.4. Techno-Economic Feasibility Analysis of Biogas Steam Reforming for Hydrogen Production

The techno-economic viability of biogas steam reforming for hydrogen production must be evaluated in order to determine its potential as a sustainable alternative to existing hydrogen production techniques [66]. Several studies have investigated the creation of hydrogen using biogas steam reformation. Bukhari et al. (2023) have evaluated, for instance, the techno-economic viability of the biogas steam reforming process for hydrogen production The study evaluated the economic viability of the process by analyzing its capital and operational costs. More research is required to optimize the design and operation of the biogas steam reforming process for the production of hydrogen [67].

Ongis et al. (2023) carried out a techno-economic evaluation of biogas steam reforming utilizing a membrane reactor for hydrogen production. The study discovered that biogas steam reforming is economically viable and may minimize carbon emissions compared to current hydrogen generation methods [68].

Di Marcoberardino et al. (2019) examined the influence of feedstock quality and process variables on the efficiency of biogas steam reforming for hydrogen production. The study indicated that the quality of the feedstock and the operating parameters of the process had a substantial impact on the process's effectiveness and profitability. Authors suggested using high-quality feedstock and optimum process conditions to attain maximum efficiency and economic viability [69].

Using life cycle assessment and cost-benefit analysis, Cvetkovi et al. (2021) analyzed the environmental and economic sustainability of biogas steam reforming for hydrogen production. The research discovered that biogas steam reforming has the potential to minimize carbon emissions and attain economic viability if renewable energy sources are utilised to produce steam [70].

Many studies have evaluated the techno-economic viability of biogas steam reforming for hydrogen production, as concluded by the research. Using high-quality feedstock and optimizing process conditions can considerably increase the process's productivity and profitability. In addition, the use of renewable energy sources for steam production can make biogas steam reforming a sustainable and economically viable alternative to conventional hydrogen production techniques.

2.5. Thermochemical Conversion of Biogas for Hydrogen Production

The increasing demand for energy and the limited supply of nonrenewable energy sources have prompted the development of alternate energy sources such as biogas [71]. During anaerobic digestion, biogas is produced from the breakdown of organic materials such as food waste, animal manure, and sewage sludge. It consists of methane, carbon dioxide, and trace quantities of other gases [72]. Biogas has the potential to reduce greenhouse gas emissions, lessen reliance on fossil fuels, and provide a source of renewable energy. Due to its poor energy density and contaminants, however, biogas cannot be utilized directly as a fuel [73]. Several thermochemical conversion technologies have been developed to convert biogas into hydrogen, which has a higher energy density and may be utilized as a clean fuel in a variety of applications, including fuel cell cars and power generation, in order to overcome these restrictions. Using heat and chemical reactions, thermochemical conversion systems convert biogas to hydrogen [74].

A number of research have examined the thermochemical conversion of biogas for hydrogen generation. For example, Lin et al. (2016) found that thermochemical conversion technologies, such as steam reforming, partial oxidation, and autothermal reformation, have been developed to convert biogas to hydrogen. Because to its great efficiency and low cost, steam reforming is the process most commonly employed for hydrogen synthesis. Biogas is combined with steam and passed over a catalyst in steam reforming to produce hydrogen and carbon dioxide [75]. Zhang et al. (2015) found that in partial oxidation, biogas reacts with oxygen in the presence of a catalyst to create hydrogen and carbon monoxide. The created gas is then treated to a water-gas shift process in order to convert carbon

monoxide to carbon dioxide and generate additional hydrogen [76].

Mu et al. (2019) describe autothermal reforming as a combination of steam reforming and partial oxidation in which biogas is combined with steam and oxygen and passed over a catalyst to generate hydrogen, carbon dioxide, and water. This approach has the benefit of producing a syngas that can be further refined into different chemicals and fuels [77].

According to Borowiecki et al. (2017), the effectiveness of various technologies differs based on operating parameters such as temperature, pressure, and gas composition. With a hydrogen yield of up to 80%, steam reforming has the highest efficiency of the three processes [78]. However, according to Batzias and Sidiras (2016), the environmental impact of biogas-based hydrogen production must also be considered. Although hydrogen produced from biogas emits fewer greenhouse gases than hydrogen produced from fossil fuels, the production process may still have an environmental impact due to the usage of energy and chemicals [79].

2.6. Advantages and Disadvantages Hydrogen Production from Biogas

Using biogas for hydrogen production has a number of advantages over conventional fossil fuels [80]. Biogas is a renewable energy source that can be generated from animal waste, agricultural waste, and municipal solid waste [81]. Methane, which is a potent greenhouse gas, is captured and utilized during biogas production, thereby reducing greenhouse gas emissions. Moreover, the production of hydrogen from biogas can result in the growth of a sustainable hydrogen economy [82]. However, the creation of hydrogen from biogas has several downsides. Biogas production can be more expensive than conventional fossil fuels [83]. Also, the quality of the biogas feedstock can influence the efficiency of the hydrogen production process. The use of biogas for hydrogen production can potentially compete with other biogas applications, such as electricity generation and direct fuel use [84]. In addition, the creation of hydrogen from biogas necessitates a substantial quantity of energy, which may be derived from nonrenewable sources.

2.7. Future Prospects for Hydrogen Production from Biogas

Significant potential exists for the establishment of a sustainable hydrogen economy through the use of biogas for hydrogen production. Future possibilities for biogas reforming for hydrogen production are contingent on the development of cutting-edge technologies that can enhance the process's efficacy and decrease its expense [8]. Integration of biogas reforming with other renewable energy sources, such as solar or wind power,

can also increase the process's sustainability [85]. Ongoing research aims to improve the biogas reforming efficiency for hydrogen production. For instance, the development of novel catalysts that can improve the efficiency of steam reforming and partial oxidation has been the focus of much research. In addition, renewable energy sources such as solar or wind power can be combined with biogas reforming to lower the process's carbon footprint [86]. The development of membrane reactors can also increase the efficiency of biogas reforming by decreasing the amount of energy needed for downstream purification [87].

To overcome the obstacles and further develop biogas reforming as a sustainable technology for hydrogen production, it is necessary to investigate a number of research fields. They include the creation of more effective and long-lasting catalysts for reforming and gas purification, as well as the optimization of operating parameters for various biogas compositions and quality [88]. Moreover, the integration of biogas reforming with other waste treatment processes, such as anaerobic digestion and wastewater treatment, should be investigated in order to increase overall efficiency and lower costs [89]. Finally, the use of hydrogen as a fuel should be encouraged through the development of hydrogen fuel cell technologies and infrastructure, as well as regulatory incentives and laws that support the use of clean energy sources [90].

2.8. Environmental Impact and Sustainability of Hydrogen Production from Biogas

The environmental impact and sustainability of hydrogen generation from biogas rely on a number of variables, including the feedstock utilized, the technique of hydrogen production, and the downstream application of hydrogen [91]. The use of biogas as a fuel for hydrogen generation has a number of environmental benefits, including the reduction of greenhouse gas emissions and the provision of a renewable resource. Yet, the generation of hydrogen still necessitates the expenditure of energy, and the utilization of hydrogen downstream might also have environmental consequences [92].

Many studies have evaluated the environmental impact and sustainability of hydrogen production from biogas, including Khan (2020), who compared the life cycle evaluation of hydrogen production from biogas to traditional hydrogen production methods. It was discovered that the production of hydrogen from biogas resulted in lower greenhouse gas emissions and energy usage compared to traditional approaches. However, the study also revealed potential environmental consequences related to the usage of catalysts and membrane materials in the manufacturing process [93].

2.9. Hydrogen Purification

During the biogas reforming procedure, the final gas combination consists of hydrogen, carbon dioxide, and other gases such as methane and nitrogen. Hydrogen must be refined to remove contaminants such as carbon dioxide in order to meet the purity requirements for specific applications, such as fuel cells [94]. The most prevalent method for purifying hydrogen is pressure swing adsorption (PSA), which separates gases based on their varied adsorption capabilities on an adsorbent material, such as activated carbon or zeolites. PSA provides various advantages over other systems, including low energy usage, great efficiency, and ease of use [95].

Many studies have investigated the use of PSA for hydrogen purification from biogas, including that of Gapp and Pfeifer (2023), who evaluated hydrogen production from biogas reforming in a membrane reactor and the following hydrogen purification using PSA. Hydrogen that has been purified can be utilized in numerous applications, including fuel cells, combustion engines, and industrial operations. Hydrogen produced from biogas is an appealing use for fuel cells due to their high efficiency and minimal emissions [96]. Numerous research have examined the use of fuel cells for the conversion of hydrogen produced from biogas, including Thiruselvi et al. (2023), who evaluated the use of a solid oxide fuel cell for the co-generation of electricity and heat utilizing hydrogen produced through biogas reforming [97].

2.10. Hydrogen Applications

Hydrogen produced from biogas can be utilized for a variety of purposes, including fuel cells, internal combustion engines, and industrial processes [98]. Fuel cells are devices that convert hydrogen and oxygen into energy and heat while generating no harmful byproducts or greenhouse gases [99]. Fuel cells have a number of advantages over conventional energy generation systems, including high efficiency, minimal noise, and low maintenance [100]. Combustion engines can also operate on hydrogen, but they generate pollutants such nitrogen oxides (NOx) and require engine modifications [101]. Hydrogen can be used as a feedstock in industrial operations such as ammonia manufacturing [102].

3. CONCLUSION

In conclusion, hydrogen production from biogas reforming is a promising technology for renewable energy production. This research provided a comprehensive overview of the latest advances in hydrogen production from biogas reforming. The study discussed the catalysts, membrane reactors, integration of renewable energy, techno-economic feasibility, and

thermochemical conversion of biogas for hydrogen production. The study shows that nickel-based catalysts are the most effective catalysts for hydrogen production from biogas reforming. The integration of renewable energy with biogas reforming has great potential to enhance the sustainability and efficiency of hydrogen production. Membrane reactors have the potential to enhance the performance of hydrogen production, but further research is required to optimize their performance. The techno-economic feasibility analysis shows that biogas steam reforming process for hydrogen production is economically feasible. The thermochemical conversion of biogas for hydrogen production is a promising technology, but further research is required to optimize the process and improve its efficiency. Overall, the research highlights the potential of hydrogen production from biogas reforming and the need for further research to optimize the process and improve its efficiency.

REFERENCES

[1] Olabi, A. G., Abdelghafar, A. A., Baroutaji, A., Sayed, E. T., Alami, A. H., Rezk, H., & Abdelkareem, M. A. (2021). Large-vscale hydrogen production and storage technologies: Current status and future directions. International Journal of Hydrogen Energy, 46(45), 23498-23528.

[2] Qyyum, M. A., Dickson, R., Shah, S. F. A., Niaz, H., Khan, A., Liu, J. J., & Lee, M. (2021). Availability, versatility, and viability of feedstocks for hydrogen production: Product space perspective. Renewable and Sustainable Energy Reviews, 145, 110843.

[3] Megía, P. J., Vizcaíno, A. J., Calles, J. A., & Carrero, A. (2021). Hydrogen production technologies: from fossil fuels toward renewable sources. A mini review. Energy & Fuels, 35(20), 16403-16415.

[4] Gür, T. M. (2022). Carbon dioxide emissions, capture, storage and utilization: Review of materials, processes and technologies. Progress in Energy and Combustion Science, 89, 100965.

[5] Fragiacomo, P., Piraino, F., Genovese, M., Corigliano, O., & De Lorenzo, G. (2022). Strategic Overview on Fuel Cell-Based Systems for Mobility and Electrolytic Cells for Hydrogen Production. Procedia Computer Science, 200, 1254-1263.

[6] McKinlay, C. J., Turnock, S. R., & Hudson, D. A. (2021). Route to zero emission shipping: Hydrogen, ammonia or methanol?. International Journal of Hydrogen Energy, 46(55), 28282-28297.

[7] Sharma, S., Agarwal, S., & Jain, A. (2021). Significance of hydrogen as economic and environmentally friendly fuel. Energies, 14(21), 7389.

[8] Qureshi, F., Yusuf, M., Kamyab, H., Vo, D. V. N., Chelliapan, S., Joo, S. W., & Vasseghian, Y. (2022). Latest eco-friendly avenues on hydrogen production towards a circular bioeconomy: Currents challenges, innovative insights, and future perspectives. Renewable and Sustainable Energy Reviews, 168, 112916.

[9] Amin, M., Shah, H. H., Fareed, A. G., Khan, W. U., Chung, E., Zia, A., ... & Lee, C. (2022). Hydrogen production through renewable and non-renewable energy processes and their impact on climate change. International Journal of Hydrogen Energy.

[10] Bertasini, D., Battista, F., Rizzioli, F., Frison, N., & Bolzonella, D. (2023). Decarbonization of the European natural gas grid using hydrogen and methane biologically produced from organic waste: A critical overview. Renewable Energy.

[11] Kumar, R., Kumar, A., & Pal, A. (2022). Overview of hydrogen production from biogas reforming: Technological advancement. International Journal of Hydrogen Energy.

[12] Amoatey, P., Al-Hinai, A., Al-Mamun, A., & Baawain, M. S. (2022). A review

of recent renewable energy status and potentials in Oman. Sustainable Energy Technologies and Assessments, 51, 101919.

[13] Sillero, L., Solera, R., & Perez, M. (2022). Biochemical assays of potential methane to test biogas production from dark fermentation of sewage sludge and agricultural residues. International Journal of Hydrogen Energy.

[14] Andriani, D., Rajani, A., Santosa, A., Saepudin, A., Wresta, A., & Atmaja, T. D. (2020, March). A review on biogas purification through hydrogen sulphide removal. In IOP Conference Series: Earth and Environmental Science (Vol. 483, No. 1, p. 012034). IOP Publishing.

[15] Lagioia, G., Spinelli, M. P., & Amicarelli, V. (2022). Blue and green hydrogen energy to meet European Union decarbonisation objectives. An overview of perspectives and the current state of affairs. International Journal of Hydrogen Energy.

[16] Cho, H. H., Strezov, V., & Evans, T. J. (2023). A review on global warming potential, challenges and opportunities of renewable hydrogen production technologies. Sustainable Materials and Technologies, e00567.

[17] Su, B., Lin, F., Ma, J., Huang, S., Wang, Y., Zhang, X., ... & Wang, H. (2022). System integration of multi-grade exploitation of biogas chemical energy driven by solar energy. Energy, 241, 122857.

[18] Minutillo, M., Perna, A., & Sorce, A. (2020). Green hydrogen production plants via biogas steam and autothermal reforming processes: energy and exergy analyses. Applied Energy, 277, 115452.

[19] Cabello, A., Mendiara, T., Abad, A., Izquierdo, M. T., & García-Labiano, F. (2022). Production of hydrogen by chemical looping reforming of methane and biogas using a reactive and durable Cu-based oxygen carrier. Fuel, 322, 124250.

[20] García, R., Gil, M. V., Rubiera, F., Chen, D., & Pevida, C. (2021). Renewable hydrogen production from biogas by sorption enhanced steam reforming (SESR): A parametric study. Energy, 218, 119491.

[21] Yu, M., Wang, K., & Vredenburg, H. (2021). Insights into low-carbon hydrogen production methods: Green, blue and aqua hydrogen. International Journal of Hydrogen Energy, 46(41), 21261-21273.

[22] Nalbant, Y., & Colpan, C. O. (2020). *An overview of hydrogen production from biogas*. Accelerating the Transition to a 100% Renewable Energy Era, 355-373.

[23] Wang, B., Liu, S., Peng, Y., Wang, C., & Zou, J. (2021). Heptane dry reforming and coupling with partial oxidation in gliding arc discharge plasma for H2 production. Fuel Processing Technology, 221, 106943.

[24] Lin, K. W., & Wu, H. W. (2020). Hydrogen-rich syngas production and carbon dioxide formation using aqueous urea solution in biogas steam reforming by thermodynamic analysis. International Journal of Hydrogen Energy,

45(20), 11593-11604.

[25] Wu, C. Y., Wang, B. W., Wu, T. H., & Chang, S. P. (2023). Using Kriging surrogate model to analyze hydrogen generation with dimethyl ether in partial oxidation catalytic fluidized bed reactor. International Journal of Hydrogen Energy.

[26] Chen, W. H., Su, Y. Q., Lin, B. J., Kuo, J. K., & Kuo, P. C. (2021). Hydrogen production from partial oxidation and autothermal reforming of methanol from a cold start in sprays. Fuel, 287, 119638.

[27] Rosha, P., & Ibrahim, H. (2022). Comparative analysis of ethanol-steam and-autothermal reforming for hydrogen production using Aspen Plus. The Canadian Journal of Chemical Engineering.

[28] Farsi, M. (2023). Reforming process design and modeling: Steam, dry, and autothermal reforming. In Advances in Synthesis Gas: Methods, Technologies and Applications (pp. 123-140). Elsevier.

[29] Alipour, Z., Borugadda, V. B., Wang, H., & Dalai, A. K. (2022). Syngas production through dry reforming: A review on catalysts and their materials, preparation methods and reactor type. Chemical Engineering Journal, 139416.

[30] Oliveira, L. G., Machado, B., de Souza, L. P., Corrêa, G. C. G., Polinarski, M. A., Trevisan, S. V. C., ... & Alves, H. J. (2022). Dry reforming of biogas in a pilot unit: Scale-up of catalyst synthesis and green hydrogen production. International Journal of Hydrogen Energy, 47(84), 35608-35625.

[31] Parente, M., Soria, M. A., & Madeira, L. M. (2020). Hydrogen and/or syngas production through combined dry and steam reforming of biogas in a membrane reactor: A thermodynamic study. Renewable Energy, 157, 1254-1264.

[32] Amin, M., Shah, H. H., Fareed, A. G., Khan, W. U., Chung, E., Zia, A., ... & Lee, C. (2022). Hydrogen production through renewable and non-renewable energy processes and their impact on climate change. International Journal of Hydrogen Energy.

[33] Zhao, Z., Situmorang, Y. A., An, P., Chaihad, N., Wang, J., Hao, X., ... & Guan, G. (2020). Hydrogen Production from Catalytic Steam Reforming of Bio-Oils: A Critical Review. Chemical Engineering & Technology, 43(4), 625-640.

[34] De Medeiros, F. G. M., Lopes, F. W. B., & Rego de Vasconcelos, B. (2022). Prospects and Technical Challenges in Hydrogen Production through Dry Reforming of Methane. Catalysts, 12(4), 363.

[35] Park, M. J., Kim, H. M., Lee, Y. H., Jeon, K. W., & Jeong, D. W. (2022). Optimization of a renewable hydrogen production system from food waste: A combination of anaerobic digestion and biogas reforming. Waste Management, 144, 272-284.

[36] Zeng, Y., Chen, G., Wang, J., Zhou, R., Sun, Y., Weidenkaff, A., ... & Tu, X. (2022). Plasma-catalytic biogas reforming for hydrogen production over K-promoted Ni/Al2O3 catalysts: Effect of K-loading. Journal of the Energy Institute, 104, 12-21.

[37] Dong, R., Yang, Z., Fu, Y., Chen, Z., Hu, Y., Zhou, Y., & Qin, H. (2022). Aminated lignin chelated metal derived bifunctional electrocatalyst with high catalytic performance. Applied Surface Science, 580, 152205.

[38] Guharoy, U., Reina, T. R., Liu, J., Sun, Q., Gu, S., & Cai, Q. (2021). A theoretical overview on the prevention of coking in dry reforming of methane using non-precious transition metal catalysts. Journal of CO2 utilization, 53, 101728.

[39] Aziz, M. A. A., Setiabudi, H. D., Teh, L. P., Annuar, N. H. R., & Jalil, A. A. (2019). A review of heterogeneous catalysts for syngas production via dry reforming. Journal of the Taiwan Institute of Chemical Engineers, 101, 139-158.

[40] Fleming, C. L., Wong, J., Golzan, M., Gunawan, C., & McGrath, K. C. (2023). Insights from a Bibliometrics-Based Analysis of Publishing and Research Trends on Cerium Oxide from 1990 to 2020. International Journal of Molecular Sciences, 24(3), 2048.

[41] Ekeoma, B. C., Yusuf, M., Johari, K., & Abdullah, B. (2022). Mesoporous silica supported Ni-based catalysts for methane dry reforming: A review of recent studies. International Journal of Hydrogen Energy.

[42] Liu, Y., Yu, S., Wu, X., Cao, X., Geng, H., Zhang, C., & Liu, S. (2023). Improving the hydrothermal stability and hydrogen selectivity of Ni-Cu based catalysts for the aqueous-phase reforming of methanol. International Journal of Hydrogen Energy.

[43] Alipour, Z., Borugadda, V. B., Wang, H., & Dalai, A. K. (2022). Syngas production through dry reforming: A review on catalysts and their materials, preparation methods and reactor type. Chemical Engineering Journal, 139416.

[44] Wu, L., Xie, X., Ren, H., & Gao, X. (2021). A short review on nickel-based catalysts in dry reforming of methane: Influences of oxygen defects on anti-coking property. Materials Today: Proceedings, 42, 153-160.

[45] Zitouni, A., Bachir, R., Bendedouche, W., & Bedrane, S. (2021). Production of bio-jet fuel range hydrocarbons from catalytic HDO of biobased difurfurilydene acetone over Ni/SiO2-ZrO2 catalysts. Fuel, 297, 120783.

[46] Wang, S., Shan, R., Gu, J., Huhe, T., Ling, X., Yuan, H., & Chen, Y. (2022). High-yield H2 production from polypropylene through pyrolysis-catalytic reforming over activated carbon based nickel catalyst. Journal of Cleaner Production, 352, 131566.

[47] Pham, C. Q., Nguyen, V. P., Van, T. T., Phuong, P. T., Pham, P. T., Trinh, T. H., & Nguyen, T. M. (2023). Syngas Production from Biogas Reforming: Role

of the Support in Nickel-based Catalyst Performance. Topics in Catalysis, 66(1-4), 262-274.

[48] Yang, X., Wang, S., & He, Y. (2022). Review of catalytic reforming for hydrogen production in a membrane-assisted fluidized bed reactor. Renewable and Sustainable Energy Reviews, 154, 111832.

[49] Sazali, N. (2020). Emerging technologies by hydrogen: A review. International Journal of Hydrogen Energy, 45(38), 18753-18771.

[50] Li, H., Tian, H., Chen, S., Sun, Z., Liu, T., Liu, R., ... & Gong, J. (2020). Sorption enhanced steam reforming of methanol for high-purity hydrogen production over Cu-MgO/Al2O3 bifunctional catalysts. Applied Catalysis B: Environmental, 276, 119052.

[51] Yaashikaa, P. R., Devi, M. K., & Kumar, P. S. (2022). Biohydrogen production: An outlook on methods, constraints, economic analysis and future prospect. International Journal of Hydrogen Energy, 47(98), 41488-41506.

[52] Kannah, R. Y., Kavitha, S., Karthikeyan, O. P., Kumar, G., Dai-Viet, N. V., & Banu, J. R. (2021). Techno-economic assessment of various hydrogen production methods–A review. Bioresource technology, 319, 124175.

[53] Wang, H., Yang, R., Wang, B., Wei, Z., Kong, H., Lu, X., & Jin, J. (2022). Thermodynamic performance of solar-driven methanol steam reforming system for carbon capture and high-purity hydrogen production. Applied Thermal Engineering, 209, 118280.

[54] Cai, L., Cao, Z., Zhu, X., & Yang, W. (2021). Effects of catalysts on water decomposition and hydrogen oxidation reactions in oxygen transport membrane reactors. Journal of Membrane Science, 634, 119394.

[55] Minutillo, M., Perna, A., & Sorce, A. (2020). Green hydrogen production plants via biogas steam and autothermal reforming processes: energy and exergy analyses. Applied Energy, 277, 115452.

[56] Amin, M., Shah, H. H., Fareed, A. G., Khan, W. U., Chung, E., Zia, A., ... & Lee, C. (2022). Hydrogen production through renewable and non-renewable energy processes and their impact on climate change. International Journal of Hydrogen Energy.

[57] Lykas, P., Georgousis, N., Bellos, E., & Tzivanidis, C. (2022). A comprehensive review of solar-driven multigeneration systems with hydrogen production. International Journal of Hydrogen Energy.

[58] Rahmat, N., Yaakob, Z., & Hassan, N. S. M. (2021). Hydrogen rich syngas from CO2 reforming of methane with steam catalysed by facile fusion-impregnation of iron and cobalt loaded MgAl2O4 catalyst with minimal carbon deposits. Journal of the Energy Institute, 96, 61-74.

[59] Hren, R., Vujanović, A., Van Fan, Y., Klemeš, J. J., Krajnc, D., & Čuček, L. (2023). Hydrogen production, storage and transport for renewable energy and chemicals: An environmental footprint assessment. Renewable and

Sustainable Energy Reviews, 173, 113113.

[60] Yıldız, S., Gunduz, H., Yildirim, B., & Özdemir, M. T. (2022). An islanded microgrid energy system with an innovative frequency controller integrating hydrogen-fuel cell. Fuel, 326, 125005.

[61] Villadsen, S. N., Fosbøl, P. L., Angelidaki, I., Woodley, J. M., Nielsen, L. P., & Møller, P. (2019). The potential of biogas; the solution to energy storage. ChemSusChem, 12(10), 2147-2153.

[62] Zhao, Q., Su, B., Wang, H., He, A., He, R., Kong, H., & Hu, X. (2021). Mid/low-temperature solar hydrogen generation via dry reforming of methane enhanced in a membrane reactor. Energy Conversion and Management, 240, 114254.

[63] Kim, J., Qi, M., Kim, M., Lee, J., Lee, I., & Moon, I. (2022). Biogas reforming integrated with PEM electrolysis via oxygen storage process for green hydrogen production: From design to robust optimization. Energy Conversion and Management, 251, 115021.

[64] Cho, H. H., Strezov, V., & Evans, T. J. (2023). A review on global warming potential, challenges and opportunities of renewable hydrogen production technologies. Sustainable Materials and Technologies, e00567.

[65] Obaideen, K., Abdelkareem, M. A., Wilberforce, T., Elsaid, K., Sayed, E. T., Maghrabie, H. M., & Olabi, A. G. (2022). Biogas role in achievement of the sustainable development goals: Evaluation, Challenges, and Guidelines. Journal of the Taiwan Institute of Chemical Engineers, 131, 104207.

[66] Wee, A. N. C. H., Erison, A. E., Anyek, E. H. E., Pakpahan, G. R., Lim, J. R., & Tiong, A. N. T. (2022). Techno-economic assessment of hydrogen production via steam reforming of palm oil mill effluent. Sustainable Energy Technologies and Assessments, 53, 102575.

[67] Bukhari, M. H., Javed, A., Kazmi, S. A. A., Ali, M., & Chaudhary, M. T. (2023). Techno-economic feasibility analysis of hydrogen production by PtG concept and feeding it into a combined cycle power plant leading to sector coupling in future. Energy Conversion and Management, 282, 116814.

[68] Ongis, M., Di Marcoberardino, G., Manzolini, G., Gallucci, F., & Binotti, M. (2023). Membrane reactors for green hydrogen production from biogas and biomethane: A techno-economic assessment. International Journal of Hydrogen Energy.

[69] Di Marcoberardino, G., Liao, X., Dauriat, A., Binotti, M., & Manzolini, G. (2019). Life cycle assessment and economic analysis of an innovative biogas membrane reformer for hydrogen production. Processes, 7(2), 86.

[70] Cvetković, S. M., Radoičić, T. K., Kijevčanin, M., & Novaković, J. G. (2021). Life Cycle Energy Assessment of biohydrogen production via biogas steam reforming: case study of biogas plant on a farm in Serbia. International Journal of Hydrogen Energy, 46(27), 14130-14137.

[71] Solaymani, S. (2021). A review on energy and renewable energy policies in Iran. Sustainability, 13(13), 7328.

[72] Song, Y. J., Oh, K. S., Lee, B., Pak, D. W., Cha, J. H., & Park, J. G. (2021). Characteristics of biogas production from organic wastes mixed at optimal ratios in an anaerobic co-digestion reactor. Energies, 14(20), 6812.

[73] Jahangir, M. H., Montazeri, M., Mousavi, S. A., & Kargarzadeh, A. (2022). Reducing carbon emissions of industrial large livestock farms using hybrid renewable energy systems. Renewable Energy, 189, 52-65.

[74] Al Rayaan, M. B. (2021). Recent advancements of thermochemical conversion of plastic waste to biofuel-A review. Cleaner Engineering and Technology, 2, 100062.

[75] Lin, J., Zhou, Z., Liu, C., & Huang, Y. (2016). Biogas steam reforming for hydrogen production: A review. International Journal of Hydrogen Energy, 41(41), 18392-18407.

[76] Zhang, X., Li, J., Li, X., Zhang, S., Liu, Y., & Li, W. (2015). Experimental study of hydrogen production from biogas partial oxidation. International Journal of Hydrogen Energy, 43(1), 622-629.

[77] Mu, D., Yang, S., & Zhang, X. (2019). Hydrogen production from biogas by autothermal reforming: A review. International Journal of Hydrogen Energy, 44(30), 15589-15602.

[78] Borowiecki, P., Nastaj, J., & Dębowski, M. (2017). Hydrogen production from biogas via steam reforming: An overview. Renewable and Sustainable Energy Reviews, 70, 665-677.

[79] Batzias, F. A., & Sidiras, D. K. (2016). Environmental impact of hydrogen production from biogas via steam reforming: Life cycle assessment. Journal of Cleaner Production, 112, 1799-1811.

[80] Salahshoor, S., & Afzal, S. (2022). Subsurface technologies for hydrogen production from fossil fuel resources: A review and techno-economic analysis. International Journal of Hydrogen Energy.

[81] Nwokolo, N., Mukumba, P., Obileke, K., & Enebe, M. (2020). Waste to energy: A focus on the impact of substrate type in biogas production. Processes, 8(10), 1224.

[82] Kolb, S., Plankenbühler, T., Hofmann, K., Bergerson, J., & Karl, J. (2021). Life cycle greenhouse gas emissions of renewable gas technologies: A comparative review. Renewable and Sustainable Energy Reviews, 146, 111147.

[83] Atelge, M. R., Krisa, D., Kumar, G., Eskicioglu, C., Nguyen, D. D., Chang, S. W., ... & Unalan, S. (2020). Biogas production from organic waste: recent progress and perspectives. Waste and Biomass Valorization, 11, 1019-1040.

[84] Bock, S., Stoppacher, B., Malli, K., Lammer, M., & Hacker, V. (2021). Techno-economic analysis of fixed-bed chemical looping for decentralized, fuel-cell-grade hydrogen production coupled with a 3 MWth biogas digester.

Energy Conversion and Management, 250, 114801.

[85] Sarker, A. K., Azad, A. K., Rasul, M. G., & Doppalapudi, A. T. (2023). Prospect of Green Hydrogen Generation from Hybrid Renewable Energy Sources: A Review. Energies, 16(3), 1556.

[86] Nandhini, R., Sivaprakash, B., Rajamohan, N., & Vo, D. V. N. (2022). Carbon-free hydrogen and bioenergy production through integrated carbon capture and storage technology for achieving sustainable and circular economy–A review. Fuel, 126984.

[87] Capa, A., Yan, Y., Rubiera, F., Pevida, C., Gil, M. V., & Clough, P. T. (2023). Process Simulations of High-Purity and Renewable Clean H2 Production by Sorption Enhanced Steam Reforming of Biogas. ACS Sustainable Chemistry & Engineering.

[88] Fan, L., Li, C. E., Aravind, P. V., Cai, W., Han, M., & Brandon, N. (2022). Methane reforming in solid oxide fuel cells: Challenges and strategies. Journal of Power Sources, 538, 231573.

[89] Khawer, M. U. B., Naqvi, S. R., Ali, I., Arshad, M., Juchelková, D., Anjum, M. W., & Naqvi, M. (2022). Anaerobic digestion of sewage sludge for biogas & biohydrogen production: State-of-the-art trends and prospects. Fuel, 329, 125416.

[90] Wang, Y., Pang, Y., Xu, H., Martinez, A., & Chen, K. S. (2022). PEM Fuel cell and electrolysis cell technologies and hydrogen infrastructure development: a review. Energy & Environmental Science.

[91] Vuppaladadiyam, A. K., Vuppaladadiyam, S. S. V., Awasthi, A., Sahoo, A., Rehman, S., Pant, K. K., ... & Leu, S. Y. (2022). Biomass pyrolysis: A review on recent advancements and green hydrogen production. Bioresource Technology, 128087.

[92] Ishaq, H., Dincer, I., & Crawford, C. (2022). A review on hydrogen production and utilization: Challenges and opportunities. International Journal of Hydrogen Energy, 47(62), 26238-26264.

[93] Khan, I. (2020). Waste to biogas through anaerobic digestion: hydrogen production potential in the developing world-a case of Bangladesh. International Journal of Hydrogen Energy, 45(32), 15951-15962.

[94] Du, Z., Liu, C., Zhai, J., Guo, X., Xiong, Y., Su, W., & He, G. (2021). A review of hydrogen purification technologies for fuel cell vehicles. Catalysts, 11(3), 393.

[95] Luberti, M., & Ahn, H. (2022). Review of Polybed pressure swing adsorption for hydrogen purification. International Journal of Hydrogen Energy.

[96] Gapp, E., & Pfeifer, P. (2023). Membrane Reactors for Hydrogen Production from Renewable Energy Sources. Current Opinion in Green and Sustainable Chemistry, 100800.

[97] Thiruselvi, D., Kumar, P. S., Kumar, M. A., Lay, C. H., Aathika, S., Mani, Y.,

... & Show, P. L. (2021). A critical review on global trends in biogas scenario with its up-gradation techniques for fuel cell and future perspectives. International Journal of Hydrogen Energy, 46(31), 16734-16750.

[98] Iannuzzi, L., Hilbert, J. A., & Lora, E. E. S. (2021). Life Cycle Assessment (LCA) for use on renewable sourced hydrogen fuel cell buses vs diesel engines buses in the city of Rosario, Argentina. International Journal of Hydrogen Energy, 46(57), 29694-29705.

[99] Atri, A., & Khosla, A. (2023). A Review of Water Electrolysis, Fuel Cells and Its Use in Energy Storage. Renewable Energy Optimization, Planning and Control: Proceedings of ICRTE 2022, 275-288.

[100] Zakaria, Z., Kamarudin, S. K., Abd Wahid, K. A., & Hassan, S. H. A. (2021). The progress of fuel cell for malaysian residential consumption: Energy status and prospects to introduction as a renewable power generation system. Renewable and Sustainable Energy Reviews, 144, 110984.

[101] Onorati, A., Payri, R., Vaglieco, B. M., Agarwal, A. K., Bae, C., Bruneaux, G., ... & Zhao, H. (2022). The role of hydrogen for future internal combustion engines. International Journal of Engine Research, 23(4), 529-540.

[102] Oliveira, A. M., Beswick, R. R., & Yan, Y. (2021). A green hydrogen economy for a renewable energy society. Current Opinion in Chemical Engineering, 33, 100701.

CHAPTER 14

MECHANICAL PROPERTIES OF CARBON NANOTUBE MODIFIED LAMINATED COMPOSITE MATERIALS

Sakine KIRATLI[1]

1 Assis. Prof. Dr., Çankırı Karatekin University, Faculty of Engineering, Department of Mechanical Engineering, 18100, Çankırı, Turkey. skiratli@karatekin.edu.tr, ORCID:0000-0001-6292-5605.

1. Introduction

Composites, which have been used since ancient times, have become popular materials for all kinds of sectors with the development of science and technology. The reason why they are used in many sectors such as aviation, automotive, marine, food, construction, etc. is that they have superior properties such as lightness, high strength, and high rigidity. In addition to these, many other properties such as mechanical strength, abrasion resistance, corrosion resistance, thermal resistance, electrical conductivity, thermal conductivity, and acoustic conductivity can be listed (Şahin, 2006).

Composite material is the combination of two or more materials at a macro level in such a way that they do not dissolve in each other (Kaw, 2005). The purpose of creating a composite material is to meet the requirements by gathering the properties of each material that makes up a single material. Composites consist of two basic components: fiber and matrix. It generally acts as a fiber carrier and matrix binder (Şahin, 2006). Glass, carbon, and aramid fibers are used as fiber materials. As matrix materials, epoxy, polyester, polyamide, etc. from the polymer group are preferred.

Today, studies are still continuing to further develop these materials and increase their usage. In particular, research focuses on the development of the fiber-matrix interface. Weak interface bonding reduces the expected properties of the composite. One of the studies carried out in recent years involves the addition of various nanoparticles into the matrix. The aim here is to reduce the brittleness of the matrix and thus increase the functionality of the composite.

Among the nanoparticles used, nanotubes take first place due to their superior properties. Studies have shown that polymer composites improve mechanical properties at low carbon nanotube amounts (Kumar et al. 2021). However, there are many different factors that contribute to the development of features. The most important of these is the homogeneous dispersion of the nanotube in the matrix. Appropriate mixing methods should be chosen as nanotubes tend to clump easily. Poor dispersion in the matrix prevents good interfacial adhesion and leads to reduced properties. Commonly used mixing methods are magnetic stirring, mechanical mixing, ultrasonic bath, ultrasonic homogenizer, etc. In addition, surface modifications are made chemically on nanotubes with molecules such as NH_2 and COOH (Cha et al. 2019). This process improves the interface interaction between the nanotube and the matrix by reducing the agglomeration tendency (Rahman et al. 2013).

The primary objective of this research is to investigate the effects of CNTs on the mechanical properties of laminated composites. The specific objectives are:

- To fabricate laminated composites reinforced with different weight percentages of CNTs.
- To characterize the mechanical properties of the laminated composites using tensile, compressive, flexural tests, etc.
- To evaluate the effects of CNTs on the mechanical properties of the laminated composites.

2. Laminated Composites

Composite materials are classified according to matrix and fiber. Polymer, metal, and ceramic matrix composites are studied according to their matrix elements. According to the fiber elements, they are named continuous and discontinuous fiber-reinforced, particle-reinforced, and laminated composites. Laminated composites are also classified as fiber-reinforced laminated composites and sandwich composites.

Laminated composites are composed of multiple layers of fibers and matrix materials arranged in a specific pattern. Laminated composites are widely used in the aerospace and automotive industries due to their high strength-to-weight ratio, stiffness, and fatigue resistance. The mechanical properties of laminated composites depend on the orientation and sequence of the layers, as well as the type and amount of fiber and matrix materials used. Figure 1 shows a typical laminated composite formed by the combination of layers with different orientations.

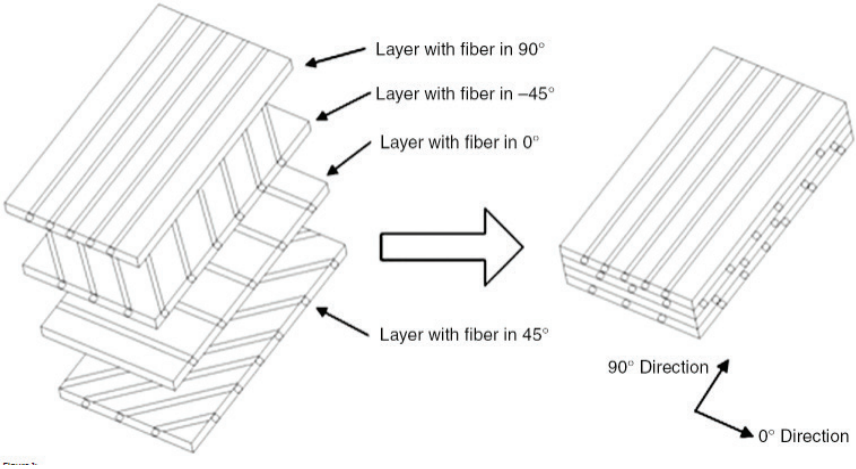

Figure 1. *Laminated composite plate (Xin et al. 2018).*

3. Materials

3.1. Nanomaterials

Materials are substances used to meet a need. They are examined under various sub-titles: metals, ceramics, polymers, composites, etc. Especially, biomaterials, smart materials, and nanomaterials are included in the new generation of material groups.

Following the discovery and use of nano-sized materials, rapid developments in technology have occurred and will continue to do so. Thanks to the superior properties of nano-sized materials, high-performance products have made our daily lives easier. The reason why materials show this performance is that the material properties change greatly at the nanoscale. Materials of this size show extraordinary mechanical, chemical, and physical properties.

Nanomaterials are more functional compared to normal materials. These are materials that are more durable, process faster, consume less energy, and occupy less space than normal materials. Among the nanomaterials, fullerene (discovered by H.W. Kroto in 1985), carbon nanotubes (discovered by S. Iijima in 1991), and graphene (discovered by Geim and Novoselov in 2004) are the most important (Demon, 2020). Apart from these, examples of nanomaterials such as nanofiber and various metal nanoparticles can be given.

3.2. Carbon Nanotubes

Carbon nanotubes (CNTs) are allotropes of carbon such as diamond, graphite, and fullerene (C60). Carbon nanotube is the name given to long, cylindrical structures formed by folding onto itself a single layer of graphite called graphene. (Yağlıkçı, 2019). Carbon nanotubes are available as single-walled (consisting of a single graphene structure) and multi-walled (consisting of multiple single-walled nanotubes that are concentrically intertwined) (Figure 2). The carbon allotropes are shown in Figure 3.

The materials have extraordinary properties in nanometer sizes. Carbon nanotubes are 10 times stronger and 6 times lighter than steel (Esawi and Farag, 2007). The reason why carbon nanotubes show extraordinary properties is the strong bonds between C–C atoms in the lattice structure with each other. Carbon atoms are covalently bonded to each other. (Yan et al. 2017).

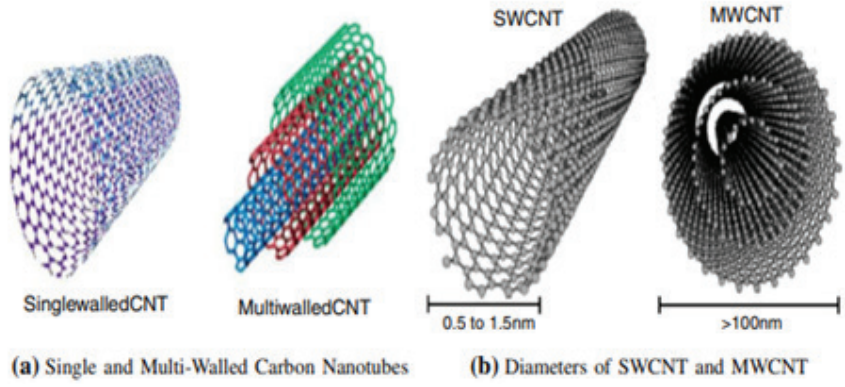

Figure 2. *Single and multi-walled carbon nanotubes (Bhattacharyya et al. 2020).*

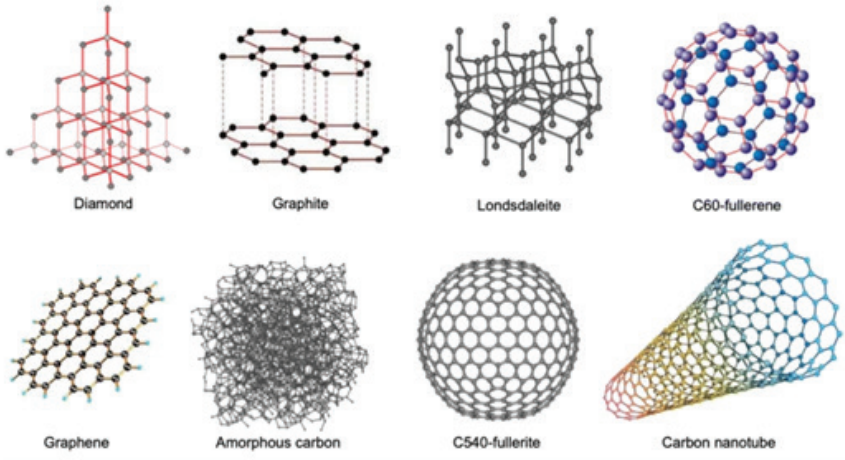

Figure 3. Allotropes *of carbon (Negri et al. 2020).*

Carbon nanotubes show extremely superior properties compared to known materials such as steel and concrete, especially in terms of mechanical properties such as tensile strength and modulus of elasticity. In addition, the thermal and electrical properties of carbon nanotubes are good. (Yağlıkçı, 2019). Carbon nanotubes have many different applications, such as sensors, thin screens, energy storage, electronic devices, and supercapacitors.

Carbon nanotubes have been used as a reinforcing material in composite materials to improve their mechanical properties. Carbon nanotubes can be dispersed in the matrix material to enhance the interfacial bonding between the reinforcement and the matrix. The presence of carbon nanotubes in the matrix material can increase the stiffness and strength of the com-

posite, while also improving its fatigue resistance and fracture toughness. Carbon nanotubes can also act as crack arresters in composite materials by absorbing and dissipating energy during crack propagation.

4. Methods

Various fabrication methods are available to fabricate laminated composites. Among them, vacuum infusion (Figure 4) and hand layup (Figure 5) methods are the most commonly used. The vacuum bagging method (Figure 6), on the other hand, is applied as a supplement to the hand layup method. The composites are reinforced with different weight percentages of carbon nanotubes. The mechanical tests are conducted according to ASTM standards. The mechanical properties of the laminated composites are characterized using tensile, compressive, flexural, shear, interlaminar shear strength, fracture toughness, etc. tests. The tests are conducted using a universal testing machine, and the strain and stress data are recorded. The effect of carbon nanotubes on the mechanical properties of the laminated composites is evaluated by comparing the results of mechanical tests for samples with and without carbon nanotubes.

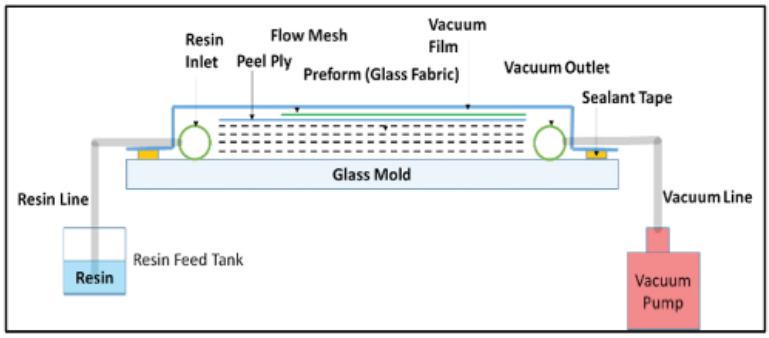

Figure 4. *Vacuum infusion method (Sunilpete and Cadambi, 2020).*

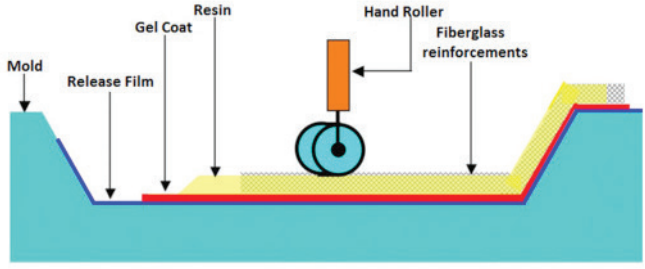

Figure 5. *Hand lay-up method (Cucinotta et al. 2017).*

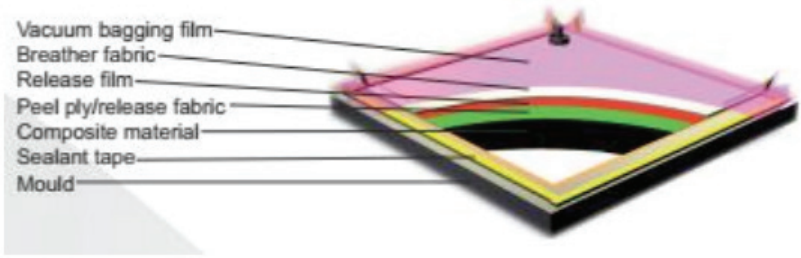

Figure 6. *Vacuum bagging method (Abdurohman et al. 2018).*

5. Mechanical Properties

The incorporation of CNTs in laminated composites has shown to improve the overall mechanical properties of the composite, such as tensile strength, flexural strength, and interlaminar shear strength. The unique properties of CNTs can significantly improve the load transfer efficiency at the matrix-reinforcement interface, resulting in improved mechanical properties of the composite. In addition, the high aspect ratio of CNTs provides a large surface area for bonding with the matrix material, which further enhances the interfacial bonding between the matrix and the reinforcement.

CNTs have been used to reinforce laminated composites, and several studies have investigated the effect of CNTs on the mechanical properties of laminated composites. Ahmadi and Karami (2017) investigated the effect of CNTs on the interlaminar shear strength of composite materials. They found that the addition of CNTs to the matrix material improved the interlaminar shear strength of the composite material. Gohardani and Khalili (2016) reviewed the use of CNTs in environmental protection and energy generation and highlighted the potential of CNTs in various applications, including water treatment, gas separation, and energy storage. Zhang et al. (2018) investigated the effects of CNTs on the mechanical properties of laminated composites. They found that the addition of CNTs to the matrix material improved the tensile and flexural strength of the composite material. Li et al. (2021) investigated the interfacial and mechanical properties of carbon fiber/epoxy composites modified with a CNT-modified sizing agent. They found that the addition of CNTs improved the interfacial bonding between the carbon fibers and the epoxy matrix, leading to improved mechanical properties. Zheng et al. (2016) reviewed the mechanical properties and failure modes of CNTs reinforced composite materials and concluded that CNTs have the potential to improve the mechanical properties of composite materials. In their study, Alnefaie et al. (2013) discovered that

multi-walled carbon nanotube composites had improved flexural strength. The tensile and bending properties of composite materials incorporating multi-walled carbon nanotubes improved, as noted by Garg et al. (2015), Shokrieh et al. (2014), and Taraghi et al. (2015). The interlaminar shear strength of materials is increased by multi-walled carbon nanotubes, according to research done on the behavior of materials under out-of-plane shear (Guo et al. 2017; Liu et al. 2017). Just a small number of researchers have conducted a study that takes into account all of the tensile, shear, and bending properties and they found that the characteristics increased (Sharma and Shukla, 2014; Subba et al. 2015).

6. Conclusions

This proposal aims to investigate the effects of carbon nanotubes on the mechanical properties of laminated composites. CNTs have been extensively studied for their exceptional mechanical properties and have been incorporated into composite materials to improve their mechanical properties. CNTs have been used to reinforce laminated composites, which are widely used in the aerospace and automotive industries due to their high strength-to-weight ratio, stiffness, and fatigue resistance. The incorporation of CNTs into laminated composites can improve their mechanical properties, including their stiffness, strength, toughness, and fatigue resistance. The studies reviewed in this paper demonstrate the potential benefits of using CNTs in laminated composites and highlight the importance of the interfacial bonding between the reinforcement and the matrix material. The findings of this research will be beneficial for the development of advanced composite materials for various industrial applications. The research will provide insights into the development of advanced composite materials and could contribute to the design of stronger and more durable composite structures. Further research is needed to optimize the incorporation of CNTs into laminated composites and to investigate the effects of varying the amount and orientation of CNTs on the mechanical properties of the composite. Additionally, the long-term durability and environmental impact of CNT-reinforced laminated composites should also be investigated.

REFERENCES

Abdurohman, K., Satrio, T., & Muzayadah, N. L. (2018, November). A comparison process between hand lay-up, vacuum infusion and vacuum bagging method toward e-glass EW 185/lycal composites. *In Journal of Physics: Conference Series* (Vol. 1130, No. 1, p. 012018). IOP Publishing.

Ahmadi, M., & Karami, G. (2017). A study on the effect of carbon nanotube on interlaminar shear strength of composite materials. *Journal of Reinforced Plastics and Composites, 36(17),* 1236-1243.

Alnefaie, K. A., Aldousari, S. M., & Khashaba, U. A. (2013). New development of self-damping MWCNT composites. *Composites Part A: Applied Science and Manufacturing*, *52*, 1-11.

Bhattacharyya, A., Seth, G. S., Kumar, R., & Chamkha, A. J. (2020). Simulation of Cattaneo–Christov heat flux on the flow of single and multi-walled carbon nanotubes between two stretchable coaxial rotating disks. *Journal of Thermal Analysis and Calorimetry*, *139*, 1655-1670.

Cha, J., Kim, J., Ryu, S., & Hong, S. H. (2019). Comparison to mechanical properties of epoxy nanocomposites reinforced by functionalized carbon nanotubes and graphene nanoplatelets. *Composites Part B: Engineering*, *162*, 283-288.

Cucinotta, F., Guglielmino, E., & Sfravara, F. (2017). Life cycle assessment in yacht industry: A case study of comparison between hand lay-up and vacuum infusion. *Journal of Cleaner Production, 142*, 3822-3833.

Demon, S. Z. N., Kamisan, A. I., Abdullah, N., Noor, S. A. M., Khim, O. K., Kasim, N. A. M., ... & Halim, N. A. (2020). Graphene-based materials in gas sensor applications: A review. *Sens. Mater, 32(2),* 759-777.

Esawi, A. M., & Farag, M. M. (2007). Carbon nanotube reinforced composites: potential and current challenges. *Materials & design, 28(9)*, 2394-2401.

Garg, M., Sharma, S., & Mehta, R. (2015). Pristine and amino functionalized carbon nanotubes reinforced glass fiber epoxy composites. *Composites Part A: Applied Science and Manufacturing*, *76*, 92-101.

Gohardani, O., & Khalili, S. M. R. (2016). Carbon nanotubes as advanced materials for environmental protection and energy generation. *Environmental Science and Pollution Research, 23(13)*, 12611-12630.

Guo, J., Zhang, Q., Gao, L., Zhong, W., Sui, G., & Yang, X. (2017). Significantly improved electrical and interlaminar mechanical properties of carbon fiber laminated composites by using special carbon nanotube pre-dispersion mixture. *Composites Part A: Applied Science and Manufacturing*, *95*, 294-303.

Kaw, A. K. (2005). Mechanics of composite materials. CRC press.

Kumar, A., Sharma, K., & Dixit, A. R. (2021). A review on the mechanical pro-

perties of polymer composites reinforced by carbon nanotubes and graphene. *Carbon Letters*, *31*(2), 149-165.

Li, J., Wang, Z., Ren, J., & Wang, G. (2021). Interfacial and mechanical properties of carbon fiber/epoxy composites modified with a carbon nanotube-modified sizing agent. *Composites Science and Technology, 201*, 108469.

Liu, W., Li, L., Zhang, S., Yang, F., & Wang, R. (2017). Mechanical properties of carbon nanotube/carbon fiber reinforced thermoplastic polymer composite. *Polymer Composites*, *38*(9), 2001-2008.

Negri, V., Pacheco-Torres, J., Calle, D., & López-Larrubia, P. (2020). Carbon nanotubes in biomedicine. *Surface-modified Nanobiomaterials for Electrochemical and Biomedicine Applications*, 177-217.

Rahman, M. M., Zainuddin, S., Hosur, M. V., Robertson, C. J., Kumar, A., Trovillion, J., & Jeelani, S. (2013). Effect of NH_2-MWCNTs on crosslink density of epoxy matrix and ILSS properties of e-glass/epoxy composites. *Composite Structures*, *95*, 213-221.

Sharma, K., & Shukla, M. (2014). Three-phase carbon fiber amine functionalized carbon nanotubes epoxy composite: processing, characterisation, and multiscale modeling. *Journal of Nanomaterials*, *2014*, 2-2.

Shokrieh, M. M., Saeedi, A., & Chitsazzadeh, M. (2014). Evaluating the effects of multi-walled carbon nanotubes on the mechanical properties of chopped strand mat/polyester composites. *Materials & Design (1980-2015)*, *56*, 274-279.

Subba Rao, P., Renji, K., Bhat, M. R., Mahapatra, D. R., & Narayana Naik, G. (2015). Mechanical properties of CNT–Bisphenol E cyanate ester-based CFRP nanocomposite developed through VARTM process. *Journal of reinforced plastics and composites*, *34*(12), 1000-1014.

Sunilpete, M. A., & Cadambi, R. M. (2020). Development of Cost Effective Out-of-Autoclave Technology–Vacuum Infusion Process with Tailored Fibre Volume Fraction. *Materials Today: Proceedings*, *21*, 1293-1297.

Şahin, Y. (2006). Kompozit Malzemelere Giriş. Seçkin Yayıncılık.

Taraghi, I., Fereidoon, A., Zamani, M. M., & Mohyeddin, A. (2015). Mechanical, thermal, and viscoelastic properties of polypropylene/glass hybrid composites reinforced with multiwalled carbon nanotubes. *Journal of Composite Materials*, *49*(28), 3557-3566.

Xin, Z., Duan, Y., Xu, W., Zhang, T., & Wang, B. (2018). Review of the mechanical performance of variable stiffness design fiber-reinforced composites. *Science and Engineering of Composite Materials*, *25*(3), 425-437.

Yağlıkçı, S.Y. (2019). Karbon nanotüp üretiminde katalizörün gaz fazı derişim profiline etkisinin incelenmesi (Doctoral Dissertation, University of Ankara).

Yan, J., Huang, Y., Wei, C., Zhang, N., & Liu, P. (2017). Covalently bonded pol-

yaniline/graphene composites as high-performance electromagnetic (EM) wave absorption materials. *Composites Part A: Applied Science and Manufacturing, 99,* 121-128.

Zhang, J., Li, X., Guo, J., & Ma, J. (2018). Mechanical properties of carbon nanotube reinforced laminated composites. *Composites Part B: Engineering, 145*, 108-115.

Zheng, W., Zhao, X., & Song, S. (2016). Mechanical properties and failure modes of carbon nanotubes reinforced composite materials: A review. Composites Part B: Engineering, 91, 545-562.

CHAPTER 15

SURVEY AND ONE-DIMENSIONAL STAKE-OUT OF BUILDINGS

Mehmet EREN[1]

1 Lecturer Dr. Mehmet EREN, Yıldız Technical University, Faculty of Civil Engineering, Department of Geomatic Engineering, https://orcid.org/0000-0002-8370-8615

1-INTRODUCTION

For cultural heritages (such as castles, inns, baths, aqueducts, and historical buildings) to be kept alive and revived in case of damage, the information on these structures should be documented. According to Article 3 of the Venice Charter (1964), "The intention in conserving and restoring monuments is to safeguard them no less as works of art than as historical evidence." defines as (Icomos, 1964). In the first applications of the surveying process, it was used as a base for restoration or reconstruction works to keep the cultural heritage alive and in documentation studies.

In recent years, it has increased the number and size of modern structures built due to technological advances. In order to beautify the appearance of these gigantic structures built for prestige purposes, exterior cladding applications are made by using different coating materials. On the other hand, external cladding systems are also used because they provide benefits such as preventing heat loss of buildings (heat insulation), reducing energy costs, and adding aesthetics to buildings. Mechanical exterior cladding systems are formed by covering the grid-shaped spaces between the carrier vertical elements and horizontal profiles mounted on the structure with panels such as granite, metal, marble, composite, or glass (Figure 1). It allows sound and heat insulation with the help of the material placed in the gaps between the cladding and the building facade. Curtain wall systems are defined by İrtem and Tığ (2006) as multi-purpose structural elements that perform different insulation functions by acting as a filter between indoor and outdoor environments (İrtem E. et al., 2006). Çetinel (2012) calculated that when the indoor-outdoor temperature difference is maximum in January, it provides fuel savings of up to 17%, depending on the type of material used (ÇETİNEL E., 2012).

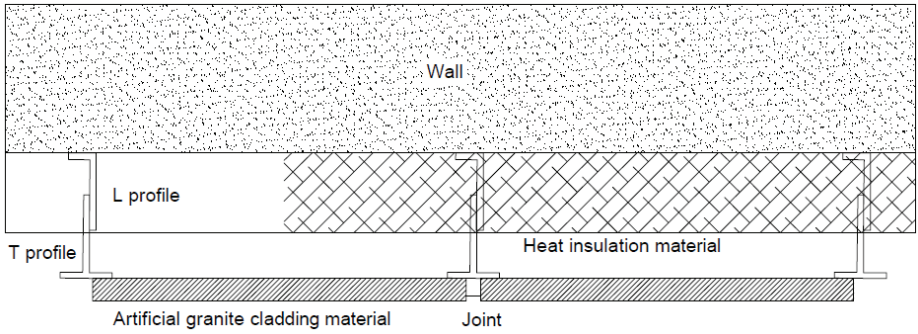

Figure 1. The application section is to be covered with artificial granite material.

The purpose of the survey measurements of buildings in exterior cladding applications is to optimize the labor cost by determining the

dimensions of the carrier element to be used between the building and the exterior cladding element. While the buildings are being built, they are carried out within the scope of a certain project. However, during the construction phase of the building, deviations from the project values are experienced due to the errors caused by the implementer. Without deviations from the project, they could have done the exterior cladding with the help of the values they took directly from the project sizes without doing a survey.

The restoration of historical buildings can be done without measuring, with sketches, photographs of the building, and detailed and well-made explanations (Reynolds, 2011). In applications to be made without geodetic measurement, the duration and cost of the work will increase. However, measuring as a "metric" using the appropriate measuring instrument will give better results both in the restoration works of the building and in the exterior works. According to (Reynolds, 2011), spatial measurements are determined by using direct measurement (Total Station (TS) / Theodolite, Global Positioning System (GPS)) or indirect measurement techniques (such as photogrammetry and laser scanning). The measurement made due to the deviation of modern buildings from the project and the surveying of historical buildings can be done with different methods. These methods are;

- Theodolite and total station measurements,
- Photogrammetric measurement,
- Laser scanners,

measurement methods can be used.

In the exterior cladding works of modern buildings, their staff make the measurements and stake-out required by the companies. Studies are carried out with the help of TS measurements in survey and application applications. Demir et al. (2005), survey measurements were carried out with the help of terrestrial techniques (total station) for the production of the elements of the main skeleton of the METU Science and Technology Museum to be made abroad (DEMİR et al., 2005) (Figure 2).

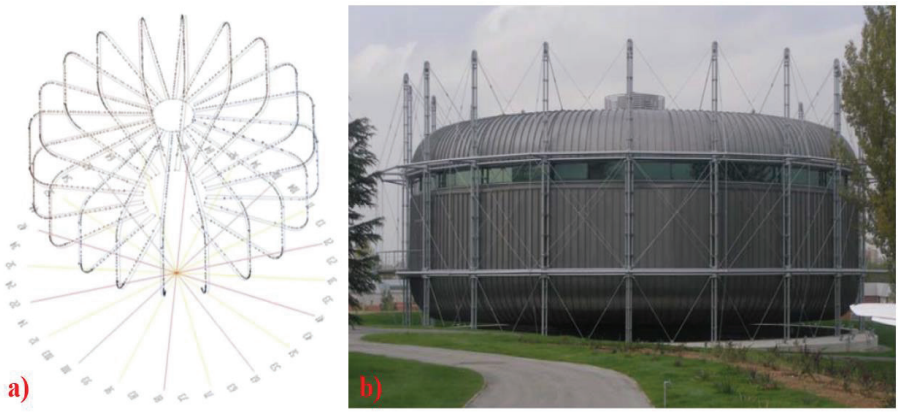

Figure 2. Object points and projection axes of the load-bearing elements (a) The finished exterior cladding of the building (b).

Yakar et al. (2011) surveyed Beyşehir Stone Bridge as a 3D model using photogrammetric measurement techniques (YAKAR et al., 2011). On the other hand, a survey of Istanbul Fatih Mosque (Figure 3) was made both with the photogrammetric method and with the help of a terrestrial laser scanner (Yastıklı, 2005).

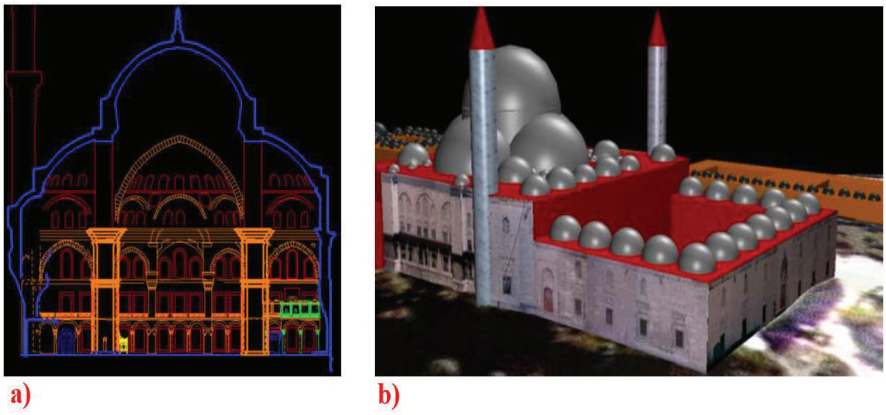

Figure 3. Measurement of Fatih Mosque with photogrammetric method (a) measurement with the laser scanner and 3D texture model (b)

In areas with measurement difficulties, Due to narrow spaces or the impossibility of surveying the roof, 3D measurements were made based on camera images in the Asinou Church studies in Cyprus (Figure 4) with the help of a quadcopter (Themistocleous et al., 2015).

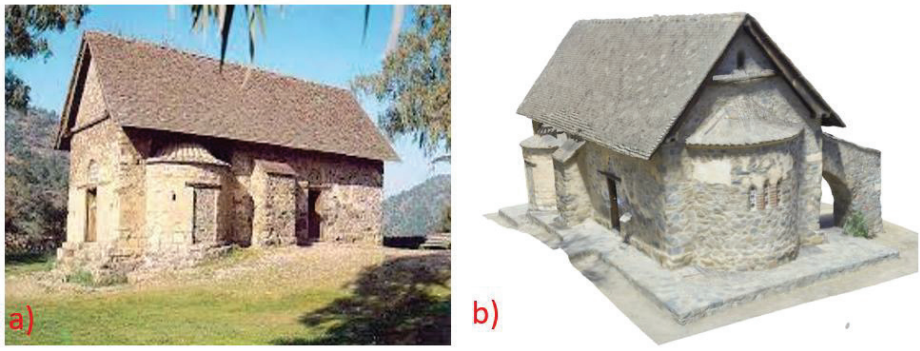

Figure 4. Asinou church (a), 3D model of the church (b).

In the survey works of the Sille Aya-i Eleni church (Figure 5), the measurements of the interiors were made with a laser scanner, the measurements of the exteriors were made with the help of three different techniques: terrestrial photogrammetric measurements and camera recordings of the roof measurements with the help of UAV's(Böge et al., 2020).

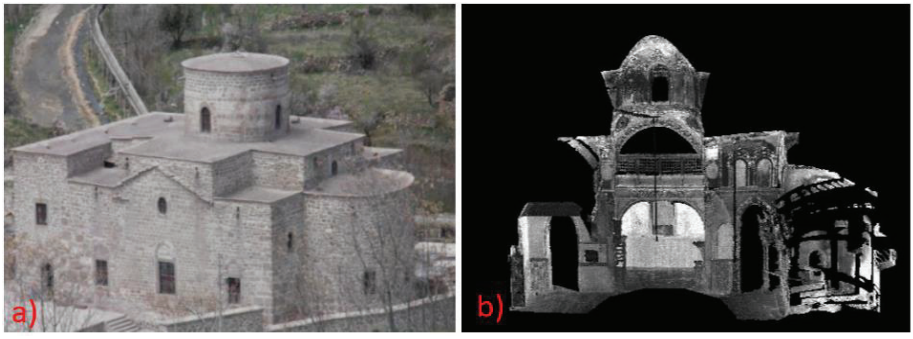

Figure 5. Sille Aya-i Eleni church (a), a section of the survey obtained from the studies (b)

The collected data is processed and projected with the help of different software (CAD, Image processing, etc.) on a computer. The coordinate data of the carrier elements are taken from the project and marked on the work area (Stake-out process).

Measurements made by laser or photogrammetric (including UAV-assisted measurements) require control points (based on terrestrial technique) that are appropriately distributed on the building or around the building and marked on the ground.

2-METHODOLOGY

Classical measurement methods such as TS or tachymetric measurement are generally used in the survey measurements of buildings. In the photogrammetric method, if the facade of the building is flat and has little detail, it is done with Rodresman (single image processing). At the same time, if there is a depth difference between the details of the facade, it is performed with the help of 3D images with help of image pairs. As another method, in the case of a large number of building detail points, surveying processes are carried out with terrestrial laser applications, which are capable of making 3D point cloud measurements inside or outside the building. Photogrammetric methods and laser measurements are generally used to measure historical buildings. However, within the scope of the study, TS measurements were carried out because the number of detail points to be measured in the external cladding systems of the measured buildings is low, and other methods are expensive and time-consuming. Within the scope of the survey measurements of the newly built buildings, it was deemed sufficient to take a limited number of details, such as the corners of the buildings, floor contour lines, window and balcony details. It was considered that it would be appropriate to use TS in the application process of the building elements designed with the help of the measurements made.

The steps to be followed before the survey measurements are made;

- For the building coordinate system (local coordinate system), two polygons are marked on the building surface and as far away as possible,
- Establishing the first point on the ground, centered on the two polygon points on the building and as far away as the terrain allows (for ease of survey measurement),
- Determination of the first point location with two-point resection problem solving (Ghilani et al., 2012),
- Then, making closed traverse calculations with the help of the measurements made on the polygons established around the building with appropriate distribution,

After the preliminary preparation, the measurement is started. Critical points of the building (building turns (Corner points), window details, floor contour lines, and balcony details) are measured in the measurement process.

When the TS is prepared for measurement, the azimuth angle (α) and vertical/zenith angle (Z) are calculated by the microprocessor of the TS from the measurements made from the known location. When the TS is prepared for measurement, the azimuth angle (α) and vertical/zenith angle

(Z) are calculated by the microprocessor of the TS from the measurements made from the known location. When the measurement button is pressed, the horizontal distance is obtained with the help of the oblique distance measured between the measured object point and the measurement point (Equation 1).

$$D_Y = D_E * Sin\ Z \quad (1)$$

After obtaining the horizontal distance, it turns into the first fundamental task of surveying solution, which is the problem of calculating the position of the new point measured with the help of the azimuth angle and distance from a known point to the point whose position will be determined (Figure 6). The coordinates of the new points are calculated using equation 2 and equation 3.

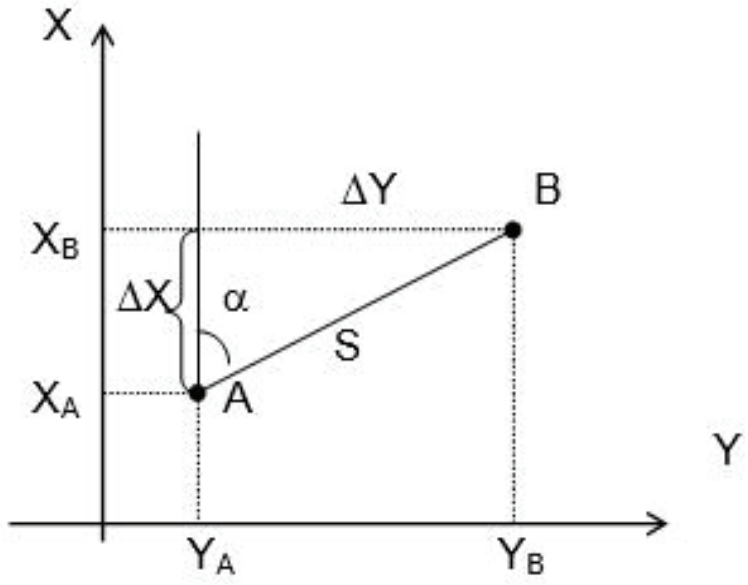

Figure 6. Graphic representation of I. fundamental task of surveying.

$$\Delta y = s \cdot \sin \alpha$$

$$\Delta x = s \cdot \cos \alpha \quad (2)$$

$$Y_B = Y_A + \Delta y$$

$$X_B = X_A + \Delta x \quad (3)$$

This calculation calculates the 2D coordinate values of all the building details. The heights of the new points are calculated using the inclined distance and the zenith angle. Based on the 3D dimensions of the building, the project is carried out with CAD software on the computer.

Thus, the 3D position of the entire building cladding element is known. The coordinate values of the exterior bearing elements are taken from the project, and stake-out is started on the building surface. The coordinate of the point where the instrument is installed is known, and the position of the point to be applied is read from the computer. With the help of the azimuth angle and the distance between these two points whose coordinates are known, the polar stake-out elements are calculated by equations 4-6 (the second fundamental task of surveying).

$$\Delta_y = Y_B - Y_A$$

$$\Delta_X = X_B - X_A \tag{4}$$

$$S = \sqrt{\Delta_y^2 + \Delta_x^2} \tag{5}$$

$$\alpha = Atn\left(\frac{Dy}{\Delta x}\right) \tag{6}$$

If $\Delta_y > 0$ ve $\Delta_x > 0$ ➔ α

If $\Delta_y > 0$ ve $\Delta_x < 0$ ➔ α + 200

If $\Delta_y < 0$ ve $\Delta_x < 0$ ➔ α + 200

If $\Delta_y < 0$ ve $\Delta_x > 0$ ➔ α + 400

For stake-out, it is sufficient to apply only these coordinate values to the coordinate axis corresponding to the building facade. For example, if the building facade corresponds to the Y coordinate value, only the y value of each element is marked. After the bearing elements are marked on the wall, the application of the covering element of the building is started. The stake-out of the cladding elements is made in one dimension again, but only the X coordinate values are applied this time. This process saves a lot of time and money.

2.1COORDINATE TRANSFORMATION

In exterior applications, the building coordinate system, which accepts one side of the building or two points on the building, is used (xy). These studies generally do not need ED-50 or projection coordinate systems (XY). However, if there is such a need, at least two of the points belonging to the building coordinate system can be transformed between the two systems by knowing the coordinates in the system to be transformed.

It is transformed with the help of transformation parameters calculated with the help of enough conjugate points whose position in both xy and XY systems is known (BAŞÇİFTÇİ et al., 2008). Similarity transformation, affine or projective transformation methods are preferred depending on the number of conjugate points used. However, within the scope of the study, only the similarity transformation will be discussed.

2.1.1 Similarity Transformation

Figure 7 shows 4 parameters, including rotation, scale, and 2 translations in the X and Y axis between both coordinate systems (Hofmann-Wellenhof et al., 2001; Mitsakaki, 2004). Two points whose coordinates are known in both systems are sufficient to solve this problem.

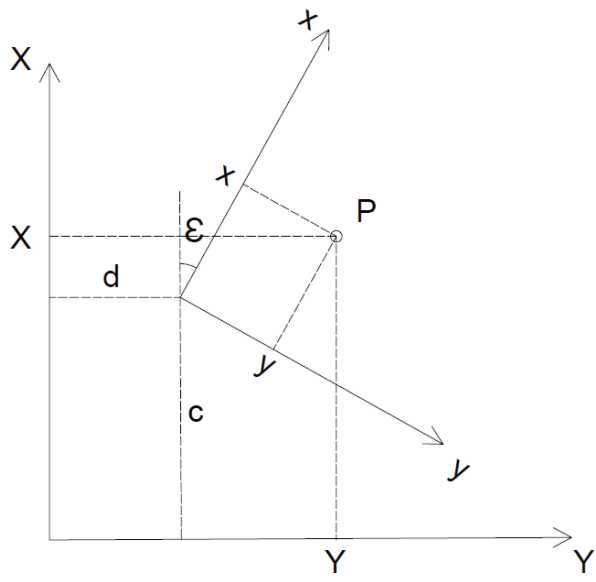

Figure 7. Similarity transformation

$$X = x.m.\cos\varepsilon - y.m.\sin\varepsilon + c$$

$$Y = x.m.\sin\varepsilon + y.m.\cos\varepsilon + d \quad (7)$$

$$a = m\cos\varepsilon \;,\; b = m\sin\varepsilon \quad (8)$$

$$X = a.x - b.y + c$$

$$Y = a.y + b.x + d \quad (9)$$

where;

x and y are the coordinates of the 1st system, X and Y are the coordinates of the 2nd system, ε is the rotation angle between the two coordinate systems, c and d are the translation elements, and m is the scale factor.

$$m = \sqrt{a^2 + b^2} \quad (10)$$

$$tan\,\varepsilon = \frac{a}{b} \quad (11)$$

If the number of conjugate points is more than two, the transformation is solved with the Least Squares (Least Squares) method with compensation. In this solution, two times the number of points residuals can be written with the help of (12) equations (Yaşayan, n.d.).

$$\begin{aligned} ax_1 - by_1 + c &= X_1 + v_{x_1} \\ ay_1 - bx_1 + d &= Y_1 + v_{y_1} \\ &\cdots \\ ax_{n1} - by_n + c &= X_n + v_{x_n} \\ ay_n - bx_n + d &= Y_n + v_{y_n} \end{aligned} \quad (12)$$

2nx4 coefficients matrix (A);

$$A = \begin{bmatrix} x_1 & -y_1 & 1 & 0 \\ y_1 & x_1 & 0 & 1 \\ \cdots & \cdots & \cdots & \cdots \\ x_n & -y_n & 1 & 0 \\ y_n & x_n & 0 & 1 \end{bmatrix} \quad (13)$$

$$X^T = [a \quad b \quad c \quad d]_{1x4} \quad (14)$$

$$l^T = [X_1 \quad Y_1 \quad \ldots \quad \ldots \quad X_n \quad Y_n]_{1x2n} \quad (15)$$

$$v^T = [v_{x_1} \quad v_{y_1} \quad \cdots \quad \cdots \quad v_{x_n} \quad v_{y_n}]_{1x2n} \quad (16)$$

Matrix of unknowns (X);

$N = A^T PA$, $n = A^T Pl$,

$X = N^{-1}n$, (17)

Residuals of conjugate points (v);

$v = AX - l$ obtained from the matrix solution. (18)

2.2 Stake-out Implementation with Total Station

The workflow algorithm, from selecting the coordinate system suitable for the building shape to implementing the stake-out operations with the total station, is shown in Figure 8.

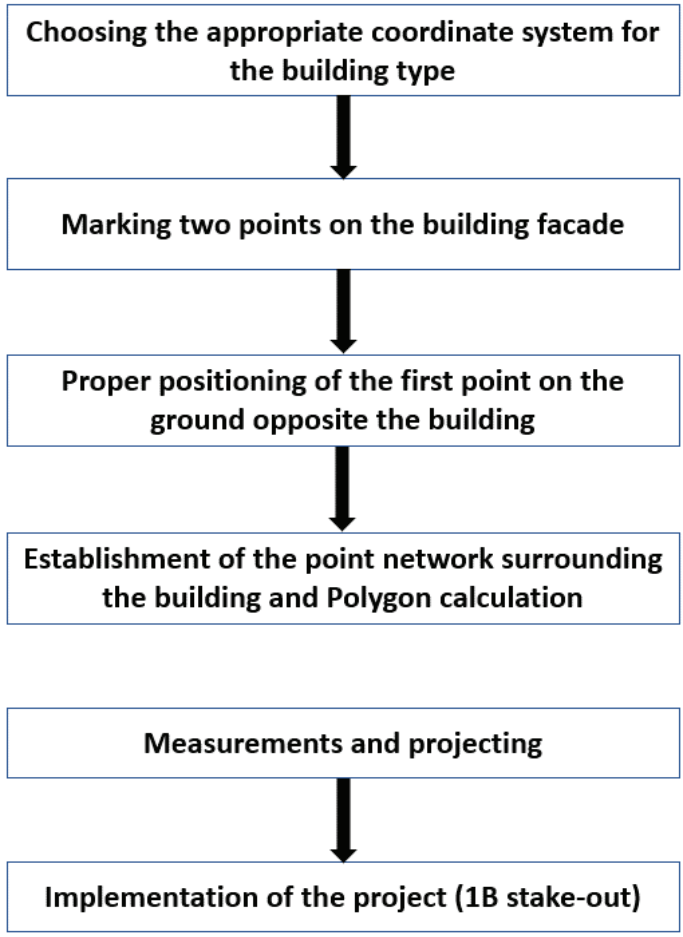

Figure-8 Stake-out workflow algorithm

3-APPLICATION

Data can be collected in the ED-50 coordinate system or the local coordinate system for the building survey made with the terrestrial technique. Due to the advantages of the building coordinate system (local coordinate system), it was preferred to be used within the scope of the study. Measurements and stake-out studies were carried out with the help of the Sokkia SET630R3 Total Station, which can measure without reflectorless. Different solutions have been proposed for projects with different geometric shapes. Buildings within the scope of the project have rectangular, circular, or circular arc or rectangular or circular forms with the arms of the blocks angled at 120º (Figure 9). This situation does not pose a problem for the surveys of the buildings. However, it is projected in Autocad 2004 software and causes 2D or 3D stake-out difficulties in the field.

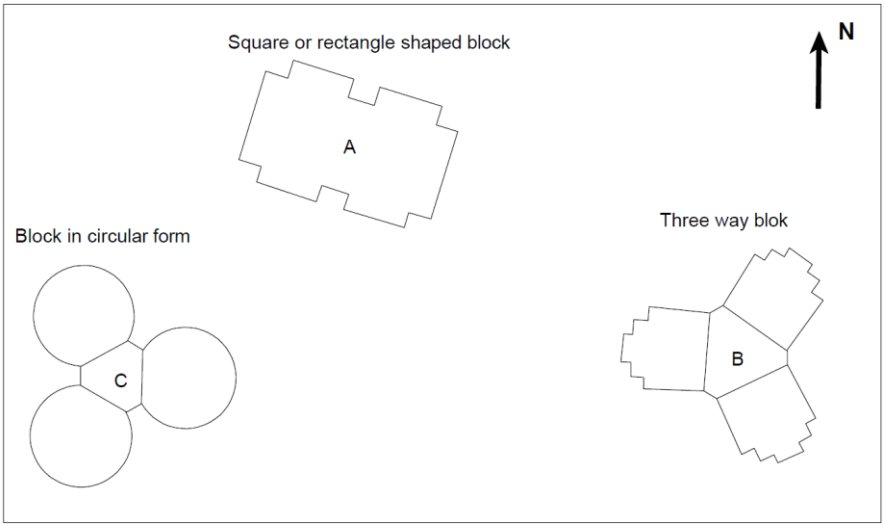

Figure 9. Three different types of building layout plans of the application area.

The building coordinate system was adopted in the studies, and stake-out to be made in 1D coordinates in rectangular or square-shaped buildings was easily applied (Figure 10). However, in buildings B and C, a single coordinate system is insufficient for problem-solving since the blocks are at an angle of 120° to each other. For B blocks, a separate coordinate system is defined for each branch (Figure 11).

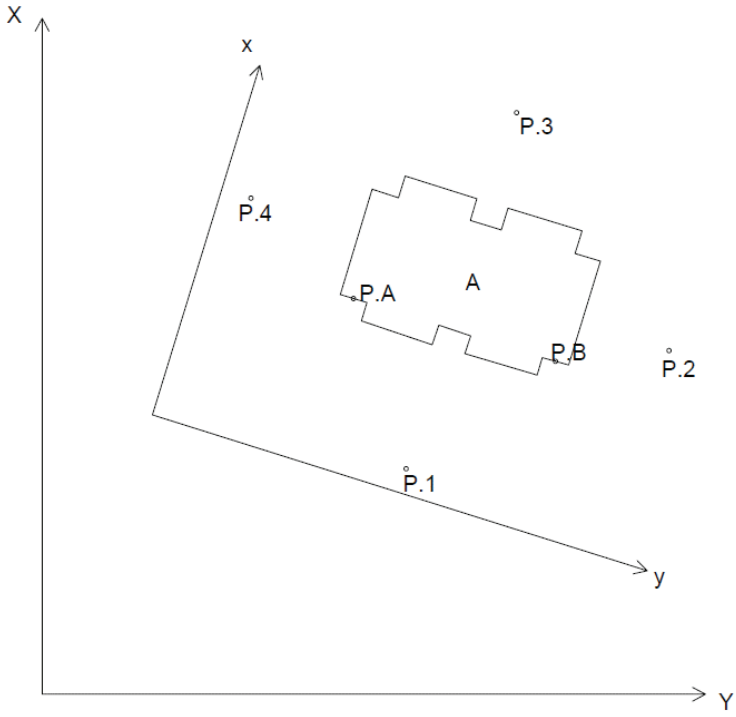

Figure 10. The coordinate system is defined in the rectangular block.

On the other hand, in buildings with a circle form, the stake-out process becomes more difficult when the angle between the center of the building and the measurement point is close to 45° (50 g) (Figure 12). In this case, two separate orthogonal coordinate systems have been proposed and planned with a 45° angle between the two coordinate systems. It has been suggested to use 6 coordinate systems in total in the application applications of C blocks (Figure 13).

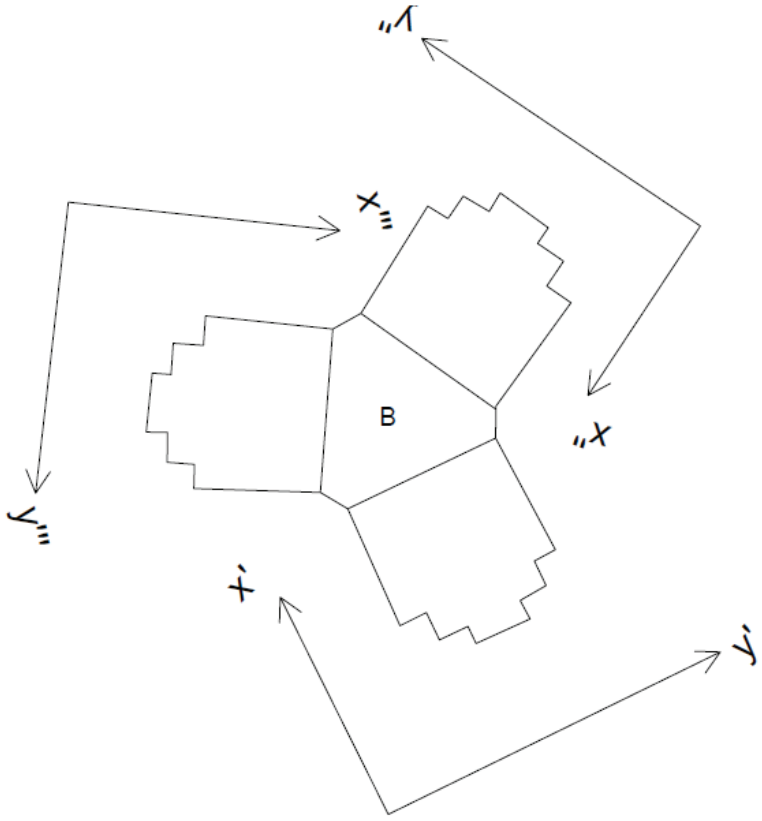

Figure 11. Three separate coordinate systems are constructed in a rectangular shape and defined by the 120° angle between the block arms.

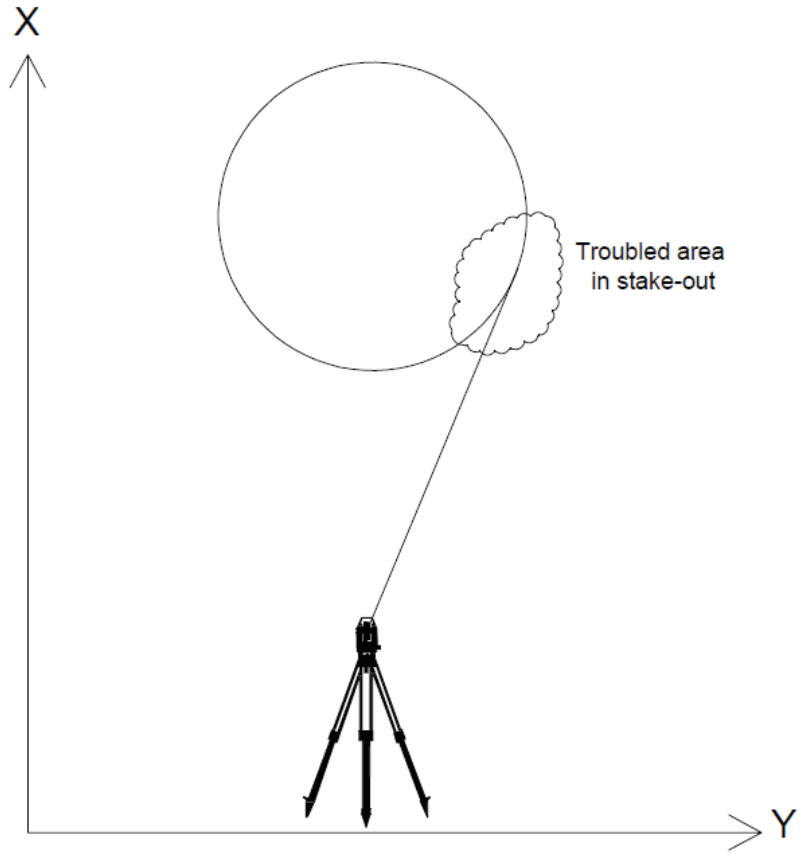

Figure 12. The problem is when the angle between the block center TS and the application point is approximately 45 degrees.

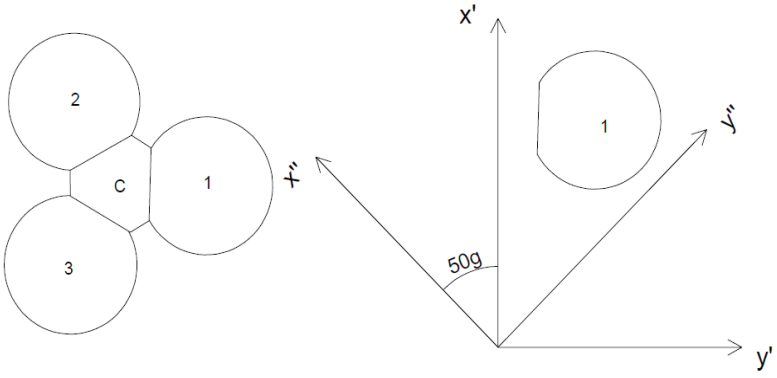

Figure 13. The application in which 6 different coordinate systems are defined in two in each arm due to the 120° angle between the blocks of the circular form.

4- CONCLUSIONS AND RECOMMENDATIONS

In survey studies, the appropriate measurement method should be used. If the number of details measured in the building is excessive, the measurements can be taken in 3D with terrestrial laser or cameras. If the number of building details is low, it can be performed in 2D by processing a single image (with Rodresman) or 3D with total station measurements.

In stake-out operations, it is recommended to use well-calibrated total stations that can measure without reflectors. Because if a reflector is used, the offset value will be different between the place where the measurement is made and the point to be measured.

One-dimensional stake-out of exterior elements;

- If the shape of the building is rectangular or square, one side of the building facade should be designed to be parallel to the x or y-axis of the coordinate system.
- If the block arms are in the form of a rectangle, making an angle of 120° to each other, a new coordinate system must be defined for each of the block arms, and a solution should be made with 3 different coordinate systems with 120° intervals.
- If the shape of the building is circular, stake-out is very difficult in the region where the angle at the time of measurement (between the building center, TS, and the stake-out point) approaches 45ô. For this reason, two separate coordinate systems should be defined to make an angle of 45 degrees with each other. For the C block, 6 coordinate systems must be defined, each of which is 2 coordinate systems.

REFERENCES

BAŞÇİFTÇİ, F., & İNAL, C. (2008). Jeodezide Kullanılan Bazı Koordinat Dönüşümlerinin Programlanması. *Bilim ve Teknoloji Dergisi*, *23*(1), 27–40.

Böge, S., & Karabörk, H. (2020). Integration of Different Methods for Architectural Survey of Historical and Cultural Heritages. *Turkish Journal of Geosciences*, *1*(2), 53–62.

ÇETİNEL E. (2012). *Tarihsel süreç içinde dış cephe kaplama malzemelerinin ısı yalıtımı açısından irdelenmesi*. Natural and Applied Sciences.

DEMİR, S., ERKAYA, H., & HOŞBAŞ, R. G. (2005, November 23). *SURVEY STUDIES FOR OUTSIDE FACING ON STEEL CONSTRUCTIONS*.

Ghilani, C. D., & Wolf, P. R. (2012). Elementary Surveying An Introduction to Geomatics Thirteenth Edition. In Pearson Education (Vol. 91, Issue 5).

Hofmann-Wellenhof, B., Lichtenegger, H., & Collins, J. (2001). Global positioning system : theory and practice In GPS.

İrtem E., & Tığ G. (2006, October 17). Giydirme Cephe Taşıyıcı Sistem Profilleri için Optimum (Ekonomik) Kesit Boyutlarının Geliştirilmesi. *3. Ulusal Çatı ve Cephe Kaplamalarında Çağdaş Malzeme Ve Teknolojiler Sempozyumu*.

Icomos. (1964). International Charter for the conservation and restoration of monuments and sites (The Venice Charter 1964). *IInd International Congress of Architects and Technicians of Historic Monuments*.

Mitsakaki, C. (2004). TS7 Reference Frame in Practice Christiana Mitsakaki TS7.2 Coordinate Transformations FIG Working Week 2004 Coordinate Transformations. *FIG Working Week 2004*.

Reynolds, C. A. (2011). Measured and Drawn: Techniques and Practice for the Metric Survey of Historic Buildings. *Collections: A Journal for Museum and Archives Professionals*, *7*(1). doi: 10.1177/155019061100700109

Themistocleous, K., Ioannides, M., Agapiou, A., & Hadjimitsis, D. G. (2015). The methodology of documenting cultural heritage sites using photogrammetry, UAV, and 3D printing techniques: the case study of Asinou Church in Cyprus. *Third International Conference on Remote Sensing and Geoinformation of the Environment (RSCy2015)*, *9535*. doi: 10.1117/12.2195626

YAKAR, M., KARASAKA, L., METİN, A., URAY, F., KAHYA, İ., & TANIK, H. (2011). *BEYŞEHİR TAŞ KÖPRÜNÜN FOTOGRAMETRİK ÖLÇÜM TEKNİKLERİ İLE MİMARİ RÖLÖVESİNİN HAZIRLANMASI VE 3 BOYUTLU MODELLENMESİ*. Antalya: TUFUAB .

Yaşayan, A. (n.d.). *Hava fotogrametrisinde iki boyutlu doğrusal dönüşümler ve uygulamaları*.

Yastıklı, N. (2005). Sayısal Fotogrametri ve Yersel Lazer Tarayıcılar ile Belgeleme ve Üç Boyutlu Modelleme. *10. Türkiye Harita Bilimsel ve Teknik Kurultayı*.